Agronomy Research

Established in 2003 by the Faculty of Agronomy, Estonian Agricultural University

Aims and Scope:

Agronomy Research is a peer-reviewed international Journal intended for publication of broad-spectrum original articles, reviews and short communications on actual problems of modern biosystems engineering incl. crop and animal science, genetics, economics, farm- and production engineering, environmental aspects, agro-ecology, renewable energy and bioenergy etc. in the temperate regions of the world.

Copyright & Licensing:

Agronomy Research online:

Agronomy Research is available online at: https://agronomy.emu.ee/

Acknowledgement to Referees:

The Editors of *Agronomy Research* would like to thank the many scientists who gave so generously of their time and expertise to referee papers submitted to the Journal.

Abstracted and indexed:

SCOPUS, EBSCO, DOAJ, CABI Full Paper and Clarivate Analytics database: (Zoological Records, Biological Abstracts and Biosis Previews, AGRIS, ISPI, CAB Abstracts, AGRICOLA (NAL; USA), VINITI, INIST-PASCAL.)

Subscription information:

Institute of Technology, EMU
Fr.R. Kreutzwaldi 56,
51006 Tartu,
ESTONIA
e-mail: timo.kikas@emu.ee

Journal Policies:

Estonian University of Life Sciences, Latvia University of Life Sciences and Technologies, Vytautas Magnus University Agriculture Academy, Lithuanian Research Centre for Agriculture and Forestry, and Editors of *Agronomy Research* assume no responsibility for views, statements and opinions expressed by contributors. Any reference to a pesticide, fertiliser, cultivar or other commercial or proprietary product does not constitute a recommendation or an endorsement of its use by the author(s), their institution or any person connected with preparation, publication or distribution of this Journal.

ISSN 1406-894X

CONTENTS

Agronomy Research **22**(S3), 1380–1404, 2024
https://doi.org/10.15159/AR.24.101

A simulation study on the comparison of Diagnosis and Recommendation Integrated System (DRIS), Modified-DRIS (M-DRIS), and Compositional Nutrient Diagnosis (CND) for pineapple nutrient diagnosis

E.C. Agbangba[1,2,*], F. Yalinkpon[1], E.L. Sossa[3], E. Ehnon Gongnet[1] and R. Glèlè Kakaï[1]

[1]Laboratoire de Biomathématiques et d'Estimations Forestières (LABEF), Faculté des Sciences Agronomiques, Université d'Abomey-Calavi, 04 BP 1525, Cotonou, Bénin
[2]Laboratoire de Recherche en Biologie Appliquée (LaRBA), Département de Génie de l'Environnement, Université d'Abomey-Calavi, 01 BP 2009 Cotonou, Bénin
[3]Laboratoire d'Enseignement des Sciences et Techniques de Production Végétale, Faculté des Sciences Agronomiques, Université d'Abomey-Calavi, 03 BP 2819 RP. Cotonou, Bénin
[*]Correspondence: agbangbacodjoemile@gmail.com

Received: May 21st, 2024; Accepted: September 19th, 2024; Published: November 19th, 2024

Abstract. Foliar diagnostic helps assess plant nutritional status and drives appropriate fertilizer recommendations to enhance quality and productivity of plants. Several foliar diagnostic methods are used but the literature is not sufficiently documented regarding the comparison of these methods using a varied range of comparison criteria. This study compared DRIS (Diagnosis and Recommendation Integrated System), M-DRIS (Modified-DRIS), and CND (Compositional Nutrient Diagnosis) in diagnosing pineapple leaf nutrient levels with varying sample sizes. Empirical data from a subtractive experiment was used to simulate and constitute a new database considering that nutrient contents were normally distributed. For each sample size, data were generated per treatment and replicated 3,000 times. DRIS, M-DRIS, and CND indices were computed from the simulated data for each nutrient. The methods were subsequently evaluated based on four criteria: (i) the Diagnosis Concordance Frequency, which assesses the consistency of diagnoses across different methods for determining nutritional indices; (ii) the sensitivity, or True Positive Rate, which gauges a model's ability to accurately identify a specific nutritional status when it is present; (iii) the precision, or Positive Predictive Value, which indicates the proportion of correctly identified diagnoses for a particular nutritional status relative to the total number of diagnoses made for that status; and (iv) the accuracy, which measures the closeness of the model's results to the true value. As results, we found that N, P, and K nutrient indices differed significantly between DRIS, M-DRIS, and CND models and with sample size. The nutritional diagnosis methods were also discordant, except DRIS versus M-DRIS (mean agreement = 66%). Compared to DRIS, and M-DRIS models, CND appeared to be the most sensitive and accurate model (average accuracy of 27.86%) for nutrient deficiency and excess diagnosis. The models' accuracy varies with the sample size, but it becomes almost unchangeable from a sample size of 330. For all sample sizes, the CND model was more accurate and efficient for N, P, and K nutrient status diagnosis, compared to DRIS and M-DRIS models.

Key words: accuracy, foliar analysis, true positive rate, precision, *Ananas comosus*.

Used abbreviations:

A: Concentration of nutrient A in the high-yielding subpopulation
AIC: Akaike Information Criterion
B: Concentration of nutrient B in the high-yielding subpopulation
CND: Compositional Nutrient Diagnosis
CV: Coefficient of Variation
DCF: Diagnosis Concordance Frequency
DRIS: Diagnosis and Recommendation Integrated System
f: DRIS function
FNA: False Negative Adequate
FND: False Negative Deficiency
FNE: False Negative Excess
FPA: False Positive Adequate
FPD: False Positive Deficiency
FPE: False Positive Excess
PFR: Potential Fertilization Response
G: Geometric mean
IA: Model Index of nutrient A
K: Potassium
LN: CND index for nutrient N
M-DRIS: Modified Diagnosis and Recommendation Integrated System
N: Azote
n: primary limiting by excess
NBIm: Nutrient Balance Index Mean
Nut: Nutrient
nz: negative or zero with lower probability
P: Phosphore
p: primary limiting by deficiency
PERMANOVA: Permutational multivariate analysis of variance
PFR: Potential Fertilization Response
PPV: Positive Predictive Value
PPAV: Positive Predictive Adequate Value
PPDV: Positive Predictive Deficiency Value
PPEV: Positive Predictive Excess Value
pz: positive or zero with lower probability
R: Residual value
RMSE: Root Mean Square Error
SD: Standard deviation
t ha^{-1}: Tonne per hectar
TPA: True Positive Adequate
TPAR: True Positive Adequate Rate
TPD: True Positive Deficiency
TPDR: True Positive Deficiency Rate
TPE: True Positive Excess
TPER: True Positive Excess Rate
TPR: True Positive Rate
VN: CND row-centred log ratio for nutrient N

INTRODUCTION

The diagnosis of the nutritional status of plants is a prerequisite for any rational fertilization. Nutrient balance determines crop yield and quality (Pineda-Álvarez et al., 2021). Foliar diagnosis can be a useful tool for correcting plant nutrient deficiencies and imbalances (Baldock & Schulte, 1996), optimizing crop production (Walworth & Sumner, 1988), and evaluating fertilizer requirements. A thorough diagnostic is essential to create appropriate fertilizer recommendations and enhance quality and productivity without negatively impacting the environment (Pacheco-Sangerman et al., 2022). However, foliar analysis can only help assess plant nutritional status if adequate methodologies for diagnosing from analytical data are available (Walworth & Sumner, 1988). Critical Levels and Sufficiency Ranges methods are commonly used to diagnose nutritional status of plants (Walworth & Sumner, 1988). Sufficiency Ranges methods have been used to investigate the nutrient status of different tomato cultivars grown under industrial greenhouse production (Osvalde et al., 2021) and to access the nutrient status of the American cranberry in Latvia (Karlsons & Osvalde, 2017). These methods involve comparing the nutrient concentration in the sample with an accepted normal value for a specific growth stage (Kania Kuhl & Callejas Rodríguez, 2011), are somewhat erroneous in that 'critical nutrient concentrations' are not independent diagnostics, but can vary in magnitude as the background concentrations of other nutrients increase or decrease in crop tissue (Bailey et al., 1997). Since nutrient uptake and distribution are affected by interactions within the plant, multi-nutrient approaches have been derived. Three common approaches used to identify nutritional imbalances are the DRIS (Beaufils, 1973), the M-DRIS (Hallmark et al., 1987), and the CND (Parent & Dafir, 1992).

DRIS is based on dual ratio functions (f(N/P), f(P/K), etc.) (DRIS, Beaufils, 1973). M-DRIS also considers nutrient contents, not just their dual relationships (Hallmark et al., 1987). CND is based on row-centred log ratios where each nutrient is adjusted to the geometric mean of all nutrients and a filling value (Parent & Dafir, 1992). These methods of nutritional diagnosis present discordant reports.

The effectiveness of the CND method compared to other methods is not often proven in the literature. Politi et al. (2013) discovered that both the CND and DRIS approaches performed comparably while analyzing the nutritional status of mango in Lower-middle San Francisco. When determining the nutritional status of sugarcane in Brazil, the CND diagnosis differed from the DRIS techniques for manganese and nitrogen (Calheiros et al., 2018). DRIS and CND methods were found similar for the evaluation of leaf nutrients in soybean in Brazil (Souza et al., 2023). The CND method was proven to be more sensitive for early detection of Zn stress in Muscat grapes compared to DRIS (Kumar et al., 2003). DRIS and/or CND have been used to diagnose the nutrient status of a range of crops including pineapple, maize, tomatoes, cotton, orange etc. (Parent et al., 1993; Magallanes-Quintanar et al., 2006; Camacho et al., 2012; Serra et al., 2016; López-Montoya et al., 2018; Morais et al., 2019; Khuong et al., 2024). The comparison of the three diagnosis methods (DRIS, M-DRIS and CND), primarily relies on the criterion of diagnosis concordance frequency (Silva et al., 2004). Since the development of the CND method, no study has compared all the existing methods (DRIS, M-DRIS and CND) based on a set of solid criteria such as the diagnosis

concordance frequency (DCF) (Silva et al., 2004), the sensitivity or rate of true positives, the precision or Positive predictive value (Trevethan, 2017) and accuracy (Morais et al., 2019; Powers, 2020; Chicco & Jurman, 2020; Tharwat, 2020).

Indeed, sensitivity or True Positive Rate (TPR) represents the proportion in which a nutritional status is identified for a nutrient when this situation is true. Sensitivity refers to a model's ability to correctly detect nutritional status when true. It refers to the efficiency of the method to correctly diagnose the cases of a true nutritional status. Precision or Positive Predictive Value (PPV) represents the proportion of correctly detected nutritional statuses relative to the total number of diagnosed cases. It reflects the performance of the prediction. The accuracy is the proximity of the model execution output to the true value. It is the ratio between the correctly detected diagnoses to the total number of diagnoses results. Furthermore, the size of the database used for the development of diagnostic methods can have an impact on the precision of the result. The scientific literature reports a wide variation in the size of the database for setting DRIS standards, from as few as 24 observations (Leite, 1993) to approximately 2,800 (Sumner, 1977) or more. In this study, we hypothesize that as CND is a multivariate method involving all nutrients, it performs better over DRIS and M-DRIS in nutrient diagnosis as a function of database size considering all solid comparison criteria (CDF, Sensitivity, PPV, and Accuracy). In this study, we are interested in the comparison of the three diagnostic methods using the major plant nutrients which are nitrogen, phosphorus and potassium. Indeed, nitrogen is the most prevalent nutrient that plants need and is a key factor in determining plant growth (Prinsi & Espen, 2015). According to Nguyen et al. (2015), this nutrient is a crucial part of cellular macromolecules like proteins, nucleic acids, chlorophyll, and plant growth regulators. Phosphorus is one of the vital macronutrients needed for the synthesis of nucleic acid, the stability and building of membranes, the metabolism of energy, and many other vital physiological and biological activities during plant growth and development (Hasan et al., 2016). Critical processes including enzyme activation, osmotic adjustment, turgor generation, cell division, membrane electric potential modulation, and pH homeostasis are all facilitated by potassium (Ragel et al., 2019). Nitrogen (N), phosphorus (P), and potassium (K) are critical macronutrients required for pineapple growth and development throughout its production cycle. Potassium is extracted in the highest amounts by the plant, and enhancing fruit weight and quality (Carr, 2012; Silva et al., 2018). Adequate potassium supply is strongly associated with improved fruit sweetness, size, and resistance to diseases (Teixeira et al., 2020). Phosphorus, often the third most required nutrient, supports root development and early plant establishment, which are important for maximizing yield potential (Roy et al., 2018). Together, these nutrients are critical for optimizing pineapple productivity and ensuring high-quality fruit production. Apart from macronutrients, certain micronutrients such as boron are essential for the full development of pineapple. Indeed, pineapple needs boron for optimal growth. Boron deficiency causes orange and yellow leaf discoloration, minimal growth, and curling. It also leads to chlorosis with red margins, multiple crowned fruits, and necrotic tissue, sometimes resulting in small spherical fruits (Py et al., 1984; Souza & Reinhardt, 2007). Therefore, this study aimed to compare DRIS, M-DRIS , and CND in diagnosing pineapple leaf nutrient levels with varying sample sizes. In this study, we used data from

the pineapple subtractive trial of Angeles et al. (1990) to generate artificial data to compare the diagnostic methods. This database was used as it includes subtractive treatments that can provide all the possible outcomes of a nutritional diagnosis: nutrient deficiencies, balances or excesses.

MATERIALS AND METHODS

Data used

We used empirical data from a subtractive experiment in N, P, and K nutrients for pineapple. These data came from the study of Angeles et al. (1990), who used a size of 1185 leaf nutrients and yield database to create DRIS norms for pineapple. They are published data sets from trials including 14 treatment combinations in which yield responses to nutrients N, P, and K were determined. In this study, five (05) treatments including 0N-0P-0K, 2N-0P-0K, 0N-1P-1K, 1N-2P-0K, and 2N-2P-2K, were chosen and used based on the subtractive nutrients. They are treatments where certain nutrients are omitted, treatments with a single dose for specific nutrients, and treatments with double doses for some nutrients. These treatments were selected to ensure adequate representation of deficiency, adequacy, and excess nutrient conditions that we aim to evaluate in our research. These 5 treatments were specifically chosen to cover a full range of responses to N, P, and K nutrients, as documented in the empirical database of the subtractive trial used. These empirical data included: treatment, mean fruit yield (response variable), and pineapple (variety smooth cayenne) foliar mineral nutrients (explanatory variables) Nitrogen (N), Phosphorus (P), and Potassium (K) contents mean and standard deviation. This dataset allowed us to evaluate the ability of DRIS, M-DRIS, and CND models to accurately detect nutrient deficiencies, balances, or excesses under these different nutrient limiting conditions.

Simulation design

The simulation was realized in four main steps: identification of probable linear or non-linear regression, generation of data, model index computation, and model comparison criteria computation.

Step 1: Identification of probable linear or non-linear regression

The variable under investigation is the pineapple fruit yield (t ha^{-1}), a continuous quantitative variable. The relationship between the dependent variable (yield) and the independent variables (N, P, and K nutrients that are continuous quantitative variables) was examined using ten models, including linear and three common non-linear models (inverse, quadratic, and logarithm). Akaike Information Criterion (AIC, Narisetty (2020)), adjusted coefficient of determination (adjusted R^2), and Root Mean Squared Error (RMSE, Nayanaka et al. (2010)) were used to test and compare these models. The AIC is given by:

$$AIC = -2 * log(likelihood\ value\ from\ the\ model) + 2 * k \quad (1)$$

where k represents the model's number of parameters.

The Root Mean Squared Error was computed as follow:

$$RMSE = \sqrt{\frac{1}{n}\left(\sum_{i=1}^{n}[Z(x_i) - Z^*(x_i)]^2\right)} \quad (2)$$

where n is the sample size, is $Z^*(x_i)$ the predicted value and $Z(x_i)$ is the observed value (Javari, 2017).

Step 2: Generation of data

The response variable (Yield) was generated using Eq. (23). The nutrient concentrations related to pineapple fruit yield have been set to follow the normal distribution with parameters presented in Table 1 (Angeles et al., 1990). Nutrient data were simulated and yield was calculated accordingly for each treatment and varied sample size to ensure an extensive dataset that meets our study conditions including having treatments where certain nutrients are omitted, treatments with a single dose for specific nutrients, and treatments with double doses for some nutrients. Data size was varied to account for the effect of this factor on the performance of the models. Ten different sample sizes (30, 70, 80, 100, 210, 270, 330, 490, 630, and 860) were randomly selected from a generated sequence of sizes ranging from 10 to 1,000 by 10 using the seq() and sample() functions in R software. For each sample size and per treatment, the simulation was replicated 3,000 times (Hoad et al., 2007). The data was generated using the R software version 4.1.3 (R Core Team, 2021).

Table 1. Parameters used for data generation

Treatment			Mean concentration (%)			Standard deviation (%)			Fruit yield
N	P	K	N	P	K	N	P	K	(t ha^{-1})
0	0	0	0.97	0.47	0.64	0.4	0.52	1.32	42.7
2	0	2	2.14	0.36	3.95	0.21	0.16	0.26	131
0	1	1	0.67	0.54	3.29	0.27	0.46	0.38	55.5
1	2	0	0.8	0.56	3.38	1.2	0.37	0.7	62.5
2	2	2	1.8	0.32	2.64	0.34	0.23	0.41	134

The first three columns refer to the fertilization treatments used in the original database; 0: a specific nutrient is omitted; 1: a single dose for a specific nutrient; 2: double doses for a specific nutrient. Source: Angeles et al. (1990)

Step 3: Model index computation

The nutritional status was evaluated using the DRIS and M-DRIS (Beaufils, 1973) methodologies, taking into account all forms of nutrient ratios (direct and inverse). Additionally, the CND approach, as described by Parent & Dafir (1992), was used for the diagnosis. The yield population was separated into two subpopulations of yields using the average yield added to half of the standard deviation (mean + 0.5*Standard deviation) as a subdivision criterion. The high-yielding subpopulation corresponds to the yield greater than the mean plus half of the standard deviation and the low-yielding subpopulation was the yield less or equal to the mean plus half of the standard deviation (Silva et al., 2004). The high-yielding subpopulation was defined as a population of reference. DRIS and M-DRIS indices were calculated using two steps. First, for each ratio of nutrients, observations were related to norms using standardization and index

equations (Hallmark et al., 1987; Bailey et al., 1997; Agbangba et al., 2010; Calheiros et al., 2018) as shown in the examples below (Eqs (3), (4) and (5)):

$$f\left(\frac{A}{B}\right) = 100\left[\frac{\frac{A}{B}}{\frac{a}{b}} - 1\right]/CV \; if \; \left(\frac{A}{B}\right) > \left(\frac{a}{b}\right) + SD \tag{3}$$

$$f\left(\frac{A}{B}\right) = 100\left[1 - \frac{\frac{a}{b}}{\frac{A}{B}}\right]/CV \; if \; \left(\frac{A}{B}\right) < \left(\frac{a}{b}\right) - SD \tag{4}$$

$$f\left(\frac{A}{B}\right) = 0 \; if \; \left(\frac{a}{b}\right) - SD \leq \left(\frac{A}{B}\right) \leq \left(\frac{a}{b}\right) + SD \tag{5}$$

where A/B is the dual relation between the 'A' and 'B' nutrient concentrations (%) of the diagnosed population; a/b, CV and SD are respectively the mean, the coefficient of variation and the standard deviation of A/B in the high-yielding subpopulation.

Next, values from the standardization equations were used to calculate indices as shown in the examples below (Eq. 6):

$$I_A = \frac{\sum_{i=1}^{n} f\left(\frac{A}{B_i}\right) - \sum_{i=1}^{n} f\left(\frac{B_i}{A}\right)}{z} \tag{6}$$

where I_A = DRIS index of 'A'; $\sum_{i=1}^{n} f\left(\frac{A}{B_i}\right)$ = Sum of functions presenting concentration of nutrient 'A' is in the numerator; $\sum_{i=1}^{n} f\left(\frac{B_i}{A}\right)$ = Sum of functions presenting concentration of nutrient 'A' is in the denominator and z = Number of DRIS functions (f).

The M-DRIS (Hallmark et al., 1987), not only considers the interdependence between nutrients but also incorporates the nutrient concentrations in its computing. The M-DRIS is calculated using the following equations:

$$f(A) = 10\left(\frac{A - a}{SD}\right) \; if \; A > a + SD \tag{7}$$

$$f(A) = 10\left(\frac{A-a}{SD}\right)\left(\frac{a}{A}\right) \; if \; A < a - SD \tag{8}$$

$$f(A) = 0 \; if \; a - SD \leq \; A \leq a + SD \tag{9}$$

where $f(A)$ = Nutrient concentration function of ; A = Sample nutrient concentration; a = High-yielding subpopulation nutrient concentration; SD = Standard deviation of the high-yielding subpopulation nutrient concentration.

The M-DRIS index is produced for each nutrient based on the outcome of each M-DRIS function, indicating that nutrient concentration as well as nutrient ratios are considered:

$$I_A = \frac{\sum_{i=1}^{n} f\left(\frac{A}{B_i}\right) - \sum_{i=1}^{n} f\left(\frac{B_i}{A}\right) + f(A)}{z + 1} \tag{10}$$

where I_A = Nutrient 'A' M-DRIS index; $\sum_{i=1}^{n} f\left(\frac{A}{B_i}\right)$ = Addition of functions in which concentration of nutrient 'A' appears in the numerator; $\sum_{i=1}^{n} f\left(\frac{B_i}{A}\right)$ = Addition of

functions in which concentration of nutrient 'A' appears in the denominator; $f(A)$ = Nutrient concentration 'A' function and z = Number of M-DRIS functions (f).

After computing the nutrient DRIS and M-DRIS indices, the mean nutritional balance index (NBI_m) (Wadt et al., 1998) was calculated. This process involves summing the absolute values of the nutrient index for each nutrient and then dividing by the number of nutrients (d), as shown in the following equation:

$$NBI_m = \frac{1}{d}\sum_{i=1}^{d} |Indice\ A_i| \quad (11)$$

In the CND model, the full composition array for d nutrient compositions in plant tissues can be described by the following simplex S^d with $d + 1$ nutrient concentrations (d nutrients plus a filling value R) (Parent & Dafir, 1992):

$$S^d = [(N, P, K, R) : N > 0, P > O, K > 0, R > 0; N + P + K + R = 100],$$

where 100 is the concentration of dry matter (%); N, P, K are the concentrations of nutrients (%); d is the number of evaluated nutrients ; and R is the filling value (residual value) between 100 and sum of the nutrients concentrations, computed as:

$$R = 100 - (N + P + K) \quad (12)$$

A geometric mean (G) computed as (Eq. 13):

$$G = (N \times P \times K \times R)^{\frac{1}{d+1}}, \quad (13)$$

was used to derive row-centred log ratios as follows (Eq. 14):

$$V_N = ln\left(\frac{N}{G}\right), \ldots, V_R = ln\left(\frac{R}{G}\right) \quad (14)$$

and $VN + VP + VK + VR = 0$, where VN is the CND row-centred log ratio expression for nutrient N.

The row-centred log-ratios were used to calculate the CND indices, represented by $I_N, \ldots, I_R$, as per Eq. (15):

$$I_N = \frac{V_N - V_N^*}{SD_N}, \ldots, I_R = \frac{V_R - V_R^*}{SD_R} \quad (15)$$

where $V_R^*, \ldots, V_R^*$ are the means and $SD_N, \ldots, SD_R$ the standard deviations of the row-centred log-ratios in the high-yielding subpopulation (> than mean + 0.5 standard deviation) of each sample.

As for the NBIm (Wadt et al., 1998) calculated for the DRIS and M-DRIS models, this index is also computed for the CND. For each sample size and treatment combination, DRIS, M-DRIS and CND index values for N, P and K nutrients were calculated using Eqs (6), (10) and (15), respectively. Each model index was applied separately for each treatment and sample size.

Step 4: Models comparison criteria

Four (04) criteria were used to compare the models. These criteria were: the Diagnosis Concordance Frequency (Silva et al., 2004), the sensitivity or True Positive Rate, the precision or Positive Predictive Value (Trevethan, 2017) and the accuracy (Morais et al., 2019; Powers, 2020; Chicco & Jurman, 2020; Tharwat, 2020). The 3,000 replications databases per treatment and sample size were used to compare the index models. The five treatments in the database involve scenarios where specific nutrients are either omitted, applied in a single dose, or applied in a double dose. The omission of

a nutrient indicates its deficiency, a single dose represents an adequate concentration, and a double dose signifies an excess of the nutrient. Specifically, 0 means a nutrient is omitted, 1 corresponds to a single dose, and 2 indicates a double dose. The models were evaluated based on their ability to detect these three situations. For instance, if a treatment has a value of 0 for a nutrient and the model correctly identifies it as deficient, then the model has accurately detected the situation.

DCF evaluates the consistency of diagnoses between different methods of determining nutritional indices. This is crucial for ensuring the reliability of the models. It is calculated based on the Potential Fertilization Response (PFR) (Silva et al., 2004). It focuses on two situations: separating nutrients and identifying the principal limiting deficient nutrient (p) and excessive nutrient (n). The following criteria were used to evaluate the degree of agreement between the diagnoses made using the various techniques for determining the nutritional indices: (i) For a nutrient, if the diagnosis (deficiency, adequate and excess, or p and n) was the same between two distinct methods, it was considered concordant; (ii) If two methods produce different diagnoses for the same nutrient, the diagnosis is considered non-concordant. The concordance rate is then calculated for all evaluated methods, providing an indicator of the consistency of different diagnoses. A high DCF indicates strong agreement between models in identifying nutrient status.

TPR: measures a model's ability to correctly identify a particular nutritional status when that status is indeed present. It refers to the efficiency of the method at correctly diagnosing the cases of a true nutritional status. This criterion includes three subcategories including the True Positive Deficiency Rate (TPDR), True Positive Adequate Rate (TPAR), and True Positive Excess Rate (TPER) that were computed for the nutritional deficiency, adequate, and excess, respectively. A high TPR for a specific nutritional status indicates that the model is able to identify this status. Indeed, TPDR is the proportion of deficiency diagnosed by a model when the nutrient is deficient, and is calculated by:

$$TPDR = \frac{TPD}{TPD + FND} = \frac{TPD}{TPD + FNA|D + FNE|D} \quad (16)$$

where TPD = True Positive Deficiency = [Deficient nutrient correctly identified as deficient]; FND = False Negative Deficiency = [Deficient nutrient incorrectly identified as excessive or adequate]; FNA|D = [Deficient nutrient incorrectly identified as adequate] and FNE|D = [Deficient nutrient incorrectly identified as excessive].

TPAR is the proportion of adequate diagnosed by a model when the nutrient is adequate, and is calculated by:

$$TPAR = \frac{TPA}{TPA + FNA} = \frac{TPA}{TPA + FND|A + FNE|A} \quad (17)$$

where TPA = True Positive Adequate = [Adequate nutrient correctly identified as adequate]; FNA = False Negative Adequate = [Adequate nutrient incorrectly identified as deficient or excessive]; FND|A = [Adequate nutrient incorrectly identified as deficient] and FNE|A = [Adequate nutrient incorrectly identified as excessive].

TPER is the proportion of excess diagnosed by a model when the nutrient is excessive, and is calculated by:

$$TPER = \frac{TPE}{TPE+FNE} = \frac{TPE}{TPE+FND|E+FNA|E}$$
$$TPER = \frac{TPE}{TPE + FNE} = \frac{TPE}{TPE + FND|E + FNA|E} \quad (18)$$

where TPE = True Positive Excess = [Excessive nutrient correctly identified as excessive]; FNE = False Negative Excess = [Excessive nutrient incorrectly identified as deficient or adequate]; FND|E = [Excessive nutrient incorrectly identified as deficient] and FNA|E = [Excessive nutrient incorrectly identified as adequate].

PPV: represents the proportion of correctly detected diagnoses of a particular nutritional status to the total number of diagnosed cases of that status. This criterion reflects the model's prediction performance. A high PPV for a specific nutrient status indicates diagnosis for that status are reliable. There are three subcategories: Positive Predictive Deficiency Value (PPDV), Positive Predictive Adequate Value (PPAV), and Positive Predictive Excess Value (PPEV). Indeed, PPDV is the proportion of deficiency that was correctly identified to the total number of deficient cases diagnosed. It is given by:

$$PPDV = \frac{TPD}{TPD + FPD} \quad (19)$$

where TPD = [Deficient nutrient correctly identified as deficient] and FPD = False Positive Deficiency = [Adequate or excessive nutrient incorrectly identified as deficient].

PPAV is the proportion of adequacy that was correctly identified to the total number of adequate cases diagnosed, and is given by:

$$PPAV = \frac{TPA}{TPA + FPA} \quad (20)$$

where TPA = [Adequate nutrient correctly identified as adequate] and FPA = False Positive Adequate = [Deficient or excessive nutrient incorrectly identified as adequate].

PPEV is the proportion of excess that was correctly diagnosed to the total number of excessive cases diagnosed, and is given by:

$$PPEV = \frac{TPE}{TPE + FPE} \quad (21)$$

where TPE = [Excessive nutrient correctly identified as excessive] and FPE = False Positive Excess = [Deficient or adequate nutrient incorrectly identified as excessive].

Accuracy: measures how close the model's results are to the true value. It is the ratio of correctly detected diagnoses to the total number of diagnosis results. Accuracy provides an overall view of the model performance. A high accuracy indicates the model performs well overall in identifying nutrient deficiencies, adequate levels, and excesses.

$$Accuracy = \frac{TPD + TPA + TPE}{TPD + TPA + TPE + FND + FNA + FNE} \quad (22)$$

where TPD = True Positive Deficiency, TPA = True Positive Adequacy, TPE = True Positive Excess, FND = False Negative Deficiency, FNA = False Negative Adequacy, and FNE = False Negative Excess.

In summary, these performance criteria provide a comprehensive picture of how well models can diagnose plant nutrient status. DCF assesses agreement between models, while TPR and PPV evaluate a model's ability to correctly identify true nutrient deficiencies, adequate levels, and excesses.

Data analysis

The fruit yield population was separated into high and low subpopulation data arrays based on the confidence interval method proposed by Silva et al. (2004). Descriptive statistics were calculated for pineapple fruit yield, leaf nutrient concentrations, nutrient ratios, and row-centred log ratio expression data (Eq. 15) using R software version 4.1.3 (R Core Team, 2021). Descriptive statistics included, means, standard deviations, CVs, skewness, and kurtosis values, where a skewness value of zero indicates perfect symmetry, and values greater than 1 indicate marked asymmetry. We computed DRIS (Eq. 6), M-DRIS (Eq. 10), and CND (Eq. 15) index values per treatment based on the index function and the row-centred log-ratios for the high-yielding subpopulation. The more negative is the index value for a nutrient, the more limiting is that nutrient. The mean nutrient balance index (NBIm) was also computed for each model. The mean indices of the three models for each nutrient and the NBIm were plotted against the sample size using plot() function from the base stats package in R software. They were plotted to see the trends for the distribution of N, P, and K indices and NBIm for the different models.

A permutational multivariate analysis of variance (PERMANOVA) test ($p < 0.05$) was performed on the nutrient indices using Euclidean method (Anderson, 2001) under the null hypothesis that there is no difference between these indices for DRIS, M-DRIS, and CND models with 0.05 significance level. Model and treatment were considered as factors. We calculated also the percentages of agreement between the models, the sensitivity (Eqs (16), (17) and (18)), precision (Eqs (19), (20) and (21)) and accuracy (Eq. 22) for each model and by sample size that were used to compare model performance. Performance criteria values including sensitivity, precision, and accuracy of each model were then averaged and plotted against the sample size using function plot from the base stats package in R software. All the computations and plots were done using R software version 4.1.3.

Interpretation of DRIS, M-DRIS, and CND indices

The nutrient index and the NBIm were used to interpret the diagnosis made by DRIS, M-DRIS, and CND (Wadt, 2005). Using this method, each nutrient's DRIS, M-DRIS, and CND index modules are compared with the NBIm. According to Wadt et al. (1998), the technique determines if the imbalance ascribed to a particular nutrient is larger or smaller than the imbalance given to the average of all nutrients. The method has the advantage of detecting even excess nutrients. According to this author, for a nutrient *Nut*, the following conclusions could be drawn:

$$Deficiency = INut < 0 \; and \; |INut| > NBIm$$

$$Adequate = |INut| \leq NBIm$$

$$Excess = INut > 0 \; and \; |INut| > NBIm$$

The DRIS, M-DRIS, and CND indices (Table 2) were interpreted using the theory of potential fertilization response (PFR) (Wadt et al., 1998). The nutrients of the high-productivity subpopulation were classified according to the potential fertilization response as follows: zero (z), positive (p), negative (n), positive or zero (pz), and negative or zero (nz).

Table 2. Criteria for interpreting DRIS, M-DRIS, and CND indices based on PFR

Nutritional state	Criteria	Potential response fertilization
Deficient and limiting	INut < 0 |INut| > NBIm INut is lower index value	Positive, with higher probability (p)
Probably deficient	INut < 0 |INut| > NBIm	Positive or zero, with lower probability (pz)
Adequate	|INut| ≤ NBIm	zero (z)
Probably excessive	INut > 0 |INut| > NBIm	Negative or zero, with lower probability (nz)
Excessive	INut > 0 |INut| > NBIm INut is higher index value	Negative, with higher probability (n)

PFR= Potential Fertilization Response, NBIm = nutrient balance index mean and INut = DRIS, M-DRIS or CND index nutrient. Source: Calheiros et al. (2018).

The flow chart (Fig. 1) below presents the different steps of this study.

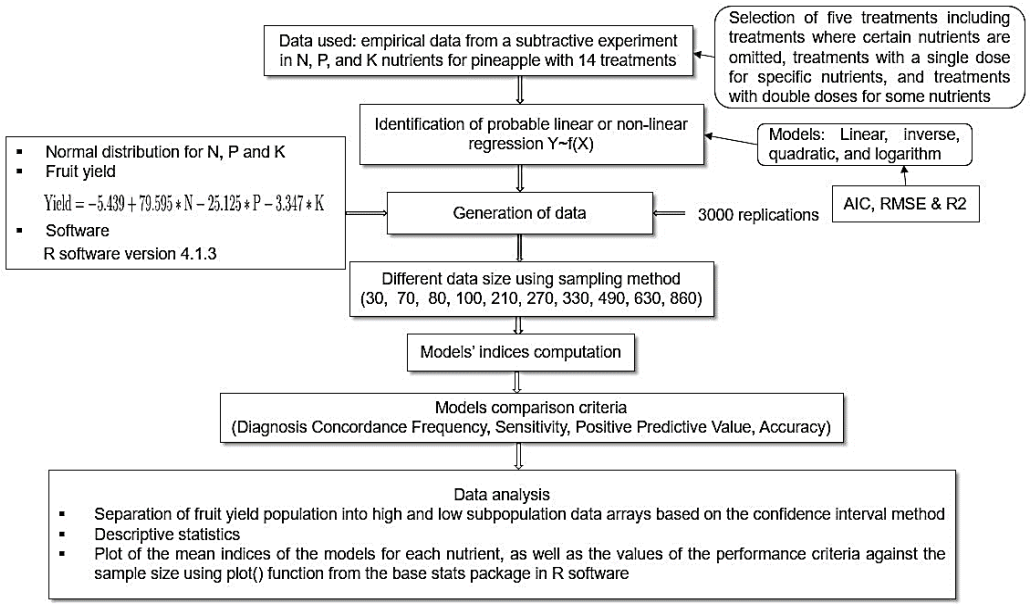

Figure 1. Research scheme.

RESULTS AND DISCUSSION

Relationship between yield and nutrients

Among the 10 regression models performed to identify the relationship between yield and nutrients, the multiple linear regression model has the lowest AIC (210.39) and RMSE (15.73) values, as well as the highest R^2 (78.01; Table 3). Therefore, it is considered the best model, and its equation is as follows:

$$Yield = -5.44 + 79.6 * N - 25.13 * P - 3.35 * K \quad (23)$$

This equation was then used to generate the yields corresponding to the nutrient levels, in keeping the linear functional link between the data.

Table 3. Linear and non linear equation to yield on the explanatory variables

Model	Equation	AIC	R^2 (%)	RMSE
Multiple linear regression	Yield = e +a*N + b*P + c*K	210.39	78.01	15.73
Logarithm transformation	Yield = e +a*log(N) + b*log(P) + c*log(K)	214.12	74.3	17.01
Inverse	Yield = e +a*(1/N) + b*(1/P) + c*(1/K)	244.09	52.85	35.98
Quadratic of N	Yield = e +a*N^2 + b*P + c*K	227.16	61.07	18.86
Quadratic of P	Yield = e +a*N + b*P^2 + c*K	241.2	60.28	28.98
Quadratic of K	Yield = e +a*N + b*P + c*K^2	225.04	63.53	20.35
Quadratic of N and P	Yield = e +a*N^2 + b*P^2 + c*K	219.45	64.12	18.25
Quadratic of N and K	Yield = e +a*N^2 + b*P + c*K^2	222.23	63.55	20.22
Quadratic of P and K	Yield = e +a*N + b*P^2 + c*K^2	235.1	60.05	28.43
Quadratic of N, P and K	Yield = e +a*N^2 + b*P^2 + c*K^2	228.64	61.75	19.62

AIC = Akaike Information Criterion; R^2: Coefficient of determination; RMSE = Root Mean Square Error; e = the intercept or constant term; a = the regression coefficient for N; b = the regression coefficient for P; c = the regression coefficient for K.

Binary nutrients ratio and row-centred log ratio statistics

Binary nutrient ratio combinations and row-centred log ratios of all three nutrients were calculated for the different sample sizes, and summary statistics were evaluated for each of the resulting nutrient ratio expressions (Table 4). We noticed that the values of the dual relations and the multi-nutrient variables with the means differed for the high-productivity subpopulation. The DRIS and M-DRIS norms, i.e. means and CVs of the nutrient ratios, for high-yielding subpopulations were presented in Table 4.

Indeed, a total of six (06) nutrient ratios were established and used to determine the DRIS and M-DRIS standards. These ratios were N/P, N/K, P/K, P/N, K/N, K/P. Considering the different sample sizes, except 30, the ratio P/N had the lowest average ratio and K/P had the highest for the control treatment (Table 4). For the treatments 2N-0P-2K, 1N-2P-0K, and 2N-2P-2K, the ratios of P/K had the lowest standard deviation, while the ratios of K/P had the highest standard deviation. On the other hand, for treatment 0N-1P-1K, the nutrient ratios of N/K had the lowest standard deviation, whereas the ratios of K/P had the highest standard deviation. These values were computed using CVs and $\overline{X}$, and were presented in Table 3. The means, standard deviation (SD), and CV (%) of ratios for high-yielding subpopulations were computed for the DRIS and M-DRIS norms. These norms were used to calculate nutrient indices of DRIS and M-DRIS and the Mean Nutrient Balance Indices.

The CND norms, i.e. means and CVs, of row-centred log ratios of N, P, and K, for the high yielding- subpopulation were presented in Table 4. N and P nutrients had the lowest and highest standard deviations, respectively, with regard to the CND criteria for all sample sizes and the control treatment. For K nutrient, the standard deviation was 0.83% (computed using $\overline{X}$ and CV; Table 4).

Table 4. Mean ($\bar{X}$) and coefficient of variation (CV) of the N, P, and K dual relations, and the CND variables in pineapple, subpopulation of high productivity. T1 = 0N-0P-0K, T2 = 2N-0P-2K, T3 = 0N-1P-1K, T4 = 1N-2P-0K, T5 = 2N-2P-2K 3

Treatment	Variable	N = 30		N = 70		N = 80		N = 100		N = 210		N = 270		N = 330		N = 490		N = 630		N = 860	
T1		$\bar{X}$ (%)	CV (%)	$\bar{X}$ (%)	CV (%)	$\bar{X}$ (%)	CV (%)	$\bar{X}$ (%)	CV (%)	$\bar{X}$ (%)	CV (%)	$\bar{X}$ (%)	CV (%)	$\bar{X}$ (%)	CV (%)	$\bar{X}$ (%)	CV (%)	$\bar{X}$ (%)	CV (%)	$\bar{X}$ (%)	CV (%)
	N/P	15.37	3,126.18	11.35	1,758.45	11.95	3,490.88	13.87	5,212.54	12.22	388.06	10.70	2,238.14	11.62	3,497.12	11.69	4,020.45	18.53	1,7751.22	14.14	1,0689.08
	N/K	4.98	1,690.33	5.74	2,261.84	5.90	3,426.84	6.99	3,298.59	5.47	145.05	8.27	9,418.30	5.32	2,242.48	6.82	4,830.60	7.09	6,515.75	6.06	4,084.55
	P/K	3.31	2,244.86	3.04	1,542.54	4.27	5,397.85	3.50	2,386.91	3.12	60.37	3.95	4,620.40	3.23	2,808.28	3.72	4,070.1	4.58	9,754.43	3.64	5,425.93
	P/N	1.45	2,965.01	1.05	758.34	1.16	1,634.93	1.04	845.66	1.25	34.03	1.28	3,754.39	1.18	1,608.89	1.54	10,641.27	1.42	5,249.52	1.26	2,650.42
	K/N	2.36	1,037.95	2.36	1,203.78	2.31	1,571.24	2.20	1,080.42	2.5	55.54	2.68	3,694.32	2.44	1,898.23	2.51	3,603.57	2.71	5,422.62	2.57	2,566.6
	K/P	18.45	3,534.8	14.35	2,859.62	14.21	2,938.93	13.04	2,258.48	14.24	550.48	13.64	3,164.33	13.77	3,555.40	13.82	4,577.69	26.84	23,281.8	16.45	12,463.73
	G	3.07	23.15	3.07	23.08	3.06	23.24	3.07	23.21	3.06	23.11	3.07	23.24	3.06	23.24	3.07	23.26	3.06	23.22	3.06	23.28
	Log (N/G)	-1.24	52.23	-1.24	-52.23	-1.24	-52.47	-1.23	-52.45	-1.23	-52.85	-1.24	-52.57	-1.23	-52.75	-1.23	-52.33	-1.24	-52.61	-1.24	-52.71
	Log (P/G)	-2.01	-55.20	-2.01	-55.20	-2.004	-54.63	-2.02	-54.82	-2.01	-54.69	-2.02	-55.002	-2.02	-54.71	-2.02	-54.94	-2.02	-55.16	-2.02	-54.93
	Log (K/G)	-1.32	-62.39	-1.32	-62.39	-1.33	-62.19	-1.33	-62.67	-1.33	-62.13	-1.33	-62.62	-1.33	-62.36	-1.33	-62.64	-1.33	-62.55	-1.33	-62.55
T2	N/P	15.03	1,724.80	15.36	2,259.69	20.11	6,309.45	12.55	1,033.16	26.13	15,606.77	14.35	2,330.56	150.6	35,245.83	15.71	3,514.99	14.41	2,598.88	17.53	8,389.27
	N/K	0.54	11.87	0.54	11.85	0.54	11.83	0.54	11.83	0.54	11.92	0.54	11.89	0.54	11.87	0.54	11.89	0.54	11.86	0.54	11.91
	P/K	0.09	43.99	0.09	44.13	0.09	43.96	0.09	43.93	0.09	44.08	0.09	44.10	0.09	44.08	0.09	43.99	0.09	44.05	0.09	43.97
	P/N	0.17	44.49	0.17	44.95	0.17	44.79	0.17	44.75	0.17	44.86	0.17	44.84	0.17	44.78	0.17	44.80	0.17	44.81	0.7	44.71
	K/N	1.86	12.06	1.86	12.02	1.86	12.03	1.86	12.04	1.86	12.13	1.86	12.08	1.86	12.08	1.86	12.09	1.86	12.07	1.86	12.11
	K/P	27.84	1,662.23	28.02	2,115.26	36.39	6,067.38	22.90	968.54	47.6	15,312.52	26.44	2,377.52	310.83	35,474.45	28.94	3,340.91	26.92	2,748.18	32.27	7,900.48
	G	4.41	1.57	4.41	1.58	4.21	1.59	4.41	1.58	4.41	1.59	4.40	1.59	4.41	1.59	4.40	1.59	4.41	1.59	4.41	1.58
	Log (N/G)	-0.73	-13.76	-0.73	0.1	-0.73	-13.78	-0.72	-13.77	-0.73	-13.86	-0.72	-13.82	-0.73	-13.78	-0.73	-13.82	-0.73	-0.73	-0.73	-13.84
	Log (P/G)	-2.65	-24.91	-2.64	-24.91	-2.64	-24.66	-2.64	-24.6	-2.65	-24.72	-2.64	-24.73	-2.65	-24.81	-2.64	-24.73	-2.64	-2.64	-2.64	-24.59
	Log (K/G)	-0.11	-44.62	-0.11	-44.63	-0.11	-44.87	-0.11	-44.51	-0.11	-44.7	-0.11	-44.92	-0.12	-44.73	-0.11	-44.74	-0.11	-0.11	-0.11	-44.68

Table 4 (continued)

T3	N/P	6.19	1,650.93	5.38	1,452.75	5.46	1,660.36	7.55	4,206.58	11.4	12,837.01	7.18	3,725.06	7.79	6,289.36	6.67	4,211.49	12.83	18,240.64	17.79	32,345.07
	N/K	0.2	41.91	0.21	41.8	0.21	41.72	0.21	41.76	0.2	41.72	0.21	41.74	0.21	41.82	0.21	41.96	0.21	41.77	0.21	41.93
	P/K	0.18	66.92	0.18	66.48	0.18	66.72	0.18	66.91	0.18	66.78	0.18	66.48	0.18	66.88	0.18	66.66	0.18	66.64	0.18	66.62
	P/N	1.47	587.16	2.59	5,853.87	4.26	12,386.18	1.73	2,742.32	1.66	2,071.21	1.93	2,716.81	1.66	2,142.14	1.7	2,416.8	1.99	5,442.97	3.42	33,140.85
	K/N	8.94	905.35	15.02	6,296.99	20.62	11,248.19	9.75	2,272.68	8.94	1,551.59	10.81	2,761.16	9.91	3,781.15	9.68	2,363.47	10.84	6,261.52	20.05	32,399.43
	K/P	31.13	1,725.96	26.64	1,396.35	28.13	1,555.03	34.04	3,137.97	44.41	7,851.88	33.87	3,194.79	36.58	5,137.91	33.44	3,780.51	57.78	14,136.23	68.42	25,110.33
	G	4.22	2.83	4.21	2.83	4.22	2.83	4.21	2.82	4.21	2.82	4.22	2.83	4.22	2.82	4.21	2.83	4.22	23.23	4.22	23.28
	Log (N/G)	-1.96	-29.7	-1.96	-29.7	-1.95	-29.45	-1.94	-29.07	-1.94	-29.04	-1.95	-29.36	-1.68	-29.22	-1.95	-29.38	-1.95	-29.32	-1.95	-29.19
	Log (P/G)	-2.29	-44.52	-2.29	-44.53	-2.29	-44.39	-2.30	-44.5	-2.3	-44.61	-2.29	-44.55	-2.3	-44.82	-2.29	-44.51	-2.3	-44.68	-2.29	-44.62
	Log (K/G)	-0.25	-35.07	-0.25	-35.07	-0.25	-35.17	-0.25	-35.02	-0.25	-34.93	-0.25	-35.03	-0.25	-34.94	-0.25	-34.97	-0.25	-34.97	-0.25	-34.95
T4	N/P	18.3	6,675.43	12.81	3,452.28	6.53	672.48	14.5	3,432.38	9.37	2,480.93	31.8	21,885.95	9.46	2,304.91	11.35	5,284.76	41.48	41,737.89	11.24	5,462.52
	N/K	0.35	79.06	0.36	79.8	0.36	80.47	0.36	79.77	0.36	79.2	0.36	79.31	0.36	79.71	0.36	79.76	0.36	80.91	0.36	79.94
	P/K	0.18	64.2	0.18	64.5	0.18	65.21	0.18	64.2	0.18	64.4	0.18	64.68	0.18	64.67	0.18	64.71	0.18	65.93	0.18	64.63
	P/N	2.61	977.89	3.50	2,290.19	5.10	5,156.76	3.15	1,779.13	624.72	32,159.3	4.68	11,755.1	3.47	2,447.74	3.95	7,641.35	4.001	6,117.44	3.5	3,386.52
	K/N	15.22	930.3	21.07	2,000.73	27.13	3,702.31	18.35	1,656.8	1,631.002	31,945.30	27.35	11,299.61	19.67	2,068.73	22.83	7,715.36	26.002	6,489.78	20.96	3,166.57
	K/P	47.15	5,113.71	1.53	3,552.3	20.42	995.8	43.29	4,806.56	27.26	2,144.36	74.38	18,235.6	33.08	4,065.54	36.51	7,780.84	60.65	26,061.09	33.58	6,103.32
	G	4.23	5.18	4.23	5.27	4.24	5.25	4.23	5.22	4.23	5.21	4.23	5.23	4.23	5.24	4.23	5.26	4.23	5.23	4.23	5.22
	Log (N/G)	-1.69	-65.23	-1.69	-65.23	-1.69	-65.22	-1.69	-65.16	-1.69	-65.15	-1.68	-65.17	-1.68	-65.25	-0.26	-65.19	-1.69	-65.21	-1.69	-65.18
	Log (P/G)	-2.25	-41.09	-2.25	-41.09	-2.25	-40.70	-2.25	-41.17	-2.25	-40.98	-2.26	-41.20	-2.25	-41.09	-2.25	-41.09	-2.26	-41.05	-2.25	-41.07
	Log (K/G)	-0.24	-67.71	-0.25	-67.71	-0.24	-68.57	-0.25	-67.38	-0.24	-67.60	-0.25	-67.81	-0.25	-67.92	-1.68	-68.11	-0.25	-67.71	-0.25	-67.78
T5	N/P	24.87	1,193.63	34.85	5,748.19	29.65	4,117.35	28.72	1,896.02	29.61	2,780.58	38.87	7,120.04	27.31	2,263.61	32.94	5691.68	32.71	7,922.83	38.17	10,933.74
	N/K	0.69	25.47	0.69	25.72	0.69	25.61	0.69	25.5	0.69	25.68	0.7	25.52	0.7	25.44	0.7	25.45	0.7	25.53	0.7	25.55
	P/K	0.13	63.5	0.13	63.98	0.13	63.99	0.13	63.47	0.13	63.55	0.13	63.66	0.13	63.40	0.13	63.49	0.13	63.61	0.13	63.61
	P/N	0.19	65.43	0.19	65.82	0.19	66.12	0.19	65.13	0.19	65.37	0.20	65.63	0.19	65.39	0.19	65.36	0.2	65.43	0.2	65.56
	K/N	1.53	26.92	1.52	27.06	1.52	28.66	1.52	26.78	1.52	26.92	1.53	26.94	1.52	26.81	1.52	26.74	1.52	26.92	1.53	26.91
	K/P	37.54	1,189.09	46.46	4,817.31	43.27	4,468.23	42.51	1,966.38	43.47	2,711.17	56.38	6,296.80	39.51	2,083.57	49.25	6,417.43	49.64	9,042.45	55.13	10,223.39
	G	3.99	3.88	3.99	3.9	4	3.89	4	3.87	3.99	3.88	3.99	3.86	3.99	3.85	4.23	3.86	3.99	3.87	3.99	2.87
	Log (N/G)	-0.82	-25.01	-0.82	-25.01	-0.81	-24.92	-0.81	-24.72	-0.81	-24.93	-0.81	-24.89	-0.81	-24.79	-0.81	-24.77	-0.81	-24.86	-0.81	-24.82
	Log (P/G)	-2.77	-34.84	-2.77	-34.84	-2.77	-34.95	-2.76	-34.85	-2.77	-35.05	-2.76	-34.93	-2.76	-34.81	-2.76	-34.71	-2.76	-34.75	-2.76	-34.77
	Log (K/G)	-0.42	-28.71	-0.42	-28.71	-0.42	-28.71	-0.42	-28.58	-0.42	-28.54	-0.42	-28.44	-0.42	-28.36	-0.42	-28.48	-0.43	-28.53	-0.42	-28.50

For the treatments 2N-0P-2K, 0N-1P-1K, and 2N-2P-2K, potassium (K) had the lowest standard deviation, while phosphorus (P) had the highest standard deviation. Potassium (K) and nitrogen (N) exhibited the lowest and highest standard deviations for the treatment 1N-2P-0K, respectively. The standard deviation of phosphorus (P) ranged between 0.91% and 0.93% (computed using $\overline{X}$ and CVs). Negative values in the CND criteria mean that the nutrient's foliar content is lower than the geometric mean of the nutritional composition in the multi-nutrient variable.

Nutrient indices computed by DRIS, M-DRIS, and CND methods

The N, P, and K indices and as well as the NBIm were calculated for each treatment and each sample size using DRIS, M-DRIS, and CND models. When all nutrient indices for DRIS, M-DRIS, and CND were plotted in one graph, the models showed different trends for the distribution of N, P, and K indices as well as NBIm (Fig. 2). Nutrient indices were different between models and with sample size. Indeed, we noticed that N, P, and K averaged indices as well as NBIm for M-DRIS (red dashed lines) were positive, whereas DRIS average indices (black lines) were negative for P and positive for K and NBIm. N varied between negative (I_N = -36.78) and positive values (I_N = 158.28). CND averaged indices (blue lines) were between negative and positive values for all nutrients with the sample size (ranging from $-1.57*10^{-16}$ to $1.31*10^{-16}$ for N, $-9.68*10^{-17}$ to $5.83*10^{-17}$ for P, and $-1.23*10^{-16}$ to $8.66*10^{-17}$) and were very close to 0, which explained the approximately linear shape of its curves in the figure.

For all three models, the calculated indices became approximately stable from the sample size of 490 (Fig. 2). P was the most limiting nutrient by deficiency, compared to the other nutrients.

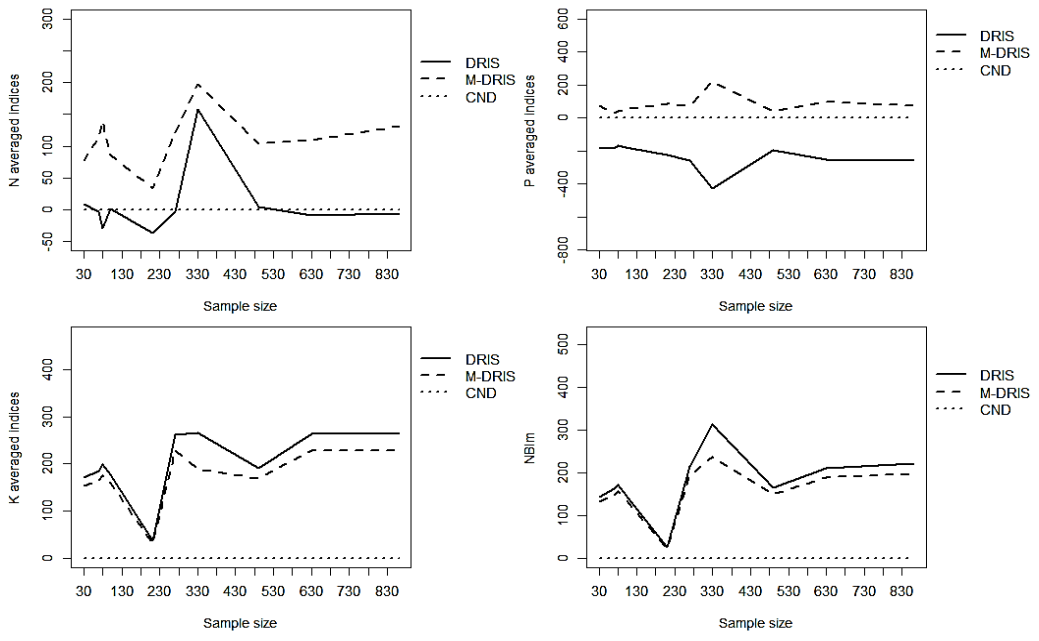

Figure 2. Averaged indices of N, P, K and mean nutrient balance index (NBIm) for DRIS, M-DRIS, and CND models relative to the different data size.

Table 5. Results of permutational multivariate analysis of variance on the nutrient indices considering the models and treatment as factors

Sample size	Source of variation	Df	Sum of squares	R^2	F	Pr(>F)
30	Model	2	276,236	0.40	5.01	0.001***
	Treatment	4	194,099	0.28	1.76	0.12
	Residual	8	220,393	0.32	-	-
	Total	14	690,729	1	-	-
70	Model	2	269,961	0.34	4.77	0.007**
	Treatment	4	288,337	0.37	2.55	0.025*
	Residual	8	226,224	0.29	-	-
	Total	14	784,522	1	-	-
80	Model	2	321,217	0.37	4.09	0.002**
	Treatment	4	233,648	0.27	1.49	0.168
	Residual	8	314,105	0.36	-	-
	Total	14	868,969	1	-	-
100	Model	2	269,792	0.36	4.45	0.004**
	Treatment	4	239,334	0.32	1.97	0.052
	Residual	8	242,563	0.32	-	-
	Total	14	751,689	1	-	-
210	Model	2	165,972,252	0.15	1.03	0.393
	Treatment	4	296,526,975	0.27	0.92	0.933
	Residual	8	646,655,531	0.58	-	-
	Total	14	1,109,154,758	1	-	-
270	Model	2	556,484	0.31	3.4	0.007**
	Treatment	4	602,948	0.33	1.84	0.076
	Residual	8	654,686	0.36	-	-
	Total	14	1,814,118	1	-	-
330	Model	2	4,802,704	0.23	1.51	0.065
	Treatment	4	3,394,142	0.16	0.53	0.913
	Residual	8	12,707,887	0.61	-	-
	Total	14	20,904,733	1	-	-
490	Model	2	303,415	0.35	4.38	0.004**
	Treatment	4	286,785	0.33	2.07	0.043*
	Residual	8	277,008	0.32	-	-
	Total	14	867,208	1	-	-
630	Model	2	579,664	0.38	4.47	0.006**
	Treatment	4	444,592	0.29	1.71	0.133
	Residual	8	519,244	0.34	-	-
	Total	14	1,543,499	1	-	-
860	Model	2	576,084	0.36	4.35	0.003**
	Treatment	4	486,791	0.31	1.84	0.048*
	Residual	8	530,319	0.33	-	-
	Total	14	1,593,194	1	-	-

Df: Degree of freedom; ***, **, and * indicate significance at 0.001, 0.01, 0.05, and 0.1 levels, respectively.

The permutational multivariate analysis of variance (PERMANOVA) results indicated that there was a significant difference between the DRIS, M-DRIS and CND indices for the sample sizes of 30 (p.value = 0.001), 70 (p.value = 0.007), 80 (p.value = 0.002), 100 (p.value = 0.004), 270 (p.value = 0.007), 490 (p.value = 0.004), 630 (p.value = 0.006), and 860 (p.value = 0.003). For the sample sizes of 210 and 330,

the nutrient indices calculated did not differ significantly between the DRIS, M-DRIS, and CND models. Considering the treatments, there was also a difference between the dispersions of the models' indices calculated for the sample size of 70 (*p*.value = 0.025) at a 5% significance level (Table 5).

Comparison of the Performance of DRIS, M-DRIS, and CND

Frequency of concordance in diagnosis using the DRIS, M-DRIS, and CND models

The comparison of multiple models employing specific norms based on the frequency of concordant diagnoses (DCF) (Silva et al., 2004) produced varying findings depending on the method of comparison and the concentration of nutrients in pineapple leaves. A set of all treatments combined was used to assess the effect of the index model and sample size. All sample sizes yielded mean values of 66% (DRIS versus M-DRIS), 43.33% (DRIS vs CND), and 28.7% (M-DRIS vs CND) (Table 6).When comparing N, P, and K nutrients, the concordance is lower with CND involved. Consequently, the DRIS and M-DRIS models showed more similarity in diagnosing nutritional status for pineapple compared to each of them versus the CND model. Overall, the models disagreed, and when it came to determining the status of N, P, and K minerals, the nutritional diagnostic obtained through the CND technique was not the same as that obtained through the DRIS and M-DRIS methods. Our results are consistent with those of Silva et al. (2004) when assessing the nutritional status of eucalyptus trees and with the work of Urano et al. (2006) when assessing the nutritional diagnosis of soybeans. They found that the DRIS and M-DRIS methods were concordant.

Table 6. Agreement percentages of concordant diagnoses of N, P, and K status in pineapple, subpopulation of high productivity, among the methods DRIS, M-DRIS, and CND for each sample size, applied to the leaves

Sample size	DRIS vs M-DRIS				DRIS vs CND				M-DRIS vs CND			
	N (%)	P (%)	K (%)	Mean (%)	N (%)	P (%)	K (%)	Mean (%)	N (%)	P (%)	K (%)	Mean (%)
30	80	20	80	60	40	20	40	33.33	60	40	40	34
70	100	80	80	86.66	40	40	80	53.33	40	40	60	27.67
80	40	20	0	20	100	40	0	46.67	40	0	40	14
100	80	60	40	60	40	20	40	33.33	60	40	80	34.67
210	80	40	80	66.67	40	0	20	20	40	60	20	33.67
270	100	20	80	66.67	60	80	60	66.67	60	40	40	34
330	100	60	80	80	40	40	20	33.33	40	60	20	33.67
490	80	40	80	66.67	40	40	60	46.67	40	40	40	27.33
630	100	60	80	80	80	20	80	60	80	0	60	27.67
860	80	60	80	73.33	60	20	40	40	60	0	20	20.33
Mean	84	46	68	66	54	32	44	43.33	52	32	42	28.7

The DCF of the potential fertilization response (PFR) for the principal limitation by deficiency (p) for DRIS vs. M-DRIS, DRIS vs. CND, and M-DRIS vs. CND were 45.32%, 50.43%, and 40.75%, respectively, for the second criterion (Table 7). Furthermore, for the same comparison, the main excess (n) constraint was 31.8%, 39.07%, and 45.82%, respectively. This comparison showed the highest degree of

similarity among the three approaches. As observed for the negative response (n), the concordance was smaller when DRIS was considered in the comparisons. M-DRIS and CND models were more consistent in identifying primary limiting by excess (n), whereas DRIS and CND were more comparable in diagnosing principal limiting by deficiency (p), when compared to the other duals.

Table 7. Agreement percentages of concordant diagnoses of the potential fertilization response in a subpopulation of high productivity, among the methods DRIS, M-DRIS, and CND using specific norms for each sample size, applied to the leaves

Sample size	Method	p (%)	n (%)
30	DRIS vs M-DRIS	26.67	33.33
	DRIS vs CND	40.67	23.33
	M-DRIS vs CND	30	55
70	DRIS vs M-DRIS	25.33	30.67
	DRIS vs CND	50	35.5
	M-DRIS vs CND	20	33.33
80	DRIS vs M-DRIS	60.33	40.67
	DRIS vs CND	26.7	60
	M-DRIS vs CND	50	10.67
100	DRIS vs M-DRIS	12.5	10
	DRIS vs CND	40	65.33
	M-DRIS vs CND	50.5	12.5
210	DRIS vs M-DRIS	70	50
	DRIS vs CND	60	24.67
	M-DRIS vs CND	45.67	75
270	DRIS vs M-DRIS	70.67	6.67
	DRIS vs CND	13.33	70
	M-DRIS vs CND	36	53.33
330	DRIS vs M-DRIS	20.33	60
	DRIS vs CND	80	27.33
	M-DRIS vs CND	20	60.67
490	DRIS vs M-DRIS	30.33	16.67
	DRIS vs CND	64.5	29.33
	M-DRIS vs CND	35.33	50.33
630	DRIS vs M-DRIS	73.33	40
	DRIS vs CND	43.67	30.5
	M-DRIS vs CND	60	67.33
860	DRIS vs M-DRIS	63.67	30
	DRIS vs CND	75.67	24.67
	M-DRIS vs CND	60	40
Mean	DRIS vs M-DRIS	45.32	31.8
	DRIS vs CND	50.43	39.07
	M-DRIS vs CND	40.75	45.82

p = primary limiting by deficiency, n = primary limiting by excess.

Sensitivity, positive predictive value and accuracy of DRIS, M-DRIS and CND models

DRIS, M-DRIS, and CND models were also compared based on their sensitivity or true positive rate (TPR, Fig. 3), positive predictive value (PPV, Fig. 4, A-C) and accuracy (Fig. 4, D). Compared with DRIS and M-DRIS, CND appeared to be more sensitive for early detection of N, P, and K deficiency and excess in pineapple leaves when the situations were true (Fig. 3, A and C). Parent & Dafir (1992) showed that CND is theoretically more robust than DRIS and M-DRIS. CND recognizes high-order interactions between nutrients, which was partially addressed by DRIS and M-DRIS (Parent & Dafir, 1992). CND has been found to be more efficient to determine the nutritional status of crops because of its sound mathematical and statistical bases (René et al., 2013; Valdez-Cepeda et al., 2013; Morais et al., 2019). In the case of pineapple, Cunha et al. (2020) found that CND was better at capturing nutrient imbalances affecting fruit development and ripening stages, suggesting that it is a more sensitive tool for managing the nutrition of fruit crops. However, for all sample sizes considered, Cunha et al. (2020) found that CND was better at capturing nutrient imbalances affecting fruit development and ripening stages, suggesting that it is a more sensitive tool for managing

the nutrition of fruit crops. However, for all sample sizes considered, the DRIS method was more sensitive to identifying N, P, and K balance in pineapple leaves when the situation was true (Fig. 3, B).

Then, the CND model was more appropriate to identify situations where nutrients were deficient or excessive. Using the CND method may be more suitable for leaves with lower or excessive nutrient contents, despite its lower sensitivity to identify non-nutritional problems. Therefore, if low productivity is due to nutritional issues, applying the CND method for nutritional diagnosis could lead to reliable recommendations for correcting imbalances and increasing crop productivity. CND was connected to DRIS and M-DRIS but, being based on compositional data analysis and principal component analysis had greater potential for improving plant leaf diagnosis (Parent & Dafir, 1992).

Furthermore, a comparison of the diagnostic precision (positive predictive value) of DRIS, M-DRIS, and CND models revealed that CND was the most precise in detecting correctly deficiency and excess to the total number of deficiency and excess cases, respectively for N, P and K nutrients, followed by the M-DRIS model (Fig. 4, A and C). Kumar et al. (2003) showed that CND appeared to be more sensitive and efficient for projecting nutrient imbalances in turmeric. CND was the sensitive diagnosis and could be instrumental in adjusting fertilization to crop needs after crop emergence (Kumar et al., 2003). However, the DRIS model was more precise in detecting correctly adequacy (sufficiency) to the total number of adequacy cases for N, P, and K nutrients in pineapple leaves (Fig. 4, B). Fig. 4, D showed the accuracy of DRIS, M-DRIS, and CND models in function of sample size.

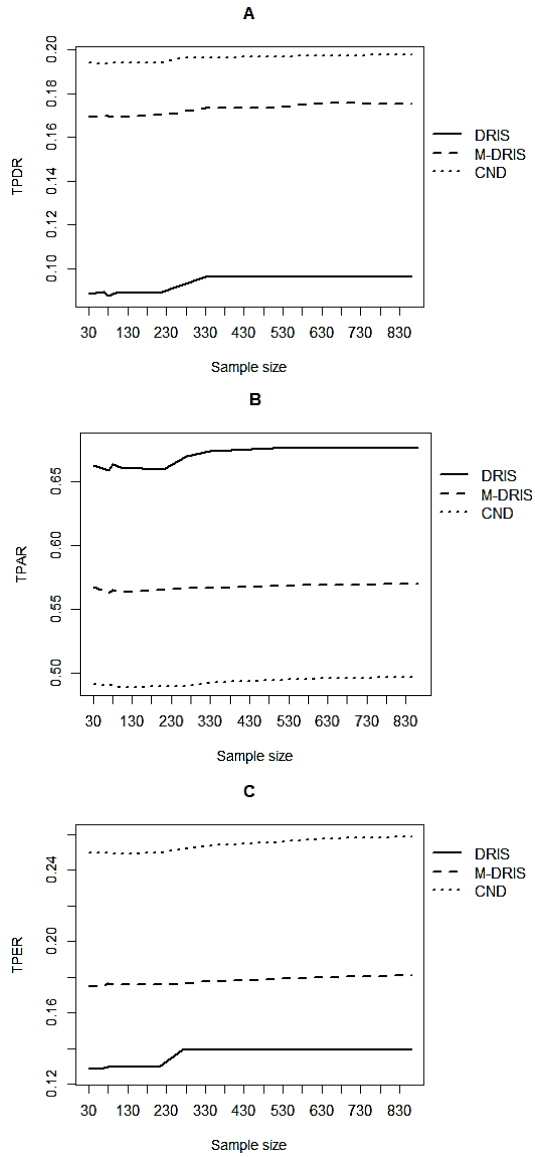

Figure 3. Sensitivity of DRIS, M-DRIS and CND models.

A = True Positive Deficiency Rate diagnosed by the models, B = True Positive Adequate Rate diagnosed by the models and C = True Positive Excess Rate diagnosed by the models.

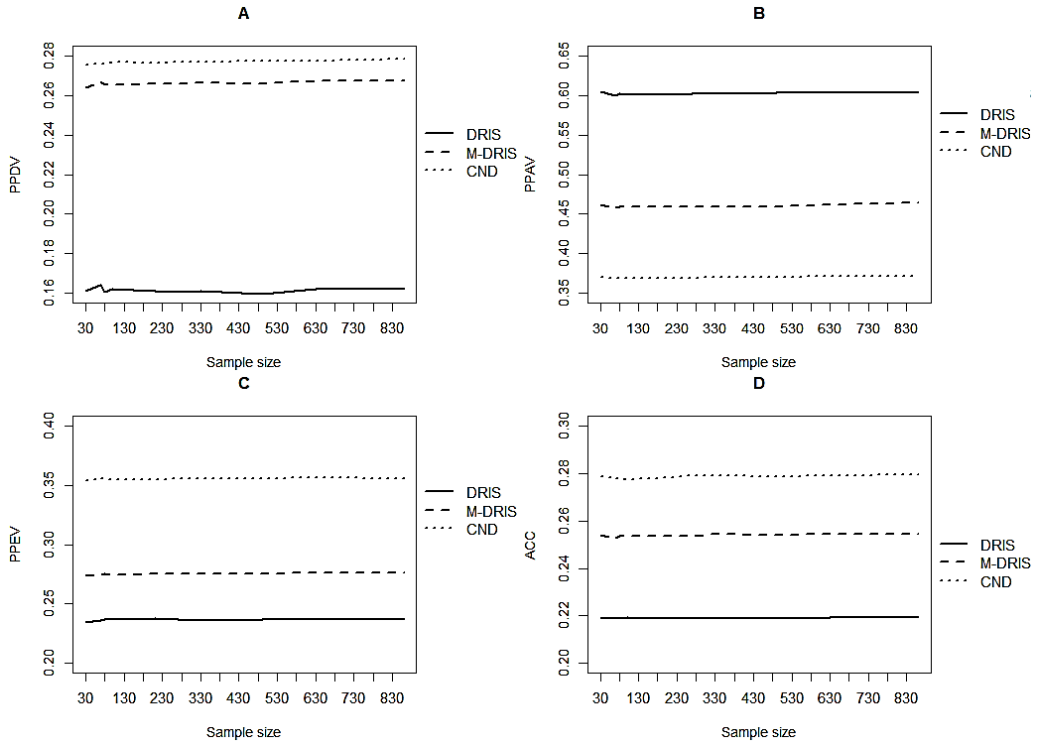

Figure 4. Positive predictive values and accuracy of DRIS, M-DRIS and CND models.
A = Positive Predictive Deficiency Value of the models, B = Positive Predictive Adequate Value of the models, C = Positive Predictive Excess Value of the models and D = Accuracy of the models.

From this figure, we saw that, for all sample sizes considered, the CND model was the most accurate (average accuracy of 27.86%) for diagnosing N, P, and K nutrients in pineapple leaves, followed by the M-DRIS method (average accuracy of 25.39%) and finally the DRIS method (average accuracy of 21.91%). The DRIS and M-DRIS methods were reportedly inferior CND in diagnosing imbalances as they assumed additivity of dual ratios (Parent & Dafir, 1992). The performance of the models varied with sample size. But, from the data size of 330, there was no higher variation in the DRIS, M-DRIS, and CND models' accuracy. The nutrient status of interest when we have low agricultural productivity is nutrient deficiency and to identify this situation, the CND model was the most appropriate, sensitive, accurate, and efficient, compared to the other models. Thes findings are consistent with the work of Tadayon et al. (2023) who conclude that CND is a better technique for assessing nutrient excesses, deficits, or balance in plant tissue. It is a multivariate approach and feneficial over the bivariate Diagnosis and Recommendation Integrated System (DRIS) techniques and conventional univariate critical value (CV) methodologies (Lisboa et al., 2024). Multivariate CND technique is superior for increased diagnostic precision for diagnosing mineral disorders when multiple nutrients are expected to limit yield simultaneously (Savita et al., 2016). Thus, in comparison to DRIS, the CND approach offers a stronger foundation for future advancements in foliar diagnostics.

CONCLUSIONS

This study compared the performance of three different systems, DRIS, M-DRIS, and CND, for diagnosing pineapple leaf nutrient levels while varying the sample size. When compared to DRIS and M-DRIS, CND performed better overall in terms of sensitivity, positive predictive value, and accuracy. Although the DRIS and M-DRIS models demonstrated certain advantages, especially in establishing nutritional balances, the CND method was more successful in detecting nutrient excess and deficiencies. Future works may focus on the comparison of the diagnosis methods for the micronutrients such as zinc, Br also essential for plant growth.

ACKNOWLEDGEMENTS. The authors receive no financial support for the research, authorship, and publication of this article.

REFERENCES

Agbangba, C.E., Dagbenonbakin, D.G. & Kindomihou, V. 2010. Establishment of the standards of the Integrated System for Diagnosis and Recommendation of the Pineapple (*Ananas comosus* (L.) Merr) Sugarloaf variety in the sub-equatorial zone of Benin. *Annales de l'Université de Parakou, Série Sciences Naturelles et Agronomie* **1**, 51–69 (in French).

Anderson, M.J. 2001. A new method for non-parametric multivariate analysis of variance. *Austral ecology* **26**(1), 32–46. doi: 10.1111/j.1442-9993.2001.01070.pp.x

Angeles, D., Sumner, M. & Barbour, N. 1990. Preliminary nitrogen, phosphorus, and potassium DRIS norms for pineapple. *HortScience* **25**(6), 652–655. doi: 10.21273/HORTSCI.25.6.652

Bailey, J., Beattie, J. & Kilpatrick, D. 1997. The diagnosis and recommendation integrated system (DRIS) for diagnosing the nutrient status of grassland swards: I. model establishment. *Plant and Soil* **197**(1),127–135. doi: 10.1023/A:1004236521744

Baldock, J.O. & Schulte, E.E. 1996. Plant analysis with standardized scores combines DRIS and sufficiency range approaches for corn. *Agronomy Journal* **88**(3), 448–456. doi: 10.2134/agronj1996.00021962008800030015x

Beaufils, E. 1973. *Diagnosis and recommendation integrated system (DRIS)*. Soil science bulletin, Pietermaritzburg, University of Natal, 132 pp.

Calheiros, L., Freire, F.J., Moura Filho, G., Oliveira, E., Moura, A.B., Costa, J., Cruz, F., Santos, A. & Rezende, J.S. 2018. Assessment of nutrient balance in sugarcane using DRIS and CND methods. *Journal of Agricultural Science* **10**(9), 164–79. doi: 10.5539/jas.v10n9p164

Camacho, M.A., Silveira, M.V.D., Camargo, R.A. & Natale, W. 2012. Normal nutrient ranges by the ChM, DRIS and CND methods and critical level by method of the reduced normal distribution for orange-pera. *Revista Brasileira de Ciencia do Solo* **36**, 193–200. doi: 10.1590/S0100-06832012000100020

Carr, M.K.V. 2012. The role of potassium in pineapple production. *Acta Horticulturae* **928**, 121–126. doi: 10.17660/ActaHortic.2012.928.17

Chicco, D. & Jurman, G. 2020. The advantages of the Matthews correlation coefficient (mcc) over f1 score and accuracy in binary classification evaluation. *BMC genomics* **21**(1), 1–13. doi : https://doi.org/10.1186/s12864-019-6413-7

Hallmark, W., Walworth, J., Sumner, M., de Mooy, C., Pesek, J. & Shao, K. 1987. Fertilizer use efficiency: Separating limiting from non-limiting nutrients. *Journal of Plant Nutrition* **10**(9–16), 1381–1390. doi: 10.1080/01904168709363670

Hasan, M.M., Hasan, M.M., Teixeira da Silva, J.A. & Li, X. 2016. Regulation of phosphorus uptake and utilization: transitioning from current knowledge to practical strategies. *Cellular & molecular biology letters* **21**, 1–19. doi: https://doi.org/10.1186/s11658-016-0008-y

Hoad, K., Robinson, S. & Davies, R. 2007. Automating des output analysis: how many replications to run. In *2007 Winter Simulation Conference*, Washington, DC, USA, IEEE, pp. 505–512. doi: 10.1109/WSC.2007.4419641

Javari, M. 2017. Spatial variability of rainfall trends in Iran. *Arabian Journal of Geosciences* **10**(4), 78. doi: 10.1007/s12517-017-2857-8

Karlsons, A. & Osvalde, A. 2017. Nutrient status of the American cranberry in Latvia (2005–2016). *Agronomy Research* **15**(1), 196–204. doi:10.17660/ActaHortic.2010.868.26

Kania Kuhl, E. & Callejas Rodríguez, R.H. 2011. Integrated Diagnostic and Recommendation System (DRIS): Tool for Foliar Analysis Interpretation. *Revista Colombiana DE Ciencias Hortícolas***12**(2), 319–328 (in Spanish). doi: 10.17584/rcch.2018v12i2.7387

Khuong, N.Q., Anh, N.H.M., Thanh Quang, L. & Xuan, L.N.T. 2024. Appraisal of the Diagnosis and Recommendation Integrated System and Nutrient Status of Pineapple (*Ananas comosus* L.) Growing Fields. *Communications in Soil Science and Plant Analysis* **55**(10), 1508–1538. doi: 10.1080/00103624.2024.2319807

Kumar, P.S., Geetha, S.A., Savithri, P., Mahendran, P. & Ragunath, K. 2003. Evaluation of DRIS and CND indexes for effective nutrient management in muscat grapevines (*Vitis vinefera*). *Journal of Applied Horticulture* **5**(2), 76–80.

Leite, R.D.A. 1993. *Evaluation of the nutritional status of conilon coffee in the state of Espírito Santo using different methods of leaf analysis interpretation*. Doctoral dissertation, Universidade Federal de Viçosa, Brasil, 87 pp. (in Portuguese).

Lisboa, B.B., Abichequer, A.D., de São José, J.F.B., Moura-Bueno, J.M., Brunetto, G. & Vargas, L.K. 2024. Compositional Nutrient Diagnosis Methodology and Its Effectiveness to Identify Nutrient Levels in Yerba Mate (*Ilex paraguariensis*). *Agriculture* **14**(6), 896. doi: 10.3390/agriculture14060896

López-Montoya, J., Fernández-Paz, J.A., Vásquez, H.D. & Menjivar-Flores, J.C. 2018. Diagnosis and Recommendation Integrated System (DRIS) for pineapple (*Ananas comosus*), honey gold variety (MD-2). *Revista Colombiana de Ciencias Hortícolas* **12**(2), 319–328. doi: 10.17584/rcch.2018vl2i2.7387

Magallanes-Quintanar, R., Valdez-Cepeda, R.D., Olivares-Sáenz, E., Pérez-Veyna, O., García-Hernández, J.L. & López-Martínez, J.D. 2006. Compositional nutrient diagnosis in maize grown in a calcareous soil. *Journal of Plant Nutrition* **29**(11), 2019–2033. doi: 10.1080/01904160600928235

Morais, T.C.B.D., Prado, R.D.M., Traspadini, E.I.F., Wadt, P.G.S., Paula, R.C.D. & Rocha, A.M.S. 2019. Efficiency of the CL, DRIS and CND methods in assessing the nutritional status of *Eucalyptus* spp. rooted cuttings. *Forests* **10**(9), 786. doi: 10.3390/f10090786

Narisetty, N.N. 2020. Bayesian model selection for high-dimensional data. In *Srinivasa Rao, A.S. & Rao, C. (eds): Principles and Methods for Data Science*- Handbook of Statistics, pp. 207–248.

Nayanaka, V.G.D., Vitharana, W.A.U. & Mapa, R.B. 2010. Geostatistical analysis of soil properties to support spatial sampling in a paddy growing alfisol. *Tropical Agricultural Research* **22**(1), 34–44. doi: 10.4038/tar.v22i1.2668

Nguyen, G.N., Rothstein, S.J., Spangenberg, G. & Kant, S. 2015. Role of microRNAs involved in plant response to nitrogen and phosphorous limiting conditions. *Frontiers in Plant Science* **6**, 629. doi: 10.3389/fpls.2015.00629

Osvalde, A., Karlsons, A. & Cekstere, G. 2021.Leaf nutrient status of tomatoes in coconut coir medium – differences in cultivars, impact on yield and quality. *Agronomy Research* **19**(4), 1850–1862. doi: 10.15159/AR.21.110

Pacheco-Sangerman, F., Prado-Hernández, V., Maldonado-Torres, R. & Robledo-Santoyo, E. 2022. Soil and foliar nutritional diagnosis in corn cultivation. *Revista mexicana de ciencias agrícolas* **13**(6), 1079–1090. doi: 10.29312/remexca.v13i6.2691

Parent, L.E. & Dafir, M. 1992. A theoretical concept of compositional nutrient diagnosis. *Journal of the American Society for Horticultural Science* **117**(2), 239–242. doi: 10.21273/JASHS.117.2.239

Parent, L.E., Karam, A. & Visser, S.A. 1993. Compositional nutrient diagnosis of the greenhouse tomato. *HortScience* **28**(10), 1041–1042. doi: 10.21273/HORTSCI.28.10.1041

Pineda-Álvarez, E.O., Villamil-Carvajal, J.E. & Cabezas-Gutiérrez, M. 2021. Diagnosis and recommendation integrated system, its application and use in agriculture. a review. *Ciencia y Agricultura* **18**(3), 29–45. doi: 10.19053/01228420.v18.n3.2021.12933

Politi, L.S., Flores, R.A., Da Silva, J.A., Wadt, P.G., Pinto, P.A.D.C. & Prado, R.D.M. 2013. Nutritional status of mango trees determined by dris and cnd methods. *Revista Brasileira de Engenharia Agrícola e Ambiental* **17**, 11–18 (in Portuguese). doi: 10.1590/S1415-43662013000100002

Powers, D.M. 2020. Evaluation: from precision, recall and f-measure to roc, informedness, markedness and correlation. *International Journal of Machine Learning Technology* **2**(1), 37–63. doi: 10.48550/arXiv.2010.16061

Prinsi, B. & Espen, L. 2015. Mineral nitrogen sources differently affect root glutamine synthetase isoforms and amino acid balance among organs in maize. *BMC plant biology* **15**, 1–13. doi: 10.1186/s12870-015-0482-9

Py, C., Lacoeuilhe, J.J. & Teisson, C. 1984. Lananas, sa culture, ses produits, techniques agricoles et productions tropicales. *Paris, France: Maisonneuve & Larose*. ACCT, 562 pp.

Ragel, P., Raddatz, N., Leidi, E.O., Quintero, F.J. & Pardo, J.M. 2019. Regulation of K+ nutrition in plants. *Frontiers in Plant Science* **10**, 281. doi: 10.3389/fpls.2019.00281

R Core Team. 2021. R: A Language and Environment for Statistical Computing. R Foundation for Statistical Computing, Vienna, Austria. https://www.R-project.org/.

Roy, E.D., Willocquet, L. & Savary, S. 2018. Phosphorus nutrition in tropical crops: A review. *Agriculture, Ecosystems & Environment* **258**, 1–12. doi: 10.1016/j.agee.2018.02.014

Savita, S., Krishnappa, R., Ngangom, B., Devi, M.T., Mishra, G., Rawat, D. & Srivastava, P. 2016. Diagnosis and recommendation integrated system (DRIS) approach on nutritional diagnosis in fruit crops-a review. *Journal of Applied and Natural Science* **8**(4), 2337–2345. doi: 10.31018/jans.v8i4.1134

Serra, A.P., Marchetti, M.E., Gonçalves, M.C., Ensinas, S.C., Mouna, B.L., da Silva, E.F., ... & de Araújo Matos, F. 2016. Nutritional Status of Cotton Plant Assessed by Compositional Nutrient Diagnosis (CND). *Cotton Research* 63. doi: 10.5772/64388

Silva, G.G.C.D., Neves, J.C.L., Alvarez, V.H. & Leite, F.P. 2004. Nutritional diagnosis for eucalypt by DRIS, M-DRIS, and CND. *Scientia Agricola* **61**, 507–515. doi: 10.1590/S0103-90162004000500008

Silva, J.A., Mendes, L.F. & Cardoso, J.M. 2018. Potassium nutrition in pineapple: Yield and quality response. *Journal of Horticultural Science & Biotechnology* **93**(4), 367–373. doi: 10.1080/14620316.2018.1428945

Souza, L.D.S. & Reinhardt, D.H. 2007. Pineapple, 325 pp.

Souza, H.A.D., Rozane, D.E., Vieira, P.F.D.M.J., Sagrilo, E., Leite, L.F.C., Brito, L.C.R.D., ... & Ferreira, A.C.M. 2023. Accuracy of DRIS and CND methods and nutrient sufficiency ranges for soybean crops in the Northeast of Brazil. *Acta Scientiarum. Agronomy* **45**, e59006. doi: 10.4025/actasciagron.v45i1.59006

Sumner, M. 1977. Application of beaufils' diagnostic indices to maize data published in the literature irrespective of age and conditions. *Plant and Soil* **46**, 359–369. doi: 10.1007/BF00010092

Tadayon, M.S., Saghafi, K. & Sadeghi, S. 2022. Applying the compositional nutrient diagnosis (CND) to pomegranate (*Punica granatum* cv.'Rabab') under saline and calcareous soil condition. *Journal of Plant Nutrition* **46**(1), 1–16. doi: 10.1080/01904167.2022.2067762

Teixeira, A.R.S., Santos, F.A. & Andrade, C.T. 2020. Influence of potassium fertilization on the yield and quality of pineapple. *Horticultura Brasileira* **38**(3), 290–296. doi: 10.1590/s0102-053620200314

Tharwat, A. 2020. Classification assessment methods. *Applied Computing and Informatics* **17**(1), 168–192. doi: https://doi.org/10.1016/j.aci.2018.08.003

Trevethan, R. 2017. Sensitivity, specificity, and predictive values: foundations, pliabilities, and pitfalls in esearch and practice. *Frontiers in public health* **5**, 307. doi: 10.3389/fpubh.2017.00307

Urano, E.O.M., Kurihara, C.H., Maeda, S., Vitorino, A.C.T., Gonçalves, M.C. & Marchetti, M.E. 2006. Evaluation of the nutritional status of soybeans. *Pesquisa Agropecuária Brasileira* **41**,1421–1428 (in Portuguese). doi: 10.1590/S0100-204X2006000900011

Valdez-Cepeda, R.D., Magallanes-Quintanar, R., Blanco-Macías, F., Hernández-Caraballo, E.A. & García-Hernández, J.L. 2013. Comparison among boltzmann and cubic polynomial models for estimation of compositional nutrient diagnosis standards: Opuntia ficus-indica L. case. *Journal of plant nutrition* **36**(6), 895–910. doi: 10.1080/01904167.2013.770020

Wadt, P., Novais, R.D., Alvarez, V.H., Fonseca, S., Barros, N. & Dias, L.1998. Three methods of calculating the DRIS to evaluate the potential response to fertilization of eucalyptus trees. *Revista Brasileira de Ciência do Solo* **22**, 661–666 (in Portuguese). doi: 10.1590/S0100-06831998000400011

Wadt, P.G.S. 2005. Relationships between soil class and nutritional status of coffee plantations. *Revista Brasileira de Ciência do Solo* **29**, 227–234. doi: 10.1590/S0100-06832005000200008

Walworth, J. & Sumner, M. 1988. Foliar diagnosis: a review. *Advances in plant nutrition* **3**, 193–241.

Agronomy Research **22**(S3), 1405–1420, 2024
https://doi.org/10.15159/AR.24.077

Exogenous phytohormones and growth-promoting microorganisms in Basilisk grass cultivation

E.B. Andrade[1,*], F.A. Teixeira[2], D.D. Fries[3], N.T. Cruz[4], R.R. Jardim[1], H.S. da Silva[1], B.E.F. dos Santos[1], T.M. Vieira[1], A.A. Seixas[1] and J.P. dos Santos[1]

[1]State University of Southwest Bahia, Postgraduate Program in Animal Science, BA 415 Highway, 45700-000, Itapetinga, Bahia, Brazil
[2]State University of Southwest Bahia, Department of Rural and Animal Technology, BA 415 Highway, 45700-000, Itapetinga, Bahia, Brazil
[3]State University of Southwest Bahia Department of Exact and Natural Sciences, BA 415 Highway, 45700-000, Itapetinga, Bahia, Brazil
[4]Federal University of Recôncavo da Bahia, Center for Agrarian, Environmental and Biological Sciences, Rui Barbosa Str., 170, 44380-000 Cruz das Almas, Bahia, Brazil
[*]Correspondence: elienezoo@gmail.com

Received: June 22nd, 2024; Accepted: July 4th, 2024; Published: August 9th, 2024

Abstract. The use of plant growth-promoting bio-inputs has been widely disseminated as a means to optimise pasture production processes. This study was conducted to evaluate the effects of applying exogenous phytohormones along with different microorganisms on the productive characteristics of Basilisk grass (*Urochloa decumbens*). The experiment was conducted in a 4×2 factorial design, in a completely randomised layout, evaluating four microorganism inoculations (no inoculation; *Azospirillum brasilense* + *Pseudomonas fluorescens*; *Rhizophagus intraradices*; *A. brasilense* + *P. fluorescens* + *R. intraradices*), combined or not with an exogenous phytohormone based on cytokinin, gibberellin and auxin. The results showed that inoculation with plant growth-promoting microorganisms stimulated an increase in root volume. In addition, the presence of the microorganisms increased the concentration of chlorophyll pigments, resulting in a 14% increase in the crude protein content of Basilisk grass compared with the control. The use of exogenous phytohormones also resulted in higher concentrations of total chlorophyll pigments and crude protein content, with increase in 25% and 9.7% respectively. The combined use of bacteria and mycorrhizal fungi, along with exogenous phytohormones, increased the accumulation of forage mass and leaf biomass. The combination enhanced carbohydrate accumulation in the leaves of Basilisk grass, thereby improving its nutritional quality. Therefore, considering the evidence found in this research, it becomes evident that the application of exogenous phytohormones, when combined with the inoculation of *A. brasilense*, *P. fluorescens*, and *R. intraradices*, represents a strategy to enhance the productivity of Basilisk grass.

Key words: diazotrophic bacteria, *Urochloa decumbens*, arbuscular mycorrhizal fungi, plant growth regulator.

INTRODUCTION

The high demand for animal-based foods for global consumption, particularly in the agricultural sector, requires Brazil to intensify technologies aimed at achieving sustainable production. However, according to Dias-Filho (2014), approximately 50% of Brazilian pastures are classified as degraded, and only 20% are in good condition for use. These factors, combined with inadequate soil management and low resource utilisation, are causing arable lands to increasingly lose their potential for nutrient cycling, microorganism activity, plant productivity and consequently, pasture supply for animals.

Thus, technologies that reduce environmental impact are increasingly being adopted. Microbiological inoculants, also known as biofertilizers, improve the development of forage species by increasing their biomass and nutritional characteristics. They also allow for the replacement of chemical fertilisers through the action of plant growth-promoting microorganisms (PGPMs) such as bacteria and fungi that act in the rhizosphere, providing benefits to the plant, such as the synthesis of phytohormones, nutrient mobilisation and phosphorus solubilisation (Hungria et al., 2010).

In this context, plant growth-promoting bacteria (PGPB) and arbuscular mycorrhizal fungi (AMF) stand out as cost-effective production systems. Examples include *Azospirillum brasilense*, *Pseudomonas fluorescens*, and *Rhizophagus intraradices*, which together reduce the need for fertilisers, increase nitrogen use efficiency through biological fixation (Cunha et al., 2014; Hourani, 2023), enhance root system development (Licea-Herrera et al., 2020), produce plant hormones that aid in cell growth, reduce water stress and improve pathogen resistance (Nadeem et al., 2014).

Moreover, there are reports on exogenous phytohormones or plant growth regulators (PGR) that promote the inhibition or modification of plant morphophysiological processes, similar to endogenous phytohormones. Under potential stress conditions, these substances positively regulate genes, thereby modulating plant responses and significantly improving water use efficiency (Colebrook et al., 2014). Alternatives involving the use of plant growth-promoting microorganisms and exogenous phytohormones have proven to be promising in forage production, stimulating growth while reducing the environmental impacts of soil degradation and nutrient loss in a sustainable and economical manner.

Thus, the aim of this study was to evaluate the application of exogenous phytohormones associated with different plant growth-promoting microorganisms in the cultivation of *Urochloa decumbens* cv. Basilisk.

MATERIAL AND METHODS

Experimental details and tratamentos

The experiment was conducted in a greenhouse located at the University of Southwest Bahia, Juvino Oliveira Campus, situated at the following coordinates: 15°38'46" south latitude, 40°15'24" west longitude, and an average altitude of 280 m, in the municipality of Itapetinga-BA, during the period from May to August 2021. The climate of the municipality, according to the Köppen classification, is 'Cw' type, humid mesothermal, and hot subhumid. The average minimum and maximum temperatures

during the experimental period were 17 °C and 36 °C, respectively. The average minimum and maximum humidity values were 22% and 86%, respectively.

The soil used was collected from the 0–20 cm depth layer at the Itapetinga Campus of the State University of Southwest Bahia (UESB). The collected soil was broken up and passed through a sieve with a 4 mm mesh size. Subsequently, the pots were filled with the soil, and samples were collected for soil analysis, which was carried out at the Department of Agricultural Engineering and Soils of UESB (Table 1).

Table 1. Physical and chemical analysis of soil

Granulometric composition (g kg^{-1})												
Sand				Silt						Clay		
555				355						90		
Chemical analysis												
pH	P	K^+	Ca^{2+}	Mg^{2+}	Al^{3+}	H^+	SB	t	T	V	m	OM
	mg dm^{-3}	----------			cmolc dm^{-3} of soil			----------		%		g dm^{-3}
6.4	14	0.87	1.6	1.7	0.0	1.7	4.2	4.2	5.9	71	0	10

SB – Sum of bases; t – Effective cation exchange capacity; T – Cation exchange capacity at pH 7; V – Base saturation; m – Aluminium saturation; OM – Organic matter.

According to the recommendations of the Soil Fertility Commission of the State of Minas Gerais, there was no need for liming, and potassium fertilisation was not necessary as it was already adequately available (Alvarez & Ribeiro, 1999). However, phosphorus availability was low, but no phosphorus fertilisation was applied due to treatments involving phosphorus-solubilising microorganisms. Nitrogen fertilisation was applied, with 50 kg ha^{-1} of N in the form of urea (44% N) being applied, corresponding to 0.35 g per pot, applied as topdressing after the uniformization cut.

To determine the field capacity, all pots with dry soil were weighed, saturated with water, and weighed again after complete drainage of water. The final weight obtained was subtracted from the dry soil weight, thus corresponding to the field capacity (FC) value, which was used to replenish losses due to evapotranspiration. The experimental units were maintained at 70% of the FC value determined.

Experimental design

The experiment was conducted in a 4×2 factorial design, with four treatments involving microorganisms: 1 – control (non-inoculated); 2 – Bacteria (*Azospirillum brasilense* + *Pseudomonas fluorescens*), 3 – Arbuscular mycorrhizal fungi (*Rhizophagus intraradices*), 4 – Bacteria (*Azospirillum brasilense and Pseudomonas fluorescens*) + Fungus (*Rhizophagus intraradices*), associated or not with phytohormones (auxin + gibberellin + cytokinin). The design was completely randomised, with five replicates, totalling 40 plastic pots, each filled with 13 kg of soil.

Before sowing, seeds were inoculated with bacteria, and phytohormones were administered in accordance with the treatments and manufacturers' recommendations. After this step, the seeds were mixed thoroughly and kept in the shade for 30 min. The commercial products BioFree®, composed of *Azospirillum brasilense* AbV6 and *Pseudomonas fluorescens* CCTB03 bacteria (300 mL per 10 kg of seeds), and Stimulate®, containing the phytohormones auxin, gibberellin, and cytokinin (10 mL per 10 kg of seeds), were used. The sowing was conducted in May 2021, with

simultaneous inoculation of the mycorrhizal fungus (*Rhizophagus intraradices*) directly into the experimental units, following the recommendations of the commercial product Rootella BR® (120 g ha^{-1} with 20,800 propagules g^{-1}).

When the plants were 15 days old, thinning was performed, maintaining four plants per pot, based on the parameters of vigour and plant homogeneity. On the 30th day after planting, a uniform cut was performed, with an average residue height of 15 cm, marking the beginning of the evaluations. Immediately after the uniform cut, nitrogen fertilisation was applied, followed by foliar re-inoculation with bacteria (500 mL ha^{-1} of Biofree®) and foliar re-application of phytohormones (500 mL ha^{-1} of Stimulate®). Bacterial re-inoculation and phytohormone re-application were performed after each cut.

Analysis of morphogenic and structural characteristics

Two cycles were conducted to evaluate the morphogenetic and structural characteristics: one between the uniform cut and the first cut, and another between the first and second cuts. In each cycle, two tillers per pot were marked. Every 3 days, the following were determined: leaf apex appearance, leaf length and width, and stem length (distance from the ground to the ligule of the youngest leaf). Based on these measurements, the following parameters were calculated: leaf appearance rate (leaves^{-1} day^{-1}), phyllochron (days^{-1} leaf^{-1}), stem elongation rate (cm), leaf width (cm), and final leaf length (cm). Height measurements were taken using a graduated ruler without compressing the forage, considering the upper limit as the height of the leaf curvature around the ruler. At the end of each evaluation period, the number of tillers in each experimental unit was counted to determine the tiller population density.

Determination of chlorophyll content and SPAD index

For the determination of the SPAD (Soil Plant Analytical Division) index, the SPAD 502 Plus device was used around 10 a.m., with readings taken on the middle third of three randomly chosen fully expanded leaves in each experimental unit. At the end of each evaluation period, two fully expanded leaves were collected from each replicate, always around 10:00 a.m., and placed in aluminium foil envelopes, which were immediately stored in ice and taken to the laboratory for determination of chlorophyll a, chlorophyll b according to the methodology of Hiscox & Israelstam (1979).

For this, 0.03 g of the fresh leaf mass collected was placed in a glass vial containing 5 mL of dimethyl sulfoxide and wrapped in aluminium foil for 72 h. The readings were taken on a spectrophotometer at absorbance wavelengths of 665, 649, and 480 nm. For the quantification of chlorophylls, the formulas defined by Wellburn (1994) were used: Chlorophyll a = (12.19×A665) - (3.45×A649); Chlorophyll b = (21.99×A649) - (5.32×A665); The values adjusted to mg g^{-1} of fresh matter. The total chlorophyll content was calculated by summing chlorophyll a and b.

Determination of productive and morphological characteristics

Two cuts were made with a residual height of 15 cm to determine dry matter production (number of days between cuts = 28). In each cut, two subsamples (two plants per subsample) were obtained from each experimental unit. The first subsample was separated into leaf, sheath + stem, and dead material. The material was weighed and placed in a forced-air oven at 55 °C for 72 h. Subsequently, the samples were weighed

again to determine dry mass, and the following characteristics were calculated: total plant dry matter production, leaf dry matter production, stem dry matter production, percentage of leaf blades, percentage of stems, and leaf-to-stem ratio.

Chemical-bromatological composition

The second sample (whole plant) was also weighed and placed in a forced-air oven at 55°C for 72 h, then weighed, ground in a knife mill with a 1-mm sieve, and subjected to chemical-bromatological analyses to determine the levels of dry matter (DM, INCT-CA method G-003/1), crude protein (CP, INCT-CA method N-001/1), mineral matter (MM, INCT-CA method M-001/1), aether extract (EE, INCT-CA method G-004/1), neutral detergent fibre (NDF, INCT-CA method F-002/1), acid detergent fibre (ADF, INCT-CA method F-004/1), hemicellulose, and lignin (INCT-CA method F-005/1), according to the techniques described by Detmann et al. (2021).

For the determination of non-fibre carbohydrates corrected for ash and protein (NFC) and total carbohydrates (TCHOT) in the samples, the equations proposed by Sniffen et al. (1992) were used. The total digestible nutrient (TDN) content of the forage was calculated using the equation proposed by Cappelle et al. (2001), and dry matter digestibility (DMD) was calculated using the equation proposed by Rodrigues (2010).

After harvesting, the collected roots were used to determine their length using a ruler graduated in centimetres. Root volume was determined using a volumetric flask containing a specific quantity of water in which fresh roots were immersed. The difference in volume before and after the immersion of the roots allowed the calculation of root volume. Subsequently, the roots were weighed and placed in a forced-air circulation oven at 55 °C for 72 h to determine the dry mass.

Statistical analysis

The data were subjected to analysis of variance using the statistical programme SAS On Demand for Academics, considering microorganisms (M), phytohormones (F), and the interaction M×F as sources of variation. The interaction was split or not when means were compared using Tukey's test at 5% significance level.

RESULTS

Morphogenetic characteristics of *Urochloa decumbens* cv. Basilisk showed no interaction effect ($P > 0.05$) between inoculation with microorganisms and the presence of phytohormones. The leaf appearance rate (LAR), phyllochron, final leaf length and width (FLL and FWL), tiller population density (TPD), and height did not show ($P > 0.05$) differences among the evaluated treatments, whereas the stem elongation rate (SER) was higher for Basilisk grass plants that received phytohormones (Table 2).

The total leaf mass and the stem percentage showed a significant interaction ($P < 0.05$) between microbial inoculation and the presence of phytohormones. However, for stem mass, leaf percentage, and the leaf-to-stem ratio, the interaction was not significant ($P > 0.05$) (Table 3).

Table 2. Morphogenic characteristics of Basilisk grass cultivated with or without microbial inoculation in the presence or absence of plant growth regulators

Item	Microorganisms				PGR		*P value*			CV
	Cont	Bac	Fun	Bac+Fun	With	Without	M*PGR	PGR	M	(%)
TApF	0.16	0.16	0.17	0.15	0.16	0.16	0.434	0.368	0.120	6.9
Phyllo	6.35	6.62	6.40	6.78	6.39	6.68	0.971	0.078	0.204	7.5
TAlC	1.14	1.12	1.16	1.11	1.15 a	1.11 b	0.892	0.032	0.363	6.0
FLL	20.62	21.11	21.16	22.06	21.49	20.98	0.110	0.345	0.306	7.9
FLW	1.51	1.53	1.56	1.63	1.54	1.58	0.574	0.359	0.164	8.0
TPD	10.32	10.57	10.07	10.82	10.5	10.3	0.257	0.474	0.27	8.3
HP	39.57	38.8	39.85	39.3	39.8	38.9	0.910	0.207	0.703	5.2

Means followed by different lowercase letters for phytohormone presence differ significantly according to Tukey's test ($P < 0.05$). TapF – leaf appearance rate (leaf^{-1} tiller^{-1} day^{-1}); Phyllo – phyllochron (day^{-1} leaf^{-1} tiller^{-1}); TAlC – stem elongation rate (cm^{-1} tiller^{-1} day^{-1}); FLL – final leaf length (cm); FLW – final leaf width (cm); TPD – tiller population density; HP – plant height (cm); Cont – control; Bac – Bacteria; Fun – Fungus; M*PGR – interaction between microorganisms (M) and plant growth regulators (PGR); CV – coefficient of variation.

Table 3. Agronomic characteristics of Basilisk grass cultivated with or without microbial inoculation in the presence or absence of plant growth regulators

Item	Microorganisms				PGR		*P value*			CV
	Cont	Bac	Fun	Bac+Fun	With	Without	M*PGR	PGR	M	(%)
TDB	9.8	9.8	11.0	11.0	10.1	10.7	0.003	0.073	0.009	10.2
LDB	6.26	6.39	6.87	6.96	6.4	6.9	< 0.001	0.07	0.084	10.6
SDB	3.7BC	3.5 C	4.1AB	4.2 A	3.8	3.9	0.257	0.608	0.001	16.5
Leaf	64.22	64.85	62.9	63.92	63.7	64.1	0.195	0.763	0.698	6.1
Stem	37.48	37.92	37.07	37.73	38.2	36.9	0.025	0.278	0.968	10.6
L/S	1.94	1.90	1.78	1.82	1.8	1.9	0.116	0.559	0.591	16.0

Means followed by different uppercase letters for microorganisms and lowercase letters for the presence of phytohormones differ significantly according to Tukey's test ($P < 0.05$). TDB – total dry biomass (g pot^{-1}); LDB – leaf dry biomass (g pot^{-1}); SDB – stem dry biomass (g pot^{-1}); leaf (%); stem (%); L/S – leaf to stem ratio; Cont – control; Bac – Bacteria; Fung – Fungus; M*PGR – interaction between microorganisms (M) and plant growth regulators (PGR); CV – coefficient of variation.

The highest accumulation of total dry biomass, leaf dry biomass, and stem percentage was achieved with co-inoculation of bacteria and fungi combined with the presence of PGR (Table 4).

Table 4. Unfolding of agronomic variables: significant interactions between microorganisms and plant growth regulators in Basilisk grass

Item	PGR	Microorganisms			
		Cont	Bac	Fun	Bac+Fun
TDB	Without	10.19Aa	10.93Aa	11.70Aa	9.92Ba
	With	9.25Ab	8.63Bb	10.29Aab	12.06Aa
LDB	Without	6.47Aa	7.39Aa	7.32Aa	6.15Ba
	With	6.05Ab	5.40Bb	6.43Aab	7.78Aa
Stem	Without	38.37Aa	35.41Aa	38.86Aa	34.80Ba
	With	36.59Aa	40.44Aa	35.30Aa	40.66Aa

Means followed by uppercase letters in the column and lowercase letters in the row differ significantly according to Tukey's test ($P < 0.05$). PGR – plant growth regulators; TDB – total dry biomass (g pot^{-1}); LDB – leaf dry biomass (g pot^{-1}); stem (%).

Root mass and volume were influenced by the interaction ($P < 0.05$) between microbial inoculation and phytohormones. Root length was influenced ($P < 0.05$) by the presence of phytohormones and was greater in plants that received this input (Table 5). The use of PGR results in a 5.96% increase in the final root length of basilisk grass.

Table 5. Root characteristics of Basilisk grass cultivated with or without microbial inoculation under the presence or absence of phytohormones

Item	Microorganisms				PGR		*P value*			CV
	Cont	Bac	Fun	Bac+Fun	Com	Sem	M*PGR	PGR	M	(%)
RB	15.5	19.0	16.0	17.1	16.1	17.4	0.002	0.004	< 0.001	8.1
RV	162.0	190.0	168.0	188.0	178	176	< 0.001	0.631	< 0.001	7.4
RL	46.4	46.8	46.2	47.1	48.0a	45.3b	0.545	0.003	0.874	5.9

Means followed by different uppercase letters for microorganisms and lowercase letters for the presence of phytohormones differ significantly according to Tukey's test ($P < 0.05$). RB – root biomass (g pot^{-1}); RV – root volume (mL); RL – root length (cm). Cont – control; Bac – Bacteria; Fung – Fungus; M*PGR – interaction between microorganisms (M) and plant growth regulators (PGR); CV – coefficient of variation.

In the presence of phytohormones, the control group plants, along with those inoculated with fungi, showed lower root mass and volume (Table 6). The use of phytohormones associated with bacteria resulted in a 37.14% increase in basilisk grass root biomass. In the absence of exogenous phytohormones, plants that were inoculated with microorganisms showed a 21% increase in root volume compared to plants in the control group (Table 6). Root volume was greater in plants without phytohormones when inoculated with microorganisms. When combined with phytohormones, bacteria had a more significant effect on root volume than fungi.

Table 6. Unfolding of the interaction between microorganisms and phytohormone on root mass and volume of Basilisk grass

Item	PGR	Microorganisms			
		Cont	Bac	Fun	Bac+Fun
RB	Without	16.62Aa	18.65Aa	17.50Aa	16.72Aa
	With	14.35Ab	19.68Aa	13.76Bb	17.50Aa
RV	Without	152Ab	188Aa	184Aa	180Aa
	With	172Aab	192Aa	152Bb	196Aa

Means followed by uppercase letters in the column and lowercase letters in the row differ significantly according to Tukey's test ($P < 0.05$). PGR – plant growth regulators; RB – root biomass (g pot^{-1}); RV – root volume (mL); Cont – control; Bac – Bacteria; Fung – Fungus.

The interaction between microbial inoculation and the presence of phytohormones was significant ($P < 0.05$) for chlorophyll a concentration, total chlorophyll, and SPAD index (Table 7).

The control group and bacteria + fungus, which were associated with the presence of phytohormones, showed higher concentrations of chlorophyll a and total chlorophyll when compared with the same groups in the absence of phytohormones (Table 8). With the addition of phytohormones, there were no differences between the inoculations with microorganisms. The combined use of phytohormones and microorganisms

(bacteria and fungi) resulted in a 20% increase in total chlorophyll. Additionally, a 25% increase was observed with the use of phytohormones alone.

Table 7. Concentration of chlorophylls and SPAD index of Basilisk grass cultivated with or without microbial inoculation in the presence or absence of phytohormone

Item	Microorganisms				PGR		*P value*			CV
	Cont	Bac	Fun	Bac+Fun	With	Without	M*PGR	PGR	M	(%)
CL*a*	0.48	0.53	0.54	0.53	0.55	0.49	0.01	<0.01	0.00	8.39
CL*b*	0.13	0.13	0.14	0.15	0.14	0.13	0.28	0.10	0.06	14.5
CLT	0.61	0.67	0.70	0.67	0.70	0.63	<0.01	<0.01	<0.01	7.2
SPD	22.76	22.85	23.38	22.71	22.95	22.91	<0.01	0.92	0.80	7.46

Means followed by different uppercase letters for microorganism differ from each other by Tukey's test ($P < 0.05$). CLa – chlorophyll *a*; CLb – chlorophyll *b*; CLT – total chlorophylls; SPAD index; Cont – control; Bac – Bacteria; Fung – fungus; M*PGR – interaction between microorganisms (M) and plant growth regulators (PGR); CV – coefficient of variation.

However, in the absence of phytohormones, higher levels of chlorophyll a and total chlorophyll were observed in the group inoculated with bacteria and isolated fungi. Basilisk grass plants exhibited a lower SPAD index when inoculated with *A. brasilense* and phytohormones. There was no difference in the SPAD index between plants that received phytohormones and those that did not, regardless of the microorganism inoculation.

Table 8. Unfolding of chlorophyll concentrations with significant interaction between microorganisms and phytohormones in Basilisk grass

Item	PGR	Microorganisms			
		Cont	Bac	Fun	Bac+Fun
CL *a*	Without	0.426Bb	0.552Aa	0.523Aa	0.496Bab
	With	0.534Aa	0.525Aa	0.575Aa	0.571Aa
CLT	Without	0.545Bb	0.690Aa	0.688Aa	0.615Bab
	With	0.682Aa	0.660Aa	0.723Aa	0.740Aa
SPAD	Without	22.3Aa	24.6Aa	22.7Aa	22.0Aa
	With	23.3Aa	21.1Ba	24.0Aa	23.5Aa

Means followed by uppercase letters in the column and lowercase letters in the row differ from each other by Tukey's test ($P < 0.05$). PGR – plant growth regulators; CL*a* – chlorophyll *a* (mg.g); CLT – Total Chlorophylls; SPAD index.

The contents of dry matter (DM), crude protein (CP), aether extract (EE), ash (ASH), total carbohydrates (TC), and non-fibrous carbohydrates (NFC) showed an interaction effect ($P < 0.05$) between inoculations and the presence of phytohormones (Table 9). The neutral detergent fibre (NDF) and lignin (LIG) contents were not affected ($P > 0.05$) by the factors evaluated in this experiment.

The levels of acid detergent fibre (ADF), hemicellulose (HEMI) and dry matter digestibility (DMD) were affected by phytohormones. Although plants that did not receive phytohormones had higher ADF content, plants that received phytohormones showed higher levels of HEMI and DMD.

Table 9. Bromatological characteristics of Basilisk grass cultivated with or without microbial inoculation under presence or absence of phytohormone

Item	Microorganisms				PGR		*P value*			CV
	Cont	Bac	Fung	Bac+Fun	With	Without	M*PGR	PGR	M	(%)
DM	19.4	20.7	18.9	20.7	20.6	19.3	0.024	0.092	0.226	11.9
CP	9.7	10.2	10.2	10.7	10.2	10.1	0.048	0.746	0.035	7.0
NDF	71.3	71.2	71.1	71.3	71.4	71.1	0.426	0.353	0.986	1.7
ADF	46.5	46.1	45.8	41.9	43.5b	46.7a	0.822	0.027	0.064	9.2
HEM	24.7	29.0	25.5	25.1	27.4 a	24.7b	0.934	0.038	0.082	15.4
LIG	4.8	5.6	5.2	5.0	5.2	5.1	0.385	0.745	0.313	19.1
ASH	7.5	8.1	8.2	8.1	8.3	7.9	0.010	< 0.001	0.217	3.3
TDN	54.1	53.1	54.1	54.0	54.0	54.1	0.426	0.353	0.988	0.9
TC	79.0	78.3	78.5	78.2	78.3	78.7	0.004	0.212	0.337	1.4
NFC	7.7	7.3	7.1	6.9	6.9	7.6	0.003	0.098	0.621	20.1
DMD	52.6	56.2	53.2	53.0	55.0a	52.5b	0.822	0.020	0.064	5.9

Means followed by different lowercase letters for phytohormone presence differ from each other by Tukey's test ($P < 0.05$). DM – dry matter; CP – crude protein; NDF – neutral detergent fibre; ADF – acid detergent fibre; HEM – hemicellulose; LIG – lignin; EE – ether extract; ASH – ash; TDN – total digestible nutrients; TC – total carbohydrates; NFC – non-fibrous carbohydrates; DMD – dry matter digestibility; Cont – control; Bac – Bacteria; Fung – fungus; M*PGR – interaction between microorganisms (M) and plant growth regulators (PGR); CV – coefficient of variation.

With co-inoculation, Basilisk grass plants exhibited higher dry matter content when phytohormones were added. In the absence of phytohormones, the dry matter content did not differ between the inoculations with microorganisms, whereas in the presence of phytohormones, the highest dry matter content was recorded for plants inoculated with bacteria and co-inoculated (Bac + Fung) (Table 10).

Table 10. Unfolding of bromatological characteristics with significant interaction between microorganisms and phytohormones of basilisk grass

Item	PGR	Microorganisms			
		Control	Bacteria	Fungus	Bac+Fung
DM	Without	20.5Aa	19.7Aa	18.6Aa	18.4Ba
	With	18.4Ab	21.7Aa	19.1Aab	24.1Aa
CP	Without	9.2Bb	9.9Aab	10.5Aab	11.0Aa
	With	10.1Aa	10.4Aa	9.9Aa	10.4Aa
ASH	Without	7.7Ba	7.9Ba	7.9Ba	8.2Aa
	With	8.2Aa	8.3Aa	8.5Aa	8.0Aa
TC	Without	80.0Aa	78.8Aab	78.7Aab	77.3Bb
	With	78.0Ba	78.2Aa	77.8Aa	79.1Aa
NFC	Without	8.9Aa	7.8Aab	8.2Aab	5.7Bb
	With	6.6Ba	6.7Aa	6.1Bb	8.1Aa

Means followed by uppercase letters in the column and lowercase letters in the row differ from each other by Tukey's test ($P < 0.05$). PGR – plant growth regulators; DM – dry matter; CP – crude protein; ASH – ash; TC – total carbohydrates; NFC – non-fibrous carbohydrates; Bac – Bacteria; Fung – fungus.

The control group, in the presence of phytohormones, showed a 9.7% increase in CP content compared to the same group that did not receive phytohormones. The highest crude protein (CP) content, when no phytohormones were added, was found in plants

that were co-inoculated; however, in the presence of the phytohormone-based product, this content did not vary with the application of microorganisms.

Plants from the control group, inoculated with bacteria and fungus individually, showed higher ash content when phytohormones were added to the system (Table 10). With or without phytohormones, the evaluated inoculations did not present differences in the mean ash content.

In the control group, Basilisk grass showed lower total carbohydrates (TC) and non-fibrous carbohydrates (NFC) content when evaluated alongside phytohormones. Conversely, plants that received co-inoculation exhibited higher TC and NFC contents when evaluated alongside phytohormones. Plants that did not receive phytohormone application showed higher total and non-fibrous carbohydrate content when they did not receive inoculation or were inoculated with bacteria and fungi individually (Table 10). In the presence of phytohormones, there was no difference between the inoculations with microorganisms.

DISCUSSION

The action of plant growth-promoting microorganisms (PGPM), such as the bacteria *Azospirillum brasilense*, *Pseudomonas fluorescens*, and the mycorrhizal fungus *Rhizophagus intraradices*, involves a symbiotic mechanism in which the host plant provides energy for the microorganism's growth while they assist the plant in its development. Among the benefits these microorganisms bring to forage plants, one can highlight the increase in water and nutrient absorption, synthesis and release of phytohormones, and activation of plant protection mechanisms (Dowarah et al., 2021; Guimarães et al., 2022; Liao et al., 2023). In this sense, the microorganism-plant interaction can alter the physiology involving mechanisms of plant tissue formation, thus resulting in modifications in the structure of morphological components of a forage plant.

The morphogenetic characteristics of forage plants are affected by a combination of factors involving their genetics and the ecological factors of the environment in which the plant is being cultivated (Cruz et al., 2022). In this study, the inoculation with microorganisms was not sufficient to alter the morphogenetic characteristics of Basilisk grass (Table 2). It is likely that the amount of nitrogen fertilisation (50 kg of N ha^{-1}) performed in all plants inferred the same pattern of morphogenetic characteristics of Basilisk grass, regardless of the use of inoculation with bio-inputs. According to Duarte et al. (2020), bacterial strains act differently depending on the forage plant species that are inserted in the pasture ecosystem. These authors reported that inoculation with different species of microorganisms did not promote changes in the phyllochron, leaf appearance rates, stem elongation, and tiller density of Xaraés (*Urochloa brizantha* cv. Xaraés) and Ruziziensis (*Urochloa ruziziensis*) grasses.

The use of plant growth-promoting bacteria (PGPB) and arbuscular mycorrhizal fungi in forage grasses has been widely advocated as a means of mitigating plant stresses (Goswami & Deka, 2020; Marro et al., 2022; Zhang et al., 2022). Thus, beyond reducing stress caused by factors existing in the pasture ecosystem, the action of these microorganisms can also aid in increasing the productivity of forage plants.

In this study, in the absence of exogenous phytohormones, inoculation with PGPB and AMF, either individually or co-inoculated, resulted in a 21% increase in root volume (Table 6) and a 14% increase in crude protein content (Table 10) compared with non-inoculated plants. These increases reveal the positive effect of the symbiotic interaction between the microorganisms and the forage plant used in this study. In support of our findings, in *Urochloa* syn. *Brachiaria* species, inoculation with *A. brasilense* (Hungria et al., 2021) and *P. fluorescens* (Lopes et al., 2018, 2021) promoted significant gains in root characteristics and chlorophyll pigment concentration of the forage plant.

Arbuscular mycorrhizal fungi can facilitate the absorption of nitrogen and phosphorus by plants with the assistance of specific proton pumps, such as H+-ATPases, which stimulate the absorption process of these nutrients (Lanfranco et al., 2018; Liu et al., 2020; Li et al., 2022). According to Hungria et al. (2021), inoculation with bacteria of the species *A. brasilense* provides nitrogen increment in pasture cultivation, thus serving as an ally for supplying the nitrogen inputs necessary for the production of forage grasses. In addition, bacteria of the species *P. fluorescens* can solubilise phosphorus present in the soil, facilitating the absorption of this nutrient by plant roots (Guimarães et al., 2022). In the bacteria-plant relationship, the facilitation mechanisms for nitrogen absorption involve physiological processes resulting from the presence of the nitrogenase enzyme complex (Kour et al., 2019), as well as the ACC-deaminase synthesis route (Danish et al., 2020), while the solubilisation and availability of phosphorus are carried out through acidification, chelation, and exchange reactions, which increase the availability and absorption of this nutrient for the plant (Senthil Kumar et al., 2018; Barin et al., 2022).

Inoculation with PGPM can promote the release of phytohormones (auxins, gibberellins, cytokinins, jasmonates, etc.) that act as regulators of plant growth (Fukami et al., 2017). Endogenous release of phytohormones is related not only to plant development and growth but also to plant survival mechanisms against stresses caused by biotic and abiotic factors (Iqbal et al., 2022), with each hormone playing a different role in the physiological maintenance of forage plants (Jogawat et al., 2021; Hussain et al., 2024). In this regard, the use of plant growth regulator (PGR) can assist in providing the hormonal boost that the plant needs for its development, thus increasing its forage production.

In light of the benefits that the association of plant growth-promoting microorganisms brings to the plant, it is possible to identify, in the data presented in this research, that the effect of co-inoculation can be enhanced with the use of PGR. Co-inoculation + phytohormones resulted in percentage increases of 21% for total mass and 26% for leaf mass compared with the absence of PGR (Table 4). This combination also benefited the percentage of grass stems, with a recorded increase of 16% compared with the control, where such gain is necessary to ensure plant support and structure. Previous studies have reported significant increases in forage production in the presence of PGR (Rocha et al., 2020) and rhizosphere microorganisms (Hungria et al., 2021; Guimarães et al., 2022).

The use of plant growth regulators as a form of bioinputs, aimed at contributing to the regrowth of Basilisk grass, could be a viable alternative, given that plants receiving the PGR showed higher rates of stem elongation (Table 2). Such a pattern can be identified in the literature where Oliveira et al. (2019) reported higher rates of stem

accumulation in Marandu grass (*Urochloa brizantha* cv. Marandu) when PGR was used, a result of the synergistic action of exogenous phytohormone utilisation. Furthermore, the beneficial effects of using plant growth regulators for Basilisk grass are evidenced by the increase in the root length (Table 5) and leaf digestibility (Table 9) of Basilisk grass.

In this experiment, the total mass and leaf mass in co-inoculated plants (PGPB + AMF) in the presence of PGR were correlated with the increase in photosynthetic activity promoted by the elevation of chlorophyll a and total (Table 8). The increase in chlorophyll content enhances the photosynthesis of the forage plant through the absorption of light and carbon, which will be used for plant growth and maintenance (Taiz et al., 2017). Thus, the elevation of photosynthetic pigments in Basilisk grass plants contributes to the increase in forage mass observed in plants inoculated with PGPB + AMF + PGR (Table 4). Furthermore, the effect of enhancing photosynthesis through the elevation of photosynthetic pigments was observed when the leaves of co-inoculated plants (PGPB + AMF) in the presence of PGR resulted in higher concentrations of carbohydrates (Table 10). This physiological increase in photosynthesis may provide greater energy reserves to be used for growth, productivity and mobilized during periods of stress experienced by the plant (Vendruscolo et al., 2021; Cruz et al., 2023).

Regardless of the use of microorganisms, plants showed longer roots with the use of phytohormones (Table 5). However, plants inoculated with fungi showed lower root mass and volume when associated with phytohormones (Table 7), but not enough to affect nutrient absorption. The presence of phytohormones can stimulate the development of root hairs in plants inoculated with AMF, thereby increasing branching and/or density. Liu et al. (2016) consider that studies reveal an increase in root hairs, especially in situations where cultivation is carried out in soil with low fertility.

Reinforcing the previously mentioned assertion, the data presented in this research infer efficient nutrient absorption by plants associated with *R. intraradices* in the presence of PGR, which obtained a 7.5% increase in mineral content in the aerial part (Table 10), surpassing plants grown without PGR, indicating a positive association between fungi and PGR on the nutritional status of the evaluated grass species. Moreover, inoculation with the association between PGPB and PGR increased the mineral content of Basilisk grass leaves by 5% compared with plants that received PGPB without growth regulators (Table 10). This indicates that the combined action of bacteria and PGR has the capacity to optimise mineral absorption and positively contribute to mineral fixation in Basilisk grass leaves.

It is still possible to identify the beneficial effect of using PGR on the nutritional quality of the forage plant when, in the data presented in this research, we identified that plants in the control group, with the addition of exogenous phytohormones, showed an increase of 9.8% and 6.4% for crude protein and mineral content (Table 10), respectively, compared with plants untreated with PGR. These results support the findings of Pezenti et al. (2022), who reported higher levels of crude protein in Napier grass (*Pennisetum purpureum* cv. Napier) when treated with plant growth regulators.

The increase in crude protein in plants treated with plant growth regulators may be related to the increase in total chlorophyll found in this study. Overall, chlorophylls are nitrogenous compounds related to the nitrogen content in the leaf, which is associated with biomass yield and improvements in the quality of this morphological component (López-Calderón et al., 2020; Kaspary et al., 2020).

Plants not inoculated with microorganisms (PGPB and AMF isolated or combined) and not treated with PGR showed lower levels of total chlorophyll, whereas plants inoculated with PGPB and AMF isolated or co-inoculated promoted an increase in chlorophyll a and total chlorophyll of 23% and 22%, respectively, for chlorophyll a and total concentration (Table 8), as well as lower levels of crude protein. Among the factors that can stimulate the reduction of photosynthetic pigments in leaves, leaf senescence promotes the degradation of chlorophylls, which are translocated to organs during growth. Thus, according to Huang et al. (2022), maintaining chlorophyll concentrations is of fundamental importance to keep the leaf in a vegetative state, delaying its senescence, which is a mechanism involving the synthesis and accumulation of ethylene that stimulates cell death, resulting in a decrease in leaf nutrients (Taiz et al., 2017; Yu et al., 2021). However, interactions between hormones, such as auxin and cytokinin, can reduce gene expression that activates leaf senescence, thereby delaying its death (Chen & Huang, 2022).

In this experiment, the PGR used comprised kinetin (which acts similarly to cytokinin), 4-indole-3-butyric acid (a form of synthetic auxin), and gibberellic acid (such as GA3). Thus, it is possible that the use of PGR delayed the process of leaf senescence, maintaining higher levels of chlorophyll and crude protein concentration compared with plants that were not treated with the growth regulator (Table 8 and 10).

CONCLUSIONS

The combination of plant growth regulators with *A. brasilense*, *P. fluorescens*, and *R. intraradices* contributes to the increase in Basilisk grass biomass. Furthermore, the use of a plant growth regulator leads to increases in crude protein content in non-inoculated plants. Inoculation with microorganisms improves the nutritional quality through the accumulation of chlorophyll pigments, resulting in the elevation of Basilisk grass's crude protein content.

ACKNOWLEDGEMENTS. To National Council for Scientific and Technological Development (CNPq, Portuguese: Conselho Nacional de Desenvolvimento Científico e Tecnológico), for the doctoral scholarship. Thanks to the State University of Southwest Bahia for the support during the research development.

REFERENCES

Alvarez, V.V.H. & Ribeiro, A.C. 1999. Liming. Recommendation for the use of correctives and fertilizers in Minas Gerais. *5th Aproximação*. Viçosa, MG: Soil Fertility Commission of the State of Minas Gerais, 359 pp. (in Brazilian Portuguese).

Barin, M., Asadzadeh, F., Hosseini, M., Hammer, E.C., Vetukuri, R.R. & Vahedi, R. 2022. Optimization of biofertilizer formulation for phosphorus solubilizing by *Pseudomonas fluorescens* Ur21 via response surface methodology. *Processes* **10**(4), 650. doi: 10.3390/pr10040650

Cappelle, E.R., Valadares Filho, S.D.C., Silva, J.F.C.D. & Cecon, P.R. 2001. Estimates of the Energy Value from Chemical Characteristics of the Feedstuffs. *Brazilian Journal of Animal Science* **30**, 1837–1856 (in Brazilian Portuguese). doi: https://doi.org/10.1590/S1516-35982001000700022

Chen, W. & Huang, B. 2022. Cytokinin or ethylene regulation of heat-induced leaf senescence involving transcriptional modulation of WRKY in perennial ryegrass. *Physiologia Plantarum* **174**(5), e13766. doi: 10.1111/ppl.13766

Colebrook, E.H., Thomas, S.G., Phillips, A.L. & Hedden, P. 2014.The role of gibberellin signalling in plant responses to abiotic stress. *Journal of experimental biology* **217**(1), 67–75. doi: 10.1242/jeb.089938

Cruz, N.T., Jardim, R.R., De Lana Sousa, B.M., Seixas, A.A., Fries, D.D., Pires, A.J.V., Dias, D.L.S., Bonomo, P., Ramos, B.L.P., Alcântara, W.Q. & Santos, A.P.D.S. 2022. Energy flows and organic reserves of forage plants. *Research, Society and Development* **11**(12), e49111234782-e549111234782. doi: 10.33448/rsd-v11i12.34782

Cruz, E.R.T., Teixeira, F.A., Fries, D.D., Jardim, R.R., Cruz, N.T., Rossa, F., Santos, A.P.S., Porto, E.M.V. & Silva, H.S. 2023. Yield and morphology of *Nopalea cochenillifera* under N fertilization and biological inoculation. *Agronomy Research* **21**(S3), 1464–1472. doi: 10.15159/AR.23.104

Cunha, F.N., Da Silva, N.F., Bastos, F.J.D.C., De Carvalho, J.J., Moura, L.M.D.F., Teixeira, M.B. & Souchie, E.L. 2014. Effect of *Azospirillum brasilense* on productivity of maize in southwest goiás. *Brazilian Journal of Maize and Sorghum* **13**(3), 261–272 (in Brazilian Portuguese). doi: 10.18512/1980-6477/rbms.v13n3p261-272

Danish, S., Zafar-Ul-Hye, M., Mohsin, F. & Hussain, M. 2020. ACC-deaminase producing plant growth promoting rhizobacteria and biochar mitigate adverse effects of drought stress on maize growth. *PLoS One* **15**(4), e0230615. doi: 10.1371/journal.pone.0230615

Detmann, E., Souza, M.A., Valadares Filho, S.C., Queiroz, A.C., Berchielli, T.T., Saliba, E.O.S., Cabral, L.S., Pina, D.S., Ladeira, M.M. & Azevedo, J.A.G. 2012. *Methods for food analysis*. 1. ed Visconde do Rio Branco: Suprema, 214 pp. (in Brazilian Portuguese).

Dias-Filho, M.B. 2014. *Diagnosis of Pastures in Brazil*. Embrapa Eastern Amazon: Belém, Brazil, 38 pp. (in Brazilian Portuguese).

Dowarah, B., Gill, S.S. & Agarwala, N. 2021. Arbuscular mycorrhizal fungi in conferring tolerance to biotic stresses in plants. *Journal of Plant Growth Regulation* **41**(4), 1429–1444. doi: doi.org/10.1007/s00344-021-10392-5

Duarte, C.F.D., Cecato, U., Hungria, M., Fernandes, H.J., Biserra, T.T., Galbeiro, S., Toniato, A.K.B. & Silva, D.R. 2020. Morphogenetic and structural characteristics of *Urochloa* species under inoculation with plant-growth-promoting bacteria and nitrogen fertilisation. *Crop and Pasture Science* **71**(1), 82–89. doi: doi.org/10.1071/CP18455

Fukami, J., Ollero, F.J., Megías, M. & Hungria, M. 2017. Phytohormones and induction of plant-stress tolerance and defense genes by seed and foliar inoculation with *Azospirillum brasiliense* cells and metabolites promote maize growth. *AMB Express* **7**, 1–13. doi: 10.1186/s13568-017-0453-7

Goswami, M. & Deka, S. 2020. Plant growth-promoting rhizobacteria—alleviators of abiotic stresses in soil: a review. *Pedosphere* **30**(1), 40–61. doi: 10.1016/S1002-0160(19)60839-8

Guimarães, G.S., Rondina, A.B.L., Santos, M.S., Nogueira, M.A. & Hungria, M. 2022. Pointing out opportunities to increase grassland pastures productivity via microbial inoculants: Attending the society's demands for meat production with sustainability. *Agronomy* **12**(8), 1748. doi: 10.3390/agronomia12081748

Hiscox, J.D. & Israelstam, G.F. 1979. A method for the extraction of chlorophyll from leaf tissue without maceration. Canadian *Journal of Botany* **57**(12), 1332–1334. doi: 10.1139/b79-163

Hourani, W. 2023. Effect of fertilizers on growth and productivity of saffron: a review. *Agronomy Research* **21**(1), 87–105. doi: 10.15159/AR.22.082

Huang, Y., Li, X., Duan, Z., Li, J., Jiang, Y., Cheng, S., Xue, T., Zhao, F., Sheng, W. & Duan, Y. 2022. Ultra-low concentration of chlorine dioxide regulates stress-caused premature leaf senescence in tobacco by modulating auxin, ethylene, and chlorophyll biosynthesis. *Plant Physiology and Biochemistry* **186**, 31–39. doi: 10.1016/j.plaphy.2022.06.029

Hungria, M., Campo, R.J., Souza, E.M. & Pedrosa, F.O. 2010. Inoculation with selected strains of *Azospirillum brasilense* and *A. lipoferum* improves yields of maize and wheat in Brazil. *Plant and soil* **331**, 413–425. doi: 10.1007/s11104-009-0262-0

Hungria, M., Rondina, A.B.L., Nunes, A.L.P., Araújo, R.S. & Nogueira, M.A. 2021. Seed and leaf-spray inoculation of PGPR in brachiarias (*Urochloa* spp.) as an economic and environmental opportunity to improve plant growth, forage yield and nutrient status. *Plant and Soil* **463**, 171–186. doi: 10.1007/s11104-021-04908-x

Hussain, S., Hafeez, M.B., Azam, R., Mehmood, K., Aziz, M., Ercisli, S., Javed, T., Raza, A., Zehra, N. & Ren, X. 2024. Deciphering the Role of Phytohormones and Osmolytes in Plant Tolerance Against Salt Stress: Implications, Possible Cross-Talk, and Prospects. *Journal of Plant Growth Regulation* **43**(1), 38–59. doi: 10.1007/s00344-023-11070-4

Iqbal, S., Wang, X., Mubeen, I., Kamran, M., Kanwal, I., Díaz, G.A., Abbas, A., Parveen, A., Atiq, M.N., Alshaya, H., El-Abedin, T.K.Z. & Fahad, S. 2022. Phytohormones trigger drought tolerance in crop plants: outlook and future perspectives. *Frontiers in Plant Science* **12**, 3378. doi: 10.3389/fpls.2021.799318

Jogawat, A., Yadav, B., Chhaya, Lakra, N., Singh, A.K. & Narayan, O.P. 2021. Crosstalk between phytohormones and secondary metabolites in the drought stress tolerance of crop plants: a review. *Physiologia Plantarum* **172**(2), 1106–1132. doi: 10.1111/pp.13328

Kaspary, T.E., Cutti, L., Bellé, C., Casarotto, G. & Ramos, R.F. 2020. Nondestructive analysis of photosynthetic pigments in forage radish and vetch. *Revista Ceres* **67**, 424–431. doi: 10.1590/0034-737X202067060001

Kour, D., Rana, K.L., Yadav, A.N., Yadav, N., Kumar, M., Kumar, V. & Vyas, P.D. 2019. Microbial biofertilizers: bioresources and eco-friendly technologies for agricultural and environmental sustainability. *Biocatalysis and Agricultural Biotechnology* **23**, 101487. doi: 10.1016/j.bcab.2019.101487

Lanfranco, L., Fiorilli, V. & Gutjahr, C. 2018. Partner communication and role of nutrients in the arbuscular mycorrhizal symbiosis. *New Phytologist* **220**(4), 1031–1046. doi: 10.1111/nph.15230

Li, Y., Zeng, H., Xu, F., Yan, F. & Xu, W. 2022. H+-ATPases in plant growth and stress responses. *Annual Review of Plant Biology* **73**, 495–521. doi: 10.1146/annurev-arplant-102820-114551

Liao, X., Zhao, J., Xu, L., Tang, L., Li, J., Zhang, W., Xiao, J., Xiao, Dan., Hu, P., Nie, Y., Zou, De. & Wang, K. 2023. Arbuscular mycorrhizal fungi increase the interspecific competition between two forage plant species and stabilize the soil microbial network during a drought event: Evidence from the field. *Applied Soil Ecology* **185**, 104805. doi: 10.2139/ssrn.4074262

Licea-Herrera, J.I., Quiroz-Velásquez, J.D. & Hernández-Mendoza, J.L. 2020. Impact of *Azospirillum brasilense*, a rhizobacterium stimulating the production of indole-3-acetic acid as the mechanism of improving plants' grow in agricultural crops. *Bolivian Journal of Chemistry* **37**, 34–39 (in Spanish) doi: 10.34098/2078-3949.37.1.5

Liu, J., Chen, J., Xie, K., Tian, Y., Yan, A., Liu, J., Huang, Y., Wang, S., Zhu, Y., Chen, A. & Xu, G. 2020. A mycorrhiza-specific H+-ATPase is essential for arbuscule development and symbiotic phosphate and nitrogen uptake. *Plant, cell & environment* **43**(4), 1069–1083. doi: 10.1111/pce.13714

Liu, C.Y., Srivastava, A.K., Zhang, D.J., Ying-Ning, Z.O.U. & Wu, Q.S. 2016. Exogenous phytohormones modulate mycorrhiza-induced changes in root hair configuration of trifoliate orange. *Notulae Botanicae Horti Agrobotanici Cluj-Napoca* **44**(2), 548–556. doi: 10.15835/nbha44210540

Lopes, M.J.S., Dias Filho, M.B., Castro, T.H.R., Gurgel, E.S.C. & Da Silva, G.B. 2021. Efficiency of biostimulants for alleviating shade effects on forage grass. *Journal of Agricultural Studies* **9**(3), 14–30. doi: 10.5296/jas.v9i3.18611

Lopes, M.J.S., Dias Filho, M.B., Castro, T.H.R. & Silva, G.B. 2018. Light and plant growth-promoting rhizobacteria effects on *Brachiaria brizantha* growth and phenotypic plasticity to shade. *Grass and Forage Science* **73**(2), 493–499. doi: 10.1111/gfs.12336

López-Calderón, M.J., Estrada-Ávalos, J., Rodríguez-Moreno, V.M., Mauricio-Ruvalcaba, J.E., Martínez-Sifuentes, A.R., Delgado-Ramírez, G. & Miguel-Valle, E. 2020. Estimation of total nitrogen content in forage maize (*Zea Mays* l.) Using Spectral Indices: Analysis by Random Forest. *Agriculture* **10**(10), 451. doi: 10.3390/agricultura10100451

Marro, N., Grilli, G., Soteras, F., Caccia, M., Longo, S., Cofré, N., Borda, V., Burni, M., Janousková, M. & Urcelay, C. 2022. The effects of arbuscular mycorrhizal fungal species and taxonomic groups on stressed and unstressed plants: a global meta-analysis. *New Phytologist* **235**(1), 320–332. doi: 10.1111/nph.18102

Nadeem, S.M., Ahmad, M., Zahir, Z.A., Javaid, A., Ashraf, M. 2014. The role of mycorrhizae and plant growth promoting rhizobacteria (PGPR) in improving crop productivity under stressful environments. *Biotechnology Advances* **32**(2), 429–448. doi: doi:10.1016/j.biotechadv.2013.12.005

Oliveira, W.F., Lima, E.M., Gomes, D.I., Alves, K.S., Santos, P.M., Azevedo, G.S. & Mezzomo, R. 2019. Agronomic performance of Marandu grass treated with plant growth biostimulants in the Amazon biome. *Arquivo Brasileiro de Medicina Veterinária e Zootecnia* **71**, 603–612. doi: 10.1590/1678-4162-10369

Pezenti, E., Dos Santos Pedreira, M., De Albuquerque Fernandes, S.A., Nery, M.S., Vitor, A.D.C.P., Silva, A.S. & Ramos, B.L.P. 2022. Use of biostimulants in elephant grass cv. Napier. *Semina ciências. agrarias* **43**(1), 91–106. doi: 10.5433/1679-0359.2022v43n1p91

Rocha, L.C., Teixeira, F.A., Pedreira, M.D.S., Frietas, D.D., Dias, D.L.S., Costa, E.G.L., Figueiredo, A.J., Seixas, A.A., Pacheco, C.C. & Santiago, B.M. 2020. Plant growth regulator and soil fertilizer improve production and growing stage of *Brachiaria decumbens*. *Grassland science* **66**(2), 102–109. doi: 10.1111/grs.12260

Rodrigues, R.C. 2010. *Food bromatological analysis methods: physical, chemical and bromatological methods.* Documentos, **306** (in Brazilian Portuguese).

Senthil Kumar, C.M., Jacob, T.K., Devasahayam, S., Stephy, T. & Geethu, C. 2018. Multifarious plant growth promotion by an entomopathogenic fungus *Lecanicillium psalliotae*. *Microbiological research* **207**, 153–160. doi: 10.1016/j.micres.2017.11.017

Sniffen, C.J., O'connor, J.D. & Van Soest, P.J. 1992. A net carbohydrate and protein system for evaluating cattle diets: II. carbohydrate and protein availability. *Journal of Animal Science* **70**(11), 3562–3577. doi: 10.2527/1992.70113562x

Taiz, L., Zeiger, E., Moller, I.M. & Murphy, A. 2017. *Plant physiology and development.* Artmed: Porto Alegre, 858 pp. (in Brazilian Portuguese).

Vendruscolo, E.P., De Oliveira, P.R., Rodrigues, A.H.A., Correia, S.R., Campos, L.F.C., Seleguini, A. & De Lima, S.F. 2021. Chlorophyll concentration and production of *Urochloa decumbens* treated with diazotrophic bacteria and thiamine in the Brazilian Cerrado. *Tropical Grasslands-Forrajes Tropicales* **9**(1), 134–137. doi: 10.17138/TGFT(9)134-137

Wellburn, A.R. 1994. The spectral determination of chlorophylls a and b, as weel o total carotenoids, using various solvents with spectrophotometers of different resolution. *Journal of Plant Physiology* **144**(3), 307–313. doi: doi.org/10.1016/S0176-1617(11)81192-2

Yu, X., Xu, Y. & Yan, S. 2021. Salicylic acid and ethylene coordinately promote leaf senescence. *Journal of Integrative Plant Biology* **63**(5), 823–827. doi: 10.1111/jipb.13074

Zhang, W., Yu, L., Han, B., Liu, K. & Shao, X. 2022. Mycorrhizal inoculation enhances nutrient absorption and induces insect-resistant defense of Elymus nutans. *Frontiers in plant science* **13**, 898969. doi: 10.3389/fpls.2022.898969

Agronomy Research **22**(S3), 1421–1433, 2024
https://doi.org/10.15159/AR.24.100

Diallel and generation analysis in F_2 soybean populations

S.B. Ferreira[1,*], B.H. Gomes[1], O.T. Hamawaki[2], P.A.S. Dias[3], C.D.L. Hamawaki[2], R.L. Hamawaki[2] and A.P.O. Nogueira[1]

[1]Universidade Federal de Uberlândia, Instituto de Biotecnologia, CEP 38405-320, Uberlândia, MG, Brasil
[2]Universidade Federal de Uberlândia, Instituto de Ciências Agrárias, CEP 38410-337, Uberlândia, MG, Brasil
[3]Instituto Federal Goiano, Campus Urutaí, Núcleo de Agronomia, CEP 75790-000, Urutaí, GO, Brasil
[*]Correspondence: ferreirasb@ hotmail.com

Received: June 14th, 2024; Accepted: September 9th, 2024; Published: Noember 19th, 2024

Abstract. The present study aimed to obtain estimates of the general (GCA) and specific (SCA) combining abilities of three soybean parents by means of the half table balanced diallel and to estimate genetic parameters of agronomic traits in F_2 populations. The experiment was organized in complete randomized blocks with ten replications. The plants obtained from the combinations between the parents UFU 510, UFUS 7415 and MG/BR 46 Conquista were individually evaluated for thirteen agronomic traits. The results indicated that the parent UFUS 7415 had the highest and most positive GCA values for the production components. The best cross was UFU 510 × UFUS 7415, with the highest number of total pods and grain production. The three combinations showed a high coefficient of heritability for the number of productive nodes. At the crossing UFU 510 × UFUS 7415, greater selection gains and higher averages were observed for the number of pods with one, two and three grains and the number of total pods.

Key words: diallel, estimation of genetic parameters, segregating populations.

INTRODUCTION

The genetic breeding of plants is essential for maintaining the global food supply and must evolve to offer products that meet population growth and cultivars capable of overcoming the effects of climate change. The world consumption of oilseeds is expected to continue, not only due to the expectation of population growth, but mainly due to the increase in the consumption of animal protein (Nadathur et al., 2024). In the Brazilian agricultural scenario, soybean crop (*Glycine max* (L.) Merrill) stands out as one of the main commodities. In this sense, investments in soybean breeding programs are indispensable for the search for more productive and adapted to climate change genotypes.

For the success of the genetic breeding of soybean, to be informed about the genetic parameters and to know the combinatorial ability of the available genotypes, makes it possible to develop segregating populations for selective processes. The analysis of

genetic parameters in soybean for agronomic traits is important to direct crosses and maximize the genetic variability of segregating populations. These and other questions can be answered from crosses that follow some genetic design (Bornhofen, 2019), such as half table balanced diallel cross.

With the diallel analysis it is possible to obtain information about the behavior of the involved parents and the hybrid combinations that result in superior segregating populations by means of estimates of the general (GCA) and specific (SCA) combining abilities (Teodoro et al., 2019). Evalutation of the combining ability of self-pollinating species often use the relation between GCA and SCA to indicate the predominant type of gene action in trait expression. GCA primarily reflects additive gene effects and additive × additive interactions, whereas SCA is associated with dominance effects, epistatic deviations, and genotype × environment interactions (Rialch & Sharma, 2019).

For soybeans, diallel analysis has proven effective in exploring genetic variability and identifying the best parents for crosses. Bagateli et al. (2020) used a partial diallel to estimate GCA and SCA for eight soybean genotypes, focusing on traits related to production, plant architecture and maturity, which enabled them to select the optimal genotypes combinations. Similarly, Soares et al. (2023) obtained valuable genetic information on ten soybean parents and their F1 hybrids through diallel analysis, allowing them to evaluate the dissimilarity between parents and crosses. Also, Chagas et al. (2023) estimated the combining ability of soybean cultivars in the F_2 generation, for agronomic, nutritional and industrial traits with the goal of identifying superior segregating parents and populations.

In soybean crop there is a limitation regarding the use of F_1 generation plants for diallel analysis due to the low availability of seeds (Friedrichs et al., 2016) and the predominance of dominance deviations. An alternative is the evaluation of the diallel in F_2 populations. In advanced generations, the dominance deviation is reduced and there is a possibility that the effect of SCA is not meaningful (Pimentel et al., 2014).

Given the above, the objectives of the study were to obtain the GCA and SCA estimates of three soybean parents through the half table balanced diallel, determine genetic parameters of important agronomic traits and estimate the gain selection in F_2 populations, in order to identify the genotypes and the combinations considered promising for the development of superior lines.

MATERIALS AND METHODS

The experiment was carried out in the 2017/2018 season, in an experimental area located at São Lourenço Farm (18° 31' 20.6" S and 46° 04' 49.5" W), in the municipality of Varjão de Minas, Minas Gerais, Brazil. The seeds of the F_2 generation were obtained from the crosses UFU 510 × UFUS 7415, UFU 510 × MG/BR 46 Conquista and UFUS 7415 × MG/BR 46 Conquista. The parents show resistance to the nematode of the galls *Meloidogyne incognita* and *Meloidogyne javanica* (MG/BR 46 Conquista), high yield potential, early cycle and tolerance to Asian soybean rust (UFUS 7415) and tolerance to white mold (UFU 510).

The area was prepared in the conventional tillage system with plowing and two harrows, followed by furrowing. Sowing fertilization was carried out with the formula NPK 02-28-18, at a dose of 400 kg ha^{-1}. Prior to sowing, the seeds were treated with fungicide (Carbendazim and Tiram) and inoculated with *Bradyrhizobium japonicum*,

SEMIA 5079 and SEMIA 5080 strains. Each F_2 generation was sown in pits, with a spacing of 0.50 m between rows and 0.25 m between plants. A randomized complete block design with ten replications was adopted. During the conduct of the experiment, the management of pests and diseases were carried out through applications of insecticides and fungicides, based on technical recommendations and the need of the crop (Embrapa, 2013). To assist in biological nitrogen fixation, 30 days after emergence, cobalt and molybdenum were applied via foliar at a dosage of 100 mL ha^{-1}.

The plants were evaluated individually to obtain information about the following agronomic traits: Plant height at flowering **(PHF)** and maturity **(PHM)**: measured in cm, from the soil surface to the end of the main stem when the plants were in the reproductive stage R1 and R8; Number of nodes on the main stem at flowering **(NNF)** and maturity **(NNM)**: determined by counting the number of nodes on the main stem, when the plants were in the reproductive stage R1 and R8; Number of productive nodes **(NPN)**: number of nodes with pods at maturity; Number of days for flowering **(NDF)** and for maturity **(NDM)**: defined as the number of days from emergence to flowering, when approximately 50% of the plants in the useful plot had at least one open flower (R1) and when 95% of the pods in the useful area of the plot were mature (R8); Insertion height of the first pod **(IHP)**: distance, in cm, measured from the soil surface to the first pod; Number of pods with one grain **(NP1)**, with two grains **(NP2)** and with three grains **(NP3)**: after harvesting, the number of pods with one, two and three grains was counted; Total number of pods per plant **(TNP)**: obtained by the sum of number of pods with one, two and three grains; Grain production per plant **(GP)**: after harvesting, the plants were traced manually, and their grains had their mass determined on an analytical balance, with four decimal places.

The data for each trait was submitted to analysis of variance and the significance level was analyzed using the F-test, at 5% probability. After obtaining the mean of the crossings for the evaluated traits, a half table balanced diallel analysis was carried out according to Griffing's (1956) method 2 and adapted by Geraldi & Miranda Filho (1988).

The effect of the treatments (averages of the three F_2 populations and the three parents) was estimated using the mathematical model:

$$Y_{ij} = \mu + g_i + g_j + s_{ij} + \overline{\varepsilon_{ij}} \quad (1)$$

where Y_{ij}: average value of the hybrid ($i \neq j$) or parent combination ($i = j$); μ: general mean of the diallel; g_i and g_j: effects of the general combining ability of the i-th and the j-th parent, respectively; s_{ij}: effect of specific combining ability for crosses between parents of order i and j; ε_i: mean experimental error.

From the phenotypic values of individuals from the generations of parents and F_2, the genetic parameters described below were estimated (Cruz et al., 2012):

Genotypic variance in F_2:

$$\hat{\sigma}^2_{G(F2)} = \hat{\sigma}^2_{F(F2)} - \hat{\sigma}^2_{e(F2)} \quad (2)$$

where $\hat{\sigma}^2_{G(F2)}$: genetic variance of the F_2 population; $\hat{\sigma}^2_{F(F2)}$: phenotypic variance of the F_2 population; $\hat{\sigma}^2_{e(F2)}$: environmental variance of the F_2 population.

Environmental variance in F_2:

$$\hat{\sigma}^2_{e(F2)} = \frac{1}{2}\left[\hat{\sigma}^2_{(P1)} + \hat{\sigma}^2_{(P2)}\right] \quad (3)$$

where $\hat{\sigma}^2_{e(F2)}$: environmental variance; $\hat{\sigma}^2_{(P1)}$: phenotypic variance of the parent 1; $\hat{\sigma}^2_{(P2)}$: phenotypic variance of the parent 2. Phenotypic variance in F_2:

$$\hat{\sigma}^2_{F(F2)} = \hat{\sigma}^2_{G(F2)} - \hat{\sigma}^2_{e(F2)} \quad (4)$$

where $\hat{\sigma}^2_{F(F2)}$: genetic variance of the F_2 population; $\hat{\sigma}^2_{G(F2)}$: phenotypic variance of the F_2 population; $\hat{\sigma}^2_{e(F2)}$: environmental variance of the F_2 population.

Heritability in the broad sense:

$$h^2_a = \frac{\hat{\sigma}^2_{G(F2)}}{\hat{\sigma}^2_{F(F2)}} \cdot 100 \quad (5)$$

where h^2_a: heritability in the broad sense; $\hat{\sigma}^2_{G(F2)}$: genetic variance of the F_2 population; $\hat{\sigma}^2_{F(F2)}$: phenotypic variance of the F_2 population.

Prediction of gains by selection:

$$\Delta G\% = \frac{\Delta G}{X_0} \quad (6)$$

where ΔG: selection gain; obtained by $DS\ x\ h^2$; DS: selection differential, given by $DS = \overline{X_s} - \overline{X_0}$: average of selected; $\overline{X_0}$: observed average of the F_2 population; h^2: heritability.

Number of genes involved in the trait expression:

$$\eta = \frac{R^2 - (1 + 0.5K^2)}{8\,\hat{\sigma}^2_G} \quad (7)$$

where η: number of genes; R: amplitude between the means of the parents or $R = \overline{P_1} + \overline{P_2}$; $\hat{\sigma}^2_G$: genetic variance.

The means were compared by the Tukey test at the 5% probability level. All analyzes were performed using the Computational Program in Genetics and Statistics - GENES (Cruz, 2016).

RESULTS AND DISCUSSION

Significant effects were found for the general (GCA) and specific (SCA) combining abilities for the agronomic traits number of days to maturity (NDM), plant height at flowering (PHF), plant height at maturity (PHM), number of pods with one and two grains (NP1 e NP2), total number of pods per plant (TNP) and grain production per plant (GP) (Table 1). The significance of the parameters for GCA indicates that there is variability in the additive gene effects and the significance for SCA indicates the predominance of dominance deviations. In breeding programs, the information about GCA and SCA are essential to identify parents that result in promising combinations (Gayosso-Barragán et al., 2019; Kibalnik et al., 2021).

The coefficients of variation (CV) were good, ranging from 0.74% (NDM) to 40.66% (NP1) (Table 1). Higher CV estimates were observed for production components (NP1 and NP3), which is common and occurs because these traits are quantitative, controlled by many genes and highly influenced by the environment (Leite et al., 2015).

The effects of SCA are more important than those of GCA, since the mean square associated with SCA was significant for most of the traits analyzed, which reinforces the greater contribution of non-additive gene action in the control of these traits (Table 1). Bagateli et al. (2020) informs that positive SCA estimates indicate the presence of numerous heterozygous loci leading to greater potential genetic variability, besides being associated with elevated mean values.

Table 1. Summary of the analysis of variance of the partial diallel involving three parents and their hybrid combinations

FV	DF	Medium square						
		NDF	NDM	PHF	PHM	NNF	NNM	NPN
Genotypes	5	1.48^{ns}	3.66**	280.36**	187.59*	2.90*	24.05^{ns}	8.56^{ns}
GCA	2	0.05^{ns}	2.05*	628.78**	184.13^{ns}	3.23^{ns}	12.35^{ns}	1.21^{ns}
SCA	3	2.44^{ns}	4.74**	48.09^{ns}	189.90*	2.68^{ns}	31.85^{ns}	13.46^{ns}
Residue	45	0.91	0.58	52.61	62.01	1.01	16.52	6.12
Overall Average		44.85	103.61	53.54	67.39	12.49	15.97	14.17
CV (%)		2.13	0.74	13.54	11.68	8.05	25.44	17.46

FV	DF	Medium square					
		HIP	NP1	NP2	NP3	TNP	GP
Genotypes	5	2.36^{ns}	260.92**	475.06**	493.43^{ns}	2,679.72*	473.84**
GCA	2	1.70^{ns}	31.89^{ns}	184.38^{ns}	410.23^{ns}	1,220.51^{ns}	225.30^{ns}
SCA	3	2.81^{ns}	413.61**	668.85**	548.90^{ns}	3,652.54*	639.54**
Residue	45	1.12	67.26	103.46	308.90	866.70	100.82
Overall Average		10.11	20.16	52.01	60.49	132.67	49.97
CV (%)		10.46	40.66	19.55	29.05	22.18	20.09

**, *: significant at the level of 1% and 5% probability, respectively, by the F and ^{ns} test, not significant by the F test. DF: Degrees of freedom; CV: coefficient of variation; NDF: number of days for flowering; NDM: number of days to maturity; PHF: plant height at flowering; PHM: plant height at maturity; NNF: number of nodes on the main stem in flowering; NNM: number of nodes on the main stem at maturity; NPN: number of productive nodes; HIP: height of insertion of the first pod; NP1, NP2 e NP3: number of pods with one, two and three grains; TNP: total number of pods per plant; GP: grain production per plant.

Colombo et al. (2018), when analyzing the GCA and SCA of soybean genotypes for agronomic attributes, also identified the predominance of SCA. In contrast, Soares et al. (2023) found highest GCA estimates, which indicates a predominance of additive gene effects in controlling the traits. The differing results can be attributed to the specific population under study, as estimates of genetic parameters are inherently tied to the target population (Soares et al., 2023). Additionally, the complexity of quantitative trait inheritance and the influence of genotype-environment interactions may account for the observed discrepancies (Goksoy et al., 2019).

Estimates of the effects of the GCA of each genotype for the evaluated traits are shown in Table 2. Positive or negative values for GCA indicate that the parent is higher or lower, respectively, than the average of the other parents (Cruz et al., 2012). For production components (NP1, NP2, NP3, TNP and GP), the UFUS 7415 genotype showed the highest and most positive values of the GCA estimates (0.74, 1.67, 3.26, 5.69 and 2.20, respectively). In the crossings in which this parent participates, there will be a contribution to the increase of production components, a desired trait in soybean breeding programs. Rocha et al. (2019) also found positive GCA values for total number of pods and for grain production per plant in segregating soybean populations.

Table 2. Estimates of the effects of the general (GCA) and specific (SCA) combining abilities of agronomic traits evaluated in a partial diallel with three parents

Genotypes	GCA												
	NDF	NDM	PHF	PHM	NNF	NNM	NPN	HIP	NP1	NP2	NP3	TNP	GP
UFU 510	0.03	0.21	-3.95	-2.10	0.01	0.26	0.06	-0.20	0.10	-2.00	-1.20	-3.19	-2.03
UFUS 7415	-0.03	-0.03	1.04	0.43	-0.25	-0.57	-0.17	0.15	0.74	1.67	3.26	5.69	2.20
MG/BR 46 Conquista	-0.00	-0.18	2.90	1.66	0.24	0.30	0.11	0.04	-0.84	0.41	-2.06	-2.49	-0.17
Genotypes	SCA												
	NDF	NDM	PHF	PHM	NNF	NNM	NPN	HIP	NP1	NP2	NP3	TNP	GP
1x1	0.10	0.25	1.43	-4.01	0.43	-1.43	-0.94	0.18	-2.79	-1.87	-6.73	-11.40	-6.64
1x2	-0.63	-0.64	-2.52	4.24	-0.20	0.42	0.68	-0.59	8.76	6.57	8.89	24.23	7.50
1x3	0.42	0.13	-0.33	3.78	-0.67	2.44	1.20	0.21	-3.18	-2.81	4.58	-1.41	5.78
2 × 2	0.31	0.65	1.90	-0.72	0.10	0.16	-0.56	0.49	-5.13	-7.69	-3.85	-16.68	-5.31
2 × 3	0.01	-0.65	-1.27	-2.78	-0.00	-0.76	0.45	-0.39	1.49	8.81	-1.18	9.13	3.13
3 × 3	-0.21	0.25	0.80	-0.49	0.33	-0.84	-0.83	0.08	0.84	-3.00	-1.70	-3.85	-4.45

NDF: number of days for flowering; NDM: number of days to maturity; PHF: plant height at flowering; PHM: plant height at maturity NNF: number of nodes on the main stem in flowering; NNM: number of nodes on the main stem at maturity; NPN: number of productive nodes; HIP: height of insertion of the first pod; NP1, NP2 e NP3: number of pods with one, two and three grains; TNP: total number of pods per plant; GP: grain production per plant; 1: UFU 510; 2: UFUS 7415; 3: BR/MG 46 Conquista.

The height of the plant at flowering and maturity is an important trait, as it influences lodging, another trait that limits the yield potential of the crop (Hwang & Geon, 2019). For PHF and PHM, the parent UFU 510 presented negative values of the GCA estimates (-3.95 and -2.10, respectively), which contributes to the reduction of the average in the analyzed traits, since soybean plants with heights less than 100 cm are ideal (Table 2). Mishra (2019), in order to evaluate six soybean genotypes by means of the general and specific combining abilities in F_1 and F_2 generations, obtained significant and negative (-2.49) value of GCA for plant height in one of the analyzed genotypes.

For the height of insertion of the first pod, the values observed were -0.20, 0.15 and 0.04 for the parents UFU 510, UFUS 7415 and MG/BR 46 Conquista, respectively (Table 2). IHP is an important trait to be analyzed, as the traditional cultivation of soybean depends on mechanized harvesting and cultivars with low values for this trait can be damaged during the harvesting process. In addition, the height of insertion of the first pod is a trait that positively correlates with yield (Jiang et al., 2018).

For the variables NNF, NNM and NPN, the MG/BR 46 Conquista genotype showed the highest positive values, which indicates that it is a promising parent for the manufacture of more productive plants (Table 2). Leite et al. (2016) observed a positive and significant genotypic correlation between the traits grain yield and number of nodes per plant, indicating that the selection of plants with a higher number of nodes would result in more productive plants. It is noteworthy that one of the main objectives of soybean breeding programs is to seek cultivars with higher and earlier values of yield.

The flowering and maturation period are important agronomic traits and it is crucial to select early maturing varieties that minimally affect seed yield and weight (Copley et al., 2018). In this perspective, the parents UFUS 7415 and MG/BR 46 Conquista presented negative estimates for NDF and NDM, which indicates the contribution of these genotypes to reduce the cycle. When considering the effects of GCA, it was observed that the traits analyzed obtained wide variation in the estimates. The parents

showed independent behaviors, which contributes to increase or decrease the average of the analyzed variables.

The SCA demonstrates the behavior of hybrids based on the general combining ability of their parents and is related to nonadditive gene effects (Cruz et al., 2012). Estimates of the effects of SCA to determine the best hybrid combinations are shown in Table 2. The cross UFU 510 × UFUS 7415 presented negative SCA estimates for the traits NDF (-0.63), NDM (-0.64), IHP (-0.59) and high magnitude and positive estimates for the production components NP1 (8.76), NP2 (6.57), NP3 (8.89), TNP (24.23) and GP (7.50). The means described in Table 3 for the traits mentioned were satisfactory and within the recommended for soybean. The good performance of the F_2 generation, which obtained values higher than its parents for the production componentes, stands out.

Table 2 shows that the combination UFU 510 × BR/MG 46 Conquista demonstrated the best positive SCA estimates for the variables NNM (2.44) and NPN (1.20). The averages (Table 3) ranged from 15.07 to 19.00 for the number of nodes on the main stem at maturity and 13.35 to 15.55 for PN. The segregating population obtained higher estimates for the traits analyzed.

Table 3. Averages of agronomic traits of three soybean parents and F_2 populations

Traits	Population A UFU 510 (P_1) x UFUS 7415 (P_2)			Population B UFU 510 (P_1) x MG/BR 46 Conquista (P_3)			Population C UFUS 7415 (P_2) x MG/BR 46 Conquista (P_3)		
	P_1	P_2	F_2	P_1	P_3	F_2	P_2	P_3	F_2
NDF	45.02	45.10	44.22	45.02	44.62	45.30	45.10	44.62	44.82
NDM	104.30	104.20	103.15	104.30	103.50	103.78	104.20	103.50	102.80
PHF	47.06	57.53	48.10	47.06	60.15	52.16	57.53	60.15	55.67
PHM	59.17	67.53	69.97	59.17	70.21	70.73	67.53	70.21	67.09
NNF	12.95	12.07	12.04	12.95	13.32	12.08	12.07	13.32	12.34
NNM	15.07	15.00	16.09	15.07	15.75	19.00	15.00	15.75	14.91
NPN	13.35	13.25	14.74	13.35	13.57	15.55	13.25	13.57	14.13
HIP	9.89	10.92	9.54	9.89	10.30	10.18	10.92	10.30	10.13
NP1	17.57	16.52	29.78	17.57	19.32	16.24	16.52	19.32	21.74
NP2	45.95	47.67	58.17	45.95	49.85	47.52	47.67	49.85	63.51
NP3	51.35	63.17	71.45	51.35	54.65	61.81	63.17	54.65	62.41
TNP	114.87	127.37	159.40	114.87	123.82	125.57	127.37	123.82	147.66
GP	39.26	49.06	57.64	39.26	45.17	53.55	49.06	45.17	55.03

NDF: number of days for flowering; NDM: number of days to maturity; PHF: plant height at flowering; PHM: plant height at maturity NNF: number of nodes on the main stem in flowering; NNM: number of nodes on the main stem at maturity; NPN: number of productive nodes; HIP: height of insertion of the first pod; NP1, NP2 e NP3: number of pods with one, two and three grains; TNP: total number of pods per plant; GP: grain production per plant; F_2: F_1 self-fertilization.

For PHF (-1.27) and PHM (-2.78), negative effects of SCA were observed on the cross UFUS 7415 × BR/MG 46 Conquista (Table 2). These observations, added to the fact that the parents have the best averages (Table 4) for the analyzed variables, allows us to affirm that this crossing brings together desirable traits, because very low plants (less than 60 cm) compromise yield and very high plants (over 100 cm) are more susceptible to lodging (Sediyama et al., 2015). Bagateli et al. (2020), in order to estimate the general and specific combining abilities of eight soybean genotypes, found negative

SCA values and averages within the recommended for soybean culture in seven of the fifteen analyzed combinations.

For the agronomic attributes of economic interest, the cross UFU 510 × UFUS 7415 presents itself as the most favorable, since it has the best means and estimates of SCA (Tables 2 and 3) and is composed of the best ranked parent from the GCA for the components of production (Table 2). Hybrid combinations involving at least one parent with favorable GCA estimates are of greater interest to breeders, as they are more important than SCA, since the objective is not to obtain hybrids, but is indicative of heterosis caused by the effects of the combination (Rocha et al., 2019).

The estimates of the variance components for quantitative traits generate information about the genetic structure of a segregating population, favoring the selection of superior genotypes. The phenotypic variance ranged from 4.47 (NDF) to 7540.82 (TNP) in the combination UFU 510 × UFUS 7415; from 2.79 (NDF) to 2748.34 (TNP) for the combination UFU 510 × BR/MG 46 Conquista; and from 2.27 (NDF) to 2753.86 (TNP) for the combination UFUS 7415 × BR/MG 46 Conquista (Table 4).

Table 4. Estimates of variances of agronomic traits for three combinations of soybean cultivars obtained from F_2 and their parents

Traits	Population A UFU 510 (P_1) x UFUS 7415 (P_2)			Population B UFU 510 (P_1) x MG/BR 46 Conquista (P_3)			Population C UFUS 7415 (P_2) x MG/BR 46 Conquista (P_3)		
	$\hat{\sigma}_f^2$	$\hat{\sigma}_e^2$	$\hat{\sigma}_g^2$	$\hat{\sigma}_f^2$	$\hat{\sigma}_e^2$	$\hat{\sigma}_g^2$	$\hat{\sigma}_f^2$	$\hat{\sigma}_e^2$	$\hat{\sigma}_g^2$
NDF	4.47	1.67	2.80	2.79	1.38	1.40	2.27	1.49	0.77
NDM	5.13	2.47	2.66	4.75	2.33	2.42	4.24	0.95	3.28
PHF	112.20	94.89	17.31	136.45	148.49	-	149.21	153.65	-
PHM	437.57	78.10	359.47	194.10	176.15	17.97	118.31	164.45	-
NNF	2.80	2.57	0.23	3.58	4.13	-	3.45	2.96	0.49
NNM	12.51	3.16	9.34	930.72	4.64	926.08	7.94	2.96	4.97
NPN	30.13	2.70	27.43	94.42	3.60	90.82	69.51	2.68	66.83
HIP	8.97	1.94	7.02	3.60	0.95	2.64	8.00	1.64	6.35
NP1	2,864.96	93.53	2771.42	76.40	79.26	-	111.85	85.31	26.53
NP2	684.64	396.26	288.38	497.64	353.11	144.53	584.39	449.33	135.06
NP3	1,343.07	962.29	380.78	1,052.21	613.38	438.82	872.99	858.42	14.57
TNP	7,540.82	2,359.35	5,181.47	2,748.34	1,500.61	1,247.73	2,753.86	2,470.63	283.23
GP	530.27	220.89	309.38	484.42	128.38	356.04	675.62	231.83	443.78

$\hat{\sigma}_f^2$: phenotypic variance; $\hat{\sigma}_e^2$: environmental variance; $\hat{\sigma}_g^2$: genotypic variance; NDF: number of days for flowering; NDM: number of days to maturity; PHF: plant height at flowering; PHM: plant height at maturity NNF: number of nodes on the main stem in flowering; NNM: number of nodes on the main stem at maturity; NPN: number of productive nodes; HIP: height of insertion of the first pod; NP1, NP2 e NP3: number of pods with one, two and three grains; TNP: total number of pods per plant; GP: grain production per plant; -: negative estimates.

In population A (UFU 510 × UFUS 7415), the genotypic variance was greater than the environmental variance for the agronomic traits NDF, NDM, PHM, NNM, NPN, IHP, NP1, TNP and GP; in population B (UFU 510 × BR/MG 46 Conquista) for NDF, NDM, NNM, NPN, IHP and GP; and in population C (UFUS 7415 × BR/MG 46 Conquista), for the traits NDM, NNM, NPN, IHP e GP (Table 4).

The highest estimates observed in the three populations for genotypic variance ranged from 283.23 to 5181.47 for TNP (Table 4), which indicates potential for the selection of that trait. The results of the present study are similar to those found by Santos et al. (2019), who observed genetic variance superior to the environmental variance for the total number of pods per plant when evaluating the genetic and agronomic parameters in soybean F_2 progenies from twenty two-parent crosses.

In breeding programs, it is essential to know the genetic variation of a given trait and the effects on the phenotype, since the variance from the environment makes it difficult to recognize superior genotypes (Hamawaki et al., 2012). Heritability is one of the most useful genetic parameters for breeding, as it enables inferences about selection gains (Silva et al., 2021). When heritability is high, it means that the phenotypic variation is mainly due to the additive (inheritable) effects of the genes (Falconer & Mackay, 1996). Heritability estimates in the broad sense of high magnitude can be observed in the three populations analyzed for the NPN. The values were between 91.03% to 96.18% (Table 5). The results observed for the NPN were higher than those found by Teixeira et al. (2017) and Vianna et al. (2019), with heritability estimates for the NPN trait of 73.57% and 48.54%, respectively.

Table 5. Estimates of genetic parameters of agronomic traits in generations P_1, P_2 and F_2 for three combinations of soybean cultivars

Traits	Population A UFU 510 (P_1) x UFUS 7415 (P_2)				Population B UFU 510 (P_1) x MG/BR 46 Conquista (P_3)				Population C UFUS 7415 (P_2) x MG/BR 46 Conquista (P_3)			
	h_a^2	η	GS (%)	Average*	h_a^2	η	GS (%)	Average*	h_a^2	η	GS (%)	Average*
NDF	62.60	6.42	-3.42	42.70	50.35	8.87	-2.11	44.34	33.94	13.13	-1.16	44.29
NDM	51.90	9.18	-1.40	101.70	50.86	13.21	-1.22	102.50	77.51	5.47	-1.77	100.97
PHF	15.43	20.35	4.16	50.11	-	-	-2.17	51.02	-	9.32	-0.70	55.28
PHM	82.15	3.54	28.67	90.03	9.25	40.17	2.35	72.40	-	-	-7.93	61.77
NNF	8.32	34.23	1.43	12.21	-	-	-2.87	11.73	14.17	65.25	2.18	12.60
NNM	74.71	2.62	20.34	19.37	99.50	12.97	63.47	31.05	62.62	11.08	14.49	17.07
NPN	91.03	10.93	33.97	19.74	96.18	5.10	51.41	23.55	96.14	7.42	48.64	21.00
HIP	78.33	4.00	30.54	12.45	73.39	4.72	16.87	11.89	79.39	8.66	24.20	12.58
NP1	96.73	4.58	137.14	70.62	-	-	-2.89	15.77	23.72	13.73	15.99	25.21
NP2	42.12	9.11	25.04	72.73	29.04	7.32	18.94	56.52	23.11	11.81	11.67	70.92
NP3	28.35	9.48	19.37	85.29	41.70	6.23	30.19	80.47	1.66	177.89	1.08	63.08
TNP	68.71	5.53	49.71	238.63	45.39	4.76	26.01	158.23	10.28	31.22	4.84	154.82
GP	58.34	6.56	31.46	75.78	73.49	4.42	42.74	76.44	65.68	3.68	41.57	77.91

h_a^2: Heritability in the broad sense; η: number of genes; GS: prediction of gains by selection; NDF: number of days for flowering; NDM: number of days to maturity; PHF: plant height at flowering; PHM: plant height at maturity NNF: number of nodes on the main stem in flowering; NNM: number of nodes on the main stem at maturity; NPN: number of productive nodes; HIP: height of insertion of the first pod; NP1, NP2 e NP3: number of pods with one, two and three grains; TNP: total number of pods per plant; GP: grain production per plant; -: negative estimates; *Average predicted for the 1st cycle after selection.

When analyzing population A, it is also observed estimates of heritability higher than 70% for the traits PHM, NNM, IHP and NP1; in population B for the traits NNM and IHP; and in population C for NDM and IHP (Table 4). Values above 70% for

heritability indicate that simple selection methods can generate considerable gains, since the environment has no significant influence on the analyzed variable (Santos et al., 2018).

Another important genetic parameter to be analyzed is the number of genes. The estimation of this parameter shows us whether the trait under study is controlled by many or few genes. According to Stacke et al. (2020) the inheritance can be classified as monogenic (one gene), oligogenic (a few genes), or polygenic (many genes). The combinations UFU 510 × UFUS 7415, UFU 510 × BR/MG 46 Conquista and UFUS 7415 ×BR/MG 46 showed the highest number of genes, respectively, for NNF (34.23), PHM (40.17) and NP3 (177.89) (Table 5) and are considered as polygenic traits. Silva et al. (2021) also found polygenic inheritance for traits related to production and plant cycle. Important agronomic traits are considered polygenics and have low heritability with their expression significantly influenced by environment conditions (Baldissera et al., 2014, Silva et al., 2021).

Based on the analysis of genetic parameters for the three crosses, the possibility of selecting superior genotypes in the F_2 generation was verified. Thus, the selection gain obtained and the average for the first cycle after selection were estimated (Table 5). The greatest genetic gains were obtained for the traits NP1 (137.14%), NNM (63.47%) and NPN (48.64%) in populations A, B and C, respectively (Table 5). In this work, greater positive selection gains were observed in the combination UFU 510 × UFUS 7415, with a higher predicted average, when compared to other crosses, for the production components NP1 (70.62), NP2 (72.73), NP3 (85.29) and TNP (238.63).

For the NDM trait, the estimates for selection gain were negative, corroborating with the results found by Amaral et al. (2020) and diverging from those found by Leite et al. (2018) who studied agronomic traits in soybeans and obtained positive values for the mentioned trait. For PHM and IHP, the selection gain was 28.67 and 30.54 for the combination UFU 510 × UFUS 7415; 2.35 and 16.87 for the combination UFU 510 × BR/MG 46 Conquista; and -7.93 and 24.20 for UFUS 7415 × BR/MG 46 Conquista (Table 5). The average predicted for PHM was between 61.77 cm and 90.03 cm and for HIFP between 11.89 cm and 12.58 cm. Thus, it was observed that the three segregating populations met the criteria considered ideal for culture.

The average predicted for GP ranged from 75.78 g to 77.91 g when analyzing the three combinations (Table 5). In addition, positive values for GP were observed in all segregating populations that ranged between 31.46% and 42.74%, which indicates the possibility of gains with the selection. Bizari et al. (2017), Teixeira et al. (2017) and Silva et al. (2021) also observed gains for grain production in segregating soybean population. Hamawaki et al. (2012) explains that selection gains are directly associated with the differences between the means of the selected group and the original population and also linked to increased heterogeneity.

CONCLUSIONS

The parent UFUS 7415 presents the highest and most positive values of the GCA estimates for the production components. The cross UFU 510 × UFUS 7415 presents the highest number of total pods and grain production. The combinations

UFU 510 × UFUS 7415, UFU 510 × MG/BR 46 Conquista and UFUS 7415 × MG/BR 46 Conquista show a high heritability coefficient for the number of productive nodes. In the population of the crossing UFU 510 × UFUS 7415, greater selection gains and higher averages are observed for the production components NP1, NP2, NP3 and TNP.

ACKNOWLEDGMENTS. The authors thank CAPES (Coordenação de Aperfeiçoamento de Pessoal de Nível Superior), Fapemig, the Soybean Breeding Program (PMG) and to Instituto Federal Goiano, Campus Urutaí, for the structural and financial support.

REFERENCES

Amaral, L.O., Bruzi, A.T., Resende, P.M. & Silva, K.B. 2019. Pure line selection in a heterogeneous soybean cultivar. *Crop Breeding and Applied Biotechnology* **19**, 277–284.

Bagateli, J.R., Bahry, C.A., Silva, R.N.O., Carvalho, I.R., Conte, G.G., Villela, F.A., Gadotti, G.I. & Meneghello, G.E. 2020. Estimates of heterosis and combining ability of soybean diallel crossings. *Plant Omics*, 7–14.

Baldissera, J.N.C., Valentini, G., Coan, M.M.D., Guidolin, A.F. & Coimbra, A.J.L.M. 2014. Genetics factors related with the inheritance in autogamous plant populations. *Revista de Ciências Agroveterinárias* **13**, 181–189 (in Portuguese).

Bizari, E.H., Val, B.H.P., Pereira, E.M., Mauro, A.O.D., Unêda-Trevisoli, S.H., Bizari, E.H., Val, B.H.P., Pereira, E.M., Mauro, A.O.D., Unêda-Trevisoli, S.H. 2017. Selection indices for agronomic traits in segregating populations of soybean. *Revista Ciência Agronômica* **48**, 110–117.

Bornhofen, E. 2019. *Genetic analysis reveals opportunities and obstacles of tolerance to the Asian soybean rust fungus*. Doutorado em Genética e Melhoramento de Plantas, Universidade de São Paulo, Piracicaba, 126 pp. (in Portuguese).

Chagas, P.H.M., Teodoro, L.P.R., Santana, D.C., Teixeira Filho, M.C.M., Coradi, P.C., Torres, F.E., Bhering, L.L. & Teodoro, P.E. 2023. Understanding the combining ability of nutritional, agronomic and industrial traits in soybean F2 progenies. *Scientific Reports* **13**, e17909.

Colombo, G.A., Carvalho, E.V., Daronch, D.J. & Peluzio, J.M. 2018. Diallel analysis of the combining ability of soybean genotypes under low latitude Brazilian cerrado conditions. *Revista de Ciências Agrárias Amazonian Journal of Agricultural and Environmental Sciences* **61**, 1–9 (in Portuguese).

Copley, T.R., Duceppe, M.O. & O'Donoughue, L.S. 2018. Identification of novel loci associated with maturity and yield traits in early maturity soybean plant introduction lines. *BMC Genomics* **19**, 167.

Cruz, C.D. 2016. Genes Software – extended and integrated with the R, Matlab and Selegen. *Acta Scientiarum Agronomy* **38**, 547–552.

Cruz, C.D., Regazzi, A. & Carneiro, P. 2012. Biometric models applied to genetic breeding. *Viçosa: Editora UFV* **1**, 514. (in Portuguese).

Embrapa - Brazilian Agricultural Research Company. 2013. *Soybean production technology* – Central Region of Brazil 2014. Londrina, 226 pp. (in Portuguese).

Falconer, D.S. & Mackay, T.F.C. 1996. *Introduction to quantitative genetics*. 4th ed. New York: Longman, 464 pp.

Friedrichs, M.R., Burton, J.W. & Brownie, C. 2016. Heterosis and Genetic Variance in Soybean Recombinant Inbred Line Populations. *Crop Science* **56**, 2072–2079.

Gayosso-Barragán, O., López-Benítez, A., Rodríguez-Herrera, S.A., Ek-Maas, J.N., Hidalgo-Ramos, D.M. & Alcala-Rico, J.S.G.J. 2019. Studies on combining ability in tomato (*Solanum lycopersicum* L.). *Agronomy Research* **17**, 77–85.

Geraldi, I.O. & Miranda Filho, J.B. 1988. Adapted models for the analysis of combining ability of varieties in partial diallel crosses. *Revista Brasileira de Genética* **11**, 419–430.

Goksoy, A.T., Sıncık, M., Erdogmus, M., Ergın, M., Aytac, S., Gumuscu, G., Gunduz, O., Keles, R., Bayram, G. & Senyıgıt, E. 2019. The parametric and non-parametric stability analyses for interpreting genotype by environment interaction of some soybean genotypes. *Turkish Journal of Field Crops* **24**, 28–38.

Griffing, B. 1956. Concept of General and Specific Combining Ability in Relation to Diallel Crossing Systems. *Australian Journal of Biological Sciences* **9**, 463–493.

Hamawaki, O.T., de Sousa, L.B., Romanato, F.N., Nogueira, A.P.O., Santos Júnior, C.D. & Polizel, A.C. 2012. Genetic parameters and variability in soybean genotypes. *Comunicata Scientiae* **3**, 76–83.

Hwang, S. & Lee, T.G. 2019. Integration of lodging resistance QTL in soybean. *Scientific Reports* **9**, 6540.

Jiang, H., Li, Y., Qin, H., Li, Y., Qi, H., Li, C., Wang, N., Li, R., Zhao, Y., Huang, S., Yu, J., Wang, X., Zhu, R., Liu, C., Hu, Z., Wi, Z., Xin, D., Wu, X. & Chen, Q. 2018. Identification of major QTLs associated with first pod height and candidate gene mining in soybean. *Frontiers in Plant Science* **9**, 1280.

Kibalnik, O., Kukoleva, S., Semin, D., Efremova, I. & Starchak, V. 2021. Evaluation of the combining ability of CMS lines in crosses with samples of grain sorghum and Sudan Grass. *Agronomy Research* **19**, 1781–1790.

Leite, W.S., Pavan, B.E., Filho, C.H.A.M., Neto, F.A., Oliveira, C.B. & Feitosa, F.S. 2016. Genetic parameters estimation, correlations and selection indexes for six agronomic traits in soybean lines F8. *Comunicata Scientiae* **7**, 302–310 (in Portuguese).

Leite, W.S., Unêda-Trevisoli, S.H., Silva, F.M., Silva, A.J. & Mauro, A.O.D. 2018. Identification of superior genotypes and soybean traits by multivariate analysis and selection index. *Revista Ciência Agronômica* **49**, 491–500.

Leite, W.D.S., Pavan, B.E., Matos Filho, C.H.A., Feitosa, F.S. & de Oliveira, C.B. 2015. Estimates of genetic parameters and correlations between morphological traits in soybean genotypes. *Nativa* **3**, 241–245 (in Portuguese).

Mishra, A.K. 2019. Estimation of Gene Action Through Combination Ability in Soybean. *Soybean Research* **17**, 22–29.

Nadathur, S., Wanasundara, J.P.D. & Scanlin, L. 2024. Feeding the globe nutritious food in 2050: obligations and ethical choices. *Sustainable Protein Sources* **2**, 649–668.

Pimentel, A.J.B., Souza, M.A., Carneiro, P.C.S., Rocha, J.R.A.S.C., Machado, J.C. & Ribeiro, G. 2014. Partial diallel analysis in advanced generations for selection of wheat segregating populations. *Pesquisa Agropecuária Brasileira* **48**, 1555–1561 (in Portuguese).

Rialch, I. & Sharma, J.D. 2019. Combining ability studies for yield and related traits in soybean (*Glycine max*). *Indian Journal of Agricultural Sciences* **89**, 1334–1339.

Rocha, M.R., Hamawaki, O.T., Nogueira, A.P.O., Machado Junior, C.S., Hamawaki, C.D.L. & Hamawaki, R.L. 2019. Combinatorial analysis of agronomic characters in soybean. *Ciência e Agrotecnologia* **43**, 1–7.

Santos, E.R., Spehar, C.R., Pereira, P.R., Capone, A. & Barros, H.B. 2019. Genetic parameters and agronomic evaluation progenies F_2 soy the federal district, Brazil. *Revista Brasileira de Ciências Agrárias (Agrária)* **14**, 1–8.

Santos, E.R., Spehar, C.R., Capone, A. & Pereira, P.R. 2018. Estimation of genetic variation parameters in F2 soybean progenies and parents with presence and absence of lipoxygenases. *Nucleus* **15**, 61–70 (in Portuguese).

Sediyama, T., Silva, F. & Borém, A. 2015. *Soybean: from planting to harvest*. Viçosa: UFV, 333 pp. (in Portuguese).

Silva, C.O., Hamawaki, O.T., Nogueira, A.P.O., Almeida, M.R.C., Castro, D.G., Marques, F.S., Hamawaki, R.L., Hamawaki, C.D.L, Cardoso, G.M. & Diniz, V.H.R. 2021. Genetic parameters and selection indexes in F2 and F2:3 soybean populations. *Agronomy Journal* **113**, 2991–3004.

Soares, S.L., Simon, G.A., Alvares, R.C. & Silva, F.H.L. 2023. Combining performance and estimated genetic diversity among soybean parents and F1 populations. *Revista Ceres* **70**, 81–90.

Stacke, R.F., Godoy, D.N., Pretto, V.E., Führ, F.M., Gubiani, P.S., Hettwer, B.L., Garlet, C.G., Somavilla, J.C., Muraro, D.S. & Bernardi, O. 2020. Field-evolved resistance to chitin synthesis inhibitor insecticides by soybean looper, *Chrysodeixis includens* (Lepidoptera: Noctuidae), in Brazil. *Chemosphere* **259**, e127499.

Teixeira, F.G., Hamawaki, O.T., Nogueira, A.P.O., Hamawaki, R.L., Jorge, G.L., Hamawaki, C.L., Machado, B.Q.V. & Santana, A.J.O. 2017. Genetic parameters and selection of soybean lines based on selection indexes. *Genetics and Molecular Research* **16**, 1–17.

Teodoro, L.P.R., Bhering, L.L., Gomes, B.E.L., Campos, C.N.S., Baio, F.H.R., Gava, R., Júnior, C.A.S. & Teodoro, P.E. 2019. Understanding the combining ability for physiological traits in soybean. *PLOS ONE* **14**, e0226523.

Vianna, M.S., Nogueira, A.P.O., Hamawaki, O.T., Sousa, L.B., Gomes, G.F., Glasenapp, J.S., Hamawaki, R.L. & Silva, C.O. 2019. Selection of lineages, genetic parameters, and correlations between soybean characters. *Bioscience Journal* **35**, 1300–1314.

Agronomy Research **22**(S3), 1434–1445, 2024
https://doi.org/10.15159/AR.24.093

Intercropping insect repellent plants (irps): a promising strategy for sustainable pest management

N. Gunaeni, W. Setiawati*, A. Muharam, A.K. Karjadi, R. Murtiningsih, T.K. Moekasan, E. Korlina, A. Hasyim, I.R. Saadah, I. Sulastrini, E. Diningsih and B.K. Udiarto

National Research and Innovation Agency, Research Center for Horticulture, Jl. Raya Jakarta-Bogor, Cibinong, ID16915 Bogor, Indonesia
*Correspondence: wiwi024@brin.go.id

Received: August 13th, 2024; Accepted: October 11th, 2024; Published: October 21st, 2024

Abstract. In current intensive crop production, the utilization of natural biological control in pest management is not fully maximized, resulting in a significant dependency on the application of insecticides. Insect-repellent plants (IRPs) have become a prominent subject of research and a widely implemented strategy for reducing both pest damage and reliance on chemical insecticides. In this study, intercropping three IRP species, coriander (*Coriandrum sativum* L.; Apiaceae), celery (*Apium graveolens* L.; Apiaceae), and bunching onion (*Allium fistulosum* l.; Amaryllidaceae), in two intercropping systems were assessed for controlling insect pests in chilli pepper. The research was carried out in the experimental field of the Indonesian Vegetable Research Institute (IVegRI) in 2022. The results revealed that intercropping systems of chilli pepper with coriander, celery, and bunching onion significantly reduced plant damage over sole crops. Among the various intercrop combinations, chili pepper intercropped with coriander resulted in the lowest damage of three major pest species on chili pepper, *Thrips parvispinus* (51.77%), *Helicoverpa armigera* (47.67%), and *Bactrocera dorsalis* (40.35%). Furthermore, this effect enhanced the productivity of chili pepper yield (43.27%).

Key words: intercropping, pest management, chili pepper, natural biological control, insecticide reduction, sustainable agriculture.

INTRODUCTION

In Indonesia, the production of chili pepper (*Capsicum annuum* L.), indeed faces challenges due to insect pests, which can significantly impact the quality and quantity of yield. Globally, yield losses in chili pepper production can range from 25% to 100%, primarily due to pest infestations. In Indonesia, chili pepper production also face similar challenges. Various pests have significantly impacted chili pepper production, causing yield losses of up to 50% (Setiawati et al., 2022). Notably, a comprehensive study has identifield 53 insect pests affecting chili peppers in both nurseries and fields. Major pests include aphids (*Myzus persicae* Sulzer, *Aphis gossypii* Glover, and *Aphis craccivora*

Koch), thrips (*Thrips parvispinus* Karny), yellow mites (*Polyphagotarsonemus latus* Banks), and whiteflies (*Bemisia tabaci* Gennadius), all of which are identified as sucking pests of chili. Additionally, certain insects directly damage chili fruits, such as fruit borers (*Helicoverpa armigera*), armyworms (*Spodoptera litura*), and the oriental fruit fly (*Bactrocera dorsalis*) (Gurlaz & Sangha, 2016; Shivalingaswamy et al., 2022).

The extensive application of chemical pesticides as a conventional method of controlling pests frequently has detrimental effects on agroecosystems. These include the development of resistance to primary pests, the resurgence of secondary pests, the eradication of natural enemies, toxic residue in food, long residual effects, and increased environmental pollution, which can adversely affect human health. This can disrupt ecosystems and lead to a decrease in biodiversity (Devi, 2018; Isman, 2020; Adeleye et al., 2022; Lishchuk et al., 2024). These factors have played to implementing environmentally friendly methods for controlling insect pests in chili peppers. Intercropping, a conventional method in agriculture and horticulture, has been investigated in several studies for its potential effects on the behavior and abundance of herbivores, their natural enemies, as well as to increase productivity and yield stability (Järvinen et al., 2023; Dubey et al., 2023). Intercropping is a farming technique that involves cultivating multiple crops in the same field simultaneously (Martin-Guay et al., 2018). This practice offers several benefits, including increased crop yield, cost savings in crop production, higher income, reduced pest infestation, and minimized reliance on broad-spectrum insecticides (Mahfudz et al., 2019; Huss et al., 2022; Mir et al., 2022; Lepse & Zeipiņ, 2023). Additionally, intercropping contributes to weed suppression, improved soil fertility, conservation of natural enemies, mitigating climate change, and efficiently reducing agriculture's negative effects on the environment (Sujay & Giraddi, 2015; Lauren et al., 2020; da Silva et al., 2021; Adeleyea et al., 2022). Furthermore, Zhang et al. (2024) reported that intercropping affects plant chemistry and enhances resistance mechanisms, which supports sustainable agriculture. According to their research, intercropping can change a plant's metabolic profiles and boost its defenses, leading to increase against herbivorous pests. This is accomplised by altering the chemistry of the leaves, which can deter pests and improve the plant’s overall defense mechanisms

Intercropping of insect-repellent plants (IRPs) alongside crops has emerged as an alternative method in pest management (Rahman et al., 2020). Many types of intercropping have been identified based on the temporal and spatial overlap of plant species. Previous studies have examined the effectiveness of Coriander (*Coriandrum sativum* L.) (Sujay & Giraddi, 2015; da Silva et al., 2021) and Celery (*Apium graveolens*) (Moekasan & Prabaningrum, 2017; Wang et al., 2021) as intercrops for chili pepper, but the impact of bunching onion (*Allium fistulosum*) has yet to be explored. Järvinen et al. (2023) reported that *Allium* sp. has shown repellency against a wide range of arthropods. Bunching onions are highly suitable for intercropping due to their sulfur compounds, like allicin, which effectively deter pests. Their perennial nature and adaptability make them sustainable for long-term use. Additionally, they offer culinary benefits and are excellent for companion planting, enhancing both agricultural productivity and economic value.

The purpose of the study was to evaluate the effects of different IRP species, such as coriander, celery, and bunching onions, as well as the type of intercropping on insect pests and the natural enemies of chili peppers. The overall goal was to improve yields, reduce pesticide usage, and promote eco-friendly pest management practices toward natural pest control.

MATERIALS AND METHODS

The research was conducted in Margahayu, an experimental field of the Indonesian Vegetables Research Institute (107° 30' EL, 60° 30' SA; 1,250 m above sea level) located in Lembang, West Bandung, Province of West Java, Indonesia, from October 2022 to February 2023. During the experiment, the averageannual rainfall was 7.24 mm year^{-1}, and the average annual temperature ranged between 24 °C and 26 °C,with humidity ranging between 84% and 88%. The soil at the experimental site was categorized as Andisol with a pH of 5.0. From an initial study conducted based on the literature, three insect-repellent plant species (IRPs) cultivated in two intercropping systems: interrow cropping (IRC) and interplant cropping (IPC) were chosen for incorporation into chili pepper cultivation as intercrops. The following seven intercropping treatments were used: A) Intercropped chili pepper + coriander (IRC); B) Intercropped chili pepper + coriander (IPC); C) Intercropped chili pepper + celery (IRC); D) Intercropped chili pepper + celery (IPC); E) Intercropped chili pepper + bunching onion (IRC); F) Intercropped chili pepper + bunching onion (IPC); and G) Sole chili pepper (without any IRPs species) (Fig. 1). The experimental treatments were arranged following a randomized complete block design (RCBD) with four replicates. Plot sizes were 10 by 1 meter. There were forty chili plants on each plot. During the experiment, no pesticides were used in the experimental area.

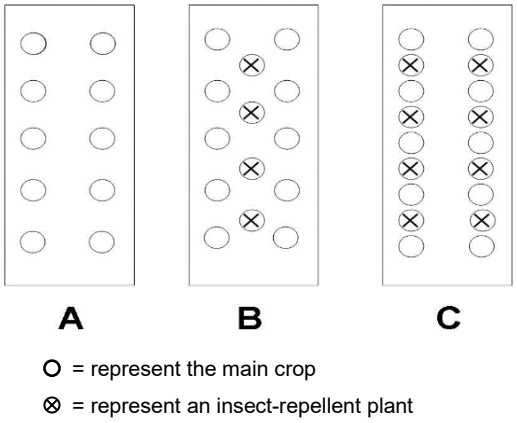

Figure 1. A schematic drawing of (A) a monoculture, (B) inter-row cropping (IRC) with ratio (100%: 50%), and (C) inter-plant cropping (IPC) with a ratio (100%:100%).

Data were collected by randomly selecting ten plants from each plot (U Shape) to collect pest intensity, natural enemies, growth performance (plant height, canopy diameter), number of chili pepper fruits, and yield. Three weeks after transplanting, weekly records of growth performance, pest intensity, and natural enemies were recorded, while the fresh weight of chili pepper fruits was recorded after harvest. The abundance of predators was determined by the average number of individuals per plant over the weeks of sampling. The intensity of plant damage due to pest infestation was calculated using Eq. 1 (Moekasan & Prabaningrum 2017):

$$P = \frac{\sum(n \, x \, v)}{N \, x \, Z} \, x \, 100\% \qquad (1)$$

where P is the percentage of damage level; v is the value of the damage category; n is the number of plants that have the same v value; Z is the highest value of the damage category (which is 9), and N is the number of observed plants. The value of v is based on the percentage of leaf area damage, with: 0 indicating no damage; 1 indicating >0 – ≤20% damage; 3 indicating >20 – ≤40% damage; 5 indicating >40 – ≤60% damage; 7 indicating >60 – ≤80% damage, and 9 indicating >80 – ≤100% damage.

The intensity of fruit bored due damage was calculated using Eq. 2 (Moekasan & Prabaningrum 2017):

$$\text{Fruit damage intensity (\%)} = \frac{\text{Number of infected fruits per plot}}{\text{Total number of fruits per plot}} \text{ x } 100\% \qquad (2)$$

The percent increase in yield over control in each of treatments was calculated as using the Equation follows:

$$\text{\% Increase in yield over control} = \frac{\text{Yield in treatment} - \text{Yield in control}}{\text{Yield in control}} \text{ x } 100\% \qquad (3)$$

Variables related to plant growth, such as plant height and canopy length, were measured once every week. The number of fruits per sample plant and yield per plot were recorded for each harvest, the average was determined and the yield per hectare was calculated. Data regarding fruit morphology parameters were recorded starting from the first harvest of the fruits. The fruits of each treatment harvested separately were used to record phenotypic parameters like fruit weight (g) fruit length (cm) and fruit diameter (cm).

A one-way analysis of variance (ANOVA) was used to examine the differences in all parameters for each of the seven treatments. A post hoc test called Tukey's honestly significant difference (HSD) was employed to separate the means to compare the variations between the seven treatments at a level of 5%.

RESULTS AND DISCUSSION

Throughout the growing season, three insect pest species were observed in chili pepper plots., namely, thrips (*T. parvispinus*), oriental fruit flies (*B. dorsalis*), and fruit borer (*H. armigera*). In most cases, intercropping with IRPs significantly affected reducing pests and relative abundances of the pests in chili peppers, but the effects varied across IPR species. Plant and fruit damages were lower in intercropped plots than in sole chili peppers. These results corroborate with other previous studies on the pest-suppressive effect of intercropping with IRPs. Fig. 2 illustrates the influence of intercrop effects on thrips damage. The statistical analysis revealed that the average amount of damage between the various dates of damage evaluation varied significantly. The percentage of thrips damage varied depending on the treatment. Plant damage caused by thrips attacks was most severe in sole chili pepper plots where there were no IRPs. Chili pepper plants intercropped with coriander had significantly less damage, with only 6.94% damage observed. This was followed by that for bunching onion (IPC), which had 8.33% damage. These damage levels represent reductions of 51.77% and 42.11%, respectively, compared to the control plots. This finding suggests that thrips damage increases with plant age. In contrast to sole chili pepper, intercropping with IRPs does not show a significant increase in thrips damage when plant age increases.

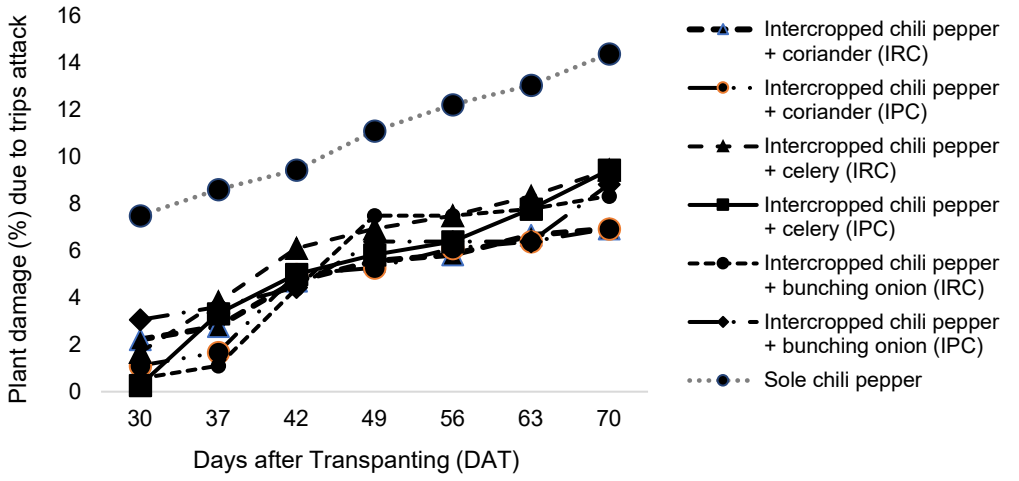

Figure 2. Plant damage due to thrips attack.

The presence of intercropping plants (IRPs) significantly affected the abundance of thrips, their predators, and the predator to thrips ratio. Although the overall number of thrips was similar across different types of intercropping (as shown in Table 1), the impact varied depending on the IRP species. Specifically, coriander intercropped plots (IRC) and bunching onion plots (IPC) had the lowest thrips populations, with reductions of 51.12% and 47.66%, respectively.

Table 1. Cumulative numbers of thrips and the total predator in chili pepper during the experiment under different treatments

No.	Treatments	Total no. of thrips/leaves	Total no. of predator/plants	Ratio of predators to thrips
A	Intercropped chili pepper + coriander (IRC)	26.75[b]	47.08 [a]	1.76:1
B	Intercropped chili pepper + coriander (IPC)	30.64[b]	45.26 [a]	1.51:1
C	Intercropped chili pepper + celery (IRC)	30.59b	45.88 [a]	1.50:1
D	Intercropped chili pepper + celery (IPC)	30.54b	49.17 [a]	1.61:1
E	Intercropped chili pepper + bunching onion (IRC)	31.01b	42.79 [a]	1.38:1
F	Intercropped chili pepper + bunching onion (IPC)	29.63b	40.29 [a]	1.36:1
G	Sole chili pepper	83.25a	32.47[b]	0.39:1
	CV (%)	19.40	17.70	

*The means in each row of a parameter followed by different letters are significantly difference ($P < 0.05$) according to the honestly significant difference (HSD) test.

A recent field study conducted by Salamanca et al. (2018) found that in control plots (sole of chili pepper), there are 2.68–3.11 times more counted thrips. Rakotomalala et al. (2023) reported that intercropping decreased arthropod pest density and abundance by 41% and 38%, respectively. The intercropped treatment exhibits lower pest densities than the sole chili pepper, which is consistent with the repellent chemical theory, which contends that VOCs from non-host plants prevent herbivores from finding and feeding on hosts. Coriander contains significant amounts of linalool, geranyl acetate, α-pinene

and β-pinene, eucalyptol, borneol, camphor, and terpinene which may be why fewer insects are present on plots where coriander is grown as an intercrop (Woldemelak, 2020). The primary active ingredients in celery that appeared to have an impact on pest selection behavior may have been D-Limonene, β-myrcene, and (E)-β-ocimene (Tu & Qin, 2017). VOCs from nonhost plants regularly affect the behavior of pests and their natural enemies, according to Yousefi et al. (2024). According to certain reports, intercropping can enhance the natural enemies of pests in agroecosystems by increasing crop biodiversity (Batista, 2017). When different intercrops are employed, however, the impact of intercrops on natural enemies differs. Our findings demonstrated that thrip population densities in both intercropping and sole chili pepper treatments decrease as predator population densities increase. The populations of predators were 51.14% and 45% higher, respectively, in the celery and coriander plots than in the sole chili pepper plots, where the populations were most numerous. The decrease in pest incidence in intercropped chili peppers may be attributed to either the low concentration of resources or the abundance of natural enemies. Natural enemies were high in okra (*Abelmoschus esculentus* L.) plots intercropped with coriander (Sujayanand et al., 2016). The same result was obtained by (Breitenmoser et al., 2022). Additionally, it was discovered that there were 53% more natural enemies of pests in the intercrop and that the number of pests had decreased from 33.5% to 53.5. The highest numbers of Coccinellidae and Syrphidae were observed on plots where carrots were intercropped with coriander. Natural enemies were unaffected by the increased plant diversity brought about by intercropping, which is advantageous for the biological control of a several of pests (da Silva et al., 2021; Li et al., 2021).

The ratio of predator-to-prey in all treatments was calculated. In general, the intercropped plots had a larger ratio of predators of thrips than the sole chili pepper plots, especially in the coliander and celery plots. When compared to the sole chili pepper plot, the ratio in these two intercropped plots increased by almost fourfold times. Thrip abundance was effectively reduced by intercropping, and the ratio of predators to pests was enhanced. In IRP intercropping, the ratio of predators to prey (pests) indicated an increased danger of predation and the possibility of improving biological control (Järvinen et al., 2023). By providing natural enemies with food, shelter, search capabilities, and oviposition sites, intercropping IRPs may improve the effectiveness of biological control by increasing the quantity and bolstering the rates of predation of these foes (Togni et al., 2016; Gurr et al., 2017; Talgre et al., 2023). Plants such as cabbage, tomatoes, carrots, eggplants, and roses attract predators such as ladybeetles (Coccinellidae), lacewings (Chrysopidae), and hoverflies (Syrphidae) when interplanted with cilantro. Plots of okra (*Abelmoschus esculentus* L.) interplanted with marigold (*Tagetes* spp.), mint (*Mentha* spp.), and coriander (*C. sativum* L.) (Sujayanand et al., 2016) had high levels of natural enemies. Furthermore, coriander flowers give their natural enemies a source of food in the form of nectar and pollen (da Silva et al., 2021).

Ladybeetles from the *Cheilomene* genus are not only the primary natural enemies for thrips but also contribute to manage the population of whiteflies (Sujayanand et al., 2016), aphids (Udiarto et al., 2023), and mites (Sumathi et al., 2019). These predators play a crucial role in managing insect pests. It is, therefore, probable that IPRs have attracted predator of thrips that could have contributed to reducing their populations in chili pepper intercropping plots. The result demonstrates the potential of IRP cropping systems to provide improved and sustainable insect pest management. Intercropping has

been suggested as an important agronomic practice for mitigating pest infestation in primary crops. This practice involves manipulating habitats to maintain ecological balance and create favorable conditions for natural enemies as well as sustaining crop productivity.

A significant difference in fruit damage between the control and the intercrop treatments was found during the experiments (Table 2). Tukey test results ($\alpha = 5\%$) showed that the lowest fruit damage due to *B. dorsalis* (8.84%) and *H. armigera* (2.13%) was recorded from chili and coriander (IRC), which was statistically similar to another treatment. The maximum fruit damage due to *B. dorsalis* (14.82%) and *H. armigera* (4.07%) was recorded from sole chili. Hence, it was confirmed that coriander was superior with a 40.35% and 47.67% reduction in fruit damage over control. To maintain production and control pest populations in the main crop, natural enemies and beneficial insects (pollinators) may be drawn to the increased plant diversity (da Silva et al., 2021; Adeleye et al., 2022).

Table 2. Effect of different treatments on fruit damage (%) due to *Bactocera dorsalis*, and *Helicoverpa armigera*

No.	Treatments	Fruits damage (%)			
		Bactocera dorsalis	Reduction of *B. dorsalis* over sole chili (%)	*Helicoverpa armigera*	Reduction of *H. armigera* over sole chili (%)
A	Intercropped chili pepper + coriander (IRC)	8.84^{c}	40.35	2.13^{b}	47.67
B	Intercropped chili pepper + coriander (IPC)	9.74^{bc}	34.28	2.76^{b}	32.19
C	Intercropped chili pepper + celery (IRC)	9.22^{bc}	37.79	2.69^{b}	33.91
D	Intercropped chili pepper + celery (IPC)	10.99^{b}	25.84	2.73^{b}	32.92
E	Intercropped chili pepper + bunching onion (IRC)	10.03^{b}	32.32	2.50^{b}	38.57
F	Intercropped chili pepper + bunching onion (IPC)	9.47^{bc}	36.1	2.25^{b}	44.72
G	Sole chili pepper	14.82^{a}	-	4.07^{a}	
	CV (%)	21.30		11.50	

*The means in each row of a parameter followed by different letters are significantly difference ($P < 0.05$) according to the honestly significant difference (HSD) test.

Additionally, according to Sandhu & Arora (2014), the IPM model, which included coriander as a plant repellent, reduced the number of *H. armigera* eggs and larvae and consequently increased productivity. Our research showed that coriander may effectively reduce *T. parvispinus, B. dorsalis*, and *H. armigera* on chili peppers in the field, suggesting that it might be a useful plant to use as an intercrop repellant. All of these results showed that IRP intercrops reduce the need for insecticidal treatments by having a variety of effects on insect pests, including direct repellence or deterrence, infestation delay, and indirect control and regulation through the recruitment of natural enemies.

Plant growth and yield of chili plants due to different treatments are presented in Table 3 and 4. At 93 DAT, the maximum plant height and canopy width in sole chili showed better performance over different intercropping combinations. However, there were no significant differences due to the effects of treatments. This was probably because intercropping with certain species of IRPs can improve soil quality by increasing soil organic nitrogen, soil water content, pH values, and available nitrogen contents (Kaci et al., 2022). The coriander was growing more, but the chili pepper was unshadow. Thus, by favoring natural enemies, the intercropping strategy suggested by IRPs can lower insect incidence while raising chili pepper yields.

The fruit length and diameter of chili pepper fruits in different treatments varied from 11.43 to 12.20 cm and 1.68 to 2.03 cm, respectively, with maximum fruit weight (18.00 cm) and fruit diameter of 2.03 cm were found in intercropping chili pepper + bunching onion (IPC), whereas the minimum fruit weight (11.43 cm) and fruit diameter (1.74 cm) were found in Intercropped chili pepper + celery (IPC). Significantly, the highest number of fruits per plant was observed in chili pepper + coriander (230.90), and the lowest was in sole chili pepper (140.50). This might be associated with the number of pests attacked. The chili pepper + coriander (IRC) system recorded the highest chili pepper yield (12.35 t ha^{-1}) followed by chili pepper + celery (IPC) (11.61 t ha^{-1}) and chili pepper + bunching onion (11.31 t ha^{-1}) compared to sole chili in the other intercropping system. The increase in yield over sole chili pepper was 43.27%, 4.29%, and 31.21%, respectively (Table 3).

Table 3. Effect of different treatments on growth and yield of chili pepper

No.	Treatments	Plant height at 93 DAT (cm)	Canopy width at 93 DAT (cm)	Yield	
				t ha^{-1}	% Increasing yield
A.	Intercropped chili pepper + coliander (IRC)	72.30	46.51	12.35[a]	43.27
B.	Intercropped chili pepper + coliander (IPC)	80.60	45.03	11.30[a]	31.09
C.	Intercropped chili pepper + celery (IRC)	71.60	50.11	11.98[a]	31.09
D.	Intercropped chili pepper + celery (IPC)	80.23	50.14	11.61[a]	34.39
E.	Intercropped chili pepper + bunching onion (IRC)	63.43	49.29	11.28[a]	30.85
F.	Intercropped chili pepper + bunching onion (IPC)	75.93	49.41	11.31[a]	31.21
G.	Sole chili pepper	74.93	50.00	8.62[b]	-
		ns	ns		
	CV (%)	7.18	8.29	7.54	

*The means in each row of a parameter followed by different letters are significantly difference ($P < 0.05$) according to the honestly significant difference (HSD) test.

Similar results of an increase in coriander and chili yield were reported by Dubey et al. (2023) who said that intercropping chili pepper and coriander with a ratio (85%: 15%) produced the highest yield. Intercropping of coriander and soybean showed much higher fresh weight per unit area than sole cropping (Weisany et al., 2021). The

beneficial impact of coriander on carrot growth and yield formation was observed (Lepse & Zeipiņ, 2023).

Among both intercropping systems, interrow cropping (IRC) showed the best results in terms of reducing pest populations and damage compared to interplant cropping (IPC). The population density of IRPs is an important tool for increasing crop production. Talukder et al. (2015) reported that 100% onion + 20% coriander and 100% onion + 30% coriander rations gave a higher yield of onion. Our studies have shown that the presence of coriander, celery, and bunching onion on chili pepper plots significantly reduces the damage caused by *T. parvispinus*, *B. dorsalis,* and *H. armigera*.

Lopes et al. (2016) reported that higher yield was positively correlated with an increase in predator populations and predation rates, with a decline in rural laborers and an increase in farmer's revenue. The results of the experiment indicate that intercropping is a practical tactic for reducing the negatif impacts of agricultural intensification on beneficial arthropods. chili pepper + coriander might be a suitable combination for higher productivity, reducing pest populations and damage, and enhancing natural enemy populations (Table 4).

Table 4. Effect of different treatments on yield contributing characters

No	Treatments	Fruit weight (g)	Fruit length (cm)	Fruit diameeter (cm)	Fruit number/plant
A	Intercropped chili pepper + coriander (IRC)	16.82^{a}	12.20^{a}	1.68^{b}	230.90^{a}
B	Intercropped chili pepper + coriander (IPC)	14.16^{ab}	13.43^{a}	1.81^{ab}	184.75^{a}
C	Intercropped chili pepper + celery (IRC)	16.14^{ab}	13.23^{a}	1.83^{ab}	211.70^{a}
D	Intercropped chili pepper + celery (IPC)	11.43^{b}	11.89^{a}	1.74^{b}	161.17^{a}
E	Intercropped chili pepper + bunching onion (IRC)	18.00^{a}	12.02^{a}	2.03^{a}	173.17^{a}
F	Intercropped chili pepper + bunching onion (IPC)	15.73^{ab}	11.98^{a}	1.74^{b}	184.20^{a}
G	Sole chili pepper	11.50^{b}	12.00^{a}	1.74^{b}	140.50^{b}
	CV	5.22	ns2.83	2.62	12.50

*The means in each row of a parameter followed by different letters are significantly difference ($P < 0.05$) according to the honestly significant difference (HSD) test.

CONCLUSIONS

This study demonstrates that intercropping chili pepper with coriander, celery, and bunching onions significantly reduces plant damage compared to sole chili pepper cultivation. Among the various intercrop combinations, chili pepper + coriander was the most effective, reducing damage from three major pest species *T. parvispinus* (51.77%), *H. armigera* (47.67%), and *B. dorsalis* (40.35%). Additionally, this combination increased the population of predatory beetles, *Cheilomenses sexmaculatus* (Coleoptera: Coccinellidae), and enhanced chili yield by 43.27%. The effectiveness of intercropping in reducing pest damage can be attributed to the repellent properties of the intercrop plants. Coriander, celery, and bunching onions release volatile organic

compounds (VOCs) that deter pests and attract beneficial predators. These natural repellents reduce the reliance on chemical insecticides, promoting a more sustainable and environmentally friendly approach to pest management.

ACKNOWLEDGMENTS. The authors are grateful to the Indonesian Vegetable Research Institute (IVEGRI), the Indonesian Agency for Agricultural Research and Development, and the Ministry of Agriculture of the Republic of Indonesia for supporting this research.

REFERENCES

Adeleye, V.O., Seal, D.R., Liburd, O.E., McAuslane, H. & Alborn, H. 2022. Pepper weevil, Anthonomus eugenii (Coleoptera: Curculionidae) suppression on jalapeño pepper using non-host insect repellent plants. *Crop Protection* **154**, 105893. doi: 10.1016/j.cropro.2021.105893

Batista, M.C., Fonseca, M.C.M., Teodoro, A.V., Martins, E.F., Pallini, A. & Venzon, M. 2017. Basil (Ocimum basilicum L.) attracts and benefits the green lacewing Ceraeochrysa cubana Hagen. *Biological Control* **110**, 98–106. doi: 10.1016/j.biocontrol.2017.04.013

Breitenmoser, S., Steinger, T., Baux, A. & Hiltpold, I. 2022. Intercropping Winter Oilseed Rape (*Brassica napus* L.) Has the Potential to Lessen the Impact of the Insect Pest Complex. *Agronomy* **12**(3), 723. doi: 10.3390/agronomy12030723

Da Silva, L.R.R, Ferreira, O.O., Cruz, J.N., De Jesus, P.F.C., Anjos, T.O.D., Cascaes, M.M., Da Costa, W.A., De Aguiar, A.E.H. & De Oliveira, M.S. 2021. Lamiaceae essential oils, phytochemical profile, antioxidant, and biological activities. *Evidence-based Complementary and Alternative Medicine*, **1**, 1–18. doi: 10.1155/2021/6748052

Devi, S. 2018. Effect of Intercropping on Sucking Insect Pests and Natural Enemies of Cotton. *International Journal of Current Microbiology and Applied Sciences* **7**(04), 1101–1109. doi: 10.20546/ijcmas.2018.704.120

Dubey, S., Singh, D. & Wesley, C.J. 2023. Inter Cropping of Chilli with Coriander and Fenugreek in Prayagraj Agro-climatic Conditions. *International Journal of Environment and Climate Change* **13**(8), 1298–1304. doi: 10.9734/ijecc/2023/v13i82073

Gurlaz, K. & Sangha, K.S. 2016. Diversity of arthropod fauna associated with chili (*Capsicum annuum* L.) in Punjab. *J Entomol Zool Stud* **4**(5), 390–396.

Gurr, G.M., Wratten, S.D., Landis, D.A. & You, M. 2017. Habitat Management to Suppress Pest Populations: Progress and Prospects. *Annual Review of Entomology* **62**(1), 91–109. doi: 10.1146/annurev-ento-031616-035050

Huss, C.P., Holmes, K.D. & Blubaugh, C.K. 2022. Benefits and Risks of Intercropping for Crop Resilience and Pest Management. *Journal of Economic Entomology* **115**(5), 1350–1362. doi: 10.1093/jee/toac045

Isman, M.B. 2020. Bioinsecticides based on plant essential oils: a short overview. *Zeitschrift Für Naturforschung C*, **75**(7–8), 179–182. doi: 10.1515/znc-2020-0038

Järvinen, A., Hyvönen, T., Raiskio, S. & Himanen, S.J. 2023. Intercropping shifts the balance between generalist arthropod predators and oilseed pests towards natural pest control. *Agriculture Ecosystems & Environment* **348**, 108415. doi: 10.1016/j.agee.2023.108415

Kaci, G., Ouaret, W. & Rahmoune, B. 2022. Wheat-Faba bean intercrops improve plant nutrition, yield, and availability of nitrogen (N) and phosphorus (P) in soil. *Agronomy Research* **20**(3), 603–616. doi: https://doi.org/10.15159/AR.22.047

Lauren, D., Snyder, M., Gómez, I. & Alison, G. 2020. Power, crop varietal mixtures as a strategy to support insect pest control, yield, economic, and nutritional services. *Frontiers in Sustainable Food Systems* **4**(60), 1–14.

Lepse, L & Zeipiņ, S. 2023. Increasing the sustainability of vegetable crops production by using intercropping. *Agronomy Research* **21**(S2), 494–503. doi: 10.15159/AR.23.026

Li, X.W., Lu, X.X., Zhang, Z.J., Huang, J., Zhang, J.M., Wang, L.K., Hafeez, M., Fernández-Grandon, G.M. & Lu, Y.B. 2021. Intercropping Rosemary (Rosmarinus officinalis) with Sweet Pepper (*Capsicum annum*) Reduces Major Pest Population Densities without Impacting Natural Enemy Populations. *Insects* **12**(1), 74. doi: 10.3390/insects12010074

Lishchuk, A., Parfenyk, A., Furdychko, O., Boroday, V., Beznosko, I., Drebot, O. & Karachinska, N. 2024. Ecotoxicological Hazard of Pesticide Use in Traditional Agricultural Technologies. *Journal of Ecological Engineering* **25**(2), 274–289. doi: 10.12911/22998993/177275

Lopes, T., Hatt, S., Xu, Q., Chen, J., Liu, Y. & Francis, F. 2016. Wheat (Triticum aestivumL.)-based intercropping systems for biological pest control. *Pest Management Science* **72**(12), 2193–2202. doi: 10.1002/ps.4332

Mahfudz, M., Saleh, S., Antara, M., Anshary, A., Bachri, S., Made, U., Hasanah, U. & Rauf, R.A. 2019. Adoption and advantages of eco-friendly technology application at the shallot farming system in Indonesia. *Agronomy Research* **17**(4), 1679–1687. doi: 10.15159/ar.19.188

Martin-Guay, M.O., Paquette, A., Dupras, J. & Rivest, D. 2018. The new Green Revolution: Sustainable intensification of agriculture by intercropping. *The Science of the Total Environment* **615**, 767–772. doi: 10.1016/j.scitotenv.2017.10.024

Mir, M.S., Saxena, A., Kanth, R.H., Raja, W., Dar, K.A., Mahdi, S.S., Bhat, T.A., Naikoo, N.B., Nazir, A., Amin, Z., Mansoor, T., Myint, M.Z., Khan, M.R., Mohammad, I. & Mir, S.A. 2022. Role of Intercropping in Sustainable Insect-Pest Management: A Review. *International Journal of Environment and Climate Change*, 3390–3404. doi: 10.9734/ijecc/2022/v12i111390

Moekasan, T.K. & Prabaningrum, L. 2017. Penggunaan rumah kasa untuk mengatasi serangan organisme pengganggu tumbuhan utama pada budidaya cabai merah di dataran tinggi. *Jurnal Hortikultura* **24**, 179–188. Indonesian with English abstract.

Rahman, M.M., Joaty, J.Y. & Islam, M.M. 2020. Intercropping for insect pest management in sustainable agriculture: A review. *Bulletin of the Institute of Tropical Agriculture, Kyushu University* **43**, 11–22. doi: 10.11189/bita.43.11

Rakotomalala, A.A., Ficiciyan, A.M. & Tscharntke, T. 2023. Intercropping enhances beneficial arthropods and controls pests: A systematic review and meta-analysis. *Agriculture Ecosystems & Environment* **356**, 108617. doi: 10.1016/j.agee.2023.108617

Sandhu, S. & Arora, R. 2014. Evaluation of oviposition efficiency on trap crops of marigold and coriander for management of tomato fruit borer,Helicoverpa armigera(Hubner) (Noctuidae: Lepidoptera) on potted plants. *Indian Journal of Agricultural Research* **48**(5), 367. doi: 10.5958/0976-058x.2014.01316.x

Salamanca, J., Souza, B. & Rodriguez-Saona, C. 2018. Cascading effects of combining synthetic herbivore-induced plant volatiles with companion plants to manipulate natural enemies in an agro-ecosystem. *Pest Management Science* **74**(9), 2133–2145. doi:10.1002/ps.4910

Setiawati, W., Muharam, A., Hasyim, A., Prabaningrum, L., Moekasan, T.K., Murtiningsih, R., Lukman & Mejana, M.J. 2022. Growth, and yield characteristics as well as pests and disease susceptibility of chili pepper (*Capsicum annuum* L.) under different plant density and pruning levels. *Applied Ecology and Environmental Research* **20**(1), 543–553. doi: 10.15666/aeer/2001_543553

Shivalingaswamy, T.M., Udayakumar, A & Mani, M.2022. Pests and their management in chilies and bell pepper. *Trends in Hortic Entomol*, 971–982. doi:10.1007/978-981-19-0343-4_39

Sujay, M.H & Giraddi, R.S. 2015. Role of intercrops for the management of chili pests. *Journal Agriculture Sciences* **28**(1), 53–58.

Sujayanand, G., Sharma, R. & Shankarganesh, K. 2016. Impact of intercrops and border crops on pest incidence in okra. *Indian Journal of Horticulture* **73**(2), 219. doi:10.5958/0974-0112.2016.00051.7

Sumathi, E., Vishnupriya, R., Ramaraju, K. & Geetha, M. 2019. Biological Control of Phytophagous Mites: A Review. *International Journal of Current Microbiology and Applied Sciences* **8**(01), 2153–2160. doi: 10.20546/ijcmas.2019.801.225

Talgre, L., Eremeev, V., Mäeorg, E. & Luik, A. 2023. Diversified cropping systems for promoting the beneficial insects-ground beetles (Coleoptera: Carabidae). *Agronomy Research* **21**(2), 592–597. doi: 10.15159/ar.23.027

Talukder, A., Rahman, J., Rahman, M., Biswas, M. & Asaduzzaman, M. 2015. Optimum Ratio of Coriander Intercropping with Onion. *International Journal of Plant & Soil Science* **4**(4), 404–410. doi: 10.9734/ijpss/2015/12600

Togni, P.H., Venzon, M., Muniz, C.A., Martins, E.F., Pallini, A. & Sujii, E.R. 2016. Mechanisms underlying the innate attraction of an aphidophagous coccinellid to coriander plants: Implications for conservation biological control. *Biological Control* **92**, 77–84. doi: 10.1016/j.biocontrol.2015.10.002

Tu, H. & Qin, Y. 2017. Repellent Effects of Different Celery Varieties in Bemisia tabaci (Hemiptera: Aleyrodidae) Biotype Q. *Journal of Economic Entomology* **110**(3), 1307–1316. doi: 10.1093/jee/tox110

Udiarto, B.K., Murtiningsih, R., Muharam, A., Moekasan, T.K., Setiawati, W., Hasyim, A., Sulastrini, I., Gunaeni, N., Korlina, E., Gunadi, N., Udiati, T., Tursilarini, T.Y., Negara, A., Ardjanhar, A. & Manzila, I. 2023. Preferences and functional response of Coccinellidae to Bemisia tabaci (Hemiptera: Aleyrodidae). *Chilean Journal of Agricultural Research* **83**(6), 715–724. doi: 10.4067/s0718-58392023000600715

Wang, J., Li, S., Fang, Y., Zhang, F., Jin, Z., Desneux, N. & Wang, S. 2021. Enhanced and sustainable control of Myzus persicae by repellent plants in organic pepper and eggplant greenhouses. *Pest Management Science* **78**(2), 428–437. doi: 10.1002/ps.6681

Weisany, W., Tahir, N.A.R. & Schenk, P.M. 2021. Coriander/soybean intercropping and mycorrhizae application lead to overyielding and changes in essential oil profiles. *European Journal of Agronomy* **126**, 126283. doi: 10.1016/j.eja.2021.126283

Woldemelak, W.A. 2020. The major biological approaches in the integrated pest management of onion thrips (Thysanoptera: Thripidae). *J. Hortic. Res*., **28**, 13–20. doi: 10.2478/johr-2020-0002

Yousefi, M., Marja, R., Barmettler, E., Six, J., Dray, A. & Ghazoul, J. 2024. The effectiveness of intercropping and agri-environmental schemes on ecosystem service of biological pest control: a meta-analysis. *Agronomy for Sustainable Development* **44**(2). doi: 10.1007/s13593-024-00947-7

Zhang, W., Zhang, T.T., Machado, R.A.R. & Dai, C.-C. 2024. Correction to: Intercropping-induced leaf metabolic changes increase plant resistance to herbivory. *Plant and Soil*. doi: 10.1007/s11104-024-06505-0

Agronomy Research **22**(S3), 1446–1459, 2024
https://doi.org/10.15159/AR.24.066

Does the level of resistance to *Acanthoscelides obtectus* of bean genotypes (*Phaseolus* spp.) change according to the seed production environment?

J.C. Jiménez-Galindo[1,*], G. Castellanos Pérez[2], M. De. La. Fuente[3], R.A. Malvar[3], N. Ramírez-Cabral[4] and D. Padilla Chacón[5]

[1]National Institute of Forestry, Agriculture and Livestock Research, Bean Genetics and Breeding Group, Av. Hidalgo No 1213, MX31500 Cuauhtémoc, México
[2]Autonomous University of Chihuahua, Agrotechnological Sciences Faculty, V. Carranza y Escorza s/n, MX31000 Chihuahua, México
[3]Biological Mission of Galicia, Maize Genetics and Breeding Group, Department of Plant Production, Carballeira 8, ES36143 Pontevedra, Spain
[4]National Institute of Forestry, Agriculture and Livestock Research, Agrometeorology and Modeling Group, Zacatecas-Fresnillo road Km. 24.5, MX98500 Calera de Victor Rosales, México
[5]Postgraduate College, CONAHCyT Postgraduate Program in Botany, Mexico-Texcoco road, km 36.5, MX56264 Montecillo, Mexico
[*]Correspondence: jimenez.cruz@inifap.gob.mx; cruz2477@yahoo.com.mx

Received: April 19th, 2024; Accepted: July 2nd, 2024; Published: July 16th, 2024

Abstract. Bean weevil (*Acanthoscelides obtectus*) cause considerable losses in warehouses in dry bean (*Phaseolus vulgaris* L). *Phaseolus acutifolius* varieties could be used for genetic studies and genetic improvement of common beans. Tepary bean varieties resistance was studied produced with irrigation and under drought conditions to *A. obtectus*. Previously, we studied A. *obtectus* colony from Spain with some of these bean varieties. In the present research, we studied a different *A. obtectus* colony from México. The varieties T-amarillo, PS-AZH-15 and T-cafe beans showed a lower ovoposition. T-amarillo, T-negro and T-cafe increased the duration of the insect biological cycle. In the varieties T-cafe, T-negro and T-amarillo increased larvae mortality before burrowing the seed in percent and reduced the number of first generation adults. Little grain weight loss is caused by small number of emerged adults, in the varieties T-amarillo, PS-AZH-15, T-cafe and T-negro. According with adult's number of first generation and grain weight loss in percent T-amarillo showed resistance and tolerance to *A. obtectus* infestation and it could be used as source of resistance for *P. vulgaris* breeding. No significant differences were found according to the seed production environment for any traits studied except for initial seed weight. Resistant varieties maintain their lethality regardless of the seed production environment. Probably *A. obtectus* is genetically different according to the area and is adapted to the varieties produced in each country or region.

Key words: bean bruchid, common bean, *P. acutifolius*, insect resistance.

INTRODUCTION

Dry bean (*Phaseolus vulgaris L.*) is an important staple crop in many countries, it is an excellent source of protein of low cost, and this legume has vitamins, minerals (Admassu Shimelis & Kumar Rakshit, 2005) as well as secondary metabolites with biological activity that help to prevent some types of cancer in humans (Cid-Gallegos et al., 2023). In 2018, harvested area with common bean, around the world, exceed 22.7 million of hectares with 28.4 million of tones (FAOSTAT, 2022).

Dry bean production is affected around the world by biotic and abiotic factors (Beebe & Corrales, 1991). Some of the major biotic constraints involving post-harvest losses caused by the bruchid species *Acanthoscelides obtectus* Say and *Zabrotes subfasciatus* Boheman. The common bean weevil *Acanthoscelides obtectu*s (Coleoptera: Bruchidae) is a global problem that causes serious damage on warehouses in regions of Latin America, Africa and Europe (Schmale et al., 2003; Silva et al., 2007). The bean weevil is the main postharvest pest of dry bean, Some studies have reported losses from 7 to 40% caused by weevil damage (Mbogo et al., 2009). This represents worldwide losses, each year of 1.95–11.16 million of tones due to weevil damage. A research carried on in Honduras in the 90´s showed that the postharvest losses could reached up to US$3.5 million dollars (Espinal et al., 2004). Infestations are more commonly detected in storage (Parsons & Credland, 2003). Females place their eggs in groups under or close to a single seed. The beetles spend their larval and pupal phases inside seeds, where the first instars larvae burrow. The last larvae stage dig chambers directly below the seed and a tiny circular aperture can reveal the existence of a larva. Unlike the majority of other bruchids, it attacks both stored seeds and field-grown beans, it has a continuous reproductive cycle without diapause (Tucić et al., 1996; Ahmed et al., 2019). Eggs are milky white color with oval shape, the larva passes through six instars with no significant differences in length or head capsule between the instars, the pupa is white-yellow color and the adult is grayish to blackish color (Ahmed et al., 2019).

There are a number of ways to control bean weevils some examples are: the use of essential oils from the next plants: *Foeniculum vulgare*, *Artemisia dracunculus*, *Lavandula angustifolia*; and isolates from entomopathogenic fungus (*Metarhizium anisopliae*) (Lak et al., 2022), *Bauveria bassiana* (Gutièrrez Jiròn, 2016), *Trichoderma spp* (Rodríguez-González et al., 2019). The egg predatory mites *Blattisocius tarsalis* and *Amblyseius swirskii* have been tested as natural enemies to control bean weevils with an efficacy of 60%, on the other side the larvae parasitoids *Anisopteromalus calandrae* and *Lariophagus distinguendus* reduced up to 38% of the pest population (Iturralde-García et al., 2020). Great farmers with large warehouses can use chemical pesticides to control the bean weevil. At the contrary, small farmers could use resistant varieties as control strategy (Mbogo et al., 2009).

Genetic breeding for pest resistance should increase grain yield contributing to a more permanent supply of common beans in countries around the world (Mbogo et al., 2009). The common bean resistant varieties against *A. obtectus*, has a number of advantages over chemical control or others. Chemical pesticides need to be repeated periodically, therefore are more expensive in comparison with the use of resistant varieties; in addition the use of chemical insecticides is associated with insecticide resistance, eradication of beneficial insects and environmental contamination (Keneni et

al., 2011). The best approach for this pest is to develop resistant lines to *A. obtectus*, the most difficult bruchid to control. For example, the number of adults present after 182 days of seed storage was low for all Tepary accessions and was high for most common bean accessions; Tepary bean may provide a useful germplasm source for *Phaseolus vulgaris* breeding (Shade et al., 1987). Seed storage protein 'arcelin' has been previously described as causing antibiosis against *Z. subfasciatus*, without providing protection against *A. obtectus* (Cardona & Kornegay, 1999; Osborn et al., 1988; Minney et al., 1990). However Osborn et al. (1988) mention that the arcelin, causes sub lethal effects in *A. obtectus* larvae, increasing the biological cycle of *A. obtectus* and reducing their adult weight. Resistance is also associated with lectin-like seed storage proteins (LLPs) (Sales et al., 2000), and α-amylase inhibitor (Fory et al., 1996). In particular, moderate resistance to *A. obtectus* has been found by Cardona et al. (1990), Kornegay & Cardona, (1991) and Kornegay et al., 1993). Seven allelic arcelin variants with differential value for insect resistance have been reported so far, with arcelin-1 (Acosta-Gallegos et al., 1998; Cardona et al., 1990; Hartweck et al., 1997). Arcelin not only prolongs the development of *A. obtectus* but also extends the period of adult emergence, thus contributing to a higher variation of host stages present at the same time (Schmale et al., 2003; Velten et al., 2008).

In the highly resistant accession G12952, resistance was expressed as antibiosis causing delayed and reduced adult emergence, high mortality of late first instar larvae, reduced female fecundity, and negative rates of population growth. The factors responsible for resistance are present in the cotyledons of seeds and are chemical in nature (Cardona et al., 1989). The natural storage protein arcelin, in G12952, causes sub-lethal effects to the bruchid *A. obtectus* (Schoonhoven et al., 1983; Kornegay & Cardona, 1991), prolonging immature development of young bruchid larvae, extending the period of adult emergence, and reducing adult weight (Osborn et al., 1988; (Velten et al., 2007).

No other sources of bruchid resistance have been detected in over 17,000 bean genotypes originating elsewhere in Latin America (Valencia et al., 2006). Few genotypes with high resistance to *A. obtectus* were found: G40199 (*Phaseolus acutifolius* A. Gray) (Kusolwa & Myers, 2011), G02770 (*P. vulgaris*), QUESS (*P. vulgaris*) (Zaugg et al., 2013), G12952 (*P. vulgaris*) (Schoonhoven et al., 1983). Recently T-amarillo and T-negro, Tepary bean varieties, were reported as resistant accessions against *A. obtectus* (Jiménez et al., 2017). And after that was reported a dominant gene for resistance to *A. obtectus* in both crosses P-saltillo × T-amarillo and T-amarillo × T-cafe using number of adults as resistance criteria (Jiménez-Galindo et al., 2020).

The novelty of this manuscript is to study how the resistance level of bean genotypes change according to seed production environment. And indirectly to validate that genetically *A. obtectus* from Spain is different of *A. obtectus* from Mexico.

MATERIALS AND METHODS

Seed material

We used ten dry bean varieties PS-AZH-15, Aluyori, PS-AZH-15/1, Azufrado Higuera (A-higuera), Rosa Bufa 60 (R-bufa-60), Pinto Saltillo (P-saltillo), Rosa Bufa-80 (R-bufa), Tepary cafe (T-cafe), Tepary amarillo (T-amarillo), and Tepary negro (T-negro). The irrigation-drought experiments were sown on July 20, 2018 and finished

on October. Performed at the Experimental Station of INIFAP in Bachiniva, Chihuahua, Mexico: 28° 47' 19.32" N, 107° 16' 11.64" E, at an altitude of 2,012 meters above sea level. In a clay loam soil with 43% sand, 28.7% silt and 28.2% clay, free of salts, high in organic matter content (2.01%). The fertilizer formula 30-50-00 was applied in both experiments. The experimental unit consisted of 1 furrow 5 meters long with 60 seeds at a distance of 8.4 cm between seeds and 0.75 m between furrows. In 2018 it rained 302 mm from July 20 to October 1, 2018 and was the total water in drought experiment. On the irrigation experiment, 20 mm irrigations were also added on July 31, August 7, August 26, August 31, September 7, September 12 and September 23 for a total of 442 mm. The application of water through irrigation are represented in green bars (Fig. 1). All seeds were harvested in 2018 from two bioassays under irrigation and drought (Table 1).

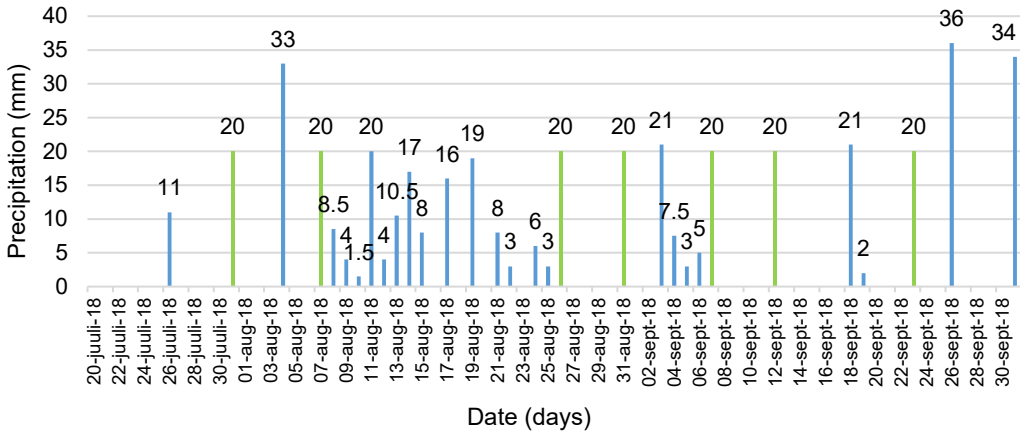

Figure 1. Precipitation and irrigation in field irrigation-drought trials in 2018 at Experimental Station of INIFAP in Bachiniva, Chihuahua.

Table 1. Characteristic of seeds of ten bean varieties from INIFAP evaluated for resistance to *A. obtectus*

Variety	Race	Species	Growth habit	Seed size
PS-AZH-15	Nueva Granada	*P. vulgaris*	II	Large
Aluyori	Nueva Granada	*P. vulgaris*	II	Large
PS-AZH-15/1	Nueva Granada	*P. vulgaris*	II	Large
A-higuera	Nueva Granada	*P. vulgaris*	II	Large
R-bufa-60	Durango	*P. vulgaris*	III	Medium
P-saltillo	Durango	*P. vulgaris*	III	Medium
R-bufa	Durango	*P. vulgaris*	III	Medium
T-cafe	Wild type	*P. acutifoilus*	III	Small
T-amarillo	Wild type	*P. acutifoilus*	III	Small
T-negro	Wild type	*P. acutifoilus*	III	Small

Experimental design

With the seed from the field experiments harvested in November 2018, two bioassays were performed on September 5, 2019 and finished on December 20, 2019 an average temperature of 22 °C in the Genetics laboratory from Experimental Station of INIFAP, in Cuauthemoc, Chihuahua, Mexico 28° 24' 15" N, 106° 52' 19" E, at an altitude

of 2050 meters above sea level. We used a completely randomized design with four replicates. We put 5 males and 5 females with 20 seeds per repetition, in plastic bottles of 5 cm diameter and 5.5 cm of height. The variables measured were: 1) 20 seed weight (g), 2) number of eggs (n), 3) larvae number (n) (that is equal to the number of eggs), 4) larvae mortality before entering the seed (n), 5) larvae mortality before entering the seed (%) [Calculated with formula: MLBES = larvae mortality before to entering the seed (n) * 100/larvae number (n)], 6) number of adults (n), 7) grain weight loss (g) [calculated with formula: SWL = initial seed weight - final seed weight, after the first generation of adults] and 8) biological cycle (days) calculated from start of bioassays to the first adult emergence on each repetition.

Statistical analysis

The analysis of the databases of the two trials was used a General Linear Model (PROC-GLM) in statistical package SAS 9.3 (SAS Institute, 2016). For mean comparisons was used the test of *MSD* (Minimum Significative Difference) from *LSD* at $p < 0.05$.

RESULTS AND DISCUSSION

Seed weight

Significant differences were found according to the seed production environment for seed weight. Significant statistical differences were found between varieties for seed weight. The best varieties that show high seed weight were PS-AZH-15, Aluyori and PS-AZH-15/1. The varieties with less seed weight were T-amarillo, T-negro and T-cafe (Fig. 2).

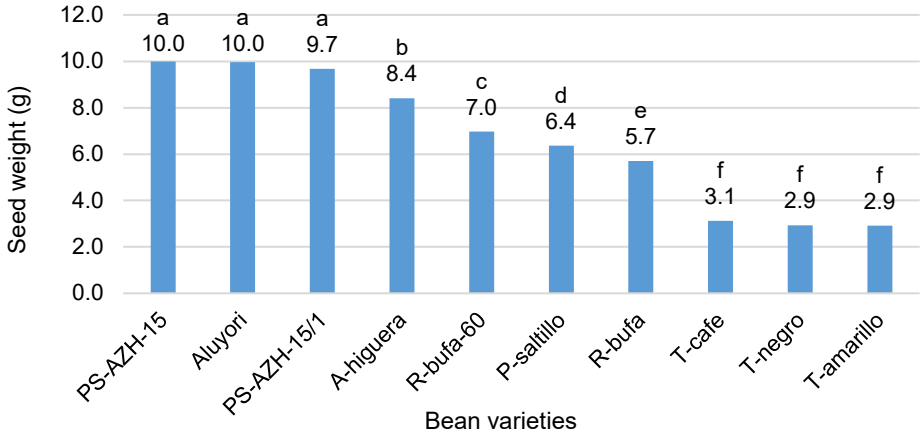

Figure 2. Twenty seed weight for 10 bean varieties. DMS = 0.55. Means followed by the same letter are not significantly different (*LSD* = 0.05).

In the present study, significant differences were found according to the seed production environment and varieties for initial seed weight, because one seed was produced under irrigation conditions and the other under rainfed conditions. The results agree with Abdalla et al. (2015) that found that the seed size and other yield components change according with the production environment.

Number of eggs

There are no differences between environments for number of eggs. Significant differences were found for number of eggs between varieties. The variety with more number of eggs was T-negro. The varieties with less number of eggs were T-amarillo and PS-AZH-15 (Fig. 3).

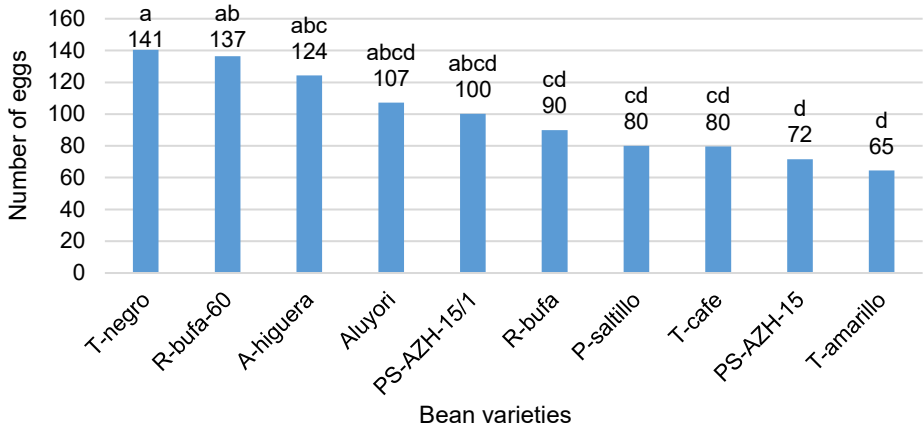

Figure 3. Number of eggs in 10 bean varieties. DMS = 49.3. Means followed by the same letter are not significantly different (*LSD* = 0.05).

Jiménez et al. (2017) found several mechanism of resistance to *A. obtectus* including a compound in seed coat that keeps the adult inactive for a long time, avoiding also oviposition. Contrastingly with Velten et al. (2007) that found varieties with high level of arcelines in cotyledons where females lay less number of eggs. Jiménez et al. (2017) found that the varieties with more number of eggs were PS-AZH-15, T-cafe and P-saltillo and the varieties with less were T-negro and T-amarillo with *A. obtectus* recollected and reared in Pontevedra, Spain. In the present study contrastingly, the varieties with more number of eggs were T-negro, R-bufa-60 and A-higuera and less P-saltillo, T-cafe, PS-AZH-15 and T-amarillo. This means that probably *A. obtectus* could be adapted to each variety that exists in each region around the world. Interestingly T-amarillo is the most resistant variety per number of eggs for both *A. obtectus* colonies, from Spain and Mexico. However, T-negro it is the one that allows the oviposition of *A. obtectus* of Mexico in the present study and decreases to oviposition of *A. obtectus* of Spain (Jiménez et al., 2017). This supports that probably the plague is genetically different in the different regions of the world, but we need more bioassays with *A. obtectus* colonies from Spain and from Mexico. Some other authors have found genetic differences between insect populations. According to our research Sword & Chapman, (1994) found that the differences in the feeding habits in different parts of their distribution of Green Bird Grasshopper (*Schistocerca shoshone*) are not simply due to the difference in food availability of different populations, but are also probably based on genetic differences between individuals. Also Jones, (1987) reported a detailed study of cabbage white butterfly (*Pieris rapae*) feeding was carried out in two populations of

native Europe, but it reached Australia where it was observed that there is a great difference in the behavior of females from different regions. When the two populations were subjected to the same environmental and food conditions, the differences were maintained, even in successive generations. Which means that probably, as in our studies of *A. obtectus*, the pests are most likely genetically different and are adapted to different environmental and nutritional conditions. In addition Bonal et al. (2019) reported differences between acorn feeding insects (*Curculio* spp.) of California and the Spain using DNA taxonomy technique. At the intra-specific level, Californian *Curculio* showed a much more marked population genetic structure compared to Iberian ones, in which genetic depauperation and a posterior intense inter-population gene-flow can be appreciated.

Larvae number

There are no differences between environments for larvae number variable. Significant statistical differences for number of larvae between varieties were found. The variety with more number of larvae was T-negro. The varieties with less number of larvae were T-amarillo and PS-AZH-15 (Fig. 4).

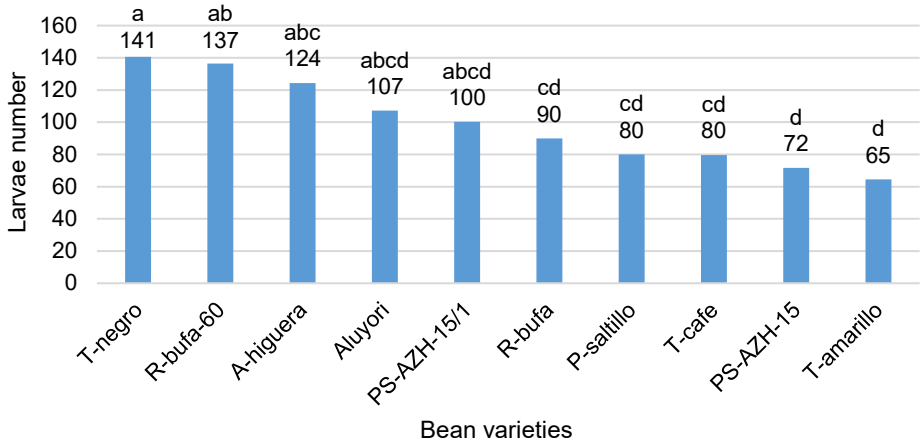

Figure 4. Larvae number in 10 bean varieties. MSD = 49.3. Means followed by the same letter are not significantly different (*LSD* = 0.05).

Larvae mortality before entering the seed (n)

There are no differences between environments for larvae mortality before to entering the seed (n). Significant statistical differences were found between varieties for larvae mortality before entering the seed (n). The varieties with more mortality of larvae were T-negro and T-cafe. The varieties with less mortality of larvae were PS-AZH-15/1, Aluyori and PS-AZH-15 (Fig. 5).

Jiménez et al. (2017) found a possible volatile compound located in testa, causing larval mortality. Such compound keeps adults inactive, avoiding oviposition, adult and larvae antixenosis, larval mortality and is not located in cotyledons, suggesting that they should be different from arcelines. These results are according with Valencia et al. (2006) that found low percentage of survivor of larvae in G40199. In addition,

Jiménez et al. (2020) found pipecolic acid in testa in two F_2 populations between T-amarillo × P-saltillo and T-cafe × T-amarillo as the responsible metabolite that keeps under control *A. obtectus* and is related to effective larvae mortality before to entering the seed and zero adults emerged from resistant lines. Jiménez et al. (2017) found that the varieties with high larvae mortality before to entering the seed were T-negro (96.1%), T-amarillo (77.6%), T-cafe (77.2%) and P-saltillo (66.2%) and less PS-AZH-15, something according with present research, where we found that the genotypes with high larvae mortality before to entering the seed were T-cafe (49.5%), T-negro (42.8%) and T-amarillo (32.5%). The mortality of larvae is lower to *A. obtectus* from Mexico and changes the order of the varieties for larvae mortality before to entering the seed, which probably means that insect pest from Spain and from Mexico, are genetically different. The varieties with less larvae mortality before entering the seed in the present study were P-saltillo, PS-AZH-15, according with Jiménez et al. (2017), PS-AZH-15/1, Aluyori, R-bufa-60, A-higuera and R-bufa. The larvae mortality before entering the seed is a very interesting resistance trait of the varieties and very few studies had quantified it, of the few reports are the authors Schmale et al. (2003) and Velten et al. (2008). Also Velten et al. (2008) found larvae mortality from 20% to 35% before entering the seed in the bean variety RAZ 94 and are according with our present results.

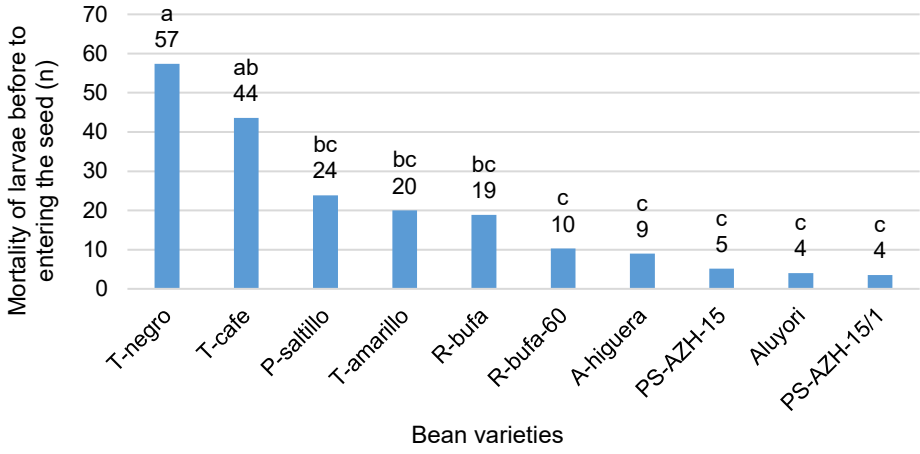

Figure 5. Larvae mortality of before entering the seed in number for 10 bean varieties. DMS = 28.7. Means followed by the same letter are not significantly different (*LSD* = 0.05).

Larvae mortality of before entering the seed (%)

There are no differences between environments for larvae mortality before entering the seed (%). Significant statistical differences between varieties were found for larvae mortality before entering the seed (%). The varieties with high larvae mortality were T-cafe, T-negro and T-amarillo. The varieties with less mortality of larvae were PS-AZH-15/1, Aluyori and R-bufa-60 (Fig. 6).

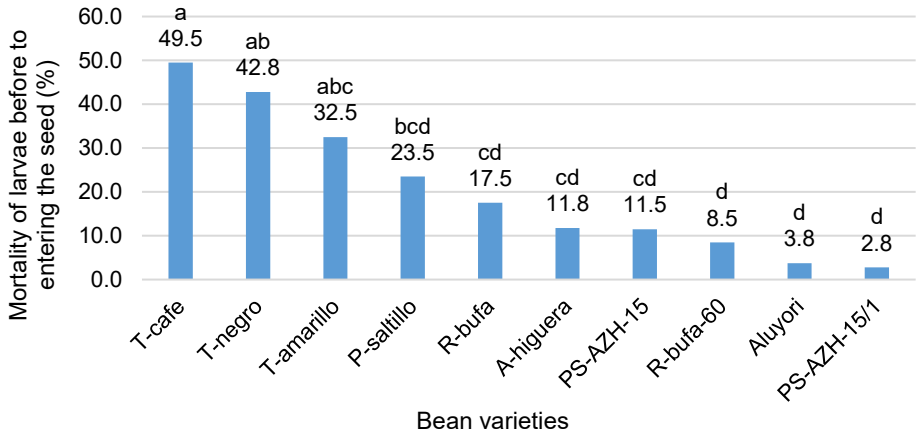

Figure 6. Mortality of larvae before to entering the seed in 10 bean varieties. DMS = 21.8. Means followed by the same letter are not significantly different *(LSD* = 0.05).

Adult's number

There are no differences between environments for adult's number. Significant statistical differences between varieties were found for adult's number. The varieties with high adults number were PS-AZH-15/1, R-bufa-60, A-higuera, Aluyori and PS-AZH-15. The varieties with less adult's number were T-amarillo, T-negro and T-cafe (Fig. 7).

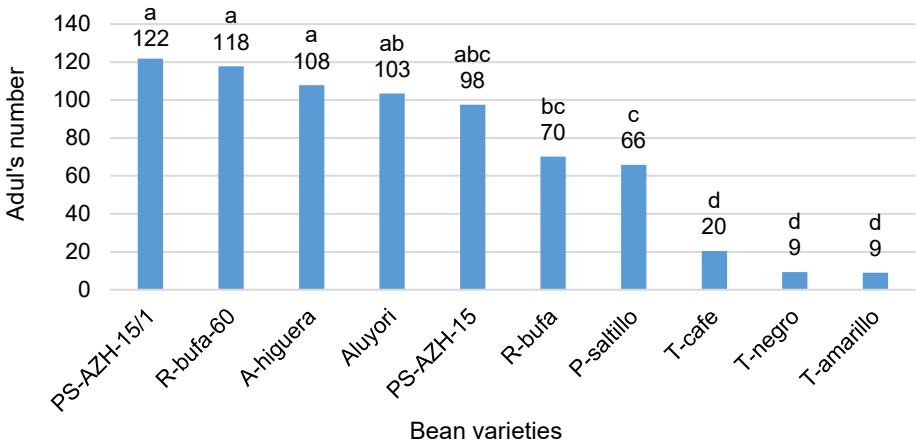

Figure 7. Number of adults in 10 bean varieties. DMS = 37.3. Means followed by the same letter are not significantly different *(LSD* = 0.05).

The varieties with more number of emerged adults of *A. obtectus* from Spain in the first generation were PS-AZH-15 (235) and P-saltillo (113) and less T-amarillo (2), T-negro (7) and T-cafe (36) (Jiménez et al., 2017). In present study we found that the varieties with more number of adults emerged from first generation of *A. obtectus* from México were PS-AZH-15/1 (122), R-bufa-60 (118 adults), A-higuera (108 adults), Aluyori (103 adults) and PS-AZH-15 (98) and interestingly the varieties are the same

with less number of adults T-amarillo (9 adults), T-negro (9 adults) and T-cafe (20 adults). The three varieties most resistant, by number of 1st adults generation, to *A. obtectus* from Spain agree with the same three that are more resistant to *A. obtectus* from Mexico. Armenta-López et al. (2021) reported Azufrado Higuera and Aluyori as resistant genotypes; at the contrary in our study we found Azufrado Higuera and Aluyori as susceptible genotypes.

Grain weight loss (%)

There are no differences between environments for grain weight loss (%). Significant differences were found for grain weight loss between varieties. The varieties with more grain weight loss were R-bufa-60 and R-bufa. The varieties with less grain weight loss were T-amarillo and PS-AZH-15 (Fig. 8).

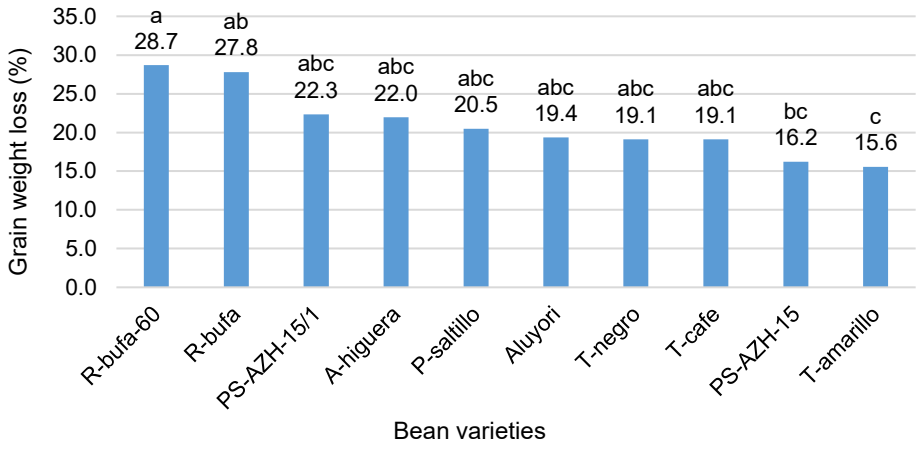

Figure 8. Grain weight loss in percent for 10 bean varieties. DMS = 8.8. Means followed by the same letter are not significantly different (*LSD* = 0.05).

Jiménez et al. (2017) reported PS-AZH-15 and P-saltillo as susceptible varieties with more grain weight loss (%) and three resistant varieties with less grain weight loss T-amarillo, T-negro and T-cafe. The results of previous research are different to present study because we found that the most susceptible varieties were R-bufa-60 and R-bufa. Likewise, P-saltillo, T-negro and T-cafe show the same level of susceptibility to *A. obtectus* from Mexico. The consistent variety is T-amarillo for resistance to both bruchids from Spain and Mexico.

Biological cycle (days)

There are no differences between environments for biological cycle. Significant statistical differences were found between varieties for biological cycle. The varieties that showed the longest biological cycle were T-amarillo, T-negro and T-cafe. The varieties with the shortest biological cycle were the rest (Fig. 9).

Velten et al. (2007) found that the arcelines in cotyledons provide clear evidence of growth inhibitor on first instar larvae. Jiménez et al. (2017) reported the biological cycle in winter and the duration of the biological cycle for the varieties at 10.5 °C was

106.5 days for T-amarillo, 98 for T-negro, 65.3 for T-cafe, 54.5 for P-saltillo and 50.8 for PS-AZH-15. These results are according with present research because we found a cycle for T-amarillo and T-negro of 73 days, 66 for T-cafe, 55 for PS-AZH-15/1, 54 for P-saltillo and 53 days for PS-AZH-15. The two bioassays were carried out at medium temperature of 14 °C. These results are consistent with Schmale et al. (2003) who reported that adult emergence in resistant varieties was from 45 to 95 days (RAZ 36, RAZ 94 and RAZ 104), while in susceptible varieties it ranges from 20 to 48 days, in the Calima bean variety.

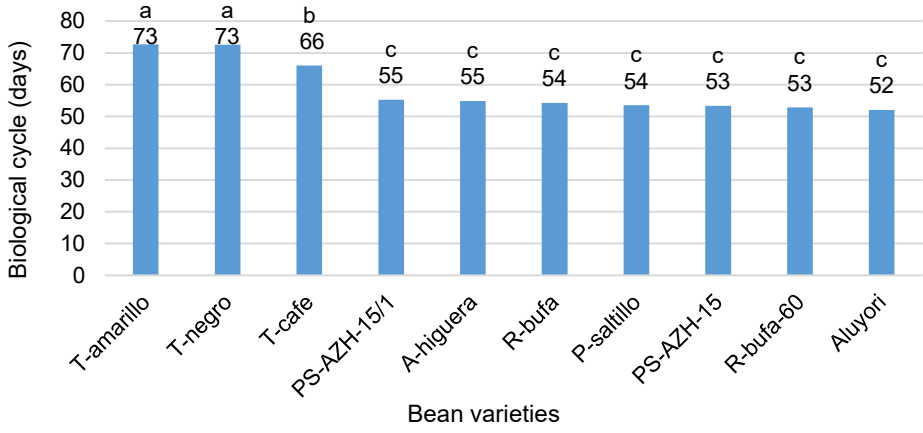

Figure 9. Biological cycle in days for 10 bean varieties. DMS = 5.2. Means followed by the same letter are not significantly different (*LSD* = 0.05).

CONCLUSIONS

The resistance level of the varieties do not changes according to the seed production environment.The most resistant varieties to *A. obtectus* from Mexico are T-amarillo, T-negro and T-cafe being T-amarillo the most resistant variety for *A. obtectus* from Mexico. The most resistant varieties had smaller seed size, lower number of eggs and larvae (except T-negro, higher larval mortality, lower number of first generation adults, lower grain weight loss and longer biologica)l cycle. T-negro has the highest number of eggs and larvae, however, also the highest number of dead larvae before entering the seed in number and percentage. The consistent variety is T-amarillo for resistance to both bruchids from Spain and Mexico. Probably *A. obtectus* from Spain is genetically different of *A. obtectus* of Mexico. The most susceptible varieties were PS-AZH-15/1, R-Bufa-60, A-higuera and Aluyori. Susceptible varieties had greater seed size, greater number of eggs and larvae, lower larval mortality, greater number of first generation adults, greater grain weight loss (except PS-AZH-15), and greater biological cycle. PS-AZH-15 presented one of the largest seed sizes; however, within the varieties with the highest seed weight, it presented a lower number of eggs and larvae and therefore lower number of adults emerged from the first generation and lower grain weight loss or lower consumption.

REFERENCES

Abdalla, A.A., Ahmed, M.F., Taha, M.B. & El Naim, A.M. 2015. Effects of Different environments on yield components of Faba Bean (*Vicia faba* L.). *International Journal of Agriculture and Forestry* **5**(1), 1–9. doi: 10.5923/j.ijaf.20150501.01

Acosta-Gallegos, J.A., Quintero, C., Vargas, J., Toro, O., Tohme, J. & Cardona, C. 1998. A new variant of arcelin in wild common bean, *Phaseolus vulgaris* L., from southern Mexico. *Genetic Resources and Crop Evolution* **45**, 235–242. doi: 10.1023/A:1008636132108

Admassu-Shimelis, E., Kumar-Rakshit, S. 2005. Antinutritional factors and in vitro protein digestibility of improved haricot bean (*Phaseolus vulgaris* L.) varieties grown in Ethiopia. *International journal of food sciences and nutrition* **56**, 377–387. doi: 10.1080/09637480500512930

Ahmed, S., Naroz, M., Abdel-Aziz, S., Awad, M. & Abdel-Shafy, S. 2019. Morphological, molecular and biological studies on common bean weevil *Acanthoscelides obtectus* (Say) in Egypt. *Journal of Entomology* **16**, 30–38. doi: 10.3923/je.2019.30.38

Armenta-López, A.R., Lugo-García, G.A., Sánchez-Soto, B.H., Romero-Félix, C.S., Cortez-Mondaca, E., Nava-Pérez, E. 2021. Resistencia del frijol al ataque del gorgojo pardo *Acanthoscelides obtectu*s (Say, 1831) (Coleoptera: Chrysomelidae) en la zona Norte de Sinaloa. *Acta zoológica mexicana* **37**, 1–18. doi: 10.21829/azm.2021.3712427

Beebe, S. &Corrales, M.P. 1991. Breeding for disease resistance. *Common beans: research for crop improvement* 561–617.

Bonal, R., Muñoz, A., Aparicio, J.M., Santoro, M. & Espelta, J.M. 2019. Filogeografía, factores históricos y especificidad parásito-hospedador: estudio comparativo de las comunidades de insectos depredadores de bellotas (*Curculio* spp.) en la Península Ibérica y California. *Ecosistemas* **28**(1), 15–25. doi: 10.7818/ECOS.1543

Cardona, C. & Kornegay, J. 1999. Bean germplasm resources for insect resistance. Global plant genetic resources for insect-resistant crops. CRC Press, Boca Raton:85–99.

Cardona, C., Kornegay, J., Posso, C.E., Morales, F. & Ramirez, H. 1990 Comparative value of four arcelin variants in the development of dry bean lines resistant to the Mexican bean weevil. E*ntomologia Experimentalis et Applicata* **56**, 197–206. doi: 10.1111/j.1570-7458.1990.tb01397.x

Cardona, C., Posso, C.E., Kornegay, J., Valor, J. & Serrano, M. 1989. Antibiosis effects of wild dry bean accessions on the Mexican bean weevil and the bean weevil (Coleoptera: Bruchidae). *Journal of Economic Entomology* **82**, 310–315. doi: 10.1093/jee/82.1.310

Cid-Gallegos, M.S., de las Mercedes Gómez, Y., Corzo-Ríos, L.J.C.-R., Sanchez-Chino, X.M., Moguel-Concha, D., Borges-Martínez, E. & Jiménez-Martínez, C. 2023. Potencial nutricional y bioactivo de frijol (*Phaseolus vulgaris*) en la salud humana. *Investigación y Desarrollo en Ciencia y Tecnología de Alimentos* **8**, 309–318. doi: 10.29105/idcyta.v8i1.42

Espinal, R., Higgins, R. & Wright, V. 2004. Economic Losses Associated with *Zabrotes subfuscintus* (Boheman) (Coleoptera: Bruchidae) and *Acanthoscelides obtectus* (Say) (Coleoptera: Bruchidae) infestations of stored dry red beans (*Phaseolus vulgaris* L.) in Southeastern Honduras. *Ceiba* **45**(2), 107–119.

FAOSTAT. Statistical Database. In Food and Agriculture Organization of the United Nations; FAO: Rome, Italy. 2022. Available online: http://faostat.fao.org/ (accessed on 20 May 2023).

Fory, L., Finardi-Filho, F., Quintero, C., Osborn, T.C., Cardona, C., Chrispeels, M.J. & Mayer, J.E. 1996. α-Amylase inhibitors in resistance of common beans to the Mexican bean weevil and the bean weevil (Coleoptera: Bruchidae). *Journal of economic entomology* **89**, 204–210. doi: 10.1093/jee/89.1.204

Gutièrrez-Jiròn, X.J. 2016. Manejo de *Acanthoscelides obtectus* (Say) en frijol común (*Phaseolus vulgaris* L.) almacenado utilizando Bauveria bassiana (Bals y Vull), Managua, Nicaragua 2016, Universidad Nacional Agraria. https://repositorio.una.edu.ni/id/eprint/3446

Hartweck, L., Cardona, C. & Osborn, T.C. 1997. Bruchid resistance of common bean lines having an altered seed protein composition. *Theoretical and Applied Genetics* **95**, 1018–1123. doi: 10.1007/s001220050656

Iturralde-García, R.D., Castañé, C., Wong-Corral, F.J. & Riudavets, J. 2020. Biological control of *Acanthoscelides obtectus* and *Zabrotes subfasciatus* in stored dried beans. *BioControl* **65**, 693–701. https://doi.org/10.1007/s10526-020-10048-5

Jiménez-Galindo, J.C., Tortosa, M., Velasco, P., De La Fuente, M., Ordás, B. & Malvar, R.A. 2020. Inheritance and metabolomics of the resistance of two F_2 populations of *Phaseolus* spp. to *Acanthoscelides obtectus*. *Arthropod-Plant Interactions* **14**, 641–651. doi: 10.1007/s11829-020-09776-3

Jiménez, J.C., de la Fuente, M., Ordás B., Domínguez, L.E.G. & Malvar, R.A. 2017. Resistance categories to *Acanthoscelides obtectus* (Coleoptera: Bruchidae) in Tepary bean (*Phaseolus acutifolius*), new sources of resistance for dry bean (*Phaseolus vulgaris*) breeding. *Crop Protection* **98**, 255–266. https://doi.org/10.1016/j.cropro.2017.04.011

Jones, R. 1987. Behavioural evolution in the cabbage butterfly (*Pieris rapae*). *Oecologia* **72**, 69–76. doi: 10.1007/BF00385047

Keneni, G., Bekele, E., Getu, E., Imtiaz, M., Damte, T., Mulatu, B. & Dagne, K. 2011. Breeding Food Legumes for Resistance to Storage Insect Pests: Potential and Limitations. *Sustainability* **3**, 1399–1415. https://doi.org/10.3390/su3091399

Kornegay, J., Cardona, C. & Posso, C.E. 1993. Inheritance of resistance to mexican bean weevil in common bean, determined by bioassay and biochemical tests. *Crop Science* **33**, 589–594. https://doi.org/10.2135/cropsci1993.0011183X003300030034x

Kornegay, J.L. & Cardona, C. 1991. Inheritance of resistance to Acanthoscelides obtectus in a wild common bean accession crossed to commercial bean cultivars. *Euphytica* **52**, 103–111. doi: 10.1007/BF00021322

Kusolwa, P. & Myers, J. 2011. Seed storage proteins ARL2 and its variants from the apalocus of wild Tepary bean G40199 confers resistance to *Acanthoscelides obtectus* when expressed in common beans. *African Crop Science Journal* **19**(4), 255–265.

Lak, F., Zandi-Sohani, N., Ghodoum-Parizipour, M.H. & Ebadollahi, A. 2022. Synergic effects of some plant-derived essential oils and Iranian isolates of entomopathogenic fungus Metarhizium anisopliae Sorokin to control *Acanthoscelides obtectus* (Say) (Coleoptera: Chrysomelidae). *Frontiers in Plant Science* **13**, 1075761. doi: 10.3389/fpls.2022.1075761

Mbogo, K., Davis, J. & Myers, J. 2009. Transfer of the arcelin-phytohaemagglutinin-α amylase inhibitor seed protein locus from Tepary bean (*Phaseolus acutifolius* A. Gray) to common bean (*P. vulgaris* L.). *Biotechnology* **8**, 285–295. doi: 10.3923/biotech.2009.285.295

Minney, B.H.P., Gatehouse, A.M.R., Dobie, P., Dendy, J., Cardona, C. & Gatehouse, J.A. 1990. Biochemical-bases of seed resistance to *Zabrotes subfasciatus* (bean weevil) in *Phaseolus vulgaris* (common bean) - a mechanism for arcelin toxicity. *Journal of Insect Physiology* **36**(10), 757–761, 763–767. doi: 10.1016/0022-1910(90)90049-L

Osborn, T.C., Alexander, D.C., Sun, S.S.M., Cardona, C. & Bliss, F.A. 1988. Insecticidal activity and lectin homology of arcelin seed protein. *Science* **240**, 207–210. doi: 10.1126/science.240.4849.207

Parsons, D.M. & Credland, P.F. 2003. Determinants of oviposition in Acanthoscelides obtectus: a nonconformist bruchid. *Physiological Entomology* **28**, 221–231. doi: 10.1046/j.1365-3032.2003.00336.x

Rodríguez-González, A., Casquero, P.A., Cardoza, R.E. & Gutiérrez, S. 2019. Effect of trichodiene synthase encoding gene expression in Trichoderma strains on their effectiveness in the control of Acanthoscelides obtectus. *Journal of Stored Products Research* **83**, 275–280. doi: 10.1016/j.jspr.2019.07.006

Sales, M.P., Gerhardt, I.R., Grossi-de-Sa, M.F. & Xavier, J. 2000. Do legume storage proteins play a role in defending seeds against bruchids? *Plant Physiology* **124**, 515–522. doi: 10.1104/pp.124.2.515

SAS Institute. Base SAS 9.4 Procedures Guide: Statistical Procedures. Version 9.4; SAS Institute: Cary, NC, USA, 2016.

Schmale, I., Wackers, F.L., Cardona, C. & Dorn, S. (2003) Combining parasitoids and plant resistance for the control of the bruchid *Acanthoscelides obtectus* in stored beans. *Journal of Stored Products Research* **39**, 401–411. doi: 10.1016/s0022-474x(02)00034-6.

Schoonhoven A.v., Cardona C.v. & Valor J. 1983. Resistance to the bean weevil and the Mexican bean weevil (Coleoptera: Bruchidae) in noncultivated common bean accessions. *Journal of Economic Entomology* **76**, 1255–1259. doi: 10.1093/jee/76.6.1255

Shade, R.E., Pratt, R.C. & Pomeroy, M.A. 1987. Development and mortality of the bean weevil, Acanthoscelides obtectus (Coleoptera: Bruchidae), on mature seeds of Tepary beans, *Phaseolus acutifolius*, and common beans, *Phaseolus vulgaris*. E*nvironmental entomology* **16**, 1067–1070. doi: 10.1093/ee/16.5.1067

Silva, F.B., Monteiro, A.C.S., Del Sarto, R.P., Marra, B.M., Dias, S.C., Fiqueiraa, E.L.Z., Oliveira, G.R., Rocha, T.L., Souza, D.S.L., da Silva, M.C.M., Franco, O.L. & Grossi-de-Sa, M.F. 2007. Proregion of *Acanthoscelides obtectus* cysteine proteinase: A novel peptide with enhanced selectivity toward endogenous enzymes. *Peptides* **28**, 1292–1298. doi: 10.1016/j.peptides.2007.03.020

Sword, G. & Chapman, R. 1994. Monophagy in a polyphagous grasshopper, *Schistocerca shoshone*. *Entomologia Experimentalis et Applicata* **73**, 255–264. doi: 10.1111/j.1570-7458.1994.tb01863.x

Tucić, N., Gliksman, I., Šešlija, D., Milanović, D., Mikuljanac, S. & Stojković, O. 1996. Laboratory evolution of longevity in the bean weevil (*Acanthoscelides obtectus*). *Journal of Evolutionary Biology* 9, 485–503. doi: 10.1046/j.1420-9101.1996.9040485.x

Valencia Cataño, S.J. 2006. Efectos subletales de resistencia antibiótica a inmaduros en la demografía de adultos de los gorgojos de frijol *Acanthoscelides obtectus* (Say) y *Zabrotes subfasciatus* (Boheman) (Coleoptera: Bruchidae). Tesis (Ingeniero Agrónomo), Universidad Nacional de Colombia, Facultad de Ciencias Agropecuarias.

Velten, G., Rott, A.S., Cardona, C. & Dorn, S. 2007. The inhibitory effect of the natural seed storage protein arcelin on the development of *Acanthoscelides obtectus*. *Journal of stored products research* **43**, 550–557. doi: 10.1016/j.jspr.2007.03.005

Velten, G., Rott, A.S., Petit, B.J.C., Cardona, C. & Dorn, S. 2008. Improved bruchid management through favorable host plant traits and natural enemies. *Biological Control* **47**, 133–140. doi: 10.1016/j.biocontrol.2008.07.009

Zaugg, I., Magni, C., Panzeri, D., Daminati, M.G., Bollini, R., Benrey, B., Bacher, S. & Sparvoli, F. 2013. QUES, a new *Phaseolus vulgaris* genotype resistant to common bean weevils, contains the Arcelin-8 allele coding for new lectin-related variants. *Theoretical and applied genetics* **126**, 647–661. doi: 10.1007/s00122-012-2008-2

Agronomy Research **22**(S3), 1460–1484, 2024
https://doi.org/10.15159/AR.24.079

Adapting agriculture to climate shifts: managing crop water needs for environmental resilience in Sindh, Pakistan

H.U. Qureshi[1,*], I. Abbas[2], S.M. H. Shah[3], Z.U. Qureshi[4], E.H.H. Al-Qadami[5], Z. Mustaffa[6] and F.Y. Teo[7,*]

[1]Associated Consulting Engineers (ACE) Limited, D-288, KDA Scheme No.1, Stadium Road, PAK75350 Karachi, Pakistan
[2]Sir Syed University of Engineering and Technology, Faculty of Civil Engineering and Architecture, Department of Civil Engineering, Main University Road, PAK75300 Karachi, Pakistan
[3]Interdisciplinary Research Centre for Membranes and Water Security, King Fahd University of Petroleum and Minerals, SA31261 Dhahran, Saudi Arabia
[4]NED University of Engineering and Technology, Department of Civil Engineering, University Road, PAK75270 Karachi, Pakistan
[5]Eco Hydrology Technology Research Centre (Eco-Hytech), Faculty of Civil Engineering and Built Environment, Universiti Tun Hussein Onn Malaysia, MY86400 Parit Raja, Malaysia
[6]Department of Civil and Environmental Engineering, Universiti Teknologi PETRONAS, MY32610 Seri Iskandar, Malaysia
[7]Faculty of Science and Engineering, University of Nottingham Malaysia, MY43500 Semenyih, Selangor, Malaysia
[*]Correspondence: harisuddinq@gmail.com; fangyenn.teo@nottingham.edu.my

Received: February 9th, 2024; Accepted: June 5th, 2024; Published: August 22nd, 2024

Abstract. Sindh is an important hub for the agricultural production in Pakistan. Therefore, this study was aimed to model the air temperature trend in Sindh and its impacts on the seasonal water requirement for Rice, Wheat, and Sugarcane under the Representative Concentration Pathways (RCP) 4.5 and 8.5 scenarios. In this study, RegCM4 with GFDL-ESM2M was used and the bias correction of RegCM4 simulations was done using Quantile Mapping. As per the analysis, the average annual temperature over the study area may rise by about 1.2 to 1.8 °C and 2.8 to 3.3 °C under RCP 4.5 and 8.5 scenarios respectively. Seasonally, warming is expected to be higher in spring and winter seasons, whereas, diurnally, the daytime temperature may increase by about 1.2 to 1.7 °C and 2.6 to 3.2 °C, while the nighttime temperature may rise by about 1.4 to 2.7 °C and 3.0 to 3.5 °C under the RCP 4.5 and 8.5 scenarios respectively. Consequentially, the seasonal water requirement for Rice in Sindh may increase by about 50–100 mm and 100–200 mm under RCP 4.5 and 8.5 scenarios respectively. For Wheat, the water requirement may rise by about 60 mm and 100 mm, whereas for Sugarcane, it may soar by about 100–150 mm and 150–200 mm under RCP 4.5 and 8.5 scenarios respectively. Conclusively, the rising crop water consumption may cause increased irrigation requirements, low crop water productivity and yield, and rising local water disputes thereby endangering the crop production and water security in the province.

Key words: climate change, crop water requirement, CROPWAT, CORDEX, food security, quantile mapping, RegCM4, SDG 13.

INTRODUCTION

Climate variability has turned out to be one of the most pressing issues for the world community due to its adverse impacts on the freshwater resources, agriculture, human health, and the overall ecosystem. Climate change is legitimately blamed to be human-induced with the main reasons including the land cover changes and unplanned development, deforestation, industrialization, burning of fossil fuels and rising Greenhouse Gases (GHGs) which destabilizes the global radiation balance and leads to the changing climate regime (Chong et al., 2021; Abbas et al., 2022). Globally, the unfavourable impacts of varying climate have been witnessed in the form of soaring temperatures, extreme meteorological events, seasonal shifts, melting glaciers, flash floods, and rising sea levels (Raihan, 2023). For instance, during the past 100 years, the mean global temperature has soared by about 0.74 °C, where in South Asia, warming increased by about 0.75 °C (Shah et al., 2020; Penev et al., 2021). Temporally, warming has been higher during the later years of century, where the earth temperature heated by about 0.18 °C per decade since 1981 alone (Akaev & Davydova, 2023). Due to the significant dependence on the natural resources and agriculture, lack of climate chnage adaptation and mitigation capacity, high population growth rate and poverty, the climate change adversities are expected to be worst in Asia, where as per the Intergovernmental Panel on Climate Change (IPCC), some parts of Asia have warmed up by 2 °C than the pre-industrial period (1850–1900), that is higher than global temperature anomaly (+1.1 °C) (You et al., 2022).

Table 1. Temporal change in global GHG levels with life span and warming potential

GHG	Level in 1870	Level in 2007	Level in 2022	Life Span in years	Warming potential (Relative to CO_2)
CO_2	280 ppm	399 ppm	420 ppm	300–1,000	1
CH_4	700 ppb	1,745 ppb	1,932 ppb	12	72
NO	270 ppb	314 ppb	334 ppb	114	310
SF6	0	3.5 ppt	10.5 ppt	3,200	16,300

Source: Rasul et al., 2012); ppt: parts per trillion; ppb: parts per billion; ppm: parts per million.

Among all major anthropogenic factors reprehensible for the changing climate patterns, the rising GHG concentrations across the globe (as shown in Table 1) is the prime cause behind the destabilizing global heat balance and consequently varrying climate patterns. For capturing the climate patterns under different GHG emission scenarios and to forumulate climate change adaptative and mitgation policy accordingly, IPCC in its 5th Assessment Report (2014) has adopted four (04) radiative forcing scenarios known as the Representative Concentration Pathways (RCPs) which depend on the magnitude of GHG concentrations and the mitigative measures adopted by the world community in the coming decades (Pedersen et al., 2022). Radiative forcing generally refers to the difference between the incoming and outgoing solar heat energy (in Watt m^{-2}), with greater the difference, the more will be the entrapped heat and

warmer will be the earth temperature. RCPs are categorized as RCP 2.6, 4.5, 6.0, and 8.5. As per IPCC, RCP 2.6 is a scenario under which the radiative forcing (global) may touch 2.6 Watt m^{-2} by 2100. Further, this scenario assumes that the CO_2 emissions begin to decrease by 2020 and drops to zero by 2100. Further, it also expects Sulphur dioxide (SO_2) emissions to around 10% of 1980 to 1990 levels, and CH_4 reduction to about half of 2020 levels by 2100. Under this scenario, the mean global temperature is expected to climb by about 1.5 to 2.0 °C by 2100 than the pre-industrial baseline. RCP 4.5 is a scenario under which the radiative forcing may reach to about 4.5 Watt m^{-2}, with the global CO_2 levels heading to 550 to 600 ppm by the end of 21st century. This scenario calls for a decline in CO_2 levels from 2045, so as to attain half of the levels of 2050 by 2100. Similarly, CH_4 emissions also need to be ceased by 2050 and decline to about 75% of CH_4 levels of 2040, while SO_2 levels are assumed to reach 20% of levels of 1980 to 1990 by 2100. In this scenario, the global temperature may warm by about 2.5 to 3.0 °C. RCP 8.5 is the worst-case scenario with no formulation and implementation of climate change mitigation policies by the world community and the global CO_2 levels marching to approximately 1,200 ppm by 2100. Under this scenario, the global temperature is expected to rise by about 5 °C by the end of century (Pedersen et al., 2022).

In order to computationally project the climate patterns under the different RCP scenarios, numerical climate models have been used (Panfilova et al., 2020). These models are categorized spatially as the Global Climate Model (GCM) and the Regional Climate Model (RCM). GCMs have a coarser (lower) spatial resoutlion (typically 150–300 km) and project the climate patterns on the global-scale, while RCMs (spatial resoultion as 20–60 km) project the climate patterns on a regional scale by using the Initial Conditions (ICs) and the Lateral Boundary Condtions (LBCs) of a GCM, and better captures the region-specific climate patterns (Barnes et al., 2024; Gutierrez et al., 2024). As per the literature, RCM projections are basically the transformed outcomes of GCMs on a finer resolution via downscaling. Downscaling refers to the transformation of lower resolution GCM outputs to a higher resolution climate data and is done using the Statistical or Dynamical appraoch (Boe et al., 2023; Zhang et al., 2023). Dynamical downscaling involves the use of a finer resolution RCM to dynamically transform the GCM projections, while in statistical downscaling, a statistical nexus is etablished between the past global and local climate trends to understand how the local climate is responding to the planetary-scale climate variability. This statistical relation is then applied on the GCM datasets to regionalize the model outcomes.

As discussed above, GCMs due to the coarser resolution are suitable only for planetary-scale climate projections as it miss the region-specific climate features and may ultimately mislead the regional climate analysis. Therefore, RCMs due to the higher resolution have been suggested and employed in various studies to conduct regional climate change assessement. For example, Raul (2017) used a RCM called REMO (2009) with the GCM named MPI-ESM-LR to study the agricultural susceptibility over Maharashtra in the Western India under the changing climate scenarios for the period 2015 to 2100. The model outcomes projected a rise in precipitation by about 80 to 250 mm and the temperature increment of about 0.5 to 2.5 °C over the study area by 2099. Ali et al. (2021) employed a RCM named RegCM4, with three (03) GCMs from the Coupled Model Intercomparison Project 5th Phase (CMIP5) namely MPI-ESM-MR, NorESM1-M and MICROC5 to determine the shift in the Monsoon rainfall over the Upper Indus Region and Pakistan. The results indicated a greater strength gain in

Monsoon under RCP 8.5 over the UIB than RCP 2.6. For Pakistan overall, a slight decline (increase) in precipitation is projected under the RCP 8.5 (RCP 2.6) scenario. Hassan et al. (2014) employed the RegCM, utilizing two experiments with ECMWF's Reanalysis data (ERA-40) and ECHAM5 for the period 1971–2000, confirming the model's accurate reproduction of air temperatures and effective analysis of Monsoon precipitation in South Asia.

RegCM is a Regional Climate Model developed by the Italy's International Center for Theoretical Physics (ICTP) for extended regional climate studies. The model solves a set of dynamical equations describing the atmosphere dynamics along with the parameterization for physical climate processes including radiation, convection, turbulent diffusion, clouds and precipitation, soil moisture and ocean fluxes, and tracer transport and chemistry to capture the atmospheric state of a region (Eghbali et al., 2022). Nevertheless, due to the regionally varyig topography and climate features, the RCM simulations often yield errors known as the Biases, which may question the reliability and raise uncertainty in the model outcomes. Therefore, different bias correction techniques have been proposed including Linear Scaling (LS), Power Transformation (PT), Local Intensity Scaling (LOCI), Distribition Mapping (DM), and the Quantile Mapping (QM) method as shown in the Table 2 (Fang et al., 2015). As per the past studies, the QM approach works well to remove biases from daily as well as monthly climate model simulations (Xue et al., 2022; Rajulapati & Papalexiou, 2023).

Table 2. Mathaemtical expressions for the commonly used bias correction methods

Bias Correction Method	Equation	
	Temperature	Precipitation
Linear scaling	$T_{corrected} = T_{Sim} + \mu(T_{obs}) - \mu(T_{sim})$	$P_{corrected} = P_{sim} \cdot \frac{\mu(P_{obs})}{\mu(P_{sim})}$ where $P_{corrected} = 0$, if $P_{sim} < P_{Thres}$
Local intensity scaling (LOCI) of precipitation	-	$P_{corrected} = P_{sim} \times S_m$ where $S_m = \frac{\mu(P_{obs} \mid P_{obs}>0)}{\mu(P_{sim} \mid P_{sim}>P_{Thres})}$
Power transformation (PT) of precipitation	-	$P_{corrected} = S_m \cdot P_{LOCI}^{b}$ where $S_m = \frac{\mu(P_{obs})}{\mu(P_{LOCI}^{b})}$ $f(b) = \frac{\sigma(P_{obs})}{\mu(P_{obs})} - \frac{\sigma(P_{LOCI}^{b})}{\mu(P_{LOCI}^{b})}$
Variance scaling (VARI) of temperature	$T_{corrected} = [T_{sim} - \mu(T_{sim})] \cdot \frac{\sigma(T_{obs})}{\sigma(T_{sim})} + \mu(T_{obs})$	-
Distribution/ Mapping (DM)	$T_{corrected} = F_N^{-1}(T_{sim} \mid \mu_{sim}, \sigma_{sim}) \mid \mu_{obs}, \sigma_{obs})$ where $f_N(x \mid \mu, \sigma) = \frac{1}{\sigma\sqrt{2\pi}} \cdot e^{\frac{-(x-\mu)^2}{2\sigma^2}}$; $x \in R$	$P_{corrected} = F_r^{-1}(F_r(P_{LOCI} \mid \alpha_{LOCI}, \beta_{LOCI}) \mid \alpha_{obs}, \beta_{obs})$ where $f_r(x \mid \alpha, \beta) = x^{\alpha-1} x \frac{1}{\beta^{\alpha}} \cdot e^{\frac{-x}{\beta}}$; $x \geq 0, \alpha, \beta > 0$
Quantile Mapping (QM)	$T_{Corrected} = x_{ms} + F_{oh}^{-1}(F_{ms}(x_{ms})) - F_{mh}^{-1}(F_{ms}(x_{ms}))$	$P_{corrected} = F_{oh}^{-1}(F_{mh}(x_{ms}))$, $x_{ms} \geq x_{th}$

Source: Fang et al., 2015.

The agriculture sector is highly susceptible to climate change due to its heavy reliance on the climate patterns and water availability (Mokrikov et al., 2019; Horváth et al., 2021; Talukder et al., 2022; Viikoja et al., 2023). Globally, agriculture is the largest consumer of freshwater as it consumes about 72% of the yearly global freshwater withdrawals (Bazrafshan et al., 2022; Rosa, 2022). A crop usually meet its water requirement through Evapotranspiration (ET). According to the Food and Agriculture Organization (FAO), Crop Water Requirement (CWR) is the depth of water required by a crop for ET (Ehteram et al., 2021; Pereira et al., 2021). Thermodynamically, evaporation only depends on weather conditions (temperature, humdity, windspeed, and solar radiation), while for transpiration, climate as well as soil properties, crop type and its growth phase, land treatment practice, and position of watertable are the influential factors (Paul et al., 2022). Furthermore, poor land fertility and soil management, high soil pH, limited and inadequate use of fertilizers, lack of disease and pest control, and low water availability also impacts (lowers) transpiration.

For crop water requirement, Reference Evapotranspiration (ET_o) is estimated which shows the evaporating potential or evaporatice demand of atmosphere and depends only on the weather conditions of region. According to FAO, ET_o is the ET from a reference crop surface (typically grass or alfalfa) 0.12 m tall, 70 s m^{-1} of surface resistance, surface albedo of 0.23, and having suffecient water on the field with non-restricting soil conditions (Srdić et al., 2023). Due to the sufficient water on the reference crop surface, the soil and crop properties do not interfere with the ET process, and thus ET_o solely indicates the energy available in the atmosphere to evaporate water from the surface. Apart from climate, the influence of soil texture, depth to water table, management practice, and the crop growth stage on crop ET is accounted with the help of a crop parameter known as Crop Coefficient (K_c). As per FAO, K_c is the ratio of actual ET from the crop field measured using the lysimeter to ET_o under the same environmental conditions. K_c is an empirical parameter and is estimated by conducting the lysimetric studies. The value of K_c noticeably varies with the crop growth stage as the crop ET is lowest during the sowing stage, starts increasing with the development phase, reaches its maximum during the late stage, and then declines as the crop march towards its harvesting phase after gaining full maturity (Liu et al., 2023).

For ET_o, FAO Penman-Monteith (PM) equation is the most reliable and widely used approach to estimate the daily as well as monthly ET_o under different climate conditions (Xing et al., 2023; Zerihun et al., 2023). For instance, Abeysiriwardana et al. (2022) used the FAO PM method to estimate ET_o in different parts of Sri Lanka. Awal et al. (2020) used the PM equation to determine ET_o over the Western Texas in USA. Ndule & Ranjan (2021) also used the PM equation to estimate ET_o over the semi-arid southern Manitoba (Canada). However, due to the large soil, crop, and weather data required for the equation which might not be available for all regions and time period, the equation proposed by Hargreaves and Samani (1985) known as the Hargreaves (HG) equation can be used for ET_o. However, the method overestimates ET_o under the humid climate conditions and underestimates under the semi-arid conditions, whereas spatially, the equation underestimates ET_o over the inland areas and overestimates nearer to the coastal zones. In order to overcome this limitation, the previous studies have proposed the local calibration of HG equation. For example, Lujano et al. (2023) calibrated the HG equation for computing ET_o in the Peruvian Altipano (Peru) by taking FAO PM

equation as a reference. Ramírez et al. (2023) used the HG equation after local adjustment for computing ET_o in the semi-arid region of Mexico. Al-Asadi et al. (2023) also used FAO PM equation as a benchmark to calibrate HG equation so as to estimate ET_o in different parts of Iraq.

Pakistan is an agrarian country with nearly 24 Million hectares (Mha) of its area under cultivation, 25% of its Gross Domestic Product (GDP) depends on the agricultural and livestock sector, and more than 90% of its freshwater resources are utilized for the agricultural and livestock production (Raza et al., 2023a). As per the Pakistan Agricultural Research Council (PARC), about 90% of the agricultural production in Pakistan depends on irrigation, as the country's precipitation can meet only 10 to 15% of the water requirements (Qureshi, 2020). The major source of freshwater in Pakistan is the mighty Indus Basin having the mean annual runoff of 146 million Acre-ft (MAF), where about 50 to 70% of its annual flow comes from the glacier and snowmelt runoff and remaining from the Monsoon and winter precipitation (Romshoo & Marazi, 2022). Apart from surface water, Pakistan also relies on groundwater for its domestic and agricultural water needs. As per the Water and Power Development Authority (WAPDA) of Pakistan, the mean annual groundwater recharge from the Indus Basin in Pakistan is about 55 MAF, where the country extracts nearly 50 MAF every year. In addition, Pakistan is the world's 3rd largest consumer of groundwater for agriculture, where approximately 73% of its irrigated area relies on groundwater. For crop production, Pakistan has two growing seasons namely Kharif (May to September) and Rabi (October to April), with the country's major crops including Rice, Wheat, Sugarcane, Cotton, chilies, fruits, and vegetables that serve as a major source of foreign exchequer to the national economy and livelihoods for the local farmers (Qureshi, 2020).

Rice is a major Kharif crop of Pakistan grown on an area of about 2.7 Mha in the country, with the per hectare yield of 2.95 tonnes and the mean annual production of 8.0 million tonnes (Ghani et al., 2023). The crop is among the highest water consuming crops consuming about 70% of the irrigation withdrawals in the country due to a continuous submergance required for its growth (Akbar et al., 2023). In Sindh, Rice is grown in between July to September on an area of about 0.75 Mha, with the annual production of about 2 million tonnes. In Sindh, the seasonal water requirement of Rice is higher than Punjab due to warmer climate, where about 1,200 to 1,500 mm is consumed in the former for Rice production (Joyo et al., 2023). Wheat is an important Rabi crop of Pakistan grown on an area of about 9.2 Mha in the country, with the mean annual production of 26 million tonnes and the per hectare yield of about 2.8 tonnes. In Sindh, Wheat is grown on an area of about 1.12 Mha in between November to March, with the mean annual production of about 4 million tonnes and the seasonal water consumption of about 400 mm (Nangraj et al., 2023). Contrarily to Rice and Wheat, Sugarcane is a perenial crop grown on an area of about 1.2 Mha in Pakistan, with the mean annual production of 64 million tonnes. In Sindh, Sugarcane is grown on an area of 0.3 Mha, with the seasonal crop water consumption in the province as 1,700 to 2,000 mm (Raza et al., 2023b).

Pakistan has repeatedly been considered among the topmost countries that are at high risk of climate change. As per IPCC, warming in Pakistan is expected to be more than the global average in coming years, where the mean temperature may increase by about 5.3 °C by the end of 21st century, that is more than the global predicted

temperature rise (3.7 °C) (Gul et al., 2022). According to the Global Change Impact Studies Centre (GCISC), warming may soar by about 4.6 °C in Sindh, 5.04 °C in Balochistan, 5.06 °C in Punjab, 5.4 °C in KPK, and 5.8 °C in Gilgit-Baltistan under RCP 8.5 scenario (Javed & Khan, 2019). Different studies have been conducted in the past to assess the climate change impacts on the crop water requirements in Pakistan. For instance, Shafeeque & Amna (2023) modeled the seasonal CWR in different parts of Pakistan under CMIP6 scenarios. As per the study, under SSP245 scenario, the Kharif seasonal CWR may increase by 0.48–0.74 mm year^{-1}, whereas in Rabi season, the CWR may increase by 0.47–0.64 mm year^{-1}. Under SSP845 scenario, the Kharif CWR may increase by 1.26–1.54 mm year^{-1}, whereas the Rabi seasonal CWR in the country may increase by 0.98–1.20 mm year^{-1} by 2100. Similarly, Ahmad et al. (2021) modeled the seasonal CWR in Rice-Wheat Punjab under RCP 4.5 and 8.5 scenarios for the period 2021–2050 and 2051–2080. The analysis projected the Wheat seasonal ET to increase by 10–13 mm and 26–37 mm during 2021–2050 and 2051–2080 respectively, whereas the Rice seasonal ET may increase by 5–22 mm and 5–25 mm during 2021–2050 and 2051–2080 respectively. Ahmed & Choi (2018) also modeled the climate change influence on ET_o over the Upper Chenab Command area of Punjab under the A1B scenario. The study projected the winter seasonal ET_o to raise by 21–26 mm and 45–55 mm during 2021–2050 and 2051–2080 respectively, while the summer seasonal ET_o may raise by 16–21 mm and 51–63 mm during 2021–2050 and 2051–2080 respectively.

The Sindh province is worst affected by climate extremes during the past decades. Therefore, this study was conducted to model the air temperature patterns in Sindh and its impacts on the seasonal CWR for Rice, Wheat, and Sugarcane under RCP 4.5 and 8.5 scenarios. The outcomes of this study may help in understanding the future climate variability and its impacts on the crop water demand and freshwater resources in Sindh, and to formulate holistic and well-integrated climate change adaptation and freshwater management measures for ensuring food and water security in the province under the climate change scenarios.

MATERIALS AND METHODS

Study Area

Sindh is an important contributor to the agricultural and livestock sector of Pakistan after Punjab. Geographically, Sindh lies in the Sub-tropical region between the latitudes 23° to 29 °N and between the longitudes 67° to 70°E, spanning on an area of about 14.09 Mha as shown in the Fig. 1. The Gross Command Area (GCA) of Sindh is about 5.53 Mha, out of which 4.87 Mha is under cultivation (Mangan et al., 2021). However, due to the poor drainage infrastructure, about 36% of GCA in the province is waterlogged and is affected by high soil salinity, with the dominant water table depth ranging from about 1.5 to 3.0 m. Climatologically, Sindh is characterized with hot and rainy summers and cold dry winters, with the maximum temperature often touches 46 °C in May, and minimum temperature as low as 2 °C during winter (January). Sindh is predominantly arid with the annual precipitation across the province ranging from about 150–350 mm, where the major fraction of its yearly rainfall is recieved during Summer season (July–September) from the Southwest Monsoon system (Kumar et al., 2023).

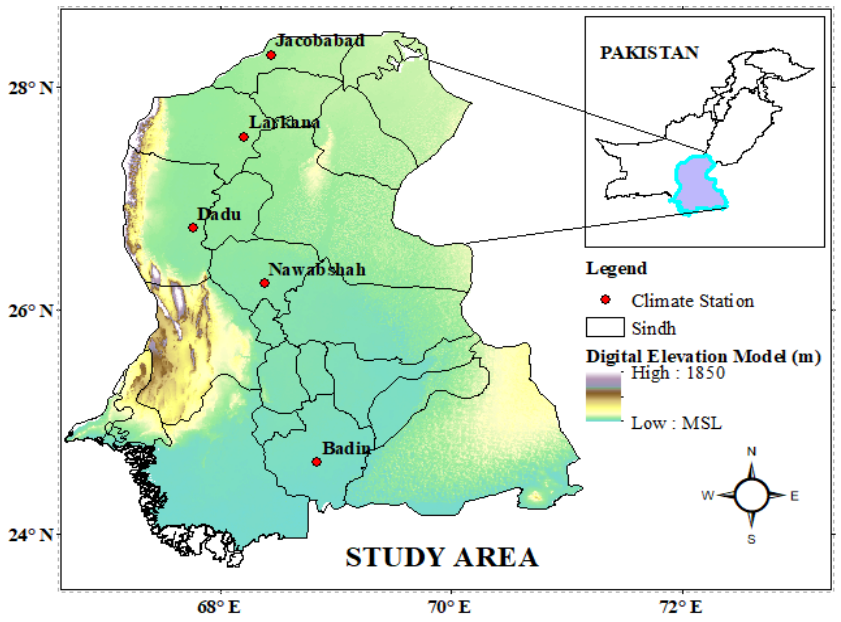

Figure 1. Study area and the selected stations.

Lithologically, based on the FAO soil classification, Sindh is classified into ten (10) different soil classes as shown in the Fig. 2, with clayey loam is the dominant soil texture, which favour crop yields due to high field capacity (as shown in Table 3).

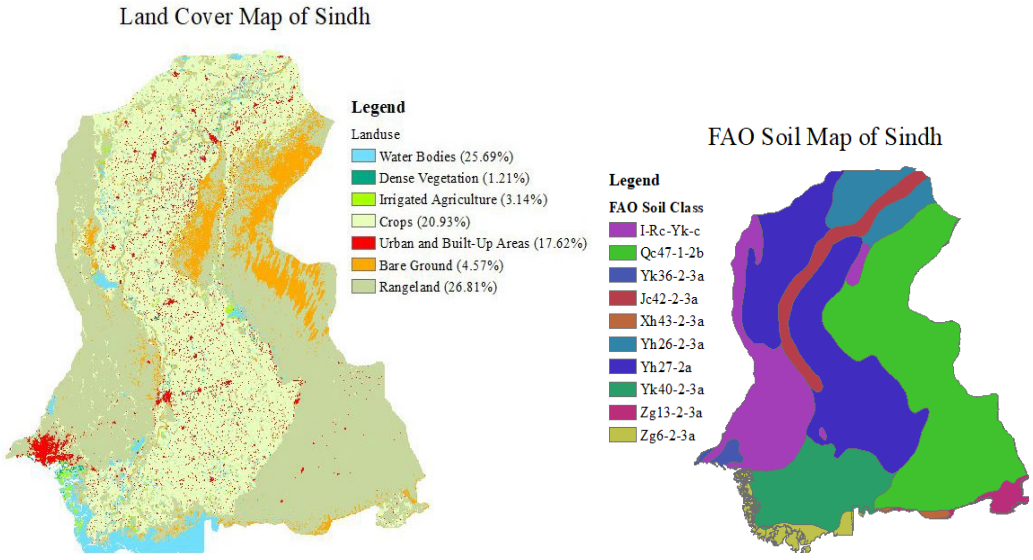

Figure 2. Landuse and FAO soil classification of Sindh, Pakistan.

On the other hand, based on the Sentinel-02 landuse classification, the dominant land cover of Sindh comprises of water bodies (25.69%), irrigated and rainfed cropfields (20.93%), urban areas (17.62%), and rangeland mainly consisting of moderate to sparse bushes, Mangrooves, shrubs and grass tufts, and savannas with less grasses, trees and other plants (26.81%).

Table 3. Representative physical properties of FAO soil classes in Sindh

FAO Soil Class	Soil texture	Soil composition			Specific gravity	Porosity (%)	Infiltration rate (mm h^{-1})	Field capacity (%)	Crop extractable water (%)
		Sand (%)	Silt (%)	Clay (%)					
I-Rc-Yk-c	Loam	35	39	26	1.3–1.5	43–49	8–20	25–36	11–17
Qc47-1-2b	Sandy Loam	79	12	9	1.4–1.6	40–47	13–76	15–27	6–12
Yk36-2-3a	Clay Loam	35	35	30	1.3–1.4	47–51	2.5–15	31–42	15–20
Jc42-2-3a	Clay Loam	27	44	29	1.3–1.4	47–51	2.5–15	31–42	15–20
Xh43-2-3a	Loam	32	42	26	1.35–1.5	43–49	8–20	25–36	11–17
Yh26-2-3a	Loam	44	30	26	1.35–1.5	43–49	8–20	25–36	11–17
Yh27-2a	Sandy Loam	52	32	16	1.4–1.6	40–47	13–76	15–27	6–12
Yk40-2-3a	Clay Loam	36	33	31	1.3–1.4	47–51	2.5–15	31–42	15–20
Zg13-2-3a	Clay Loam	26	35	39	1.3–1.4	47–51	2.5–15	31–42	15–20
Zg6-2-3a	Clay	25	27	48	1.2–1.3	51–55	0.1–1	39–49	19–24

(Source: Cuenca, 1987).

Hydrologically, as per the Indus River System Authority (IRSA) of Pakistan, Sindh receives about 48.76 MAF annually from the Indus River, with 33.94 MAF in Kharif season and 14.82 MAF in Rabi season. The Indus Basin Irrigation System (IBIS) has the province as one of its main beneficiaries with three (03) barrages in the province, diverting 48.76 MAF annually to the 14 main canal commands with a complex system of 117 branch canals, 1,400 distributaries and minors, and about 42,000 water courses across the province (Simons et al., 2020). Based on the crop type, climate, water availability, and cropping practice, Sindh has two major agro-climatic zones including Cotton-Wheat Sindh and Rice-Other Sindh. Cotton-Wheat Sindh serves as a major zone for cultivating Cotton, Sugarcane, Wheat, And Rice in the province, while in Rice-Other Sindh, Barley, Rice, Sugarcane, Wheat, pulses, vegetables, and fruits are the prominent crops (Sadiq et al., 2019).

For this study, a number of five (05) stations in Sindh namely Badin, Dadu, Jacobabad, Larkana, and Nawabshah having rich growing fields of Rice, Wheat, and Sugarcane were selected. The climate data needed for this purpose was taken from the Pakistan Meteorological Department (PMD) for the years 1990–2022. The climate normal for the selected stations are shown in the Fig. 3.

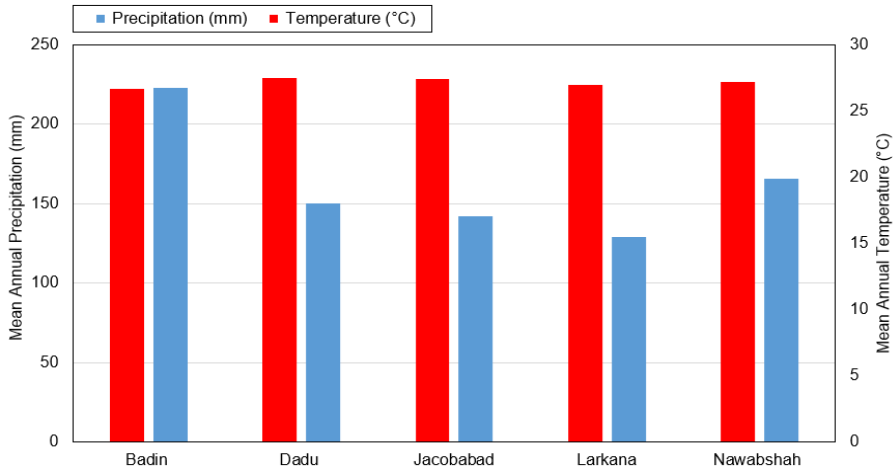

Figure 3. Mean annual precipitation (mm) and temperature (℃) of the selected stations.

Methodology

Selection of Regional Climate Model

In this study, the Regional Climate Model Version 4 (RegCM4) was selected with NOAA-GFDL-ESM2M as the driving Atmosphere-Ocean Global Circulation Model (AOGCM). The daily historical and future RegCM4 climate projections for the study area were acquired from the CORDEX data portal (https://cordex.org/data-access/regional-data-portals) for both RCP 4.5 and 8.5 scenarios. The Coordinated Regional Downscaling Experiment (CORDEX) is a program supported by the World Climate Research Program (WCRP) to forumulate a modifed framework via global co-ordination with a prime aim to generate the regional-scale downscaled climate projections for different regions of the world by considering the region-specific climate features, so as to faciltate the impact assessment studies on the regional scale. The climate data was obtained for the period 1990 to 2099, with 1990 to 2005 taken as the validation period, and 2020 to 2099 was taken as the modeling period as shown in the Table 4.

Table 4. Description of RCM-GCM combination used in the study

RCM	CORDEX Domain	Driving GCM	Spatial resolution	Climate variables	Temporal resolution	Time period
RegCM4	WAS-44i	NOAA-GFDL-ESM2M	50 km	T_{max} and T_{min}	Daily	1990–2099

Bias Correction of RCM Simulations

As discussed earlier, the RCM climate simulations often contain biases that result in misinterpretation and erroneous reproduction of local climate features and may ultimately mislead the analysis. In this study, the air temperature (T_{min} and T_{max}) simulated by RegCM4 showed the presence of warm biases (overestimation) for all stations during the validation period. Therefore, in order to remove biases from the RegCM4 temperature simulations, the Quantile Mapping (QM) technique was used.

Quantile mapping (QM)

In this study, QM technique was used to bias correct the daily temperature projections for all stations. The method works by establishing a statistical nexus between the histroical model simulations and the actual data of same period by replacing the model values with the actual data at the same Cumulative Density Function (CDF) of the employed distribution, and this statsitical relation is then applied on the future climate dataset of the climate model to obtain statisitcally improved projections. In QM approach, Gamma distribution is used to correct precipitation, Normal distribution for temperature, and Beta distribution for the solar radiation. The mathematical expression employed by QM for correcting the temperature values (historical as well as the future values) is shown in the Eq. 1 as under (Gupta et al., 2019):

$$\bar{x}_{ms.corr}\,(\text{Temperature}) = x_{ms} + F_{oh}^{-1}\left(F_{ms}(x_{ms})\right) - F_{mh}^{-1}(F_{ms}(x_{ms})) \quad (1)$$

where, F is the Cumulative Density Function (CDF), F^{-1} is its inverse, and subscripts o is the actual data, m is the model predicted value, s and h are the simulation and past period respectively, and $\bar{x}_{ms.corr}$ is the bias corrected value.

Estimation of reference evapotranspiration (ET_o)

FAO Penman-Monteith equation

The FAO PM Equation for ET_o is shown in the Eq. 2 as under:

$$ET_o = \frac{0.408\Delta(R-S)+\gamma\frac{900}{T+273}v(e_s-e_a)}{\Delta+\gamma(1+0.34v)} \quad (2)$$

where S is the soil heat flux density (MJ m^{-2} per day), R is net solar radiation at the field surface (MJ m^{-2} per day), Δ is the slope of vapour pressure curve (KPa $°C^{-1}$), γ is the psychometric constant (KPa $°C^{-1}$), T is the average daily air temperature at 2 m altitude (°C), v is the wind speed at 2 m height (m s^{-1}), e_s and e_a are the saturation and actual vapour pressures (KPa) respectively. Herein, this study involved the utilization of a computer model called CROPWAT 8.0 to assess ET_o following the FAO PM equation (Ma et al., 2023).

Hargreaves equation

The Hargreaves Equation is shown in the Eq. 3 as under:

$$ET_o = BR_a\,(T+17.8)(T_{max}- T_{min})^{0.5} \quad (3)$$

where, B is a constant assigned the value 0.0023, ET_o represents reference evapotranspiration (in millimeters per day), Ra denotes extraterrestrial solar radiation (in Mega-joules per square meter per day), and T, T_{max}, and T_{min} refer to the mean, maximum, and minimum air temperatures, respectively, measured in degrees Celsius (Habeeb et al., 2021).

Calibration of Hargreaves equation

The calibration process (with 2005–2019 taken as the calibration period) involved the estimation of a calibration factor (B) for all selected stations so as to adjust the HG equation on monthly scale, and to align with the specific climatic conditions of the locality by taking PM equation as a reference.

$$ET_o\,(PM) = B\,ET_o\,(HG)$$

$$ET_o\,(PM) = BR_a\,(T+17.8)(T_{max}- T_{min})^{0.5}$$

By taking Y= ET_o (PM) and X= ET_o (HG), the expression can be rewritten as: Y = BX.

Afterwards, by calculating the Coefficient of determination (R^2) and the Root Mean Square Error (RMSE) between the ET_o estimates of HG and PM equations for each year within the calibration period, the calibration factor 'B' was determined for each station. The parameter B was selected based on the year exhibiting the highest R^2 and the lowest RMSE value. The equations used for the estimation of R^2 and RMSE as under (Majeed et al., 2017):

$$R^2 = \frac{[\sum_{i=1}^{n}(x_i - \bar{x})(y_i - \bar{y})]^2}{\sum_{i=1}^{n}(x_i - \bar{x})^2 \sum_{i=1}^{n}(y_i - \bar{y})^2} \quad (4)$$

$$RMSE = \sqrt{\frac{\sum_{i=1}^{n}(y_i - x_i)^2}{n}} \quad (5)$$

where 'yi' denotes the estimated average monthly reference evapotranspiration (ET_o) using the PM equation for month 'i' in millimeters per day, 'xi' represents the estimated average monthly ET_o using the HG equation for month 'i' in millimeters per day, and '$\bar{x}$' and '$\bar{y}$' signify the averages of xi and yi, respectively.

Computation of seasonal crop water requirement

As per FAO, the equation used to estimate the daily water requirement for a crop is given in Eq. 6 as below:

$$\text{Crop Water Requirement (CWR)} = ET_o \times K_c \quad (6)$$

In this study, the monthly and seasonal water requirements for the selected crops under RCP 4.5 and 8.5 scenarios were estimated using Eqs 7 and 8 respectively given as under:

$$\text{Monthly Crop Water Requirement} = \sum \text{Daily Crop Water Requirement} \quad (7)$$

$$\text{Seasonal Crop Water Requirement} = \sum \text{Monthly Crop Water Requirement} \quad (8)$$

RESULTS AND DISCUSSION

Bias correction of RCM simulations

In this study, the RegCM4 simulations for the study area were bias corrected using the QM approach for the period 1990 to 2005. The evaluation of bias corrected outputs was performed using the two statistical parameters as RMSE and R^2 between the historical actual and simulated data to validate how close the simulated values are to the actual climate data after bias correction. The validation results are shown as under:

Table 5. Goodness of fit between the observed and simulated climate data before and after bias correction for RCP 4.5 scenario

Station	Nawabshah		Dadu		Badin		Jacobabad		Larkana	
	T_{min} (°C)									
	RMSE	R^2	RMSE	R^2	RMSE	R^2	RMSE	R^2	RMSE	R^2
Before Bias Correction	4.91	0.76	5.25	0.81	4.23	0.77	5.86	0.74	4.66	0.82
After Bias Correction	3.26	0.80	2.87	0.85	2.56	0.84	2.97	0.88	1.85	0.90
	T_{max} (°C)									
Before Bias Correction	6.91	0.67	3.61	0.74	4.50	0.65	5.43	0.67	3.60	0.74
After Bias Correction	2.71	0.78	2.48	0.88	2.09	0.86	2.98	0.79	2.05	0.89

Table 6. Goodness of fit between the observed and simulated climate data before and after bias correction for RCP 8.5 scenario

Station	Nawabshah		Dadu		Badin		Jacobabad		Larkana	
	T_{min} (°C)									
	RMSE	R^2	RMSE	R^2	RMSE	R^2	RMSE	R^2	RMSE	R^2
Before Bias Correction	3.32	0.79	4.10	0.79	3.22	0.78	4.31	0.79	4.13	0.81
After Bias Correction	2.03	0.85	1.80	0.89	1.55	0.89	2.07	0.88	1.60	0.90
	T_{min} (°C)									
Before Bias Correction	5.65	0.68	3.78	0.70	4.31	0.65	5.20	0.69	3.82	0.70
After Bias Correction	1.63	0.84	2.46	0.86	2.22	0.70	2.85	0.81	2.23	0.87

Temperature projections in study area under the climate change scenarios

In this study, after the removal of biases from the RegCM4 temperature projections, the temperature patterns under the RCP 4.5 and 8.5 scenarios in the selected stations were comprehensively analysed using the Sen's Slope method for the period 2020 to 2099 using R (a programming language). The results obtained from the analysis are shown as under:

The above analysis showed a significant rise in air temperature in the selected stations. Annually, the air temperature over the study area may rise by about 1.3–1.8 °C under the RCP 4.5 scenario as shown in the Table 7, whereas under the RCP 8.5 scenario, warming may soar by about 2.8–3.3 °C by the end of century as shown in the Table 8. It is pertinent to understand that the seasonal temperatures also hold significance for agriculture. For instance, for Rabi crops, winter and the early spring temperatures govern the crop water needs, crop water productivity, soil moisture availability, and the crop yield. While for the Kharif crops, the late spring and summer seasonal temperatures are highly influential. As per the analysis, for Spring season, temperature may increase by about 1.8–3.5 °C under RCP 4.5 scenario, whereas under the RCP 8.5 scenario, warming may increase by about 3.5–5.7 °C by the year 2100. For summer season, temperature may increase by about 0.3–0.9 °C under RCP 4.5 scenario, while under the RCP 8.5 scenario, temperature may warm by about 0.7–1.5 °C. For winter season, a rise of about 3.1–4.9 °C under the RCP 4.5 scenario may be recorded, whereas under the RCP 8.5 scenario, warming may soar by about 4.3–5.9 °C.

Table 7. RegCM4 projected temperature change (°C) over the selected stations under RCP 4.5 scenario

S.No.	Station	Temperature Change (°C)			
		Annual	Spring	Summer	Winter
1	Badin	+1.8	+2.4	+0.7	+4.9
2	Dadu	+1.3	+1.8	+0.9	+3.3
3	Jacobabad	+1.6	+3.5	+0.3	+4.3
4	Larkana	+1.3	+2.0	+0.3	+3.1
5	Nawabshah	+1.6	+3.0	+0.5	+4.7

Table 8. RegCM4 projected temperature change (°C year^{-1}) over the selected stations under RCP 8.5 scenario

S.No.	Station	Temperature Change (°C)			
		Annual	Spring	Summer	Winter
1	Badin	+3.1	+4.0	+0.9	+5.7
2	Dadu	+3.0	+3.7	+1.5	+4.5
3	Jacobabad	+3.3	+5.7	+0.5	+5.4
4	Larkana	+2.8	+3.6	+1.3	+4.3
5	Nawabshah	+3.3	+4.9	+0.7	+5.9

Apart from the mean daily temperature, the maximum (daytime) and minimum (nighttime) temperatures of a day also holds a significant importance for the crops, as the best photosynthesis is linked to high daytime and low nighttime temperatures. Moreover, the maturing of crops is also effected due to variations in the nighttime temperature. In this study, RegCM4 projected a higher magnitude of warming of nighttime temperature in Sindh than the daytime temperature. Under RCP 4.5 scenario, the daytime temperature in the province may increase by about 1.2 to 1.7 °C, while the nighttime temperature may increase by about 1.4 to 2.8 °C by the year 2100 as shown in the Table 9. On the other hand, under RCP 8.5 scenario, the daytime temperature may increase by about 2.6 to 3.2 °C, whereas the minimum temperature may increase by about 3.0 to 3.5 °C.

Table 9. RegCM4 projected daytime and nighttime temperature change (°C) over the selected stations under RCP 4.5 and 8.5 scenarios

S.No.	Station	RCP 4.5		RCP 8.5	
		T_{max}	T_{min}	T_{max}	T_{min}
1	Badin	+1.7	+2.8	+3.0	+3.3
2	Dadu	+1.2	+1.4	+2.8	+3.1
3	Jacobabad	+1.6	+1.5	+3.2	+3.3
4	Larkana	+1.2	+1.4	+2.6	+3.0
5	Nawabshah	+1.5	+1.7	+3.1	+3.5

Conclusively, it is pertinent to mention that the selected stations in this study serve as the major agricultural zones in Sindh province for growing important food and horticultural crops in the country. Therefore, the warming air temperature patterns as projected by the analysis may adversely impact the agricultural production in the province, as the rising temperatures may result in increased evapotranspiration and consequently more crop water consumption, soil moisture desiccation, declining crop-water use efficiency, crop water stress conditions, and ultimately reduced crop yield, thereby threatening the food as well as the water security in the country.

Calibration of Hargreaves equation

In this study, HG equation was calibrated for all selected stations on the monthly scale to minimize the overestimation of ET_o. The results of local calibration are shown as under:

Table 10. Summary of Hargreaves Equation local calibration for selected stations in Sindh

Station	Nawabshah		Dadu		Badin		Jacobabad		Larkana	
	Tmin (°C)									
	RMSE	R^2	RMSE	R^2	RMSE	R^2	RMSE	R^2	RMSE	R^2
Before Bias Correction	6.72	0.93	6.83	0.89	3.87	0.80	7.71	0.87	7.22	0.90
After Bias Correction	0.93	0.96	0.82	0.92	0.80	0.85	0.85	0.92	0.99	0.92

The above calibration results (Table 10) indicated that RMSE was higher and the value of R^2 was comparatively lower between the results of the original HG equation and the FAO PM equation before calibration. However, after the calibration of HG equation by finding the calibration factor (B), the correlation in results between the two methods improved statistically and the deviation in results (RMSE) dropped significantly, with the correlation (R^2) improved further. Thus, the calibrated Hargreaves equations showed a good match of ET_o estimates with that of FAO PM equation. The resulting calibrated HG

equations to estimate the monthly ET_o are shown in the Table 11 as under.

The above calibrated Hargreaves equations were then used to estimate ET_o over the selected stations under the RCP 4.5 and 8.5 scenarios.

Table 11. Calibrated Hargreaves equations for the selected stations

Station	Calibrated Hargreaves equation
Badin	$ET_o = 0.0013\ R_a\ (T+17.8)(T_{max}- T_{min})^{0.5}$
Jacobabad	$ET_o = 0.00125\ R_a\ (T+17.8)(T_{max}- T_{min})^{0.5}$
Dadu	$ET_o = 0.00123\ R_a\ (T+17.8)(T_{max}- T_{min})^{0.5}$
Larkana	$ET_o = 0.00115\ R_a\ (T+17.8)(T_{max}- T_{min})^{0.5}$
Nawabshah	$ET_o = 0.00127\ R_a\ (T+17.8)(T_{max}- T_{min})^{0.5}$

Projected seasonal ET_o in study area under the climate change scenarios

In this study, after the local calibration of Hargreaves equation for the selected stations, the change in seasonal reference evapotranspiration was estimated for Kharif and Rabi seasons for all stations under the RCP 4.5 and 8.5 scenarios using the calibrated HG equations. The results obtained from the analysis are shown as under.

As discussed earlier, ET_o indicates the eveporative demand of atmosphere at a location and greatly influence the crop water requirements. The above results (Table 12) showed that under the RCP 4.5 scenario, the ET_o for the Kharif season in the study area may increase by about 60 to 80 mm at the rate of about 0.7 to 1.0 mm year^{-1} by 2100. Under RCP 8.5 scenario, the ET_o for Kharif season may increase by about 80 to 130 mm at the rate of about 1.0 to 1.7 mm year^{-1} by the end of century. For Rabi season, ET_o in the study area may increase by about 30 to 60 mm under the RCP 4.5 scenario, whereas under RCP 8.5 scenario, ET_o is expected to increase by about 90 to 140 mm at the rate of about 1.3 to 1.7 mm year^{-1} by the year 2100.

Table 12. Projected station-wise change in seasonal ET_o in mm year^{-1} under the climate change scenarios

Station	RCP 4.5		RCP 8.5	
	Kharif	Rabi	Kharif	Rabi
Badin	+0.76	+0.73	+1.04	+1.72
Dadu	+0.95	+0.48	+1.63	+1.63
Jacobabad	+0.82	+0.38	+1.61	+1.20
Larkana	+0.98	+0.44	+1.62	+1.18
Nawabshah	+0.80	+0.49	+1.14	+1.30

Projected seasonal crop water requirements in study area under the climate change scenarios

In this study, the calibrated Hargreaves equations along with the bias corrected temperature data were used to compute ET_o for the modelling period. After the estimation of ET_o, the seasonal water requirements for Rice, Wheat, and Sugarcane were estimated using Eq. 8 under the RCP 4.5 and 8.5 scenarios. The results obtained from the analysis are shown as under.

Projected seasonal water requirement of rice in study area under the climate change scenarios

The projected seasonal crop water requirement of Rice under RCP 4.5 and 8.5 scenarios over the study area are shown in the Figs 4−8 as under:

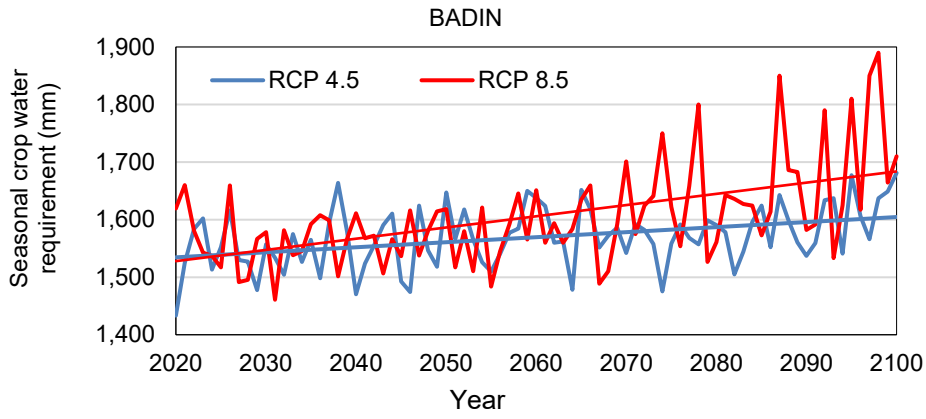

Figure 4. Projected Seasonal water requirement of Rice in Badin under RCP 4.5 and 8.5 scenarios.

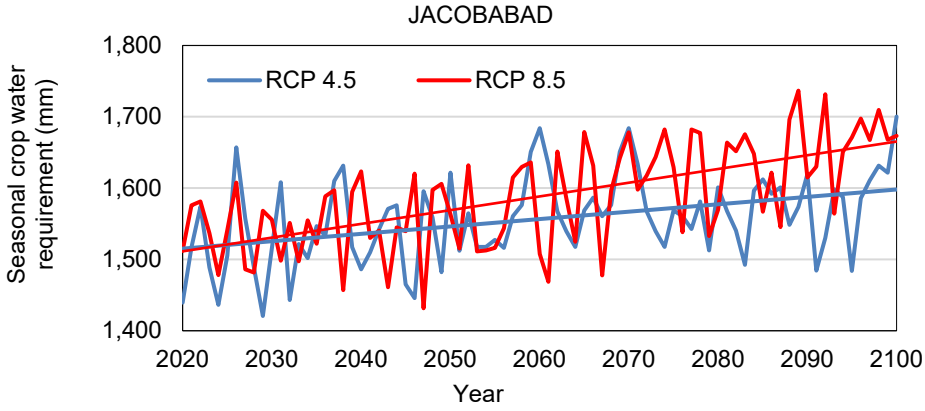

Figure 5. Projected Seasonal water requirement of Rice in Jacobabad under RCP 4.5 and 8.5 scenarios.

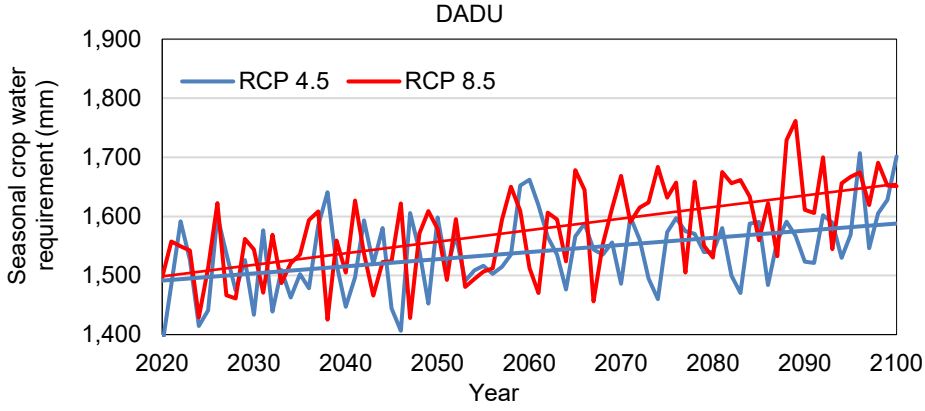

Figure 6. Projected Seasonal water requirement of Rice in Dadu under RCP 4.5 and 8.5 scenarios.

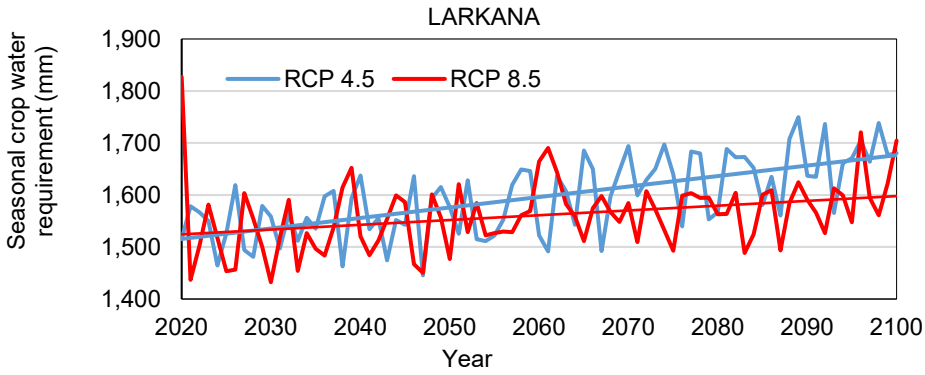

Figure 7. Projected Seasonal water requirement of Rice in Larkana under RCP 4.5 and 8.5 scenarios.

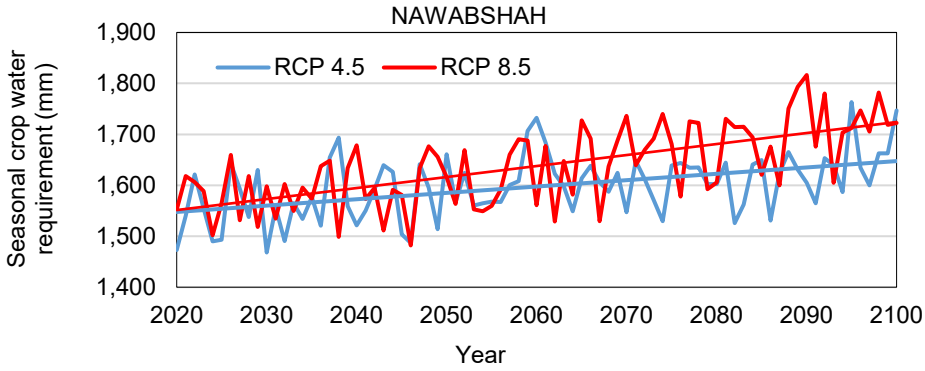

Figure 8. Projected Seasonal water requirement of Rice in Nawabshah under RCP 4.5 and 8.5 scenarios.

Projected seasonal water requirement of wheat in study area under the climate change scenarios

The projected seasonal crop water requirement of Wheat under RCP 4.5 and 8.5 scenarios in the study area are shown in the Figs 9−13 as under:

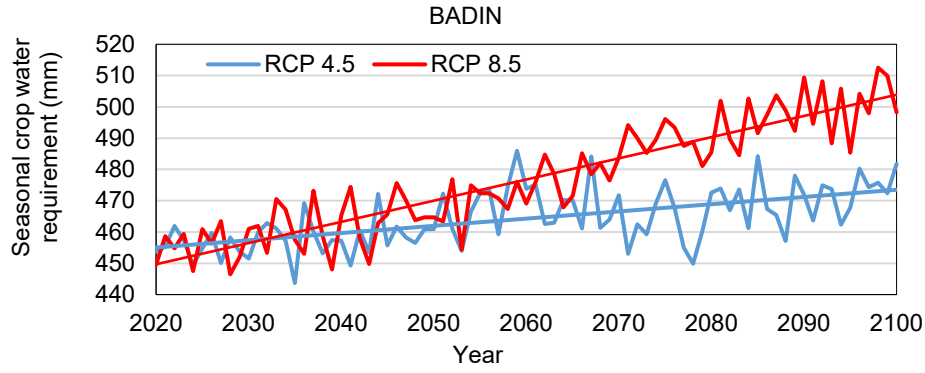

Figure 9. Projected Seasonal water requirement of Wheat in Badin under RCP 4.5 and 8.5 scenarios.

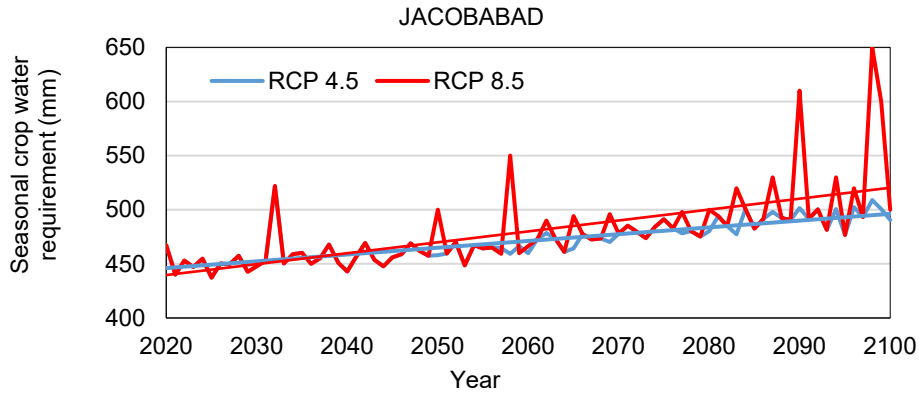

Figure 10. Projected Seasonal water requirement of Wheat in Jacobabad under RCP 4.5 and 8.5 scenarios.

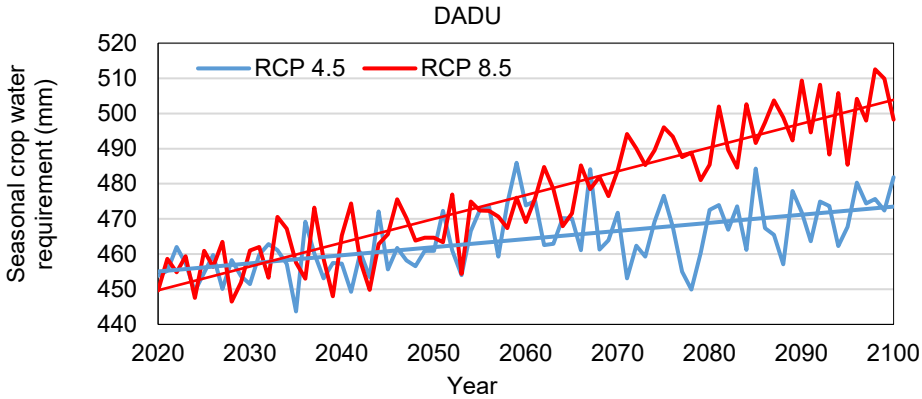

Figure 11. Projected Seasonal water requirement of Wheat in Dadu under RCP 4.5 and 8.5 scenarios.

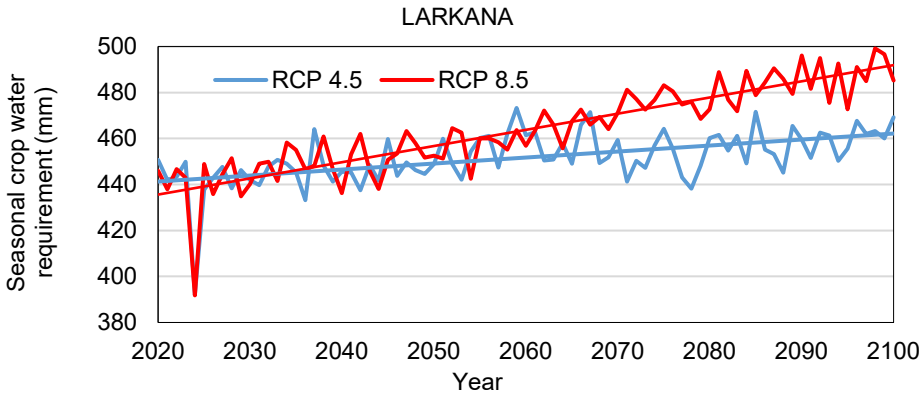

Figure 12. Projected Seasonal water requirement of Wheat in Larkana under RCP 4.5 and 8.5 scenarios.

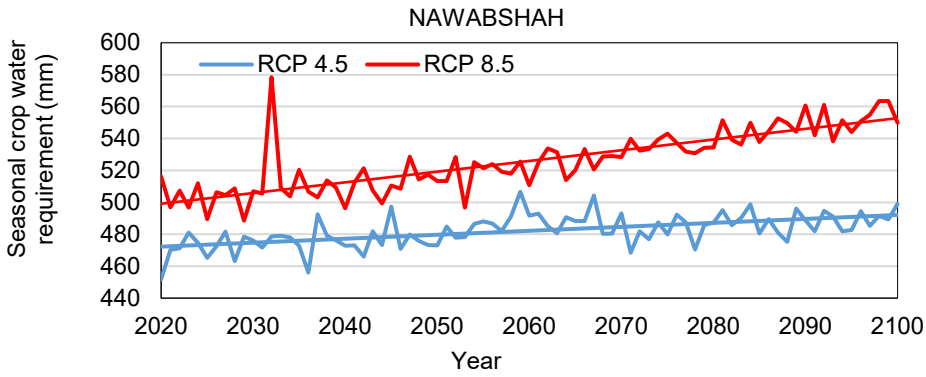

Figure 13. Projected Seasonal water requirement of Wheat in Nawabshah under RCP 4.5 and 8.5 scenarios.

Projected seasonal water requirement of sugarcane in study area under RCP 4.5 and 8.5 scenarios

The projected seasonal crop water requirment of Sugarcane under RCP 4.5 and 8.5 scenarios in the study area are shown in the Figs 14−18 as under:

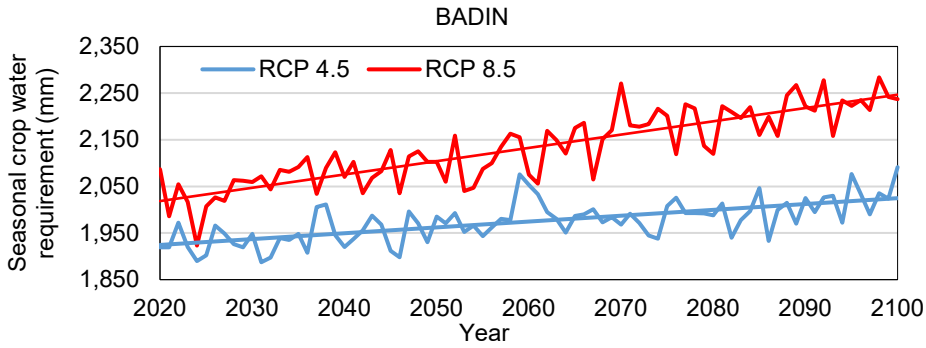

Figure 14. Projected Seasonal water requirement of Sugarcane in Badin under RCP 4.5 and 8.5 scenarios.

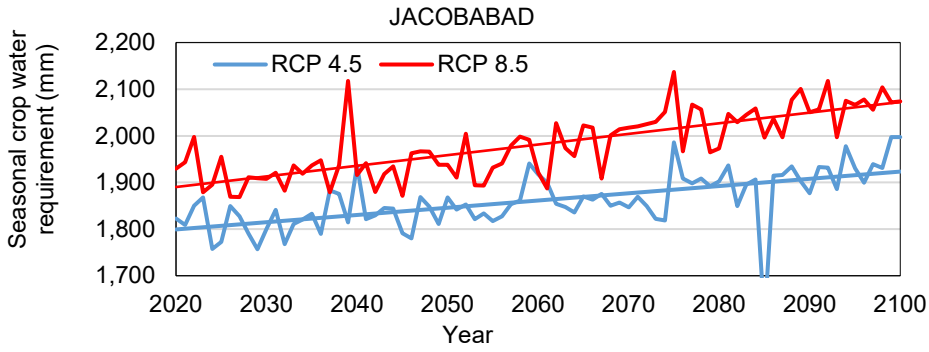

Figure 15. Projected Seasonal water requirement of Sugarcane in Jacobabad under RCP 4.5 and 8.5 scenarios.

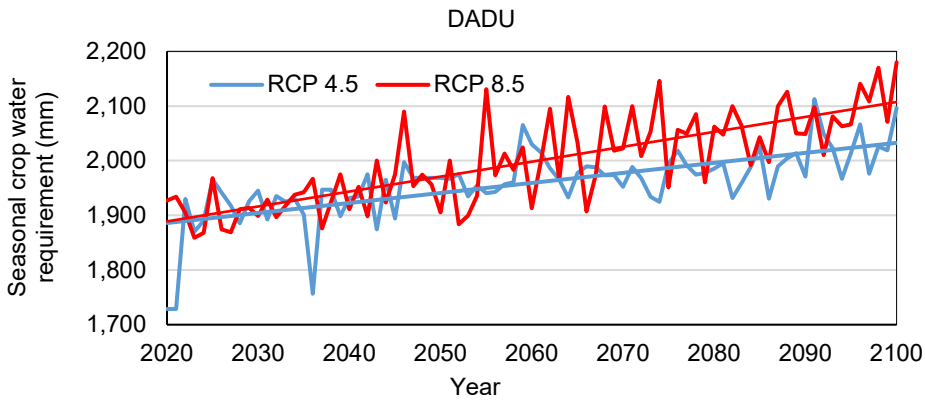

Figure 16. Projected Seasonal water requirement of Sugarcane in Dadu under RCP 4.5 and 8.5 scenarios.

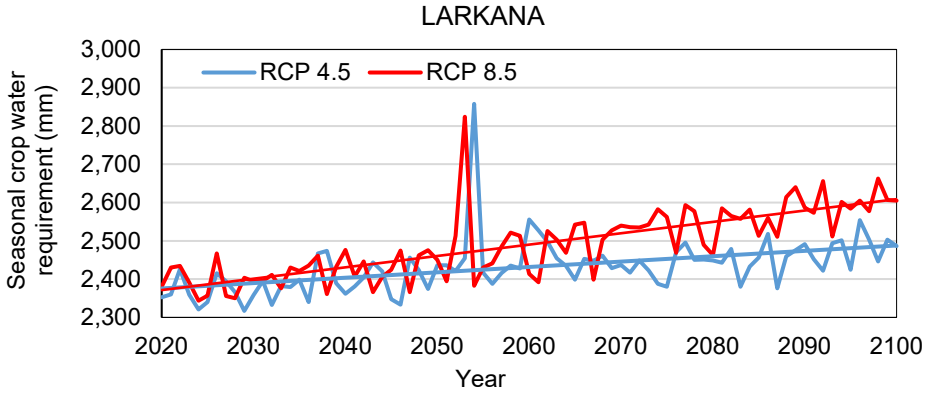

Figure 17. Projected Seasonal water requirement of Sugarcane in Larkana under RCP 4.5 and 8.5 scenarios.

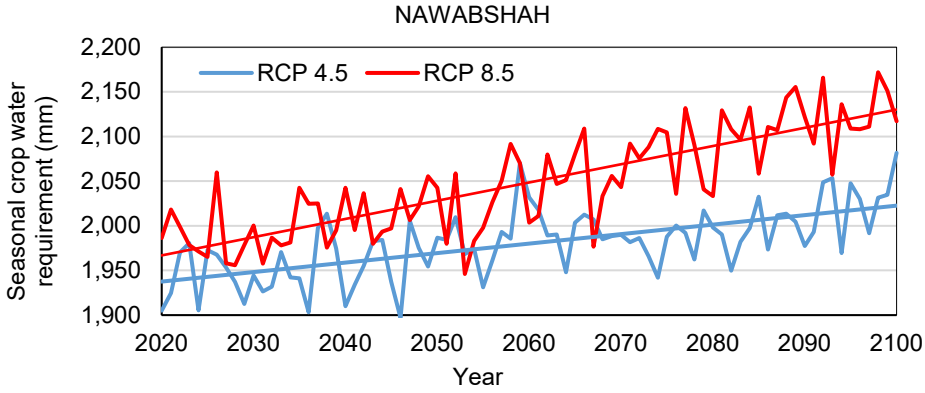

Figure 18. Projected Seasonal water requirement of Sugarcane in Larkana under RCP 4.5 and 8.5 scenarios.

The above analysis projected a noticeable rise in the seasonal water requirements for Rice, Wheat, and Sugarcane in Sindh under the climate change scenarios. For Rice, the seasonal crop water requirement may increase from about 1,500 to 1,550 mm currently to about 1,600 to 1,650 mm in Sindh under RCP 4.5 scenario, while under RCP 8.5 scenario, the water consumption may increase to about 1,700 mm, as shown in the Figs 4 and 5. For Wheat, the seasonal crop water requirement may increase from about 400 to 450 mm currently to about 500 mm under the RCP 4.5 scenario, while under the RCP 8.5 scenario, the water requirement may reach to about 550 mm, as shown in the Figs 6 and 7. For Sugarcane, the seasonal crop water requirement may increase from about 1,700 to 1,900 mm currently to about 2,000 to 2,050 mm under the RCP 4.5 scenario, whereas under the RCP 8.5 scenario, the water requirement may reach to about 2,100 mm by the end of century as shown in the Figs 8 and 9.

Conclusively, Rice, Wheat, and Sugarcane are among the major crops of Pakistan, consuming significant amount of irrigation withdrawals in the country, and serve as livelihood for the local farmers and an important source of foreign exchequer for the national economy. Therefore, the increasing crop water requirements due to climate change as predicted in this study may cause increased freshwater consumption in Sindh for crop production, pressurizing the already stressed freshwater resources of the country and rise in local water disputes, ultimately posing an eminent threat to the country's food and water security.

CONCLUSION AND RECOMMENDATIONS

The prime objective of this study was to model the temperature patterns over the Sindh province and to project its impacts on the reference evapotranspiration and seasonal water requirements for the major crops of country including Rice, Wheat, and Sugarcane under the climate change scenarios. Following conclusions have been made based on the analysis performed:

1. The RegCM4 bias corrected outputs showed that under RCP 4.5 scenario, the average annual temperature in Sindh may warm by about 1.3–1.8 °C, while about 2.8–3.3 °C under the RCP 8.5 scenario by the end of 21st century. Seasonally, warming was projected to be mainly focused on the spring and winter seasons. For spring season, temperature may increase by about 1.8–3.5 °C under RCP 4.5 scenario, and about 3.5–5.7 °C under RCP 8.5 scenario. For winter season, warming may increase by about 3.1–4.9 °C under RCP 4.5 scenario, and about 4.3–5.9 °C under RCP 8.5 scenario.

2. Diurnally, RegCM4 projected a higher increase in nighttime temperature as compared to the daytime temperature. As per the model outputs, the daytime temperature may increase by about 1.2–1.7 °C, while the nighttime temperature may increase by about 1.4–2.8 °C under RCP 4.5 scenario. Under RCP 8.5 scenario, the maximum temperature may rise by about 2.6–3.2 °C, while the minimum temperature may increase by about 3.0–3.5 °C by the end of century.

3. For ET_o, the analysis revealed that under the RCP 4.5 scenario, the Kharif seasonal ET_o may increase by about 60–80 mm, while the Rabi seasonal ET_o may increase by about 30–60 mm by 2100. Under RCP 8.5 scenario, the Kharif seasonal ET_o may increase by about 80–130 mm, whereas the Rabi seasonal ET_o may soar by about 90–150 mm by the end of century.

4. Due to the warming air temperatures, a noticeable rise in crop water consumption in the province was predicted. For Rice, the seasonal water requirement may increase by about 50–100 mm under the RCP 4.5 scenario, and about 100–200 mm under the RCP 8.5 scenario. For Wheat, the seasonal water requirement may increase by about 60 mm under the RCP 4.5 scenario, and about 100 mm under RCP 8.5 scenario. For Sugarcane, the water requirement may increase by about 100–150 mm and 150–200 mm under RCP 4.5 and 8.5 scenarios respectively.

5. In view of the study outcomes, the authors recommend the formulation of a holistic and well-integrated climate change adaptation and mitigation strategy to deal with the unfavorable aspects of the global climate shift in the country. Moreover, to cater the increasing agricultural water demand under the warming scenarios, a timely shift to conservative utilization and management of water resources is suggested.

ACKNOWLEDGEMENT. The authors would like to acknowledge the Climate Data Processing Centre (CDPC) of Pakistan Meteorological Department for their support by supplying the required climate data for the study.

REFERENCES

Awal, R., Habibi, H., Fares, A. & Deb, S. 2020. Estimating Reference Evapotranspiration under limited climate dataset in West Texas. *Journal of Hydrology: Regional Studies.* **28**, 100677.

Abeysiriwardana, H.D., Muttil, N. & Rathnayake, U. 2022. A Comparative Study of Potential Evapotranspiration Estimation by Three Methods with FAO Penman-Monteith Method across Sri Lanka. *Hydrology* **9**(11), 206.

Ali, S., Reboita, M.S. & Kiani, R.S. 2021. 21st century precipitation and monsoonal shift over Pakistan and Upper Indus Basin (UIB) using high-resolution projections. *The Science of the Total Environment* **797(**1), 149139.

Ahmed, M.J. & Choi, K.S. 2018. "Climatic Influence on the Water Requirement of Wheat-Rice Cropping System in UCC Command Area of Pakistan. *Journal of Korean Society of Agricultural Engineers* **60**(5), 69−80.

Ahmad, M.J., Cho, G.H., Kim, S.H. & Lee, S. 2021. Influence Mechanism of Climate Change over Crop Growth and Water Requirements for Wheat-Rice System of Punjab, Pakistan. *Journal of Water and Climate Change* **12**(4), 1184−1202.

Abbas, K., Qasim, M.Z., Song, H., Murshed, M., Mahmood, H. & Younis, I. 2022. A review of the global climate change impacts, adaptation, and sustainable mitigation measures. *Environmental Science and Pollution Research* **29**(28), 42539−42559.

Akaev, A. & Davydova, O. 2023. Climate and Energy: Energy Transition Scenarios and Global Temperature Changes Based on Current Technologies and Trends. Reconsidering the Limits to Growth: A Report to the Russian Association of the Club of Rome. Springer, 53−70.

Al-Asadi, K., Abbas, A.H., Dawood, A.S. & Duan, J. 2023. Calibration and Modification of the Hargreaves–Samani Equation for Estimating Daily Reference Evapotranspiration in Iraq. *Journal of Hydrologic Engineering* **28**(5), 05023005.

Akbar, G., Hameed, S. & Islam, Z. 2023. Assessing water productivity and energy use for irrigating rice in Pakistan. *Irrigation and Drainage* **72**(2), 478−486.

Barnes, C.R., Chandler, R.E. & Brierley, C.M. 2024. A comparison of regional climate projections with a range of climate sensitivities. *Journal of Geophysical Research: Atmospheres* **129**(2), e2023JD038917.

Bazrafshan, O., Ehteram, M.S., Latif, D., Huang, Y.F., Teo, F.Y., Ahmed, A.N. & El-Shafie, A. 2022. Predicting crop yields using a new robust Bayesian averaging model based on multiple hybrid ANFIS and MLP models. *Ain Shams Engineering Journal* **13**(5), 101724.

Boe, J., Mass, A. & Deman, J. 2023. A simple hybrid statistical–dynamical downscaling method for emulating regional climate models over Western Europe. Evaluation, application, and role of added value. *Climate Dynamics* **61**(1), 271−294.

Cuenca, R.H. 1987. *Irrigation System Design: An Engineering Approach*, Prentice Hall Inc. Eaglewood Cliffs, New Jersey.

Chong, X.Y., Vericat, D., Batalla, R.J., Teo, F.Y., Lee, K.S.P. & Gibbins, C.N. 2021. A review of the impacts of dams on the hydromorphology of tropical rivers. *Science of The Total Environment* **794**(1), 148686.

Eghbali, A., Babaeian, I., Azadi, M., Nokhandan, M.H. & Zarrin, A. 2022. Optimal configuration of RegCM 4.5 model for rainfall forecasting in Iran based on climatic zones (November-May), Case study: 2019−2014. *Journal of Climate Research* **1401**(49), 1−14.

Ehteram, M., Teo, F.Y., Ahmed, A.A.N., Latif, S.D., Huang, Y.F., Abozweita, O., Al-Ansari, N., El-Shafie, A. & Rahman,A. 2021. Performance improvement for infiltration rate projection using hybridized adaptive neuro-fuzzy inferences system (ANFIS) with optimization algorithms. *Ain Shams Engineering Journal* **12**(2), 1665−1676.

Fang, G., Yang, J., Chen, Y.N. & Zammit, C. 2015. Comparing bias correction methods in downscaling meteorological variables for a hydrologic impact study in an arid area in China. *Hydrology and Earth System Sciences* **19**(6), 2547−2559.

Gul, A., Chandio, A.A., Siyal, S.A., Rehman, A. & Xiumin, W. 2022. How climate change is impacting the major yield crops of Pakistan? An exploration from long− and short−run estimation. *Environmental Science and Pollution Research* **29**, 26660-26674.

Ghani, H.U., Mahmood, A., Finkbeiner, M., Kaltschmitt, M. & Gheewala, S.H. 2023. Evaluating the absolute eco-efficiency of food products: A case study of rice in Pakistan. *Environmental Impact Assessment Review* **101**(1), 107119.

Gupta, R., Bhattarai, R. & Mishra, A. 2019. Development of climate data bias corrector (CDBC) tool and its application over the agro-ecological zones of India. *Water* **11**(5), 1102.

Gutierrez, R.A., Junquas, C., Armijos, E., Sorensson, A.A. & Espinoza, J.C. 2024. Performance of Regional Climate Model Precipitation Simulations Over the Terrain-Complex Andes-Amazon Transition Region. *Journal of Geophysical Research Atmospheres* **129**(1), e2023JD038618.

Hassan, M., Penfei, D., Iqbal, W., Can, W. & Ba, W. 2014. Temperature and Precipitation Climatology Assessment over South Asia using the Regional Climate Model (RegCM4.3): An Evaluation of Model Performance. *Journal of Earth Science and Climatic Change* **5**(7), 214.

Habeeb, R., Zhang, X., Hussain, I., Hashmi, M.Z., Elashkar, E.E., Khader, J.A., Soudagar, S.S., Shoukry, A.M., Ali, Z. & Al-Deek, F.F. 2021. Statistical analysis of modified Hargreaves equation for precise estimation of reference evapotranspiration. *Dynamic Meteorology and Oceanography* **73**(1), 1−12.

Horváth, E., Gombos, B. & Szeles, A. 2021. Evaluation phenology, yield and quality of maize genotypes in drought stress and non-stress environments. *Agronomy Research* **19**(2), 408−422.

Javed, M.N. & Khan, A.W. 2019. Climate Change in South Asia and it Impacts on Pakistan: Causes, Threats and Measures. *Pakistan Journal of Social Sciences* **39**(4), 1571−1582.

Joyo, A.A., Channa, Z.H., Khan, M.B., Joyo, A.S. & Bhutto, N.A. 2023. Impact of climate change on agricultural productivity in sindh province of pakistan: analysis of major crops in eight districts. *Pakistan Journal of Agriculture, Agricultural Engineering and Veterinary Sciences* **39**(2), 141−148.

Kumar, P., Shah, S.F., Khokhar, R.B., Uqaili, M.A., Kumar, L. & Zafar, R.F. 2023. Meteorological drought mitigation for combating climate change: A case study of Southern Sindh, Pakistan. *Mehran University Research Journal of Engineering & Technology* **42**(3), 129−153.

Lujano, A., Sanchez, M. & Lujano, E. 2023. Improvement of Hargreaves–Samani Reference Evapotranspiration Estimates in the Peruvian Altiplano. *Water* **15**(7), 1410.

Liu, Z., Lu, L., Haotian, L., Na, L., Hongxi, W. & Liwei, S. 2023. Changes and influencing factors of crop coefficient of summer maize during the past 40 years in the North China Plain. *Chinese Journal of Eco-Agriculture* **31**(9), 1355−1367.

Ma, Y., Niu, Z., Wang, X., Sun, D. & Jia, L. 2023. The Influence of Meteorological Variables on Reference Evapotranspiration Based on the FAO PM Model- A Case Study of the Taohe River Basin, NW China. *Water* **15**(12), 2264.

Majeed, A., Mehmood, S., Sarwar, K., Nabi, G. & Kharal, M.A. 2017. Assessment of Reference Evapotranspiration by the Hargreaves Method in Southern Punjab Pakistan. *European Journal of Advances in Engineering and Technology* **4**(1), 64−70.

Mangan, T., Dahri, G.N., Ashfaq, M., Culas, R., Baig, I., Punthakay, J.F. & Nangraj, M. 2021. Improving groundwater management to enhance agriculture and farming livelihoods: Socio-economic assessment for improving groundwater management in the Left Bank Command of the Sukkur Barrage, Sindh Pakistan. *ILWS Report*, No. **157**, Australian Centre for International Agricultural Research (ACIAR).

Mokrikov, G., Minnikova, T., Kazeev, K. & Kolesnikov, S. 2019. Influence of precipitation and moisture reserves on the yield of crops under different tillage. *Agronomy Research* **17**(6), 2350−2358.

Ndulue, E. & Ranjan, R.S. 2021. Performance of the FAO PM equation under limiting conditions and fourteen reference evapotranspiration models in southern Manitoba. *Theoretical and Applied Climatology* **143(**3−4), 1285−1298.

Nangraj, A.N., Solangi, T., Manzoor, B., Khan, N.M., Talpur, B.A. & Dahri, G.N. 2023. Impact of Procurement Policy of Wheat on Farmers in District Khairpur Mir's, Sindh, Pakistan. *Journal of Education and Social Studies* **4**(3), 655−663.

Panfilova, A., Mohylnytska, A., Gamayunova, V., Fedorchuk, M., Drobitko, A. & Tyshchenko, S. 2020. Modeling the impact of weather and climatic conditions and nutrition variants on the yield of spring barley varieties. *Agronomy Research* **18**(2), 1388−1403.

Paul, E., Revill, A., Maier, R., Buchmann, N. & Damm, A. 2022. Insights for the Partitioning of Ecosystem Evaporation and Transpiration in Short-Statured Croplands. *Journal of Geophysical Research: Biogeosciences* **127**(7), e2021JG006760.

Pedersen, J.T.S., Vuuren, D.V., Gupta, J., Santos, F.D., Edmonds, J. & Swart, R. 2022. IPCC emission scenarios: How did critiques affect their quality and relevance 1990–2022, *Global Environmental Change* **75**, 102538.

Penev, T., Dimov, D., Marinov, I. & Angelova, T. 2021. Study of influence of heat stress on some physiological and productive traits in Holstein-Friesian dairy cows. *Agronomy Research* **19(**1), 210−223.

Pereira, L.S., Paredas, P., Hunsaker, D.J., Urrea, R.L. & Shad, Z.M. 2021. Standard single and basal crop coefficients for field crops. Updates and advances to the FAO56 crop water requirements method. *Agricultural Water Management* **243**, 106466.

Qureshi, A.S. 2020. Groundwater governance in Pakistan: From colossal development to neglected management. *Water* **12**(11), 3017.

Raihan, A. 2023. A review of the global climate change impacts, adaptation strategies, and mitigation options in the socio-economic and environmental sectors. *Journal of Environmental Science and Economics* **2**(3), 36−58.

Ramirez, D., Gonzalez, M.A.B., Nolasco, A.Q., Perez, A.L. & Avalos, J.E. 2023. Estimation of Reference Evapotranspiration in a Semi-Arid Region of Mexico. *Sensors* **23**(15), 7007.

Rasul, G., Afzal, M., Zahid, M. & Bukhari, S.A.A. 2012. *Climate Change in Pakistan: Focussed on Sindh Province*. Pakistan Meterological Department (PMD), Technical Report No PMD-25/2012.

Raul, T. 2017. Future Climate Change Scenario over Maharashtra, Western India: Implications of Regional Climate Model (REMO-2009) for the Understanding of Agricultural Vulnerability. *Pure and Applied Geophysics* **178**(3−4), 155−168.

Raza, H.A., Hameed, M.U., Islam, M.S., Lone, N.A., Raza, M.A. & Sabagh, A.E.L 2023a. Environmental and Economic Benefits of Sustainable Sugarcane Initiative and Production Constraints in Pakistan: A Review. In: Ahmed, M. (eds), *Global Agricultural Production*: *Resilience to Climate Change,* Springer, Switzerland, 441−468.

Raza, M. Y.,Wu, R. & Lin, B. 2023b. A decoupling process of Pakistan's agriculture sector: Insights from energy and economic perspectives. *Energy* **263**, 125658.

Romshoo, S.A. & Marazi, A. 2022. Impact of climate change on snow precipitation and streamflow in the Upper Indus Basin ending twenty-first century. *Climatic Change* **170**(1−2), 6.

Rosa, L. 2022. Adapting agriculture to climate change via sustainable irrigation: Biophysical potentials and feedbacks. *Environmental Research Letters* **17**(6), 063008.

Rajulapati, C.R. & Papalexiou, S.M. 2023. Precipitation Bias Correction: A Novel Semi-parametric Quantile Mapping Method. *Earth and Space Science* **10**(4), e2023EA002823.

Shafeeque, M. & Amna, B. 2023. Assessing the Impact of Future Climate Scenarios on Crop Water Requirements and Agricultural Water Supply across Different Climatic Zones of Pakistan. *Frontiers in Earth Science* **11**, 1283171.

Sadiq, S., Saboor, A., Jamshaid, F., Mohsin, A.Q. & Khalid, A. 2019. Assessment of Farmers' Vulnerability to Climate Change in Agro-Climatic Zones of Pakistan: An Index Based Approach. *Sarhad Journal of Agriculture* **35**(3), 734−740.

Shah, M.I., Khan, A., Akbar, T.A., Hassan, Q., Khan, A.J. & Dewan, A. 2020. Predicting hydrologic responses to climate changes in highly glacierized and mountainous region Upper Indus Basin. *Royal Society open science* **7**(8), 191957.

Simons, G.W.H., Bastiaanssen, W.G.M., Cheema, M.J.M., Ahmad, B. & Immerzeel, W.W. 2020. A novel method to quantify consumed fractions and non-consumptive use of irrigation water: Application to the Indus Basin Irrigation System of Pakistan. *Agricultural Water Management* **236**, 1−14.

Srdic, S., Srdevic, Z., Stricevic, R., Cerekovic, N., Benka, P., Rudan, N., Rajic, M. & Todorovic, M. 2023. Assessment of empirical methods for estimating reference evapotranspiration in different climatic zones of Bosnia and Herzegovina. *Water* **15**(17), 3065.

Talukder, S., Al-Mamun, M.A., Hossain, M.S., Khan, M.A.R., Rahman, M.M., Talukder, M.R., Haque, M.M. & Biswas, J. 2022. Duration of low temperature changes physiological and biochemical attributes of rice seedling. *Agronomy Research* **20**(1), 1163−1174.

Viikoja, R., Alaru, M., Keres, I., Lillak, R., Voor, I. & Loit, E. 2023. Impact of changing weather on the crops yield stability in different cropping systems. *Agronomy Research* **21**(2), 979−993.

Xing, L., Feng, Y., Cui, N., Guo, L., Du, T., Wu, Z., Zhang, Y., Wen, S., Gong, D. & Zhao, L. 2023. Estimating reference evapotranspiration using Penman-Monteith equation integrated with optimized solar radiation models. *Journal of Hydrology* **620**, 129407.

Xue, P., Zhang, C., Wen, Z., Park, E. & Jakada, H. 2022. Climate variability impacts on runoff projection under quantile mapping bias correction in the support CMIP6: An investigation in Lushi basin of China. *Journal of Hydrology* **614**, 128550.

You, Q., Jiang, Z., Yue, X., Guo, W., Liu, Y., Cao, J., Li, W., Wu, F., Cai, Z., Zhu, H., Li, T., Liu, Z., He, J., Chen, D., Pepin, N. & Zhai, P. 2022. Recent frontiers of climate changes in East Asia at global warming of 1.5° C and 2° C. *Npj Climate and Atmospheric Science* **5**(1), 80.

Zerihun, D, Sanchez, C.A. & French, A.N. 2023. Derivation of the Penman–Monteith equation with the thermodynamic approach: A review and theoretical development. *Journal of Irrigation and Drainage Engineering* **149**(5), 04023007.

Zhang, M., Guo, Z.Y., Dong, G.T. & Tan, J.G. 2023. Projected heat wave increasing trends over China based on combined dynamical and multiple statistical downscaling methods. *Advances in Climate Change Research* **14**(5), 758−767.

Agronomy Research **22**(S3), 1485–1503, 2024
https://doi.org/10.15159/AR.24.080

Management alternatives for sandy soils to overcome edaphic limitations in irrigated okra cultivation

N.F. Rodrigues[1,*], S.R.L. Tavares[2], F.C. Silva[3], C.M. Hüther[3] G.M. Corrêa[4], J.R. Oliveira[4], L.S. Hamacher[3] and E.P. Clemente[5]

[1]Federal Rural University of Rio de Janeiro, Posgraduate Program in Agronomy, Rodovia BR 465, Km 7, 23890-000, Seropédica, Brazil
[2]Brazilian Agricultural Research Corporation (Embrapa), Embrapa Soils, Rua Jardim Botânico, 1024 - Jardim Botânico, 22460-000 Rio de Janeiro, RJ, Brazil
[3]Federal Fluminense University, School of Engineering, Department of Agricultural and Environmental Engineering, Rua Passo da Pátria, 156 - São Domingos, 24210-240 Niterói, RJ, Brazil
[4]Federal Fluminense University, Postgraduate Program in Biosystems Engineering, Rua Passo da Pátria, 156 - São Domingos, 24210-240 Niterói, RJ, Brazil
[5]Brazilian Agricultural Research Corporation (Embrapa), Embrapa Maize and Sorghum, Rodovia MG 424, Km 45, 35701-970 Sete Lagoas, MG, Brazil
[*]Correspondence: rodriguesnataliafe@gmail.com

Received: June 6th, 2024; Accepted: August 2nd, 2024; Published: August 23rd, 2024

Abstract. Sandy soils are often unsuitable for agriculture due to their poor physical and chemical properties. However, using conditioners can improve these parameters, making these soils viable for cultivation. This study evaluated Red-Yellow Argisol (Clay), Biochar, and Ceramic residues as soil conditioners for Planosol. The experiments were conducted in pots in a greenhouse and the experimental design was completely randomized with three treatments and five replications, compared to a control (100% P). Treatments included Clay (50% P + 570.6 t ha^{-1} A), Biochar (50% P + 189.9 t ha^{-1} B), and Ceramic (50% P + 459.9 t ha^{-1} C). Okra (*Abelmoschus esculentus* L.) was used to assess the impact on development and productivity over 90 days from transplanting (DAT). Granulometry of conditioners, and the carbon, hydrogen, nitrogen, and ash content were analyzed. For constructed soils, granulometry, bulk density, particle density, and water retention capacity (CRA) were measured before planting. Chemical parameters, including Ca^{2+}, Mg^{2+}, K^{+}, Na^{+}, Al^{3+}, H^{+}, pH, and others, were measured at 0 and 90 DAT. Okra growth parameters, such as height, stem diameter, leaf number, leaf area, stomatal conductance, and chlorophyll a fluorescence dry biomass and leaf nutrient contents (N, P, K, Ca, Mg, Na) were assessed at 90 DAT. Results indicated that conditioners improved the physical and chemical properties of the Planosol and the physiological parameters of okra. Biochar increased phosphorus and potassium, while Clay enhanced nitrogen and sodium for okra cultivation.

Key words: *Abelmoschus esculentus* L., horticulture, soil conditioners.

INTRODUCTION

Global food demand is expected to increase by 1.3% annually over the next decade due to population growth and rising incomes, primarily in low- and middle-income countries. According to estimates from the OECD (Organisation for Economic Co-operation and Development) (2022), a 20% increase in global food production is needed over the next decade to provide enough food for the world's population, expected to rise from 7.7 billion in 2020 to 8.5 billion in 2030 (OECD-FAO Agricultural Outlook 2022–2031). With agricultural land expansion contributing only 6% to this growth, light sandy soils, which lack nutrients and water retention, are increasingly incorporated into agriculture for crops other than pastures.

These sandy soils pose challenges due to their low fertility, organic matter, acidity, and water retention capacity (Santos et al., 2015). Research is needed to address these issues, as improving soil management practices can mitigate their inherent fragility. Practices that enhance organic matter, cation exchange capacity, nutrient content, and vegetative cover are crucial for sustainable agriculture (Lamarca, 1996; Amado et al., 1999; Aita et al., 2004; Mafra et al., 2008).

In order to increase the organic matter content, CEC, pH, Water Retention Capacity (WRC), improve structure, increase microbiota, etc., several techniques can be evaluated individually or in combination. Among them, the use of conditioners to improve the chemical, physical, and biological characteristics of the soil is noteworthy, especially with the joint application of fertilizers, manures, and amendments (Shinde et al., 2019; Babla et al., 2022).

Conditioner selection should consider soil properties, potential benefits, and logistical and economic feasibility. Many conditioners such as zeolite, biochar, organic materials, peat, humic and fulvic acids, sludge have been evaluated for soil regeneration (Babla et al., 2022). However, few studies explore using construction residues like ceramics and clayey soils removed from other areas. Biochar is a material composed of carbon of high stability and chemical recalcitrance, characterized by possessing complex organic structures (Singh et al., 2022).

The use of biochar as a soil conditioner for the improvement of physical-hydraulic and nutritional properties can be visualized in the so-called Terra Preta de Indio (TPI), an anthropogenic formation in which, over the years, people buried organic and inorganic materials in the soil (Glaser et al., 2003). After the action of biotic and abiotic factors on these soils, significant visual, biological, physical-hydraulic, and fertility changes were observed (Neves Junior, 2008). These lands are characterized by dark-coloured soil patches, high fertility, nutrient retention, presence of ceramics, and lithic artifacts in the surface horizons (Neves Junior, 2008) and consist of 35% to 45% pyrogenic or charcoal carbon (Glaser et al., 2000).

However, the biochar use does not present a consensus regarding the results on the physical and chemical parameters of the soil, as some authors point out positive results such as its ability to mobilize Pb, carbon sequestration (Gurwick et al., 2013; Igalavithana et al., 2019), influence on hydraulic parameters and water retention in the soil (Razzaghi et al., 2020), nutrient availability (Hussain et al., 2020), pH increase (Xu et al., 2014), reduction of Al^{3+} levels (Falcão et al., 2013), improvement of aggregate stability (Yang & Lu, 2021), and reduction of trace elements in contaminated soils (Riedel et al., 2015). The literature also presents negative results such as reduced

productivity and increased greenhouse gas emissions (Mukherjee & Lal, 2014) or even indifferent, without significant effects, for sandy soils (Jeffery et al., 2015).

Ceramics, present in the TPI from buried artifacts, are a poorly evaluated conditioner. Traditionally, red ceramics mainly use clay as raw material in the manufacture of ceramic pieces. The production of red ceramic pieces presents significant environmental impacts due to failures in the production process. In addition to the waste generated in the production process, there are also those generated in logistics, construction, and demolition forming part of the so-called Construction and Demolition Waste (CDW). There is, therefore, a global trend towards mitigating the generation and maximising the resource efficiency of these CDWs, driven by more stringent environmental regulations, public policies, and increased societal awareness (Akhtar & Sarmah, 2018).

Among the few properties studied when applied to soil, low toxic contents, a tendency to increase soil pH, potential use as a soil conditioner (Ramalho & Pires, 2009), and a source of potassium (Nobre et al., 2011; Nobre et al., 2012) can be mentioned. Rodrigues et al. (2021) described the composition of ceramics, emphasizing that it may vary according to the region, consisting mainly of silica (SiO_2), alumina (Al_2O_3), and hematite (Fe_2O_3).

The addition of clay to sandy soils, according to Hall et al. (2010), can lead to an increase in agricultural production. This can occur due to changes in stability and the formation of new aggregates (Silva et al., 2014). Thus, the presence of clay modifies the texture and its relationship with the amount of retained water, as well as factors such as orientation and shape of the grains (Donagemma et al., 2016). Research indicates that it becomes an important ally for C sequestration (Shi & Marschner, 2013), greater retention of nutrients such as Nitrogen and Potassium, and decreased natural leaching of sandy soils (Tahir & Marschner, 2017).

Due to this, one of the crops that can be associated with sandy soils in tropical climate regions due to its hardiness is Okra (*Abelmoschus escurentes* L.), a vegetable of the *Malvaceae* family (Santos et al., 2020). Its origins are attributed to Ethiopia (Sathish Kumar et al., 2013) and it has applications in various sectors, including food, pharmaceutical, and paper. The green pod of okra is a great source of fiber, minerals, vitamins C, proteins, and lipids (Ofori et al., 2020; Paul et al., 2023; Paul et al., 2024). The ideal soils for the crop are those with clayey-sandy (light) textures, pH between 6.0 and 6.5, and rich in organic matter (CATI, 1999).

The hypothesis of this research is that incorporating clay, biochar, or ceramic residue into sandy soils will improve soil fertility and structure, thereby enhancing okra cultivation. The objectives are to evaluate the effects of these soil conditioners on sandy soils and determine the optimal conditioner for successful irrigated okra cultivation.

MATERIALS AND METHODS

Soil and conditioners selection and characterization

The Haplic Planosol used in this research was chosen as the target of this study due to its textural composition of 643 g kg^{-1} coarse sand (2–0.2 mm), 234 g kg^{-1} fine sand (0.2–0.05 mm), 63 g kg^{-1} silt (0.05–0.002 mm), 60 g kg^{-1} clay (< 0.002 mm), and 0.8 g kg^{-1} organic carbon. Thus, this soil, totaling almost 88% sand in its pedological profile in depth, is classified in the textural triangle proposed by the United States

Department of Agriculture (USDA) (SOIL SURVEY STAFF, 1951) as Loamy Sand, which is highly representative in Brazilian soils. In order to improve the physical characteristics, and consequently chemical, nutritional, etc., of this soil, three conditioners were tested: Clay (argisol), Biochar, and Ceramic.

This soil (Planosol) was collected in a soil toposequence in Seropédica, Rio de Janeiro, Brazil (S22°46'11"), and the Red-Yellow Argisol was also collected in this toposequence in Seropédica, Rio de Janeiro, Brazil (O43°42'28") presenting 361 g kg^{-1} coarse sand (2–0.2 mm), 77 g kg^{-1} fine sand (0.2–0.05 mm), 55 g kg^{-1} silt (0.05–0.002 mm), 507 g kg^{-1} clay (< 0.002 mm), and 1.9 g kg^{-1} organic carbon. Both soils were initially characterized regarding their chemical parameters (Table 1) according to Teixeira et al. (2017).

Table 1. Analysis of the soils collected in Seropédica - RJ

Analysis	Unity	Argisol	Planosol
pH (water)		5.3	5.1
pH (KCl)		4.9	4.2
Ca^{2+}	$cmol_c\ kg^{-1}$	1.2	0.1
Mg^{2+}	$cmol_c\ kg^{-1}$	0.6	
K^+	$mg\ kg^{-1}$	3.9	3.9
Na^+	$mg\ kg^{-1}$	13.8	2.3
S Value	$cmol_c\ kg^{-1}$	1.9	0.1
Al^{3+}	$cmol_c\ kg^{-1}$	0	0.1
H^+	$cmol_c\ kg^{-1}$	2.0	0.4
T Value	$cmol_c\ kg^{-1}$	3.9	0.6
V Value	%	49	17
P[1]	$mg\ kg^{-1}$	< 1	1

[1] Assimilable P.

The biochar was obtained from commercial charcoal, derived from the pyrolysis of eucalyptus wood at approximately 400ºC, and the ceramic was obtained from construction waste, specifically from the disposal of red ceramic bricks collected at a brickyard in the municipality of Itaboraí/RJ - Brazil.

For the biochar, elemental analyses of carbon (C), hydrogen (H), and nitrogen (N) contents were also performed, determined by dry combustion in a CHN elemental analyzer (Perkin Elmer 2400), in triplicate. The ash content of the biochar was determined in triplicate by weighing 0.5 g of biochar sample in porcelain crucibles, which were heated in a muffle furnace at 800 °C for six hours. After this period, the samples were placed in a desiccator for one hour to cool down and then weighed on an analytical balance with an accuracy of four decimal places (ASTM D1762-84) (ASTM, 2007). The oxygen (O) content was obtained by the difference between 100 and the sum of the contents of C, H, N, and ash (KIM et al., 2012).

Therefore, the elemental characterization of the biochar was 70.44 ± 1.25% carbon, 2.62 ± 1.14% hydrogen, and 0.56 ± 0.01% nitrogen. The ash content obtained was 7.11%, totalling 19.27% oxygen (O). The molar ratios of H/C and O/C in the biochar are 0.03 and 0.27, respectively.

Conduction of the experiment and experimental design

The study was conducted at the Gragoatá campus of the Federal Fluminense University in Niterói - RJ, Brazil, 22°54'S latitude, 43°08'W longitude, and 8 m elevation with an Aw climate, according to the Köppen classification, meaning a tropical climate with a dry winter and rainy summer, with an average annual temperature of 23 °C and average annual precipitation of 1,200 mm, during the period from December 14, 2021, to April 13, 2022.

The experiments were conducted inside a greenhouse, in plastic pots with a volume of 4 dm^3, using 5 kg of soil with conditioners per pot. The experimental design was completely randomized with four treatments segregating each of the aforementioned conditioners and the control, with 5 replications, totalling 20 experimental units. The percentage composition of the conditioners for each treatment was 50% of the volume of Planosol and 50% of the volume of the conditioner (Table 2).

Table 2. Treatment Description % (v/v) Tonnes per hectare

Treatment	Original soil	Conditioner	
	%	t ha^{-1}	%
Planosol	100	-	0
Clay	50	570.6	50
Biochar	50	189.9	50
Ceramic	50	459.9	50

To ensure the homogeneity of the experiment, the conditioners and soils were passed through a 2 mm sieve, then weighed for the individual preparation of each experimental unit. After weighing, they were placed in plastic bags and shaken for 2 minutes.

To ensure the homogeneity of the experiment, the conditioners and soils were passed through a 2 mm sieve, then weighed for the individual preparation of each experimental unit. After weighing, they were placed in plastic bags and shaken for 2 minutes.

Soil correction and fertilization were carried out according to the Liming and Fertilization Manual of the State of Rio de Janeiro (Freire et al., 2013), where each treatment had its pH corrected to a range between 6.0 and 6.5. The same fertilization was applied to all treatments considering the needs of okra plants. Thus, at planting, 20 kg ha^{-1} of nitrogen was incorporated through urea, 80 kg ha^{-1} of phosphorus through single superphosphate, and 40 kg ha^{-1} of potassium through potassium chloride.

The assembly of the pots was carried out by weighing each component individually, homogenizing them in plastic bags, and incubating them for 30 days, with the moisture maintained at 70% of field capacity.

After this period, two *Santa Cruz* 47 okra seedlings were transplanted, with 20 days after seedling (DAS). At 40 DAS, thinning was carried out, leaving only one plant per pot.

Irrigation during the experiment was carried out using the gravimetric method, considering the water retention capacity (CRA) and soil density of each treatment estimated by the Soil Analysis Methods Manual of Embrapa Solos (Teixeira et al., 2017).

Soil Treatments Analysis

Undisturbed soil samples from the experiments were collected before the okra transplanting (40 DAS) and after harvest (110 DAS). The samples were taken from each experimental unit and later mixed to obtain composite samples per treatment. They were then directed for chemical and physical analysis at Embrapa Solos laboratories, following the methodologies described by Teixeira et al. (2017).

At the end of the experiments (110 DAS), undisturbed samples from each treatment were taken using a cylindrical ring with a known volume to determine the final soil density by the volumetric ring method. The samples were dried in a forced air circulation oven at 105 °C for 24 hours, and after this period, weighed to determine the soil dry mass.

Plant growth and okra analysis

At 110 DAS, the following parameters were collected: plant height (H), stem diameter (SD), number of leaves (NL), and leaf area (LA). Stem diameter was measured at a height of three centimeters from the plant collar using a digital caliper graduated in millimeters; plant height was measured from the plant collar (soil surface) to the tip of the main stem, using a tape measure graduated in centimeters; the leaf area of each experimental unit, expressed in cm^2, was determined by averaging the area of two fully expanded young leaves using a tape measure graduated in centimeters to measure length versus width (x) versus a correction factor of 0.63, specific to okra cultivation (Oliveira et al., 2014); in addition to leaf number (NL).

The leaves and stems were separated with pruning shears, placed in paper bags, properly identified, and directed for drying in a forced air circulation oven at 65 °C for 72 hours. After drying, the samples were weighed on an analytical balance to determine the dry leaf mass (DLM) and dry stem mass (DSM) in grams for each experimental unit.

In the greenhouse, after removing the aboveground plant material, the roots were removed from the pots by soil disaggregation and passing through a 2 mm sieve. Then, the collected roots were washed in running water using a sieve and placed in paper bags, properly identified, for subsequent drying in a forced air circulation oven at 65 °C for 72 hours. After drying, the samples were weighed on an analytical balance to determine the dry root mass (DRM) in grams.

The dried leaf and root material were ground in a Wiley-type knife mill and directed for determination of N, P, K contents using the methodology described in the Manual of Soil, Plant, and Fertilizer Chemical Analysis (EMBRAPA, 2009).

After the beginning of fruiting, the number of fresh fruits was counted, and successive harvests of fruits were carried out considering the commercial harvest point where they were tender, fiberless, and had an intense green color. The fruit length (FL) was determined with a ruler graduated in cm, the fruit diameter (FD) with the use of a digital caliper in mm, and the fruit mass using a precision balance in grams. Productivity was determined by the total fruit production per plant and transformed from g $plant^{-1}$ to t ha^{-1}.

Chlorophyll (Greenness) fluorescence parameters

The measurements were taken on the upper middle third of the plants on young, fully expanded, and non-detached leaves. Evaluations were conducted on 3 leaves from each sample unit, which were previously adapted to dark conditions for 30 minutes using a portable fluorometer Model Handy-PEA (Hansatech Instruments, King's Lynn, Norfolk, UK). Determinations were made after the dark period, followed by a saturating pulse of 3,400 μmol photons m^{-2} s^{-1}, which was applied to induce the OJIP transient fluorescence. Transient fluorescence intensities were measured between 50 μs (initial fluorescence - F0) and 1 second; after obtaining the values of transient fluorescence, the JIP Test parameters were calculated (Table 3) (Strasser & Strasser, 1995; Tsimilli-Michael & Strasser, 2008). The analyses were performed at the end of the experiment (110 DAS).

Table 3. JIP Test Parameters

	Fluorescence parameters extracted
tFm	Time (in ms) to reach F_m
	Fluorescence parameters calculated from primary data
FV/FM	Maximum quantum yield of PSII
FV/F_0	Quantum yield of primary photochemistry of PSII
	Specific activity per reaction center (RC)
ABS/RC	Apparent size of the antenna system or the absorption flux per RC
TR_0/RC	Maximum rate at which an exciton is trapped by the RC resulting in plastoquinone (QA-) reduction
ET_0/RC	QA- reoxidation via electron transport at an active RC
DI_0/RC	Total dissipation ratio of unquenched excitation energy per total RC, with dissipation in this case being energy loss in the form of heat
RE_0/RC	Reduction of the final electron acceptor on the electron acceptor side of PSI by RC
	Energy efficiencies and flux rates
φP_0	Maximum photochemical quantum yield
φ_{E0}	Quantum yield of electron transport from QA- to the intersystem electron acceptors
φ_{R0}	Quantum yield of electron transport from QA- to the final electron acceptor of PSI
ψ_{E0}	Probability (at time 0) that an exciton captured can move an electron in the electron transport chain after QA-
δ_{R0}	Efficiency with which an electron can move from reduced intersystem electron acceptors to the final electron acceptors of PSI
	Performance Index
PI_{ABS}	Total performance index
PI_{TOTAL}	Total performance index, measuring performance up to the final electron acceptors of PSII

[1] (Sousa, 2012. Adapted from: Strasser et al., 2004 and Yusuf et al., 2010).

Data analysis

The results were subjected to the Shapiro-Wilk test to check for data normality and subsequently submitted to analysis of variance to determine significance. Afterwards, the Tukey's test for mean comparison was conducted at a 5% probability level using the R® software (R Core Team, 2024).

RESULTS AND DISCUSSION

The planosol and biochar were classified texturally as sandy loam; the argisol was classified as sandy clay loam; and the Ceramic as loamy sand (Table 4). The Available Water Capacity was respectively 0.66 mm cm^{-1} for the planosol; 0.93 mm cm^{-1} for the argisol; 0.61 mm cm^{-1} for the Biochar and 0.52 mm cm^{-1} for the ceramic residue. It was observed that the addition of ceramic resulted in worsened granulometric conditions, as a large percentage (81%) of this material was in the form of gravel and could effectively be disregarded in the granulometry used.

The biochar had a significant impact on soil density, as its individual application led to a 28% decrease in density. This result was also observed by Esmaeelnejad et al. (2016), who found a reduction in soil density in all treatments with different types of biochar applied to a sandy clay loam soil.

Table 4. Physical analyses of treatments

Analysis	Unity	Control	Clay	Biochar	Ceramic
Coarse sand	g kg^{-1}	602	456	617	690
Fine sand	g kg^{-1}	164	123	172	134
Silt	g kg^{-1}	72	135	109	75
Clay	g kg^{-1}	162	286	102	101
Particle density	g cm^{-3}	2.54	2.55	2.00	2.46
Bulk density	g cm^{-3}	1.42	1.29	1.02	1.22
Total porosity	cm^3 100 cm^{-3}	84.4	84.58	80.44	83.88
Water retention capacity	%	26	33	43	23

Total porosity decreased with the addition of biochar, due to its low density and presence of fine particles, leading to the filling of macropores in the Planosol and an increase in micropores. Carvalho et al. (2020) reported that the addition of 25 t ha^{-1} of biochar resulted in a 63% reduction in density compared to the control, affecting mainly the volume of soil micropores.

The incorporation of ceramic and clay into the planosol showed similar behaviors, resulting in a reduction in soil density. This practice may have also influenced the micropores, as observed by Primo (2020), where the addition of clay resulted in significant improvements in microporosity, making it the most beneficial parameter.

Since the conditioners impacted porosity and density, they consequently modified the soil's water retention capacity. Biochar promoted an increase of about 65.4% in Available Water Capacity (AWC), while Clay showed an increase of 26.9% and ceramic a decrease of 11.5%. Other authors support the results found for biochar incorporation, as in the case of Lucon (2019) who found values of 63.73% (kg dm^{-3}) and Bibar (2014) values of 80 and 81% (kg dm^{-3}), with biochar pyrolysis temperatures of 400 and 700 °C, respectively. However, there are no references that contextualize the incorporation of ceramic and clay.

Despite the negative results of ceramic, literature has shown that the specific surface area of these ceramic materials and biochars has the potential to increase their efficiencies as they degrade in the soil, promoting increased fertility, nutrient cycling, microbiota activity, and water and air availability, as these factors are intrinsically interconnected (Petter, 2010) and can provide greater benefits to sandy soils (Troeh & Thompson, 2005). Probably a greater crushing of the ceramic residue, providing finer particles, can increase the contribution of this conditioner.

Therefore, nutritional parameters in the soil were evaluated before transplanting (40 DAS) and at the end of the experiment (110 DAS) to verify the behavior of nutrients in the different treatments (Table 5).

Through the solution fertilizations carried out, it was found that biochar showed a greater tendency to retain phosphorus. However, the same did not occur for potassium, as there was a decrease with a similar trend to potassium, nitrogen, calcium, and magnesium.

The conditioners tend to promote greater nutrient retention. The presence of more stable materials in the soil promotes interaction sites that can influence carbon storage and nutrient retention, significantly altering the soil's cation exchange capacity (CEC).

Table 5. Nitrogen (N), phosphorus (P), potassium (K), calcium (Ca), magnesium (Mg), organic carbon (C), C/N ratio, and pH of the treatments at 40 DAS (i) and 110 DAS (f)

Analyses		40 DAS				110 DAS			
		Control	Clay	Biochar	Ceramic	Control	Clay	Biochar	Ceramic
N	g kg^{-1}	0.7	1.1	0.8	0.7	0.8	1.3	1.2	1.0
P[1]	mg kg^{-1}	1,213	1,152	1,195	1,113	1,199	1,325	1,820	1,240
K^{+}	$cmol_c$ kg^{-1}	1.67	2.02	1.83	1.80	0.41	1.14	0.53	0.65
Ca^{2+}	$cmol_c$ kg^{-1}	12.0	15.3	11.8	9.5	8.0	13.9	12.2	8.8
Mg^{2+}	$cmol_c$ kg^{-1}	1.3	3.1	1.3	1.2	1.0	1.5	0.3	0.7
C[2]	g kg^{-1}	11.5	13.3	23.4	8.7	8.3	12.8	22.4	9.9
C/N	-	16	12	29	12	10	10	19	10
pH	Água	6.5	6.1	5.6	6.1	6.0	5.9	5.5	5.2
	KCl	6.4	6.0	5.3	6.0	6.0	5.2	6.0	5.8

According to IBI (2015), the H/C molar ratio should be less than 0.7, ensuring a large proportion of aromatic rings in the biochar structure. This value is still used to distinguish biochar from other biomasses that have not undergone partial thermochemical alteration or have been only partially altered.

In addition to biochar, the clay promotes mineral interactions, where there is a greater specific surface area and, in a basic medium, there is deprotonation and binding with cations from the soil solution. The ceramic, despite originating from clay, undergoes mineralogical and chemical changes according to the temperature used during the calcination process, which promotes the combustion of organic matter and pyrite (200 °C – 400 °C), allotopic transformation of crystalline silica (573 °C), changes in crystalline structures (800 °C – 930 °C) (Souza Santos, 1989), and vitrification process (900 °C) (Callister, 2006).

The processes involved in ceramic formation modify the active sites capable of establishing ionic exchanges and, therefore, modify their adsorptive properties. This was verified in the treatment where ceramic was inserted, making the results even lower than the control treatment. Thus, the material in this granulometry does not have a specific enough surface to adsorb cations and improve the soil's CEC. Therefore, it is not indicated individually for this purpose.

Total organic carbon was widely influenced by the addition of conditioners, with the treatment with biochar showing a greater tendency to introduce carbon into the soil. It is worth noting that the treatment with ceramic had a lower carbon content. Petter (2010) reported on the increasing linearity of soil C content with increasing doses of applied biochar. However, Hamer et al. (2004) described that despite the higher amount of carbon, it is highly aromatic and not readily accessible as an energy source for the microbiota; therefore, the effects of the material occur due to the greater surface area it promotes microbial growth and activity.

The chlorophyll *a* transient parameter of the treatments with conditioner compositions (Fig. 1), referring to the sequential energy transduction indicated by reaction centers (RC), showed an increase in the reduction of the final electron acceptor on the PSI acceptor side (RE0/RC) for all conditioners, along with an increase in energy dissipated as heat per RC (DI0/RC), leading to a decrease in performance indices (PI).

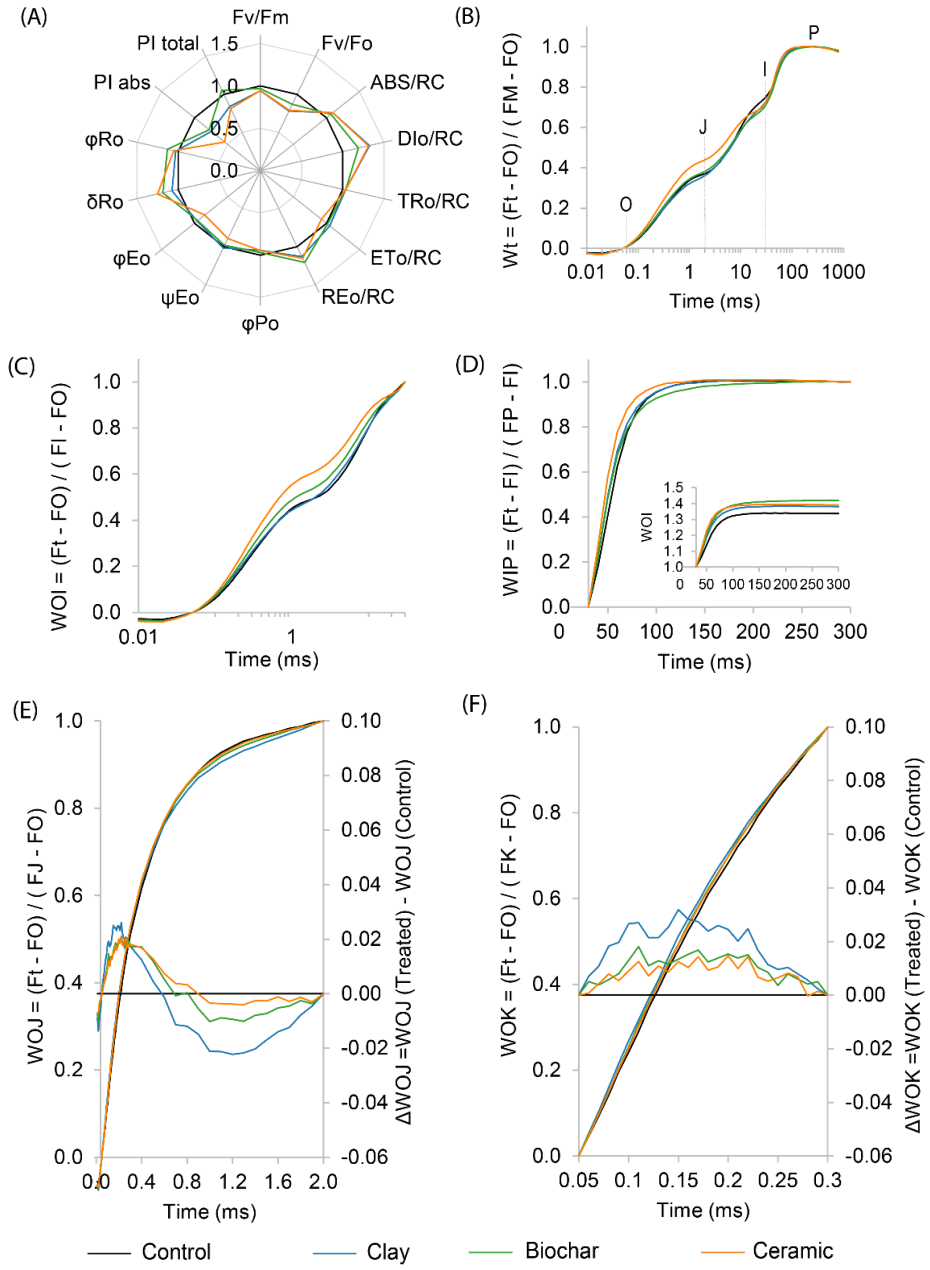

Figure 1. Chl α fluorescence transients of dark-adapted leaves of Okra (*Abelmoschus esculentus* L.) grown in different soil conditioners at 110 DAS.

Parameters of the JIP Test, in relation to the respective control, obtained from the transient OJIP fluorescence of rice plants grown under different extracts applied to the leaves and roots (A). Relative variable fluorescence between the steps O and P (Wt; B) on logarithmic time; Relative variable fluorescence between the steps O and I (WOI; C) on logarithmic time; Relative variable fluorescence between the steps I and P (WIP; D) and WOI in the insert. Relative variable fluorescence between the steps O and J (WOJ; E) and average kinetics (right vertical axis) depicted between the steps O and J (ΔWOJ), revealing the K-band; Relative variable fluorescence between the steps O and K (WOK; F) and average kinetics (right vertical axis) depicted between the steps O and K (ΔWOK). N = 15.

The decrease in both the performance index (potential) for energy conservation of the exciton for the reduction of electron acceptors of the intersystem (PIABS) and in the performance index (potential) for energy conservation of the exciton for the reduction of electron acceptors of photosystem I (PItotal) indicates a decrease in the functionality of the electron transport chain of the plants, resulting in increased energy flows for absorption (ABS/RC; which measures the apparent size of the antenna (total absorption or total chlorophyll per active RC)) mainly for the ceramic and clay, since the biochar showed no differences in PItotal when compared to the control. Regarding quantum yields and efficiencies, no significant differences were observed in the maximum quantum yield for primary photochemistry (φPo). Ceramic was the only one that showed a decrease in electron transport from QA^- to the intersystem (ψEo and φEo). However, the final electron acceptor of PSI (φRo and WIP phase) showed an increase. Another evidence of electron flow interruption is the intensity of fluorescence levels in the J step, which demonstrates that most of the QA^- is completely reduced (Strasser & Strasser, 1995). This results in a decrease in the photosynthetic performance (PItotal) of the plants, and energy loss through fluorescence (Wt) and heat (DI0/RC).

The chlorophyll *a* fluorescence transients (Fig. 1, b) exhibited typical polyphasic OJIP chlorophyll *a* fluorescence transient (Wt), increasing from initial fluorescence (FO) to maximum fluorescence (FM). However, a slight decrease in fluorescence was observed, demonstrated by a decrease in relative variable fluorescence curves in step I and, specifically for ceramic, an increase in step J. The normalization between steps O and I (WOI) mainly affected the ceramic and, subsequently, the biochar in events from exciton capture by PSII to plastoquinone (PQ) reduction (Fig. 1, c). On the other hand, Figure 1d (with its respective insertion graph) shows an increase in the sequence of events from PSI-driven electron transfer to the final electron acceptor on the PSI acceptor side, starting from PQH2 (plastoquinol) (WIP).

The kinetic evaluations revealed the presence of the L band (ΔWOK) and the K band (ΔWOJ). The positive K band (Fig. 1, e) could mean that the oxygen-evolving complex (OEC) becomes permeable and offers access to non-aqueous electron donors evidenced by a reduced quinone (QA) reduction rate, the primary electron acceptor of PSII, from QA to QA-. The presence of a positive K band reflects an increase in the functional antenna size of PSII and/or an inactivation of the oxygen-evolving complex (Yan et al., 2013), as evidenced by an increase in ABS/RC. The presence of a positive L band (Fig. 1, f) indicates lower energy connectivity and more inefficient consumption of excitation energy, giving lower stability (Pollastrini et al., 2017).

Thus, any disorder in these factors promoted by stress will be observed by the alteration of the vitality index (Han et al., 2009). According to Novák et al. (2020), under regular conditions, biochar-enriched soils promote photosynthesis and stomatal conductance. Therefore, the evaluation of these indices showed that the crop underwent biotic and abiotic stresses, and it can be observed that the lower the PIABS at the end of the experiment, and possibly the greater the stress it was subjected to, mainly evidenced for the ceramic treatment.

Plants under stress exhibit several key responses, such as stomatal closure to minimize transpirations, reduced cell growth, and decreased turgor pressure. Theses physiological changes lead to lower water content, reduced dry weight, and diminished plant height (Guo et al., 2018). Thus, such factors related to chlorophyll *a* directly impact the growth parameters of okra (Table 6).

Biochar significantly impacted okra cultivation, as the plants exhibited smaller size, reduced leaf area, and more leaves, this is likely due to biochar's capacity to enhance initial plant growth by effectively retaining and storing water, while also contributing essential nutrients (Syaranamual et al., 2024). This finding aligns with Petter (2010), who noted that charcoal also had significant effects on the height parameter of soybeans, and with Melo (2016), who observed similar effects on cowpea beans. However, it contrasts with Liu et al. (2021), who found no significant height differences in okra when biochar was applied. These results may be linked to the stress factors observed in chlorophyll *a* fluorescence parameter, which altered the crop parameters for better performance, as indicated by the increase in PItotal.

Table 6. Growth parameters of okra (*Abelmoschus esculentus* L.) at 110 DAS under different soil compositions

Treatments	Plant height, cm	Leaf area, cm^2	Stem diameter, mm	No of leaves per plant, un
Control	161.6 a	186.6 ab	15.32 ab	14.6 b
Clay	151.8 ab	209.8 a	15.08 b	14.0 b
Biochar	144.2 b	154.4 c	15.94 ab	16.4 a
Ceramic	158.6 a	160.1 bc	16.21 a	15.2 ab
CV (%)	4.01	9.80	6.56	5.56

[1] Same letters in the column, for the same day of analysis, in each parameter, do not differ statistically from each other at a 5% probability level according to Tukey's test. Values represent means of $n = 15$.

The other treatments and the control displayed more similar behaviors to each other, as observed by Nobre et al. (2012), who found that adding ceramic powder to banana seedling production did not enhance height, as this material lacks essential macro and micronutrients.

Consequently, these factors directly influenced the dry mass production of each part of the okra plant (Fig. 2). The increased root production in the treatments Control > Biochar > Ceramic may be related to the amount of macropores and resistance to root penetration in the constructed soil and/or the low nutrient availability, prompting greater root exploration in the soil volume in search of nutrients. Liu et al. (2021) did not corroborate the data found, as they identified a 40% increase in root biomass in the biochar treatment compared to the control. Milla et al. (2013) also reported increases in biomass factors, root depth, leaf width, and stem size with the application of rice husk charcoal. Ismail & Ozawa (2007) observed an increase in biometric attributes of cucumber and corn with the addition of clay, particularly in roots.

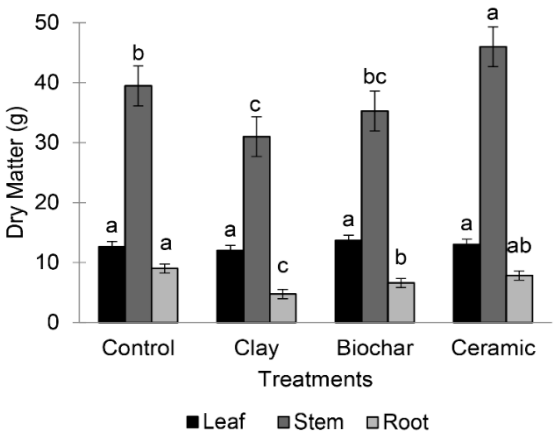

Figure 2. Dry mass of leaves, stems, and roots of okra for the treatments at the end of the experiment (110 DAS).

*Same letters among treatments for the same parameter do not differ statistically from each other at a 5% probability level according to the Tukey test. The values represent the means of $n = 5$.

Regarding the aerial part, Primo (2020) reported that increasing the percentage of clay in the soil did not significantly affect the dry matter of sorghum. However, Song et al. (2020) obtained higher corn biomass in soils with 40% clay content due to higher water retention. Lucon (2019) and Petter (2010) did not observe a relationship between charcoal levels in the soil and increased dry matter in corn and soybean crops, respectively.

Thus, since there were differences in the photosynthetic factors and the parameters related to the physiology of okra, it is necessary to evaluate its foliar contents to check for nutritional differences (Table 7).

Table 7. Foliar contents of nitrogen (N), phosphorus (P), potassium (K), calcium (Ca), magnesium (Mg), and sodium (Na), in g kg^-1, of okra (Abelmoschus esculentus L.) subjected to different soil compositions

Treatments	N	P	K	Ca [ns]	Mg [ns]	Na
	---------- g kg^{-1} ----------					
Control	17.86 c	9.58 b	41.01 b	48.60	9.33	0.28 b
Clay	25.35 a	9.49 b	41.77 b	43.84	9.26	0.32 a
Biochar	21.83 b	12.21 a	44.30 a	41.97	9.25	0.28 b
Ceramic	21.00 b	9.11 b	41.86 b	42.87	9.58	0.28 b
CV (%)	5.92	5.12	2.77	9.60	9.60	4.45

[1] Same letters in the column, for the same day of analysis, in each parameter, do not differ statistically from each other at a 5% probability level according to Tukey's test; Values represent means of $n = 15$; ns = not significant.

It was found that there was a significant difference for nitrogen, phosphorus, potassium, and sodium. The treatment composed of clay stood out in the promotion of nitrogen (N) and sodium (Na), while biochar stood out in the promotion of potassium (K) and phosphorus (P). Hussain et al. (2020) described that the use of biochar promotes higher concentrations of nitrogen (N), phosphorus (P), and potassium (K), and, in combination with other conditioners, promotes greater productivity, nutrient absorption, and growth for maize.

Moreover, biochar's influence manifests through the generation of anionic species via complex oxidation-reduction interactions with soil oxygen. Consequently, biochar demonstrates significant efficacy in nutrient retention for enhanced plant assimilation (Joseph et al., 2010; Bolan et al., 2022). Primo (2020) corroborates these results by reporting that in soil with 26% clay, there was greater nitrogen absorption by plants compared to levels of 10%, 15%, and 31%.

Thus, the use of biochar can be a good ally for phosphate and potassium fertilization, as phosphorus plays a significant role in the flowering and fruiting of plants, promoting good development of the root system and increased production (Raij, 1991), participating in the regulation of enzyme activity, synthesis of sucrose, phospholipids and cellulose, and the release of energy from ATP (Malavolta, 2008). Potassium, in turn, acts as an enzyme activator in the synthesis and degradation of organic compounds, in the processes of stomatal opening and closing, and osmoregulation (Marschner, 1995).

Consequently, this culminated in the productivity of the crop (Fig. 3), where about 99% of the harvested fruits were classified as Prime, i.e., fruits over 12 cm in length, regardless of the treatment (data not shown) (Filgueira, 2005). Productivity was significantly affected by the inclusion of conditioners; however, there were no significant differences between them, only compared to the control.

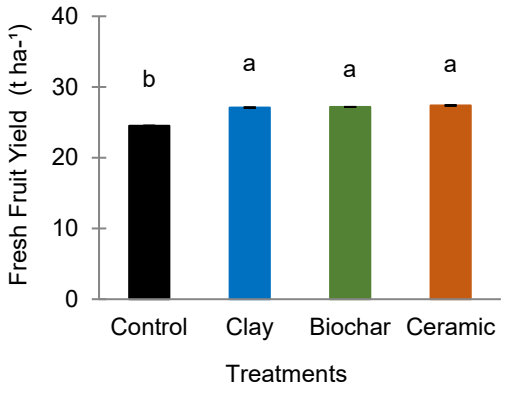

Figure 3. Productivity of okra (*Abelmoschus esculentus* L.) for treatments.

Values followed by the same letter within the same column are not significantly different from each other at a 5% probability level according to Tukey's test. Values represent the means of $n = 5$.

However, these values may present different results in subsequent harvests, as biochars can undergo biodegradation and transformation (Madari et al., 2006), potentially resulting in an increase in the availability of electrochemical sites. The utilization of biochar in nutrient-deficient soils represents a potential strategy to enhance agricultural productivity (Widiasri et al., 2022; Xu et al., 2017). This was observed by Yakubu et al. (2020), who reported an increase in productivity starting from the second year of okra cultivation, and by Major et al. (2010), who noted an increase in corn productivity in the second year of planting. Melo (2016) observed an increase of up to 60% in the productivity of dry caupi beans in Fluvic Neosol between the application of zero dose and a dose of 10.5 t ha^{-1}.

CONCLUSIONS

As the conditioners are highly stable materials, it is natural for the modifications to take time to appear over time. However, it was found that ceramic induced greater photosynthetic stress, was not efficient in retaining nutrients in the soil, nor did it promote chemical and/or physical qualities. Despite this, it significantly increased productivity. Biochar, on the other hand, was effective in retaining more water in the soil, retaining phosphorus, making it available for okra cultivation, increasing its absorption along with potassium, and increasing organic carbon content. Clay increased the levels of sodium and nitrogen in the crop. There was no difference between the conditioners in increasing productivity, only compared to the control.

Given that these results are preliminary, for future research, it is recommended to conduct experiments with doses and combinations of conditioners. Additionally, should be made experimentation in an open system (field) and medium and long-term trials.

REFERENCES

Aita, C., Giacomini, S.J., Hubner, A.P., Chiapinotto, I.C. & Fries, M.R. 2004. Intercropping cover crops in autumn/winter preceding no-till maize: nitrogen dynamics in the soil. *Brazilian Journal of Soil Science* **28**, 739–749 (in Portuguese). doi: 10.1590/S0100-06832004000400014

Akhtar, A. & Sarmah, A.K. 2018. Construction and demolition waste generation and properties of recycled aggregate concrete: a global perspective. *Journal of Cleaner Production* **186**, 262–281. doi: 10.1016/j.jclepro.2018.03.085

Amado, T.J., Mielniczuk, J., Fernandes, S.B.V. & Bayer, C. 1999. Cover crops, total nitrogen accumulation in the soil, and maize yield. *Brazilian Journal of Soil Science* **23**, 679–686 (in Portuguese). doi: 10.1590/S0100-06831999000300022

ASTM International ASTM D1762-84.2021 'Standard Test Method for Chemical Analysis of Wood Charcoal'. ASTM International 1–2, West Conshohocken. doi: 10.1520/D1762-84R21

Babla, M., Katwal, U., Yong, M-T., Jahandari, S., Rahme, M., Chen, Z-H. & Tao, Z. 2022. Value-added products as soil conditioners for sustainable agriculture. *Resources, Conservation and Recycling* **178**, 106079. doi10.1016/j.resconrec.2021.106079

Bibar, M.P.S. 2014. *Agricultural potential of biochars from alternative biomass*. Dissertation (Master's) - Agronomic Institute of Campinas, Campinas, Brazil, 115 pp. (in Portuguese).

Bolan, N., Hoang, S.A., Beiyuan, J., Gupta, S., Hou, D., Karakoti, A., Joseph, S., Jung, S., Kim, K.H., Kirkham, M.B., Kua, H.W., Kumar, M., Kwon, E.E., Ok, Y.S., Perera, V., Rinklebe, J., Shaheen, S.M., Sarkar, B., Sarmah, A.K., … Van Zwieten, L. 2022. Multifunctional applications of biochar beyond carbon storage. *International Materials Reviews* **67**(2), 150–200. https://doi.org/10.1080/09506608.2021.1922047

Callister, W.D. 2006. *Fundamentals of Materials Science and Engineering: An Integrated Approach.* 2nd ed. Rio de Janeiro, Brazil, 824 pp. (in Portuguese).

Carvalho, M.L., De Moraes, M.T., Cerri, C.E.P. & Cherubin, M.R. 2020. Biochar amendment enhances water retention in a tropical sandy soil. *Agriculture* **10**(3), 62. doi: 10.3390/agriculture10030062

CATI. 1999. *Comprehensive Technical Assistance Coordination* / *Coordenadoria de Assistência Técnica Integral, SP*. Okra – Agricultural Technologies, 39 pp. (in Portuguese).

Donagemma, G.K., Freitas, P.L., Balieiro, F.C., Fontada, A., Spera, S.T., Lumbreras, J.F., Viana, J.H.M., Filho, J.C.A., Santos, F.C., Albuquerque, M.R., Macedo, M.C.M., Teixeira, P.C., Amaral, A.J., Bortolon, E. & Bortolon, L. 2016. Characterization, agricultural potential, and perspectives for the management of light soils in Brazil. *Brazilian Agricultural Research* **51**(9), 1003–1020. doi: 10.1590/S0100-204X2016000900001

Esmaeelnejad, L., Shorafa, M., Gorji, M. & Hosseini, S.M. 2016. Enhancement of physical and hydrological properties of a sandy loam soil via application of different biochar particle sizes during incubation period. *Spanish Journal of Agricultural Research* **14**(2), e1103, pp. 14. doi: 10.5424/sjar/2016142-9190

Freire, L.R., Balieiro, F.C., Zonta, E., Anjos, L.H.C., Pereira, M.G., Lima, E., Guerra, J.G.M., Ferreira, M.B.C, Leal, M.A.A., Campos, D.V.B. & Polidoro, J.C. 2013 *Lime and Fertilisation Manual for the State of Rio de Janeiro*. Brasília, DF: EMBRAPA, Seropédica, RJ. Editora Universidade Rural, 430 pp. (in Portuguese).

Falcão, N.P.S., Souza, L.A.G. & Oliveira, D.M. 2013. Effect of adding charcoal and sawdust to a Yellow Latosol soil in Central Amazonia on the development and natural nodulation of cowpea. In H. Noda, L.A.G. de Souza, & D.F. da Silva Filho (Eds.), *Agricultural Research for Sustainable Agriculture in Central Amazonia* Chapter **16**, 233–252. Manaus, Amazonas: NERUA – CSAS – INPA, Brazil (in Portuguese).

Filgueira, F.A.R. 2005. *New Horticulture Manual: Modern Agrotechnology in the Production and Marketing of Vegetables* (2nd ed.). Viçosa, MG: UFV Press, Brazil, 412 pp. (in Portuguese).

Glaser, B., Balashov, E., Haumaier, L., Guggenberger, G. & Zech, W. 2000. Black carbon in density fractions of anthropogenic soils of the Brazilian Amazon region. *Organic geochemistry* **31**(7–8), 668–678. doi: 10.1016/S0146-6380(00)00044-9

Glaser, B., Guggenberger, G., Zech, W. & Ruivo, M.D L. 2003. Soil organic matter stability in Amazonian Dark Earths. In J. Lehmann, D. C. Kern, B. Glaser, & W. I. Wodos (Eds.), *Amazonian dark earths,* 141–158, Springer. doi: 10.1007/1-4020-2597-1_12

Guo, Y.Y., Yu, H.Y., Yang, M.M., Kong, D.S. & Zhang, Y.J. 2018. Effect of drought stress on lipid peroxidation, osmotic adjustment and antioxidant enzyme activity of leaves and roots of Lycium ruthenicum Murr. seedling. *Russian J. Plant Physiol.* **65**(2), 244–250. doi: 10.1134/S1021443718020127

Gurwick, N.P., Moore, L.A., Kelly, C. & Elias, P. 2013. A Systematic Review of Biochar Research, with a Focus on Its Stability in situ and Its Promise as a Climate Mitigation Strategy. *PLoS ONE* **8**(9), e75932. doi: 10.1371/journal.pone.0075932

Hall, D.J.M., Jones, H.R., Carbtree, W.L. & Daniels, T.L. 2010. Claying and deep ripping can increase crop yields and profits on water repellent sands with marginal fertility in southern Western Australia. *Australian Journal of Soil Research* **48**(2), 178–187. doi: 10.1071/SR09078

Hamer, U., Marschner, B., Brodowski, S. & Amelung, W. 2004. Interactive priming of black carbon and glucose mineralization. *Organic Geochemistry* **35**(7), 823–830. doi: 10.1016/j.orggeochem.2004.03.003

Han, S., Tang, N., Jiang, H.X., Yang, L.T. & Chen, L.S. 2009. CO_2 assimilation, photosystem II photochemistry, carbohydrate metabolism and antioxidant system of citrus leaves response to boron stress. *Plant Science* **176**(1), 143–153. doi: 10.1016/j.plantsci.2008.10.004

Hussain, A., Ahmad, M., Mumtaz, M.Z. & Ali, S. 2020. Integrated Application of Organic Amendments with Alcaligenes sp. AZ9 Improves Nutrient Uptake and Yield of Maize (Zea mays). *Journal of Plant Growth Regulation* **39**(3), 1277–1292. doi: 10.1007/s00344-020-10067-7

IBI. 2015. International biochar initiative: Standardized product definition and product testing guidelines for biochar that is used in soil, 2015. *http://www.biochar-international.org/characterizationstandard*. Accessed 13.12.2023

Igalavithana, A.D., Kwon, E.E., Vithanage, M., Rinklebe, J., Moon, D.H., Meers, E., Tsang, D.C.W. & Ok, Y.S. 2019. Soil lead immobilization by biochars in short-term laboratory incubation studies. *Environment International* **127**, 190–198. doi: 10.1016/j.envint.2019.03.031

Ismail, S. & Ozawa, K. 2007. Improvement of Crop Yield, Soil Moisture Distribution and Water Use Efficiency in Sandy Soils by Clay Application. *Applied Clay Science* **37**(1–2), 81–89. doi: 10.1016/j.clay.2006.12.005

Jeffery, S., Meinders, M.B.J., Stoof, C.R., Bezemer, T.M., van de Voorde, T.F.J., Mommer, L. & van Groenigen, J.W. 2015. Biochar application does not improve the soil hydrological function of a sandy soil. *Geoderma* **251–252**, 47–54. doi: 10.1016/j.geoderma.2015.03.022

Joseph, S.D., Camps-Arbestain, M., Lin, Y., Munroe, P., Chia, C.H., Hook, J., Van Zwieten, L., Kimber, S., Cowie, A., Singh, B.P., Lehmann, J., Foidl, N., Smernik, R.J. & Amonette, J.E. 2010. An investigation into the reactions of biochar in soil. Australian Journal of Soil Research **48**(6–7), 501–515. doi: 10.1071/SR10009

Kim, K.H., Kim, J.Y., Cho, T.S., Choi, J.W. 2012. Influence of Pyrolysis Temperature on Physicochemical Properties of Biochar Obtained from the Fast rolysis of Pitch Pine (Pinus rigida). *Bioresource Technology* **118**, 158–162. doi: 10.1016/j.biortech.2012.04.094

Lamarca, C.C. 1996. *Stubble over the soil.* Madison: American Society of Agronomy, pp. 245.

Liu, Q., Meki, K. & Ma, X. 2021. Enhanced Growth of Okra (Abelmoschus esculentus) in Soil Amended with Biochar and Fulvic acid. *E3S Web of Conferences* 251, 02067. doi: 10.1051/e3sconf/202125102067

Lucon, I.M. 2019. *Biochar on the physical and chemical attributes and productivity of maize in soil under tropical climate*. PhD Thesis, IAC, Brazil, 92 pp. (in Portuguese).

Madari, B.E., Costa, A.R., Castro, L.M., Santos, J.L.S., Benites, V.M., Rocha, A.O. & Machado, P.L.O.A. 2006. Charcoal as a soil conditioner for upland rice (cultivar primavera): A prospective study. *Embrapa Arroz e Feijão* **125**, 2 pp. (in Portuguese).

Mafra, A.L., Guedes, S.F.F., Klauberg Filho, O., Santos, J.C.P., Almeida, J.A. & Dalla Rosa, J. 2008. Organic carbon and chemical attributes of soil in forest areas. *Revista Árvore* **32**(2), 217–224. doi: 10.1590/S0100-67622008000200004

Major, J., Rondon, M., Molina, D., Riha, S. & Lehmann, J. 2010. Maize yield and nutrition during 4 years after biochar application to a Colombian savanna oxisol. *Plant Soil* **333**(1), 117–128. doi: 10.1007/s11104-010-0327-0

Malavolta, E. 2008. The future of plant nutrition, considering agronomic, economic, and environmental aspects. *Agronomic Information* **121**, 1–10 (in Portuguese).

Marschner, H. 1995. *Functions of Mineral Nutrients: Micronutrients*. In: Mineral Nutrition of Higher Plants, 2nd Edition, Academic Press, London, 313–404.

Melo, I.G.C. 2016. *Effects of charcoal on soil and cowpea cultivation in a protected environment*. Ph.D. Thesis, Federal Rural University of the Semi-Arid Region, 97 pp. (in Portuguese).

Milla, O.V., Rivera, E.B., Huang, W.J., Chien, C.C. & Wang, Y.M. 2013. Agronomic properties and characterization of rice husk and wood biochar and their effect on the growth of water spinach in a field test. *Journal of Soil Science and Plant Nutrition* **13**(2), 251–266. doi: 10.4067/S0718-95162013005000022

Mukherjee, A. & Lal, R. 2014. The biochar dilemma. *Soil Research* **52**(3), 217–230. doi: 10.1071/SR13359

Neves Junior, A.F. 2008. *Physical quality of soils with an anthropic horizon (Terra Preta de Índio) in Central Amazonia*. Ph.D. Thesis, São Paulo University, Brazil. doi: 10.11606/T.11.2008.tde-28072008-155658 (in Portuguese).

Nobre, L.L.S., Araújo, F.S. & Leite, J.Y.P. 2011. Analysis of red ceramic waste and its application as a source of potassium in agriculture. *HOLOS* **5**, 3–9. doi: 10.15628/holos.2011.769 (in Portuguese).

Nobre, L.L.S., Leite, J.Y.P., Dutra, M.F.B., Medeiros, A.J.R.P. & Pereira, E.C. 2012. Analysis of the behaviour of red ceramic waste as a source of potassium in banana cultivation. *HOLOS* **5**, 34–41. doi: 10.15628/holos.2012.1101 (in Portuguese).

Novák, V., Křížová, K. & Šařec, P. 2020. Biochar dosage impact on physical soil properties and crop status. *Agronomy Research* **18**(4), 2501–2511.

OECD/FAO. 2022. OECD-FAO Agricultural Outlook 2022–2031, OECD Publishing, Paris. doi:10.1787/f1b0b29c-en

Ofori, J., Tortoe, C. & Agbenorhevi, J.K. 2020. Physicochemical and functional properties of dried okra (Abelmoschus esculentus L.) seed flour. *Food Science Nutrition* **8**(8), 4291–4296. doi:10.1002/fsn3. 1725

Oliveira, S.P., Melo, E.N., Mota de Melo, D.R., Costa, F.X. & Mesquita, E.F. 2014. Seedling formation of okra with different organic substrates and biofertilizer. *Revista Terceiro Incluído* **4**(2), 219–235. doi: 10.5216/teri.v4i2.35280 (in Portuguese).

Paul, S.K., Gupta, D.R., Ino, M., Hirooka, Y. & Ueno, M. 2023. Biological characterization of *Fusarium buharicum*-induced wilt of okra and its management. *Journal of Plant Pathology*. doi:10.1007/s42161-023-01557-0

Paul, S.K., Gupta, D.R., Ino, M. & Ueno, M. 2024. Development of a PCR-based assay for specific and sensitive detection of *Fusarium buharicum* from infected okara plant. *PLoS ONE*, **19**(4), e0302256. doi: 10.1371/journal

Petter, F.A. 2010. *Charred biomass as a soil conditioner: agronomic and environmental aspects of its use in Cerrado soils*. Ph.D Thesis, Federal University of Goiás, Brazil, 13 pp. (in Portuguese).

Pollastrini, M., Nogales, A.G., Benavides, R., Bonal, D., Finer, L., Fotelli, M., Gessler, A., Grossiord, C., Radoglou, K., Strasser, R.J. & Bussotti, F. 2017. Tree diversity affects chlorophyll a fluorescence and other leaf traits of tree species in a boreal forest. *Tree Physiol* **37**(2), 199–208. doi: 10.1093/treephys/tpw132

Primo, B.A. 2020. *Use of organic and inorganic conditioners in the quality of sandy soil in the northeastern semi-arid region*. Master's Dissertation, Federal University of Ceará, Brazil, 48 pp. (in Portuguese).

Raij, B.V. 1993. Principles of correction and fertilization for seedlings and commercial production. In: Symposium on Nutrition and Fertilization of Vegetables, Piracicaba, *POTAFOS*, 75–84 (in Portuguese).

Ramalho, A.M. & Pires, A.M.M. 2009. Viability of agricultural use of construction and ceramic industry waste: chemical attributes. In: *Interinstitutional Congress of Scientific Initiation*, 3rd, Campinas, Brazil, pp. 6 (in Portuguese).

Razzaghi, F., Obour, P.B. & Arthur, E. 2020. Does biochar improve soil water retention? A systematic review and meta-analysis. *Geoderma* **361**, 114055. doi: 10.1016/j.geoderma.2019.114055

R Core Team. 2024. R: A Language and Environment for Statistical Computing. R Foundation for Statistical Computing, Vienna, Austria. https://www.R-project.org/.

Riedel, T., Hennessy, P., Iden, S.C. & Koschinsky, A. 2015. Leaching of soil-derived major and trace elements in an arable topsoil after the addition of biochar. *European Journal of Soil Science* **66**(4), 823–834. doi: 10.1111/ejss.12256

Rodrigues, M.I.B., Soares, B.S., Neta, I.A.B., Rodrigues, A.W.B. & Neiva, L.S. 2021. Sustainable development for waste generated in the Red Ceramic Industries in the Cariri region - CE. *Brazilian Journal of Development* **7**(4), 40689–40702. doi: 10.34117/bjdv7n4-500 (in Portuguese).

Santos, F.C., Resende, A.V., Filho, M.R.A., Borin, A.L.D.C. & Passos, A.M.A. 2015. *Dynamics of fertility in fragile soil*s. In: Fragile soils: characterization, management, and sustainability, Brazil, 367 pp. (in Portuguese).

Santos, E.A., Vale, L.S.R., Oliveira, H.F.E. & Miranda, T.M. 2020. Seed quality of okra produced under different irrigation depths. *Research, Society and Development* **9**(11), e52591110184. doi: 10.33448/rsd-v9i11.10184 (in Portuguese).

Sathish Kumar, D., Eswar Tony, D., Praveen Kumar, A, Ashok Kumar, K, Bramha Srinivasa Rao, D. & Nadendla, R. 2013. A Review on: Abelmoschus esculentus (Okra). *International Research Journal of Pharmaceutical an Applied Sciences* **3**(4), 129–132.

Shi, A. & Marschner, P. 2013. Addition of a clay subsoil to a sandy top soil alters CO_2 release and the interactions in residue mixtures. *Science of the Total Environment* **465**, 248–254. doi: 10.1016/j.scitotenv.2012.11.081

Shinde, R., Sarkar, P.K. & Thombare, N. 2019. Soil conditioners. *Agriculture & Food: e-Newsletter* **1**(10), 1–5.

Silva, A.S., Silva, I.F., Bandeira, L.B., Dias, B.O. & Neto, L.F.S. 2014. Clay and organic matter and effects on aggregation in different soil uses. *Ciência Rural* **44**(10), 1783–1789. doi: 10.1590/0103-8478cr20130789 (in Portuguese).

Singh, H., Northup, B.K., Rice, C.W. & Vara Prasad, P.V. 2022. Biochar applications influence soil physical and chemical properties, microbial diversity, and crop productivity: a meta-analysis. *Biochar* **4**, 8. doi: 10.1007/s42773-022-00138-1

SOIL SURVEY STAFF. 1951. *Soil survey manual*. Washington: Department of Agriculture Handbook **18**.

Song, Z., Bi, Y., Zhang, J., Gong, Y. & Yang, H. 2020. Arbuscular mycorrhizal fungi promote the growth of plants in the mining associated clay open. *Scientific Reports* **10(**2663), 1–9. doi: 10.1038/s41598-020-59447-9

Sousa, C.P. 2012. *Action of herbicides on the photosynthetic activity of plants with C3 and C4 metabolism*. Ph.D. thesis, Federal University of Pelotas, Brazil, 122 pp. (in Portuguese).

Souza Santos, P. 1989. *Science and Technology of Clays*, 2nd ed. São Paulo, Brazil, 408 pp. (in Portuguese).

Strasser, B.J. & Strasser, R.J. 1995. Measuring fast fluorescence transients to address environmental questions: The JIP-test. Photosynthesis: From Light to Biosphere, pp. 977–980. doi: 10.1007/978-94-009-0173-5_1142

Strasser, R.J., Tsimilli-Michael, M. & Srisvastava, A. 2014. *Analysis of the Chlorophyll a Fluorescence Transient*. In: Papageorgiou, G.C., Govindjee (eds) Chlorophyll a Fluorescence. Advances in Photosynthesis and Respiration, vol **19**, Springer, Dordrecht. doi: 10.1007/978-1-4020-3218-9_12

Syaranamual, S., Tuhumena, V.L., Syufi, Y., Daeng, B., Muyan, Y., Karamang, S., Martanto, E.A., Baan, S., Musaad, I., Amriati, B., Purnomo, D.W., Sarungallo, A.S. & Tubur, H.W. 2024. The implementation of sustainable urban agriculture: response of mustard (Brassica juncea L.) towards planting media composition of top soil, biochar and manure at vertical farming. *Agronomy Research* **22**(S2), 712–726. https://doi.org/10.15159/AR.24.027

Tahir, S. & Marschner, P. 2017. Clay Addition to Sandy Soil Reduces Nutrient Leaching – Effect of Clay Concentration and Ped Size. *Communications in Soil Science and Plant Analysis* **48**(15), 1813–1821. doi: 10.1080/00103624.2017.1395454

Teixeira, P.C., Donagemma, G. K., Fontana, A. & Teixeira, W.G. 2017. *Manual of Soil Analysis Methods*, 3rd ed. Brasília, Brazil, 574 pp. (in Portuguese).

Troeh, F.R. & Thompson, L.M. 2005. *Soils and Soil Fertility*. Sixth Edition, Blackwell, Ames, Iowa, 489 pp.

Tsimilli-Michael, M. & Strasser, R. 2008. In vivo assessment of stress impact on plants' vitality: applications in detecting and evaluating the beneficial role of Mycorrhization on host plants. In: Varma, A. (Ed.). *Mycorrhiza: state of the art, genetics and molecular biology, ecofunction, biotechnology, eco-physiology, structure and systematic*. Uttar Pradesh: Springer, 679–703. doi: 10.1007/978-3-540-78826-3_32

Widiasri, E., Maulani, R.R., Nofitasari, D., Lambangsari, K., Manurung, R. & Abduh, M.Y. 2022. Enrichment of growing media using biochar, compost, and nanosilica for the cultivation of Oryza sativa L. *Agronomy Research* **20**(Special Issue I), 1175–1186. https://doi.org/10.15159/AR.22.061

Xu, G., Sun, J.N., Shao, H.B. & Chang, S.X. 2014. Biochar had effects on phosphorus sorption and desorption in three soils with differing acidity. *Ecological Engineering* **62**, 54–60. doi: 10.1016/j.ecoleng.2013.10.027

Xu, X., Zhao, Y., Sima, J., Zhao, L., Masek, O. & Cao, X. 2017. Indispensable Role of Biocharinherent Mineral Constituents in Its Environmental Application: A Review. *Bioresources Technology* **214**, 887–899.

Yakubu, A., Danso, E.O., Arthur, E., Kugblenu-Darrah, Y.O., Sabi, E B., Abenney-Mickson, S., Ofori, K. & Andersen, M.N. 2020. Rice straw biochar and irrigation effect on yield and water productivity of okra. *Agronomy Journal* **112**(4), 3012–3023. doi: 10.1002/agj2.20230

Yan, K., Chen, P., Shao, H., Shao, C., Zhao, S. & Brestic, M. 2013. Dissection of photosynthetic electron transport process in sweet sorghum under heat stress. *PLoS ONE* **8**, 62100. doi: 10.1371/journal.pone.0062100

Yang, C.D. & Lu, S.G. 2021. Effects of five different biochars on aggregation, water retention and mechanical properties of paddy soil: A field experiment of three-season crops. *Soil and Tillage Research* **205**, 104798. doi: 10.1016/j.still.2020.104798

Yusuf, M., Kumar, D., Rajwanshi, R., Strasser, R.J., Tsimilli-Michael, M.G. & Sarin, N.B. 2010. Overexpression of γ-tocopherol methyl transferase gene in transgenic Brassica juncea plants alleviates abiotic stress: Physiological and chlorophyll a fluorescence measurements. *Biochimica et Biophysica Acta – Bioenergetics* **1797**(8), 1428–1438. doi: 10.1016/j.bbabio.2010.02.002

Agronomy Research **22**(S3), 1504–1516, 2024
https://doi.org/10.15159/AR.24.064

Influence of coconut fiber incorporation on the mechanical behavior of adobe blocks

N.A. da Silva[1,2], D. Cecchin[1,*], C.A.A. Rocha[1], R.D. Toledo Filho[2], J. Pessin[1], G. Rossi[3], G. Bambi[3], L. Conti[3] and P.F.P. Ferraz[4]

[1]Federal Fluminense University - UFF, Department of Agricultural and Environmental Engineering; Rua Passo da Pátria, 156, PO Box 21065-230, Niterói, Brazil
[2]Federal University of Rio de Janeiro - UFRJ, Civil Engineering Department, Rio de Janeiro, Brazil
[3]University of Firenze, Department of Agriculture, Food, Environment and Forestry (DAGRI), Via San Bonaventura 13, IT50145 Firenze, Italy
[4]UFLA - Federal University of Lavras, Department of Agricultural Engineering, Campus Universitário, PO Box 3037, Lavras, Minas Gerais, Brazil
[*]Correspondence: daianececchin@id.uff.br

Received: January31st, 2024; Accepted: June 7th, 2024; Published: July 11th, 2024

Abstract. Adobe is an ancient construction technique, simple and low cost, still used in some parts of the world, mainly in rural areas. Normally, in these regions, a considerable amount of agricultural waste is generated that can be used for different purposes. An agricultural waste that has been increasingly studied in the construction sector is natural fibers. The addition of natural fibers in the soil matrix has been gaining prominence as it is a natural and easily accessible stabilizer. This work aimed to analyze and characterize adobe blocks reinforced with coconut fibers, with the addition of 1% and 2% compared to the reference block (without the addition of coconut fiber) through capillary absorption, fiber-soil adhesion, durability in the presence of water and mechanical, properties through of compression bending tests. The adobe blocks with the addition of fibers showed mechanical results above those required by the standard NBR 16814. The addition of fibers promoted higher capillary absorption results than the samples consisting only of soil and when exposed to drip erosion, no significant damage was observed in the adobe structure.

Key words: adobe, coconut fiber, rural buildings.

INTRODUCTION

The construction with earth resurged significantly in 1970, where the global scenario was witnessing the oil crisis and the increasing environmental issues such as the rise in pollutant emissions related to high energy consumption and extraction of non-renewable raw materials (Santos & Lima Bessa, 2020). A technique used in the past in prehistoric dwellings reemerges as a low-cost, highly available, and environmentally friendly alternative (Cordeiro et al., 2020).

In Brazil, an important milestone occurred in 2020 regarding earthen construction, which was the publication of the standard NBR 16814 by the Brazilian Association of Technical Standards (ABNT, 2020a). This brought visibility and credibility to the adobe construction technique.

Adobe is the most commonly used technique due to its ease of fabrication (Jalali & Eires, 2008). Christoforou et al. (2016) conducted a cradle-to-gate Life Cycle Assessment (LCA) of adobe blocks under different scenarios. In the local production scenario with regionally sourced soil and reinforcement, the global warming potential (GWP) impact category was 1.76E-03 $kgCO_2eq$. The embodied energy value was 0.34 MJ/block, demonstrating that adobe has a significantly lower energy footprint than concrete blocks (12.5 MJ/block) and fired clay bricks (4.25 MJ/block).

When associated with rural constructions, it is an interesting alternative not only because of the ease of construction but also because it requires simple maintenance, low cost, and contributes to sustainable rural development in construction when compared to conventional building materials.

According to Faostat data, in 2019, the global production of coconut was 62.9 million tons, and Brazil was the fifth largest producer globally, accounting for 3.7% of the total produced, behind only Indonesia, the Philippines, India, and Sri Lanka (FAOSTAT, 2021). Coconut is frequently found in places with tropical climates, such as Brazil, and the residue from its processing, when not discarded properly, can create environmental problems (Lertwattanaruk & Suntijitto, 2015). Natural fibers have been increasingly utilized in construction materials due to their characteristics and potential to enhance the mechanical properties of products (Ferreira et al., 2021). Among these fibers, acai fiber (Rocha et al., 2021), pineapple fibers (Azevedo et al., 2021), and coconut fibers (Ferreira et al., 2022) have been mentioned.

The characteristics of coconut residues include reduced cost, high lignin content, low density, abundant availability, while the fibers have high elongation at break, and low modulus of elasticity (Adeniyi et al., 2019). These characteristics of coconut residues make coconut fibers a promising choice as reinforcement for adobe blocks, as they can improve their mechanical properties. The objective of this study was to evaluate adobe blocks reinforced with the addition of coconut fiber for potential use in rural constructions.By investigating this combination, the study hopes to contribute to the development of more sustainable and accessible construction techniques, promoting both economic and environmental benefits.

MATERIALS AND METHODS

Soil

The soil used in the research was derived from excavation at a construction site in the state of Rio de Janeiro. Physical characterization tests (bulk density, moisture content, liquid limit, plastic limit, and plasticity index), granulometric analysis, and chemical composition analysis were conducted.

For the granulometric analysis, the soil was prepared according to the NBR 7181 (ABNT, 2016a) standard, which determines analysis by sieving and sedimentation (to distinguish the silt and clay fractions). In this study, the sedimentation test was replaced by laser diffraction analysis using the MasterSizer 2000 equipment, which provides precise

grain size measurements down to 0.0001 mm. It employs a light scattering technique where the angles of laser diffraction are measured and related to particle diameters.

The bulk density was determined according to NBR 6458 (ABNT, 2016b). Fifty grams of soil were separated, immersed in distilled water for 24 hours, and then transferred entirely to the dispersion cup and dispersed for 15 minutes. Subsequently, the sample was transferred to the pycnometer, where vacuum was applied to remove all air. After the test was completed, the set (pycnometer + soil + water) was weighed.

For determining the moisture content, the procedure followed the NBR 6457 (2016) standard. Three samples of 30 g each were taken in metallic capsules. The capsules along with the soil were weighed initially and then placed in an oven at 105 °C until a constant mass was achieved. Subsequently, the set was weighed again, the dry mass was recorded, and the moisture content was calculated according to Eq. (1).

$$w(\%) = \frac{Mu - Ms}{Ms} x100 \quad (1)$$

where w – Soil moisture content; Mu – Mass of the soil in its natural state; Ms – Mass of the soil when dry.

The plasticity index of the soil was determined by the decrease in the liquid limit, which is found through the test described in NBR 6459 (ABNT, 2016c), and the plastic limit test conducted according to NBR 7180 (ABNT, 2016d). The Liquid Limit (LL) is the transition from the liquid state to the plastic state, and the Plastic Limit (PL) is the transition from the plastic state to the semi-solid state. The Plasticity Index (PI) physically represents the amount of water needed to add to the soil to transition it from the plastic to the liquid state.

For the plastic limit test, 50 g of soil, a glass plate, and an oven were required. The soil used was the one passing through a 0.42 mm sieve. This soil was mixed with distilled water in a porcelain container until a homogeneous mixture was obtained. Then, 10 g of this sample was taken and formed into a small ball, which was rolled on the glass plate to form a cylinder with a diameter of 3 mm and a length of 100 mm. When the cylinder fragmented with these dimensions, the sample was transferred to a container, weighed, and placed in the oven to determine its moisture content. To determine the liquid limit, the Casagrande apparatus and 200 g of soil were required. After preparing the soil, a portion was transferred to the Casagrande apparatus. Once the apparatus was filled, a chisel was used to divide the material, and the apparatus was operated to perform the necessary blows until the lower edges of the groove joined. After this process, a portion of the soil was removed to determine the moisture content, and this test was repeated two more times to obtain mixtures covering the range of 15 to 35 blows. With the results obtained, a graph of the number of blows versus moisture content was plotted, and the liquid limit of the soil is the moisture content corresponding to 25 blows.

The chemical composition was determined through X-ray fluorescence (XRF) analysis using the Shimadzu model EDX-720.

Coconut fiber

The coconut fibers used were purchased from the company Coco Verde, located in Duque de Caxias, Rio de Janeiro. The fibers were subjected to a crusher, with the aim of reducing their length and contributing to the adobe production process.

The coconut fibers underwent physical characterization (bulk density and moisture content) and Scanning Electron Microscopy (SEM) analysis. The moisture content of

the coconut fiber was determined according to the NBR 9939 standard (ABNT, 2011). Three samples of 30 g each were separated and distributed in metal trays, then placed in an oven at 105 °C until reaching a constant mass.

To determine the bulk density, the procedure followed the NBR NM 52 (ABNT, 2009) standard. Initially, the fibers were submerged in water for 24 hours and then exposed to air to superficially dry. They were then placed in bottles with water up to the 500 ml mark. The bottles were left to rest in a water bath at 21 °C for 1 hour. Afterward, the bottles were topped up with water, and the entire set was weighed to record the total mass. Finally, the samples were removed and placed in ovens to dry at 105 °C until a constant mass was achieved.

Adobe

Adobe Production. Nine adobe blocks were produced (three for each treatment) and the production steps were as follows:

a. Production of wooden molds: The dimensions of the adobe mold were based on the criteria established by NBR 16814 (ABNT, 2020a), which are: 7×15×31 cm (height × width × length).

b. Preparation of the mixture: Three different mixtures were prepared, including a reference mixture with soil and water, and two others with the addition of 1% and 2% of fiber relative to the soil mass. The water-to-soil ratio was fixed at 0.35.

c. Molding and demolding: With the mixture ready, the mold was completely filled, the surface was leveled, and the adobe was demolded onto a flat surface.

d. Drying: The drying time was 20 days, ensuring uniform drying on all faces of the block.

Analysis. The adobe blocks underwent tests for: Mechanical characterization (uniaxial compression and flexural strength), absorption, density, durability, erosion test), and fiber-soil interface (pull-out test).

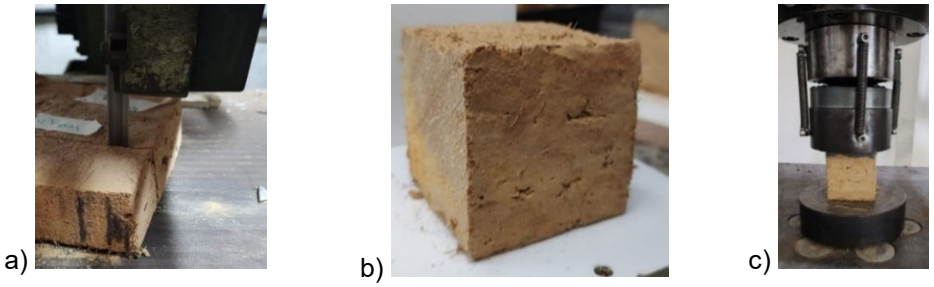

Figure 1. Uniaxial compression test: (a) sample cutting; (b) samples after cutting; and (c) uniaxial compression test of the adobe.

The uniaxial compression test was conducted according to NBR 16817 (ABNT, 2020b) standards using a Universal Testing Machine with a load capacity of 1,000 kN at a speed of 0.30 MPa min^{-1}. Two cubic test specimens of 6 cm were cut from each adobe block using a band saw (Fig. 1, a and b). To regularize the faces, a capping layer of up to 3 mm thickness was applied using a mix of cement and fine sand in a ratio of 1:2 by mass. The setup of the tests is illustrated in Fig. 1, c.

The flexural test was conducted using a Shimadzu Universal Testing Machine with a loading capacity of 100 kN. The test speed used was 0.3 mm min^{-1}. Prismatic specimens measuring (40×40×160 mm) were positioned for the three-point flexural test with a support span of 120 mm (Fig. 2).

For the calculation of flexural strength, Eq. (2) was used, according to the Araya-Letelier et al. (2019).

$$\tau f = \frac{3PL}{2BH^2} \qquad (2)$$

where P – maximum applied load; L – distance between supports; B – width of the sample; H – height of the sample.

The density of the blocks was determined according to BS EN 771:1 (2003). According to the standard, the specimens were placed in ovens at 110 °C for 48 hours until a constant mass was reached, and then weighed. The dimensions are collected, and the volume is calculated. Density is calculated using Eq. 3.

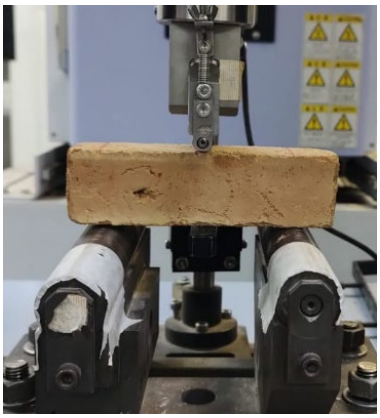

Figure 2. Three-point flexural test.

$$\rho = \frac{m}{V} \qquad (3)$$

where ρ – density (kg m^{-3}); m – mass (kg); V – volume (m^3).

For the determination of water absorption by capillarity, the procedures were based on the NBR 9779 (ABNT, 2012) standard. The specimens were placed in an oven at 105 °C for 24 hours, and after this process, they were cooled to room temperature to determine their masses. Then, they were wrapped with plastic film, leaving a 5 mm strip without plastic, as it is the region that was in direct contact with water. The specimens were immersed in a 5 mm layer of water, arranged in a glass container. During the test, the mass of the specimens was recorded at 3, 6, 24, 48, and 72 hour intervals.

The drip erosion test was based on the NBR 17014 standart (ABNT, 2022). In this test, the block was placed on a surface with a 1:2 slope so that the center of gravity of the larger face is on the axis of water drip application. A container with 100 mL of water was positioned 400 mm above the block. Water dripped onto the block for approximately 30 minutes, and after this process, the depth of the hole was measured using a vernier caliper and ruler. Depending on the depth, the adobe mixture can be classified as erosive, highly erosive, or failure.

The analysis of the fiber-soil interface was conducted through the pullout test, where the fiber is pulled out of the soil, and force and displacement data are collected, performed as described by Mendonça (2018). To conduct this test, a machine called Tytron 250 was used, equipped with a 50 N load cell. The test speed was set at 0.4 mm min^{-1}, and the samples consisted of a coconut fiber inserted into a PVC tube filled with soil, with an immersion length of 10 mm. For the calculation of the maximum tension (τmáx), it was compute using Eq. (4)

$$\tau máx = \frac{Pmáx}{lfPe} \qquad (4)$$

where $Pmáx$ – maximum load during pullout; lf – fiber embedment length; Pe – fiber perimeter.

To obtain the perimeter of the fiber, images from the SEM (Scanning Electron Microscope) and the Image J software were used.

RESULTS AND DISCUSSION

Soil

The grain size distribution curve of the soil is presented in Fig. 3, where the grain diameters and the percentages retained and passed through the soil are observed, according to the distribution of sieves described in NBR 7181 (ABNT, 2016).

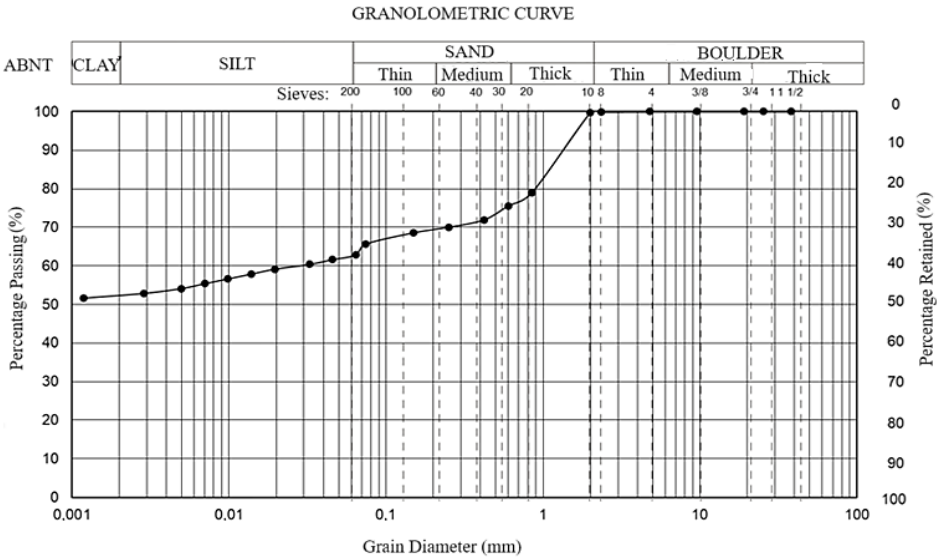

Figure 3. Granulometric distribution curve of the soil.

The grain size composition of the soil (Table 1) showed a higher concentration of clay (52%), followed by sand (37%), and finally silt (10%). According to NBR 16184 ABNT, 2020), the grain size composition should preferably meet (the following parameters: sand (between 45% and 65%); silt (up to 30%); and clay (between 25% and 35%).

Analyzing the grain size distribution of the soil selected for this study, the clay and sand contents do not meet the parameters specified by the standard. In this case, the standard suggests conducting physical and mechanical behavior tests on the produced adobes to determine if they meet performance specifications.

The results of the soil's physical properties can be observed in Table 2.

Table 1. Granulometric composition of the soil

Gravel	Coarse Sand	Medium Sand	Fine Sand	Silt	Clay
1%	24%	6%	7%	10%	52%

Table 2. Soil physical properties and coefficient of variation (in parentheses)

Bulk density (BD)	Plastic limit (PL)	Liquid limit (LL)	Plasticity index (PI)	Moisture Content (MC)
2.37 g cm^{-3} (2.19)	31.65% (4.50)	56.25% (6.12)	24.75%	3.11% (0.80)

The average soil moisture content at the time of the test was 3.11%, and the bulk density was 2.37 g cm^{-3}. When analyzing the consistency limits, it is important to note that this property is related to the physical state in which the soil is found in the presence of moisture and is divided into four groups: liquid (soil with fluid appearance), plastic (moldable soil), semi-solid (soil that shrinks when drying), and solid (soil that no longer undergoes volumetric variation) (Silva, 2022). According to Burmister (1949), a soil with a PI between 20–40, which is the case of the soil in this study (24.75%), is considered to have high plasticity, a characteristic of more clayey soils. Table 3 presents the chemical composition of the soil in the form of oxides, and it is noticeable that the highest contents are silica (SiO_2), alumina (Al_2O_3), and hematite (Fe_2O_3). According to Brian & Carleton (1982), these chemical elements, after oxygen, are the most abundant in the Earth's crust, and these contents may vary in percentages depending on the location.

Table 3. Chemical composition of the soil

Element	Content (%)
SiO_2	41.13
Al_2O_3	38.43
Fe_2O_3	15.78
SO_3	1.66
TiO_2	1.55
BaO	0.66
K_2O	0.26
others	0.53

Coconut fiber

The bulk density and moisture content of coconut fibers yielded the following results and coefficients of variation, respectively: 1.06 g cm^{-3} (8.4) and 8.77 (4.1). Vegetable fibers in general do not have a defined cross-section, and their dimensions can vary along the length (Ribeiro, 2021). Fig. 4, a shows an image of the cross-section of coconut fiber, which appears to have an approximately circular shape.

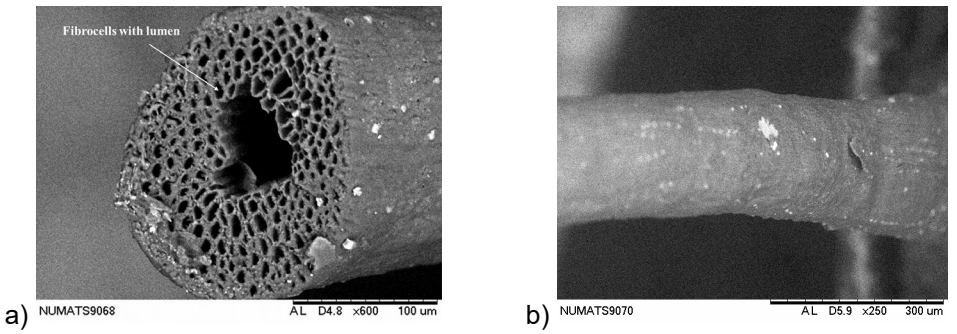

Figure 4. Scanning Electron Microscopy (SEM) images of coconut fibers: a) cross-section and b) outer surface.

Coconut fibers have a significant number of fibrocells, and their cell walls are thinner compared to other vegetable fibers such as sisal, jute, and curauá (Pereira, 2012). In Fig. 4, b, the outer surface of the fiber can be analyzed, showing a slight roughness that, according to Nunes et al. (2022), may be due to its vegetal origin and the extraction processes, which can result in the presence of impurities, fats, and organic residues adhered.

Adobe

The values of bulk density of the adobe blocks (reference (without fiber addition), 1% fiber addition, and 2% fiber addition) and their respective coefficients of variation were: 1,790 kg m^{-3} (4.1), 1,714.77 kg m^{-3} (3.6) and 1,675 kg m^{-3} (2.4). Since coconut fibers are very light (density 1.06 g cm^{-3}), when incorporated into the soil matrix, there is a reduction in densities compared to the reference mixture. This reduction ranges from 4.20% for the mixture with 1% of fibers to 6.40% for the mixture with 2% of fibers.

In the adobe blocks reinforced with fibers, an increase in water absorption by capillarity is observed (Fig. 5). This increase is attributed to the water absorbed by the cellulose of the fibers and the voids created by the fibers in the blocks, allowing more water to be absorbed. During the mixing process, the fibers absorb water and expand, and after the drying process, the fibers retract, creating these voids (Ghavami et al., 1999; Danso et al., 2015).

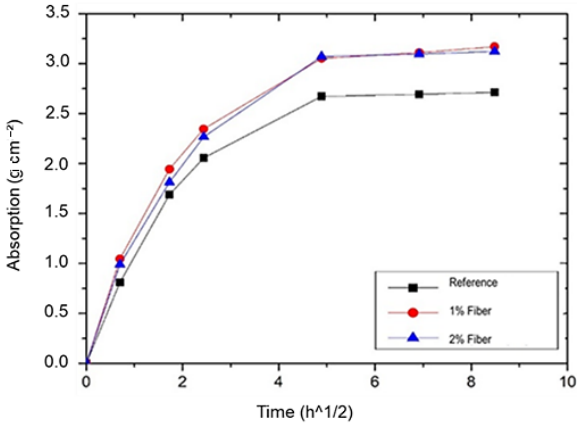

Figure 5. Capillary absorption curves of the adobe blocks.

Upon analyzing the results from the drip erosion analysis, it was noted that there were no significant changes on the surface of the blocks. In fact, the 17014 standard (ABNT, 2022) recommends dripping 100 mL of water onto the block's surface for 20 to 60 minutes. In this study, double the amount of water was tested, and consequently, the time also doubled, to simulate a more severe scenario. However, no significant impact was observed.

According to Danso et al. (2015), when using water jets with higher pressures, the durability of the blocks is more affected. The authors concluded that fiber-reinforced blocks protect soil particles from being carried away, thus reducing the effects of erosion.

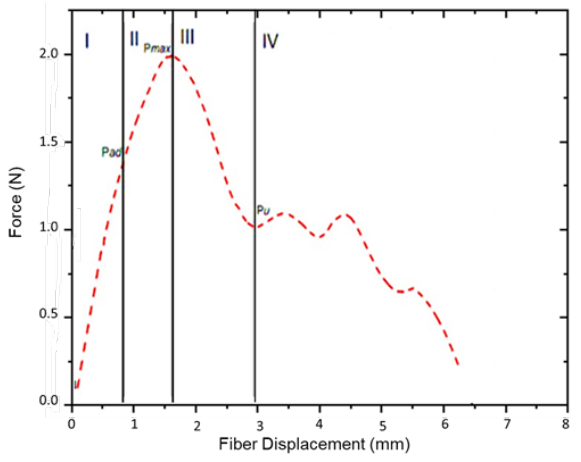

Figure 6. Typical force-displacement curve of the fiber from the pull-out test.

For the analysis of fiber-soil adhesion, the coconut fiber was inserted into the matrix and subjected to a tensile force. As the fiber displaced, a force-displacement curve of the fiber was obtained (Fig. 6). According to Naaman et al. (1991), the adhesion between fiber and matrix is a result

of the combined action of many elements, including physical-chemical adhesion between the fiber and the matrix, anchorage, and friction.

According to Ribeiro (2021), this behavior can be divided into four phases: Phase I: In this initial phase, the behavior is linear until the point where the superficial shear stress results in the breakage of the chemical adhesion between the fiber and the matrix, at which point the Pad (adhesion load) is reached. Analyzing the curve, it is noted that in the case of coconut fiber with the soil matrix, this breakage of chemical adhesion occurred at 1.2 N. Phase II: The displacement is no longer linear, and partial decohesion of the fiber-matrix interface occurs until the pull-out force reaches the maximum value, Pmax (2N). With this load, it was possible to calculate the adhesive stress (τ_{max}), which was 0.28 MPa, as shown in Table 4. Phase III: In the post-peak phase, the fiber was gradually pulled out of the matrix, reducing the force. The fissure of the fiber-matrix interface, which began in phase II, propagates throughout the fiber's length, characterized by the point Pu (0.88 N). Phase IV: It is characterized by the total pull-out of the fiber along its embedding length.

Table 4. Average results and coefficient of variation of the coconut fiber pull-out test

Perimeter (μm)	P*ad* (kN)	P*max* (kN)	P*u* (kN)	τ_{max} (MPa)
1,027.92 (9.4)	1.20 (8.7)	2.00 (5.6)	0.88 (7.8)	0.28 (3.2)

P*ad*: adhesion load; P*max*: peak load; P*u:* fiber debonding force; τ_{max}*: bond stress.*

The uniaxial compression strength was analyzed according to NBR 16814 (ABNT, 2020a), where the individual compression strength of adobe should be ≥ 1.5 MPa. All mixtures produced and tested in this study were above 1.5 MPa (Table 5), hence they can be used in constructions. It is noticeable that as the fiber content increases, the compression strength reduces. This phenomenon is related to the porosity of the material, which can cause additional microcracks due to fiber detachment and the formation of cracks at the fiber-matrix interface (Li, 1992; Ribeiro, 2021).

Table 5. Average results and coefficient of variation of the uniaxial compression test

Mixtures	*fca* (MPa)	Coefficient of variation (%)
Reference (0% fiber)	2.19	8.37
1% fiber	2.05	6.50
2% fiber	1.95	9.50

Abdulla et al. (2020) investigated the mechanical properties of straw fiber-reinforced adobe and obtained a compressive strength of 1.45 MPa after 28 days of curing. Rodríguez-Mariscal & Solís (2020) evaluated the mechanical properties of unreinforced adobe blocks in compression and found a value of 1.13 MPa. Pinto et al. (2021) subjected unreinforced adobe blocks to compression and found a value of 1.97 MPa; when reinforced with sisal, the value significantly increased to 3.28 MPa. Comparing the values found in this study with those in the literature, it is evident that the results are within the observed ranges.

Regarding the behavior of adobes during rupture, it is important to note that this behavior begins with the formation of microcracks, and when fibers are added, there is a delay in the propagation of cracks, preventing catastrophic failure (Ribeiro, 2021). Fig. 7, b and 7, c represent this type of behavior, while Fig. 7, a shows that the reference formed a continuous crack map, leading to abrupt rupture shortly thereafter.

Figure 7. Samples broken after uniaxial compression test: a) reference (0% fiber); b) 1% fiber; and c) 2% fiber.

In regards to the three-point bending test, only the reference adobe blocks and those with 2% fiber were tested, as it has the highest volumetric fraction of fibers. The values obtained for flexural strengths (Fig. 8) for the reference adobe block were 0.61 MPa (6.8), and for the samples with 2% fiber, the strength was approximately 0.56 MPa (9.4).

The load-displacement curve of the reference sample initially exhibits a linear behavior, and when the first crack appears (peak), there is an abrupt reduction in load, classifying this behavior as brittle. The characteristic crack opening of these samples can be observed in Fig. 9. The curve representing the samples with 2% fiber initially shows a linear segment until the first crack, and as micro-cracking begins, the randomly arranged fibers limit this propagation, improving resistance and ductility. The rupture process is characterized by the pulling out of fibers until the opening of a single crack.

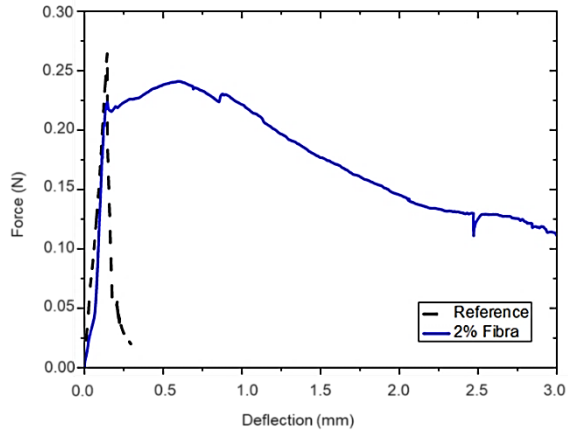

Figure 8. Load-displacement behavior of the adobe blocks.

Figure 9. Adobe samples after the bending test:(a) Reference and (b) 2% fiber.

CONCLUSIONS

With the incorporation of fibers, there was a reduction in the apparent densities of the adobe blocks.

When inserted into the adobe production process, the fibers absorb a certain amount of water from the mixture, which leads to an expansion process of their structure. As the block drying process occurs over time, these fibers undergo a retraction process, and the fiber-matrix interface experiences micro-cracks that end up providing pathways for a greater amount of water to penetrate, resulting in higher capillary absorption.

The evaluated adobe blocks did not show any significant damage related to water erosion when exposed to water dripping.

All blocks surpassed 1.5 MPa when subjected to compression loads, confirming the potential application of adobe. It was observed that the fibers provided mechanical gains regarding both the rupture and stabilization of the blocks, not only in compression but also in flexion.

Applying coconut fibers in earth constructions, specifically adobe, is a safe, low-cost possibility that requires low technology and contributes to the environment.

For future research, it is suggested to test the durability of adobe blocks under different climatic conditions by exposing them to prolonged cycles of rain, sun, wind, and temperature variations. Additionally, it is proposed to explore other natural fibers such as jute, sisal, and bamboo, with the aim of identifying alternatives that can further improve the strength and sustainability of these construction materials.

ACKNOWLEDGEMENTS. To the Ministério da Agricultura, Pecuária e Abastecimento (MAPA) for the scholarship granted to the first author during the Postgraduate Course - Residency in Agricultural Practices and Technical Assistance and Rural Extension (ATER).

REFERENCES

Abdulla, K.F., Cunningham, L.S. & Gillie, M. 2020. Experimental study on the mechanical properties of straw fiber–reinforced adobe masonry. *Journal of Materials in Civil Engineering* **32**(11), 04020322. doi_ 10.1061/(asce)mt.1943-5533.0003410

ABNT - Associação Brasileira de Normas Técnicas. 2016a. *Soil-Particle Size Analysis*, NBR 7181, ABNT: Rio de Janeiro, Brazil, 2016, 12 pp. (in Portuguese).

ABNT - Associação Brasileira de Normas Técnicas. 2016d. *Soil-Determination of Plastic Limit*, NBR 7180; ABNT: Rio de Janeiro, Brazil, 2016; 3 pp. (in Portuguese)

ABNT - Associação Brasileira de Normas Técnicas. 2020a. *Adobe - Requirements and Testing Methods*, NBR 16814 Rio de Janeiro, Brazil (in Portuguese).

ABNT - Associação Brasileira de Normas. 2009. *Fine Aggregate - Determination of Specific Gravity and Apparent Specific Gravity*, NBR NM 52, Rio de Janeiro, Brazil, 6 pp. (in Portuguese)

ABNT - Associação Brasileira de Normas. 2011. *Coarse Aggregate - Determination of Total Moisture Content - Test Method,* NBR 9939, ABNT: Rio de Janeiro, Brazil, 3 pp. (in Portuguese).

ABNT - Associação Brasileira de Normas. 2012. *Hardened mortar and concrete - Determination of water absorption by capillarity*, NBR 9779, ABNT: Rio de Janeiro, Brazil, 3 pp. (in Portuguese).

ABNT - Associação Brasileira de Normas. 2016c. *Soil-Determination of Liquid Limit*, NBR 6459, ABNT: Rio de Janeiro, Brazil, 2016, 5 pp. (in Portuguese).

ABNT - Associação Brasileira de Normas. 2020b. *Non-destructive testing - Conventional radiography - Procedure qualification* NBR 16817, ABNT: Rio de Janeiro, Brazil, 4 pp. (in Portuguese).

ABNT - Associação Brasileira de Normas. 2022. *Rammed earth construction - Requirements, procedures, and control*, NBR 17014, Rio de Janeiro, Brazil, 34 pp. (in Portuguese).

Adeniyi, A.G., Onifade, D.V., Ighalo, J.O. & Adeoye, A.S. 2019. A review of coir fiber reinforced polymer composites. *Composites Part B: Engineering* **176**, 107305. doi: 10.1016/j.compositesb.2019.107305

Araya-Letelier, G., Concha-Riedel, J., Antico, F.C. & Sandoval, C. 2019. Experimental mechanical-damage assessment of earthen mixes reinforced with micro polypropylene fibers. *Construction and Building Materials* **198**, 762–776. doi: 10.1016/j.conbuildmat.2018.11.261

Azevedo, A.R.G., Rocha, H.A., Marvila, M.T., Cecchin, D., Xavier, G.C., Silva, R.C., Ferraz, P.F.P., Conti, L. & Rossi, G. 2021. Application of pineapple fiber in the development of sustainable mortars. *Agronomy Research* **19**(3), 1387–1395, doi: 10.15159/AR.21.140

Brasileira de Normas Técnicas. 2016b. *Soil Sample—Preparation for Compaction Tests and Characterization Tests*, NBR 6457, ABNT: Rio de Janeiro, Brazil, 8 pp. (in Portuguese).

Brian, M. & Carleton, B.M. 1982. *Principles of geochemistry*. 4.ed. New York, John Wiley, 344 pp.

BRITISH STANDARDS INSTITUTION. 2003. *BS EN 771-1: Specification for masonry units– Part 1: Clay masonry units*.

Burmister, D.M. 1949. Principles and techniques of soil identification. In: *Proceedings of the Highway Research Board. National Research Council.* Washigton, DC **29**, 402–434.

Christoforou, E., Kylili, A., Fokaides, P.A. & Ioannou, I. 2016. Cradle-to-Site Life Cycle Assessment (LCA) of adobe bricks. *Journal of Cleaner Production* **112**, 443–452 (in Portuguese).

Cordeiro, C.C.M., Brandão, D.Q., Durante, L.C., Callejas, I.J.A. & Campos, C.A.B. 2020. Thermophysical characterization of lateritic soil for manufacturing rammed earth walls. *Matéria (Rio de Janeiro)* **25**(1) e-12564. doi: 10.1590/S1517-707620200001.0889

Danso, H., Martinson, B., Ali, M. & Williams, J. 2015. Effect of fibre aspect ratio on mechanical properties of soil building blocks. *Constr. Build. Mater*. **83**, 314–319. https://doi.org/10.1016/j.conbuildmat.2015.03.039

FAOSTAT (Food and Agriculture Organization of The United Nations). 2021. *Crops and livestock products.* Available on: https:// www.fao.org/faostat/en/#data/. Accessed in: 18 jan 2024.

Ferreira, G.M.G., Cecchin, D., De Azevedo, A.R.G., Valadão, I.C.R.P., Costa, K.A., Silva, T.R., Ferreira, F., Amaral, P.I.S., Huther, C.M. & Sousa, F.A. 2021. Bibliometric analysis on the use of natural fibers in construction materials. *Agronomy Research* **19**, 1–12. doi: 10.15159/AR.21.131

Ferreira, G.M.G., Cecchin, D., Valadão, I.C.R.P., da Silva, T.R., do Carmo, D.d.F., Moll Hüther, C., Ferreira, F. & de Azevedo, A.R.G. 2022. Evaluation of the Technological Properties of Soil–Cement Bricks with Incorporation of Coconut Fiber Powder. *Eng*. **3**(3), 311–324. https://doi.org/10.3390/eng3030023

Ghavami, K., Toledo Filho, R.D. & Barbosa, N.P. 1999. Behaviour of composite soil reinforced with natural fibres. *Cement and Concrete Composites* **21**(1), 39–48. doi: 10.1016/S0958-9465(98)00033-X

Jalali, S. & Eires, R. 2008. *Scientific Innovations in Earthen Construction. In: Internacional Conference-Angola: Teaching, Research and Development* (EIDAO 080), 7. (in Portuguese).

Lertwattanaruk, P. & Suntijitto, A. 2015. Properties of natural fiber cement materials containing coconut coir and oil palm fibers for residential building applications. *Constr. Build. Mater*. **94**, 664–669. doi: 10.1016/j.conbuildmat.2015.07.154

Li, V.C.A. 1992. Simplified micromechanical model of compressive strength of fiber-reinforced cementitious composites. *Cement and Concrete Composites* **14**(2), 131–141. doi: 10.1016/0958-9465(92)90006-H

Mendonça, Y.G.S. 2018. *Micromechanical Dosage of Cementitious Composites Reinforced With Jute Fibers*. Master's Thesis, Federal University of Rio de Janeiro, Rio de Janeiro, Brazil, 120 pp. (in Portuguese).

Naaman, A.E., Adce, M., Namur, G.C., Alwan, J.M. & Najm, H. 1991. Fiber pullout and bond slip. I: Analytical study. *Journal of structural engineering* **11**(9), 2769–2790.

Nunes, J.V.S., da Silva, E.X.B., Miranda, M.H.P., Rios, A.S. & de Deus, E.P. 2022. Mechanical and Morphological Characterization of Surface-Treated Coconut Fibers for Use as Reinforcement in Polymers. *Matéria* **27**(2). doi: 10.1590/1517-7076-RMAT-2022-0046 (in Portuguese).

Pereira, T.V.C., Fidelis, M.E.A., Gomes, O.F.M., Silva, F.A. & Toledo Filho, R.D. 2012. Investigation of Morphological Influence via Image Analysis on the Tensile Strength of Natural Fibers. In: *Congresso Anual da ABM*, ABM WEEK-67, Rio de Janeiro, Brasil, pp. 31–03. (in Portuguese).

Pinto, B.R. 2021. *Thermal and mechanical performance of alkaline activated adobe masonry reinforced with sisal fiber*. Master's Thesis, Federal University of Paraíba, Paraíba, Brazil 146 pp. (in Portuguese).

Pinto, B.R. 2021. *Thermal and mechanical performance of alkaline activated adobe masonry reinforced with sisal fiber*. Master's Thesis, Federal University of Paraíba, Paraíba, Brazil 146 pp. (in Portuguese).

Rocha, H.A., Azevedo, A.R.G., Marvila, M.T., Cecchin, D., Xavier, G.C., Silva, R.C., Ferraz, P.F.P., Conti, L. & Rossi, G. 2021. Influence of different methods of treating natural açai fibre for mortar in rural construction *Agronomy Research* **19**(S1), 910–921. doi: 10.15159/AR.21.062

Rodríguez-Mariscal, J.D. & Solís, M. 2020. Towards a methodology fort the experimental characterization of the compressive behaior of adobe masory. *Informes de la Construcción* **72**(557). doi: 10.3989/ic.67456 (in Spanish).

Santos, D.P. & Lima Bessa, S.A. 2020. The Use of Adobe in Brazil: A Literature Review. *MIX Sustentável* **6**(1), 53–66 (in Portuguese).

Silva, R.W.G.da. 2022. *Correlations for Preliminary Identification of Optimum Moisture Content of Brazilian Soils*. Trabalho de Conclusão de Curso. Universidade Federal do Rio Grande do Norte, 18 pp. (in Portuguese).

Agronomy Research **22**(S3), 1517–1530, 2024
https://doi.org/10.15159/AR.24.085

Metabolite profiling, terpenoid and kaurenoic acid production of *Adenostemma platyphyllum* at different concentrations of hydroponic solutions in the wick system

A.H.N. Tamsin[1], R. Nurfalah[1], Trivadila[2], I. Batubara[2,3,*], M. Rafi[2,3], T. Ridwan[3], S.A. Aziz[3,4], and H. Takemori[5]

[1]IPB University, Faculty of Mathematics and Natural Sciences, Departement of Chemistry, ID16680 Bogor, West Java, Indonesia
[2]IPB University, Faculty of Mathematics and Natural Sciences, Graduate Program of Chemistry, ID16680, Bogor, West Java, Indonesia
[3]IPB University, Tropical Biopharmaca Research Center, 16680 Bogor, West Java, Indonesia
[4]IPB University, Faculty of Agriculture, Department of Agronomy and Horticulture, ID16680 Bogor, West Java, Indonesia
[5]Gifu University, Faculty of Engineering, Department of Chemistry and Biomolecular Science, JP501-1193 Gifu, Japan
[*]Correspondence: ime@apps.ipb.ac.id

Received: March 9th, 2024; Accepted: June 27th, 2024; Published: August 29th, 2024

Abstract. *Adenostemma platyphyllum*, a medicinal plant belonging to the Asteraceae family, has gained increasing attention due to its potential as a source of bioactive compounds with diverse therapeutic properties but has not been widely cultivated. This work aims to obtain the optimum concentration of AB-mix solution to produce higher terpenoid and kaurenoic acid, as well as metabolite profiling in cultivating *A. platyphyllum* using a hydroponic wick system. This research uses a one-factor randomized block design of different concentrations of AB-mix nutrient solutions. Total terpenoids were quantified using the UV-Vis spectrophotometric method, total kaurenoic acid was determined using a high-performance liquid chromatography (HPLC) method, and the metabolite profiling was analyzed using a liquid chromatography-tandem mass spectrometry (LC-MS/MS) instrument. Several terpenoid compounds have been identified in *A. platyphyllum*, including Ent-17-Oxo-15-kauren-19-oic acid, andrographolide, cafestol, alpha-Farnesene, curcumene, as well as ent-11α-hydroxy-15-oxo-kaur-16-en-19-oic acid (11αOH-KA) and 11α,15-dihydroxy-16-kauren-19-oic acid (11α,15OH-KA), which belong to the kaurenoic acid group. The plants had the highest total terpenoid and kaurenoic acid found in 1,300 mg L^{-1} nutrient concentrations. On the other hand, the highest terpenoid and kaurenoic acid productivity were found in plants with 900 and 1,300 mg L^{-1} AB-mix solution, respectively. Therefore, the optimum concentration of nutrient solution to produce optimum terpenoid and kaurenoic acid levels in *A. platyphyllum* cultivation by hydroponic wick system was 1,300 mg L^{-1}.

Key words: *Adenostemma platyphyllum*; hydroponic; kaurenoic acid; plant growth; total terpenoid.

INTRODUCTION

Adenostemma genus, a plant of the Asteraceae family, has received much attention due to its traditional and widespread use in herbal medicine. *A. platyphyllum* from this genus contains diverse bioactive compounds associated with therapeutic properties, such as terpenoids (Fauzan et al., 2018). A large and diverse natural product derived part of isoprene, like terpenoids, is known for its various biological activities, including anti-inflammatory, anti-melanogenic, and antioxidant properties (Bisht et al., 2021). Apart from this, the agricultural potential of this genus needs to be explored and studied further.

Kaurenoic acids, a type of diterpenoid, are a group of compounds found in *A. lavenia*, another species from the *Adenostemma* genus. This compound is responsible for 50% of the anti-melanogenic activity in the extract (Hamamoto et al., 2020). On the other hand, there is no investigation of the total terpenoid and kaurenoic acid levels in *A. platyphyllum* species. Understanding the total terpenoid of *A. platyphyllum* is crucial for clarifying the chemical basis of its therapeutic effects and exploring its potential as an herbal medicine.

To conduct a comprehensive analysis of plant content, a substantial sample size is necessary. However, the *A. platyphyllum* species remains uncultivated and thrives in its natural habitat within tropical regions. Therefore, a cultivation method is needed to produce plants with high levels of secondary metabolite, for example hydroponic method. Cultivating plants using hydroponic systems has demonstrated efficiency and sustainability in enhancing plant biomass and boosting secondary metabolite production (Majid et al., 2021).

In hydroponic systems, the composition of the AB-mix nutrient solution plays a vital role in plant growth (Ghatage et al., 2019) and the synthesizing of the phytochemicals responsible for the medicinal properties (Bulawa et al., 2022). According to a study conducted by Attarzadeh et al. (2020), it was found that the utilization of hydroponic systems with nutrient solutions rich in elements like phosphorus demonstrated the potential to enhance the synthesis of secondary metabolites in plants belonging to the Asteraceae family. This research aims to comprehensively examine the effect of different concentrations of the AB-mix solution in a hydroponic wick system on the growth parameters and phytochemical production of *A. platyphyllum*.

MATERIALS AND METHODS

Experimental material: The experiment was carried out from December 2021 to January 2022 in the greenhouse of the Faculty of Agriculture, IPB University, Bogor, Indonesia. The study area lies at -6°55’ 10.8” S, 106°71’ 57.6” E, 159 m above sea level. Seeds of *A. platyphyllum* were collected from forests in Karanganyar, Pekalongan, Indonesia. The plants' identification was conducted by curators affiliated with the Bandungen Herbarium (FIPIA) at the SITH ITB (Nurlela et al., 2022). Specimens verifying the plants were deposited at the Bandungense Herbarium (FIPIA) at SITH ITB, assigned with collection numbers FIPIA-DEP35, FIPIA-DEP36, and FIPIA-DEP37. The stem cutting of *A. platyphyllum* was transferred into a rock wool medium and cultitaved with wick system of hydroponic method that are generally passive aerated system.

Treatments: In this study, a one-factor randomized block design was employed, focusing on different concentrations of AB mix fertilizer. The five AB-mix concentrations were replicated three times (in three groups: group 1, group 2, and group 3), resulting in 15 experimental units. Each experimental unit comprised five hydroponic containers, totaling 75 containers. Within each container, nine plants were grown, resulting in a total of 675 *A. platyphyllum* plants across all treatments. The concentration of AB-mix fertilizer was set in 5 concentrations of 0, 700, 900, 1,100, and 1,300 mg L^{-1}. The fertilizer used as the nutrient solution is AB mix fertilizer manufactured by CV. Agrifam. The environmental conditions in the greenhouse have a 14% UV plastic roof, a 50-mesh insect net, and a 50% shaded net.

Preparation of AB-mix Nutrient Solution

The nutrient solution is prepared by dissolving separate stocks of A and B, both produced by CV. Agrifam. Each stock, weighing 500 g, is dissolved in 5 L of water to create concentrated solutions. Subsequently, these concentrated stocks A and B are combined. The resulting nutrient solution is then poured into plastic tubs, with each tub containing a water volume of 7 L.

Observation of Plant Growth

The plants were harvested six weeks after applying treatment at each concentration. During the cultivation period, non-destructive observations were also made, including the leaf and branch number and plant height at once-a-week intervals. Destructive observations included determining leaf area, relative growth rate (RGR), net assimilation rate (NAR), and chlorophyll content. RGR calculation refers to Saharuddin et al. (2018), based on the dry weight of plants per unit time based on the following formula :

$$\text{RGR (g week}^{-1}) = 1\ W\ X\ \Delta W\ \Delta t = \ln W2 - \ln W1\ t2\text{-}t1 \quad (1)$$

where W1: ln dry weight of plants at observation 1; W2: ln dry weight of plants at observation 2; t1: observation time 1; t2: observation time 2.

NAR calculations refer to those carried out by Saharuddin et al. (2018), based on dry weight and plant area per unit time using the following formula:

$$\text{NAR (g cm}^{-2}\text{week}^{-1}) = 1\ A\ X\ \Delta W\ \Delta t = \ln A2 - \ln A1\ A2\text{-}A1\ X\ \ln W2 - \ln W1\ t2\text{-}t1 \quad (2)$$

where W1: ln plant dry weight at observation 1; W2: ln plant dry weight at observation 2; t1: observation time 1; t2: observation time 2; A1: ln leaf area 1; A2: ln leaf area 2.

Sample Preparation

Subsequently, after harvested the leaves were dried, and their wet and dry weights were measured. Finally, the dried leaves were ground using a blender. A 1 g sample of the powder was extracted with 7 mL of methanol using a Sartorius shaker for one hour. The resulting mixture was then filtered through Whatman filter paper number 93. The residue underwent two additional solvent extractions until the solvent volume reached 20 mL. To determine the moisture content of *A. platyphyllum*, the gravimetric method was employed, specifically following the guidelines outlined in AOAC 2012, chapter 4, item 4.1.06, method 930.15.

Determination of Total Terpenoid Content

Determination of chlorophyll content was carried out referring to Sims and Gamon (2003) by weighing 0.02 g of fresh sample, at that point putting the sample in a mortar and including 1 mL of acetone, then grinding until homogeneous. The homogenized sample was transferred into a 2 mL microtube, then the mortar and pestle were washed with acetone solution and after that the wash water was included into the microtube until the volume was full. The sample within the microtube was then isolated using centrifugation at a speed of 18.845 g for 10 seconds. The isolated supernatant was then transferred 1 mL into a test tube and after that homogenized until the precipitate disappeared. The samples were then analyzed using a UV-Vis spectrophotometer at wavelengths of 537, 647 and 663 nm. The equation for deciding chlorophyll content is appeared within the condition below. The coefficients contained within the equation are decided based on the particular retention coefficients recorded in Lichtenthaler (1987).

Determination of Total Terpenoid Content

According to Łukowski et al. (2022), a total of 0.2 g of A. platyphyllum leaf simplicia was combined with 2.8 mL of cold methanol. The mixture was then macerated for 48 hours at low temperature and subsequently centrifuged at 4,000 g for 15 minutes. The resulting supernatant was filtered and transferred to a test tube. Next, 1.5 mL of chloroform and 100 µL of H_2SO was added. The absorbance was analyzed by UV-Vis spectrophotometer at a wavelength of 520 nm. The total terpenoid content was determined based on the standard nerol curve ($y = 0.1817x + 0.0249$; $R^2 = 0.9912$). Terpenoid productivity (mmol nerol plant^{-1}) is determined by multiplying the total terpenoid concentration, mmol nerol equivalent/g dry weight units (mmol NE g^{-1} DW), by the dry weight of the plants at harvest (g plant^{-1}). Average mass of a plant and the dry matter content, as results are given (g plant^{-1}) based on previous research (Tamsin, et al., 2023).

Determination of Kaurenoic Acid Content

Determination of kaurenoic acid content by high-performance liquid chromatography (HPLC) refers to the method used by Hamamoto et al. (2020). A 10 mg sample of the extract was combined with 1,000 µL of 50% methanol. After homogenization for 1 hour, the mixture underwent centrifugation at 14,500 g for 5 minutes. The resulting supernatant was transferred to a microtube, from which 10 µL was drawn using a syringe and injected into the HPLC injector port. The column specifications included a C18 ODS column (4.6 mm × 50 mm: RP-18 GP, Kanto Kagaku, Tokyo, Japan) with acid A solvent (0.1% formate in distilled water) and solvent B (100% acetonitrile). The gradient elution profile consisted of 10% solvent B at 0.0–0.1 minutes, followed by 10.0–35.0% at 1.0–7.0 minutes, 35.0% – 47.5% solvent B at 7.0–10.0 minutes, and 47.5% – 100% solvent B at 10.0–12.0 minutes. The system was then maintained at 100% solvent B for an additional 5 minutes. Detection of the 11αOH-KA compound occurred via UV absorption at a wavelength of 245 nm. The concentration of the 11αOH-KA compound in A. platyphyllum was determined using a standard curve based on 11αOH-KA isolated from A. lavenia plant ($y = 3953.2x + 64465$; $R^2 = 0.9982$). Kaurenoic acid productivity (mmol/plant) is determined by multiplying the total kaurenoic acid concentration (mmol g^{-1} DW) by the dry weight of the plants at harvest (g plant^{-1}).

Metabolite Profiling with LC-MS/MS

Metabolite profiling from methanol extract of *A. platyphyllum* leaves prepared before was investigated through UHPLC Vanquish Tandem Q Exactive Plus Orbitrap HRMS ThermoScientific system according to Rafi et al. (2020), with Accucore™ Vanquish C18 column (100×2.1 mm, 1.5 µm) was used for separation. The positive scan mode of an MS ES (electrospray ionization) was used to acquire accurate masses in the 200−1,500 m/z range. The injection volume used was 2 µL with a flow rate of 0.2 mL min^{-1} and a column temperature of 30 °C. The gradient separation used 0.1% formic acid in H_2O (phase A) and 0.1% formic acid in acetonitrile (phase B) as a mobile phase. The eluent composition was 5% phase B at 0–1 min, 90-5% phase A, and 10–95% phase B at 1–17 min, 100% phase B at 17–18.5 min, and 5% B at 18.5 min. Three sample replicates were blank-corrected.

The UHPLC-Q-Orbitrap HRMS analysis involved several additional conditions. Fragmentation was achieved using collision energies of 18, 35, and 53 eV. The spray voltage was set at approximately 3.9 kV, and the capillary temperature was maintained at 320 °C. Sheath gas and auxiliary gas flow rates were set to 15 and 3 mL min^{-1}, respectively. We used scan type full MS/dd MS^2 for positive ion mode. The potential identification of detected metabolites in *A. platyphyllum* extracts was made by analyzing the mass spectrum obtained from UHPLC-Q-Orbitrap HRMS. The data was processed using Compound Discoverer version 2.2. Furthermore, the obtained MS/MS spectra were subjected to another compound identification and characterization by utilizing various databases, including PubChem, ChemSpider, HMDB (Human Metabolome Database), and CFM-ID (Compound Fragmentation Mass Spectrometry Identification).

Statistical analysis

The data were subjected to an ANOVA test. Duncan's multiple range test (DMRT) was used for mean separation. Data were analyzed using SAS on Demand for academic programs. LC-MS/MS data were processed using Thermo Scientific Xcalibur software. Afterward, Origin software was employed to generate chromatograms and perform data visualization.

RESULTS

Plant Growth

The growth observations were carried out 1 to 6 weeks after planting (WAP). Parameters observed during the study were plant height (Fig. 1, a), leaf number (Fig. 1, b), branch number (Fig. 1, c), and leaf area (Fig. 1, d), aimed to know a plant's response during the cultivation period to the treatment applied. Increasing the concentration of the hydroponic nutrient solution in *A. platyphyllum* plants tends to improve their growth. AB-mi concentrations significantly increased the plant height, branch number, leaf number, and leaf area.

The growth of *A. platyphyllum* plants without adding AB-mix nutrient solution did not increase every week, resulting in significantly lower plant height, leaf number, branch number, and leaf area. In contrast, the growth of plants with concentrations of 700, 900, 1,100, and 1,300 mg L^{-1} AB-mix increased constantly. However, there was no significant difference between the four treatments on growth parameters at the end of the cultivation period.

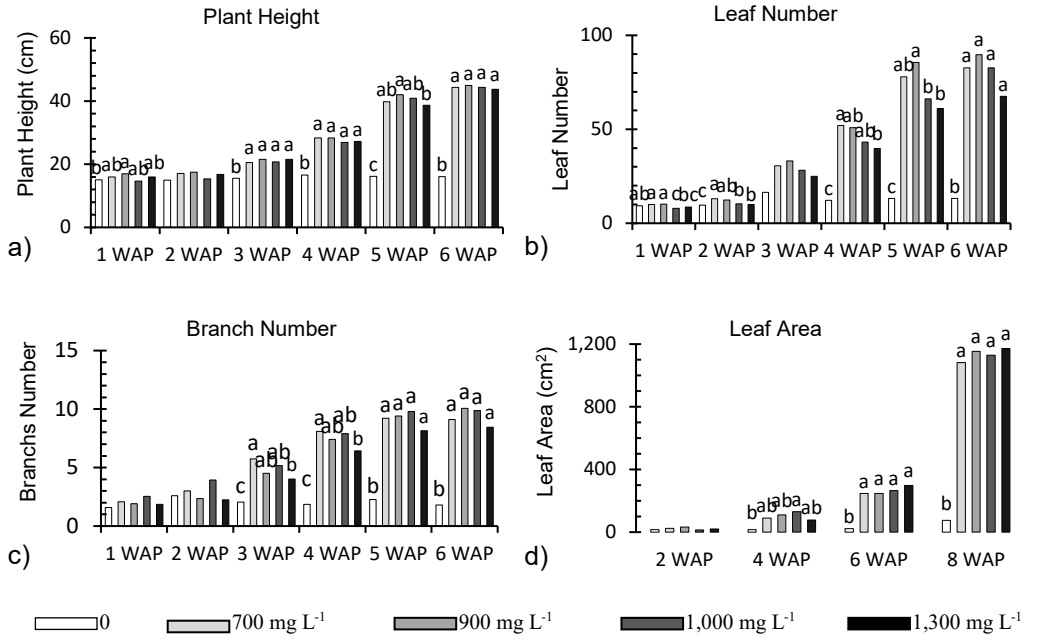

Figure 1. Plant height (a); leaf number (b); branch number (c); and leaf area (d) of *A. platyphyllum*. Different bar charts followed by different letters are significantly different based on DMRT 5%

Relative Growth Rate

The relative growth rate (RGR) or the relative increase in plant biomass per unit of time from *A. platyphyllum* is illustrated in Table 1. Comparing RGR values between treatments allows for identifying factors influencing plant growth. Based on plant growth observation, different concentrations of AB-mix solution did not significantly affect *A. platyphyllum* RGR.

Table 1. The relative growth rate of *A. platyphyllum*

Treatment	Relative Growth Rate ± SD (g $g^{-1}day^{-1}$)		
	Weeks 2 & 4	Weeks 4 & 6	Weeks 6 & 8
0	0.0118 ± 0.0095^{b}	0.0235 ± 0.0149	0.0653 ± 0.0349
700	0.0806 ± 0.0699^{ab}	0.0220 ± 0.0149	0.1128 ± 0.0066
900	0.0793 ± 0.0581^{ab}	0.0258 ± 0.0174	0.1308 ± 0.0748
1,100	0.1278 ± 0.0617^{a}	0.0425 ± 0.0136	0.1170 ± 0.0331
1,300	0.0311 ± 0.0197^{b}	0.0516 ± 0.0538	0.1039 ± 0.0894

Different numbers followed by letters differ significantly with DMRT 5%.

Net Assimilation Rate

In contrast to RGR, the net assimilation rate (NAR) measures plants' photosynthetic ability to produce dry matter (biomass). Based on the data shown in Table 2, the net assimilation rate of *A. platyphyllum* at 6−8 WAP, the plant experienced a significant difference.

Table 2. Net assimilation rate of *A. platyphyllum*

Treatment	Net Assimilation Rate ± SD (g cm^{-2} day^{-1})		
	Weeks 2 & 4	Weeks 4 & 6	Weeks 6 & 8
0	0.0002 ± 0.0001^{b}	0.0003 ± 0.0002	0.0007 ± 0.0002^{a}
700	0.0006 ± 0.0005^{ab}	0.0001 ± 0.0001	0.0004 ± 0.0001^{b}
900	0.0005 ± 0.0004^{ab}	0.0001 ± 0.0001	0.0005 ± 0.0003^{ab}
1,100	0.0009 ± 0.0005^{a}	0.0002 ± 0.0001	0.0005 ± 0.0002^{ab}
1,300	0.0004 ± 0.0003^{ab}	0.0003 ± 0.0004	0.0004 ± 0.0004^{b}

Different numbers followed by letters differ significantly with DMRT 5%.

Chlorophyll Content

The chlorophyll content obtained from the *A. platyphyllum* plant is shown in Table 3, the highest value was obtained from the *A. platyphyllum* with 1,100 mg L^{-1} AB-mix solution. Meanwhile, plants treated with concentrations of 700, 900, and 1,300 mg L^{-1} did not significantly differ. On the other hand, plants without AB-mix solution produced the lowest chlorophyll content.

Table 3. Chrolophyll content of *A. platyphyllum*

Treatment	Chrolophyll a ± SD (µmol cm^{-2})	Chrolophyll b ± SD (µmol cm^{-2})	Total Chrolophyll ± SD (µmol cm^{-2})
0	0.0055 ± 0.00087^{c}	0.0025 ± 0.00039^{c}	0.008 ± 0.00131^{c}
700	0.0079 ± 0.00043^{b}	0.0036 ± 0.00019^{b}	0.0114 ± 0.00048^{b}
900	0.0087 ± 0.0004^{ab}	0.0039 ± 0.00018^{ab}	0.0126 ± 0.0002^{ab}
1,100	0.0094 ± 0.00085^{a}	0.0042 ± 0.00038^{a}	0.0136 ± 0.00094^{a}
1,300	0.0084 ± 0.00073^{ab}	0.0034 ± 0.00032^{ab}	0.0123 ± 0.00032^{ab}

Different numbers followed by letters differ significantly with DMRT 5%.

Total Terpenoid Concentration and Productivity

A. platyphyllum without AB-mix solution treatment resulted in a significant minimum total terpenoid concentration, 3.46 mmol NE g^{-1} DW (Fig. 2, a). Total terpenoids increased significantly with increased AB-mix concentration. The highest total terpenoid concentration was found in plants with 1,300 mg L^{-1} of AB-mix treatment (9.65 mmol NE g^{-1} DW). Moreover, the highest terpenoid productivity was found in plants treated with 900 mg L^{-1} AB-Mix solution (24.38 mmol NE $plant^{-1}$).

Total Kaurenoic Acid Concentration and Productivity

The total kaurenoic acid contained in *A. platyphyllum* was significantly affected by the concentration of the AB-mix nutrient solution (Fig. 2, b). The results of the analysis using the HPLC instrument stated that AB-mix concentration of 1,300 mg L^{-1} produced the highest total kaurenoic acid and kaurenoid acid productivity in *A. platyphyllum,* 2.74 mM g^{-1} DW and 5.91 mM $plant^{-1}$ respectively. On the other hand, plants without AB-mix solution generate the lowest total kaurenoid acid and productivity, 1.85 mM g^{-1} DW and 0.46 mM $plant^{-1}$, respectively.

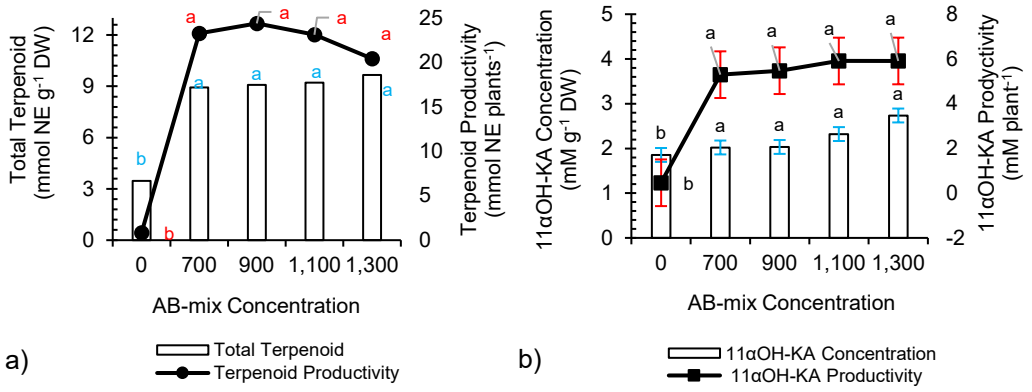

Figure 2. Total terpenoid and terpenoid productivity (a); Total kaurenoic acid and kaurenoic acid productivity (b) of *A. platyphyllum.* Different bar/line charts followed by different letters are significantly different based on DMRT 5%.

Metabolite Analysis by LC-MS/MS

A total of 17 metabolites from six prominent compounds were putatively identified (Table 3) in the treatment methanol extract of *A platyphyllum* using UHPLC-Q-Orbitrap-HRMS (Fig. 3, a). A cluster analysis was conducted on the metabolites identified in *A. platyphyllum*. The results were visualized using a heatmap format (Fig. 3, b).

DISCUSSION

Plant growth observations are crucial for understanding plant development and assessing crop performance. Plant growth can be explained as increased plant volume and mass, with or without constructing new structures such as organs, tissues, cells, and organelles. Growth is usually associated with development and reproduction (Brukhin & Morozova, 2011). Observations of plant growth provide valuable insights into plant strength, biomass accumulation, and productivity.

According to Wang et al. (2020), nitrogen in the AB-mix nutrient solution is a factor affecting plant height, which is required in large quantities for plant growth because it functions in the formation of cells, tissues, and plant organs. In addition, nitrogen also plays a role in various metabolic processes, including photosynthesis, that trigger vegetative growth. Increasing the available nitrogen will produce large amounts of protein, so plant tissue growth will also increase. A lack of nitrogen elements will inhibit plant growth because it cannot form cells or tissues (Jiaying et al., 2022), causing the plant height of *A. platyphyllum* at a concentration of 0 mg L^{-1} to become stunted.

Another parameter of plant growth is relative growth rate (RGR) and net assimilation rate (NAR). RGR measures a plant's average growth rate over time by quantifying the increase in plant biomass per unit of time (Rajput, 2017). Determining the RGR provides insight into resource utilization efficiency, overall growth potential, and the impact of different processing and environmental conditions. The RGR during the 2−4-week period after planting exhibited a statistically significant variation, primarily attributed to the ongoing adaptive responses of plants to the environmental conditions.

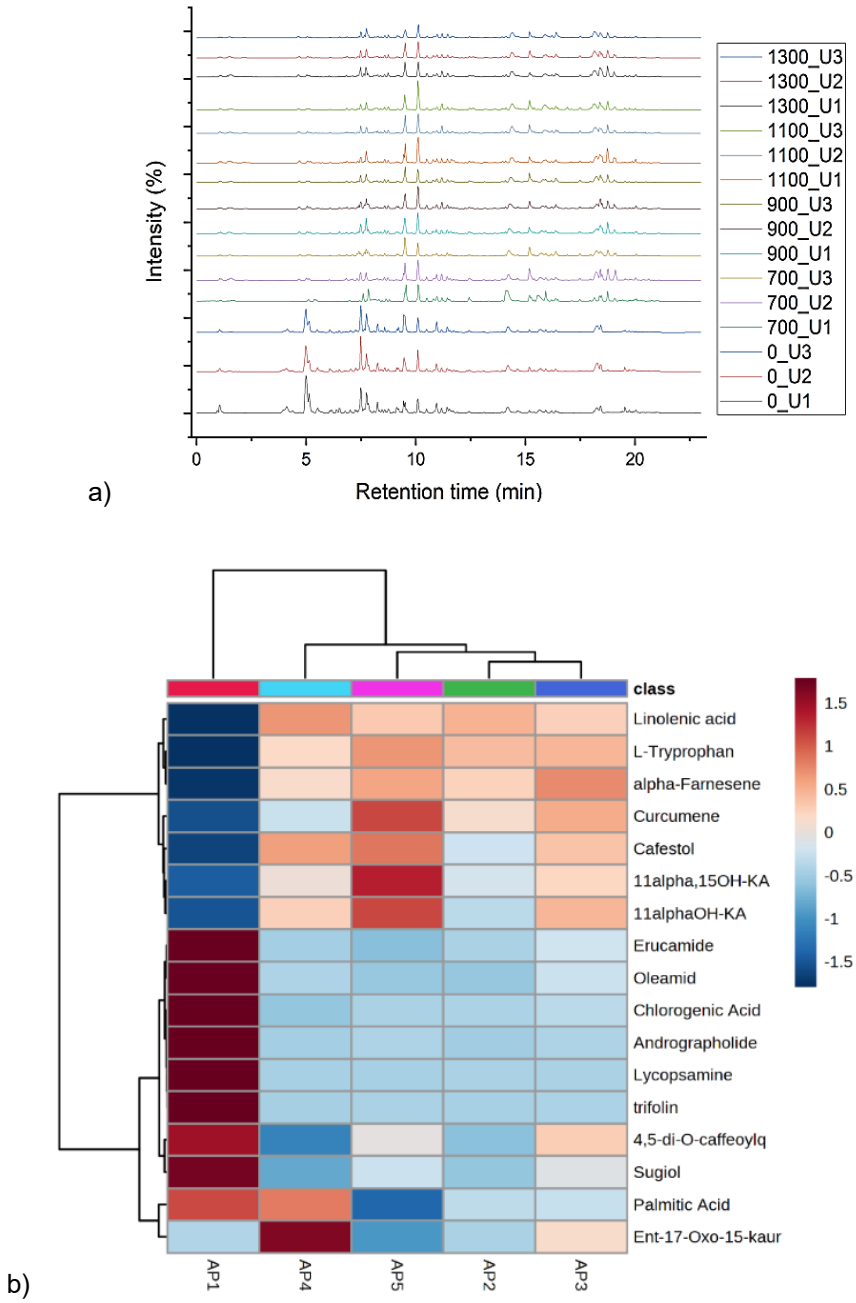

Figure 3. The base peak of the LC-MS/MS chromatogram in the positive ionization mode of *A. platyphyllum* (a); Heatmap analysis of identified compound in *A. platyphyllum* (b). K0 is 0 mg L^{-1}, K1 is 700 mg L^{-1}, K2 is 900 mg L^{-1}, K3 is 1,100 mg L^{-1}, and K4 is 1,300 mg L^{-1}.

The environmental adaptation process induces stunted growth in plants (Li et al., 2021), manifested by a wilted appearance and reduced turgidity in their morphological characteristics. Moreover, during 4−6 WAP and 6−8 WAP, the growth of *A. platyphyllum* exhibited a recovery phase, with the relative growth rate showing an upward trend compared to the preceding weeks. However, the analysis of variance revealed no significant influence of varying concentrations of AB mix fertilizer on the RGR values during the 4−6 and 6−8 WAP time intervals.

The NAR value expresses how plants convert assimilated carbon into new biomass (Safitri et al., 2018). The NAR exhibited significant variations between 2−4 and 6−8 weeks after planting, indicating dynamic physiological responses. Conversely, at the 4−6 weeks marker, the NAR values showed no significant distinctions, implying comparable photosynthetic capacities across the five treatments assessed. Statistical analyses revealed that plants without AB-mix solution exhibited significantly higher NAR values than the 700 and 1,300 mg L^{-1} treatments.

Notably, leaf area is among the influential factors affecting NAR, wherein plants with broader leaves typically exhibit higher NAR due to increased photosynthetic surface area and subsequent biomass production (Lewar & Hasan, 2022). However, an inverse relationship between leaf area and NAR was observed in the 700 and 1,300 mg L^{-1} treatments, whereby a higher leaf area resulted in reduced NAR and could be attributed to shading effects caused by lush leaves, hindering efficient photosynthesis in the shaded portions of leaves (Safitri et al., 2018).

Chlorophyll content determination in plant leaves is crucial in evaluating photosynthetic efficiency and plant health. Chlorophyll content in plants can be influenced by various factors, including intrinsic factors, which pertain to plant-specific characteristics, and extrinsic factors, which refer to environmental influences (Li et al., 2018). One factor that influences chlorophyll content is nutrient availability.

Plants without AB-mix solution exhibit nutrient deficiency, resulting in an insufficient energy supply to support growth and photosynthesis. Nitrogen is an essential component of the chlorophyll molecule, especially in the form of the magnesium porphyrin complex (Borah & Bhuyan, 2017). The presence of sufficient nitrogen promotes chlorophyll synthesis and increases chlorophyll content. Limited nitrogen levels can limit chlorophyll production, lower chlorophyll levels, and cause chlorosis or leaf yellowing (Sakuraba, 2022).

Determining phytochemicals, like total terpenoid and kaurenoic acid content in *A. platyphyllum*, is essential in evaluating the plant's potential medicinal and pharmacological properties. One factor that affects the production of phytochemical content is nutrient availability. Plants treated with AB-mix solution tended to have higher total terpenoids caused by several mechanisms. The availability of adequate nutrients, particularly nitrogen (N), phosphorus (P), and potassium (K), provides the necessary for plants' building blocks (Xu et al., 2020) and energy for secondary metabolite biosynthesis, as well as terpenoid synthesis.

These macronutrients are essential to biosynthesis precursors, enzymes, coenzymes, and energy carriers. For example, sufficient phosphorus promotes some precursors for terpenoid production. The terpenoid precursors IPP (isopentenyl diphosphate), DMAPP (dimethylallyl pyrophosphate), GDP (geranyl diphosphate), and FDP (farnesyl diphosphate) possess high-energy phosphate bonds. In addition, phosphorus is part of ATP and NADPH molecules needed for terpenoid synthesis via the mevalonate (MVA)

and methylerythritol phosphate (MEP) pathways, hence phosphorus may be an essential element for terpenoid biosynthesis (Bustamante et al., 2020).

A. platyphyllum, a wild species, has been introduced into cultivation for the production of terpenoids. Research conducted on cultivated sunflower (*Helianthus annuus*) has indicated significant compositional diversity of volatiles among the studied lines of *H. annuus*. This diversity includes a notable reduction in the total abundance of volatiles compared to wild *H. annuus* (Bahmani et al., 2023). The findings of this study suggest that the possibility of volatile terpenoids diversity for breeding the *A. platyphyllum*.

One of the terpenoid compounds found in *Adenostemma* is kaurenoic acid. Previous studies by Maeda et al. (2022) have reported the presence of at least three different types of kaurenoic acid in *A. lavenia,* namely ent-11α-hydroxy-15-oxo-kaur-16-en-19-oic acid (11αOH-KA), 9,11α-dehydroxy-15-oxo-kauren-16-en-19-oic acid (9,11αOH-KA), and 11α,15-dihydroxy-16-kauren-19-oic acid (11α,15OH-KA). Additionally, Batubara et al. (2020) have researched *A. lavenia* and highlighted that the terpenoid compound 11αOH-KA, successfully extracted from this plant, exhibits significant biological activities such as antitumor, anti-melanogenesis, and anti-inflammatory effects. This compound belongs to the diterpenoid classification, which has four repeated isoprene units, as described by (Hamamoto et al., 2020).

Plant secondary metabolite productivity refers to the capacity of plants to produce and accumulate secondary metabolites. The quantification of secondary metabolite productivity can be assessed by multiplying the biomass of the harvested plants with the total concentrations or levels of the secondary metabolite (Abbasi et al., 2019). Plants without AB mix nutrient solution exhibited the lowest terpenoid and kaurenoic acid productivity due to their significantly lower biomass.

Insufficient nutrient availability negatively impacts plant biomass, leading to reduced terpenoid production. The observed low secondary metabolite productivity reflects the poor ability of plants to synthesize secondary metabolites due to suboptimal nutrition conditions (Bahmani et al., 2020). In contrast, the four other treatments demonstrated comparable productivity levels for total terpenoids and kaurenoic acid. Statistical analysis indicated no significant differences among these treatments, demonstrating similar performance in secondary metabolite production.

The chemical content from the methanol extract of *A. platyphyllum* analyzed using UHPLC-Q-Orbitrap-HRMS resulted in 17 compounds. These metabolites were identified based on their mass spectra and fragmentation patterns that belonged to various compound groups, specifically, the primary metabolite represented by L-tryptophan, which belonged to the amino acid group. The fatty acid group was represented by four compounds, erucamide, oleamide, palmitic acid, and α-Linolenic acid. The secondary metabolites belonging to the alkaloid group were represented by lycopsamine. The flavonoid group was expressed by trifolin, and the phenolic group included chlorogenic acid, 4,5-O-caffeoylquinic acid, and sugiol.

Additionally, seven metabolites were identified from the terpenoid group, represented by ent-17-Oxo-15-kauren-19-oic acid, 11αOH-KA, 11α,15OH-KA, andrographolide, cafestol, α-farnesene, and curcumene. The dominant compounds in *A. platyphyllum* were phenolic compounds, originated lipids (fatty acid), and terpenoids, as reported by Fauzan et al. (2018). Furthermore, the comprehensive metabolite profiling verified the high total terpenoid content in *A. platyphyllum*, confirming numerous

compounds derived from the terpenoid group found in the *A. platyphyllum* plant. This concurrence between the quantitative analysis and secondary metabolite profile reinforces the rich terpenoid diversity within the *A. platyphyllum* plant.

Hierarchical cluster analysis visually represents the variations in metabolite content among *A. platyphyllum*, which is cultivated using different concentrations of AB-mix solution types through a heatmap. Upon the heatmap pattern displayed in Figure 3, the color intensity corresponding to secondary metabolites derived from the terpenoid group, present in *A. platyphyllum* treated with the AB-mix solution (AP2, AP3, AP4, and AP5), exhibited a significant increase compared to the plants without AB-mix solution (AP1). Specifically, the color pattern exhibited by the *A. platyphyllum* plant treated with a concentration of 1,300 mg L^{-1} AB-mix resulted in the highest intensity of red color for the metabolites 11αOH-KA and 11α,15OH-KA, which both belonged to the kaurenoic acid group. These findings corroborate the results obtained from the HPLC analysis, which demonstrated that *A. platyphyllum* treated with a 1,300 mg L^{-1} AB-mix solution displayed the highest total kaurenoic acid content.

CONCLUSION

A. platyphyllum possesses various beneficial properties and bioactive compounds. The plant has been found to contain metabolites from diverse classes, including flavonoids, phenolics, and terpenoids. The highest terpenoid and kaurenoic acid productivity were found in plants with 900 and 1,300 mg L^{-1} AB-mix solution, respectively. Secondary metabolite compounds from the kaurenoic acid group were identified in *A. platyphyllum*, namely 11αOH-KA and 11α,15OH-KA, which have a wide range of biological activities and have potential, especially in the health and pharmaceutical industries.

ACKNOWLEDGMENTS. This research received support from the bilateral exchange program of the Directorate General of Higher Education and the Japan Society for Promoting Science under the joint research project with reference number 023.17.1.690439/2022.

REFERENCES

Abbasi, B.H., Siddiquah, A., Tungmunnithum, D., Bose, S., Younas, M., Garros, L., Drouet, S., Giglioli-Guivarc'h, N. & Hano, C. 2019. Isodon rugosus (Wall. ex Benth.) codd in vitro cultures: Establishment, phytochemical characterization and in vitro antioxidant and anti-aging activities. *Int J Mol Sci*. **20**(452), 1–22. doi:10.3390/ijms20020452

Attarzadeh, M., Balouchi, H., Rajaie, M., Dehnavi, M.M.,& Salehi, A. 2020. Improving growth and phenolic compounds of Echinacea purpurea root by integrating biological and chemical resources of phosphorus under water deficit stress. *Ind Crops Prod*. **154**(April), 1–13. doi:10.1016/j.indcrop.2020.112763

Bahmani, K., Giguere, M., Dowell, J.A. & Mason, C.M. 2023. Germplasm diversity of sunflower volatile terpenoid profiles across vegetative and reproductive organs. *Agronomy Research* **21**(1), 4–27. https://doi.org/10.15159/AR.22.084

Bahmani, M., Jalilian, A., Salimikia, I., Shahsavari, S. & Abbasi, N. 2020. Phytochemical screening of two Ilam native plants *Ziziphus nummularia* (Burm.f.) Wight & Arn. and Ziziphus spina-christi (Mill.) Georgi using HS-SPME and GC-MS spectroscopy. *Plant Sci. Today*. **7**(2), 275–280. doi:10.14719/pst.2020.7.2.714

Batubara, I., Astuti, R.I., Prastya, M.E., Ilmiawati, A., Maeda, M., Suzuki, M., Hamamoto, A. & Takemori, H. 2020. The anti-aging effect of active fractions and ent-11α-hydroxy-15-oxo-kaur-16-en-19-oic acid isolated from Adenostemma lavenia (L.) O. Kuntze at the cellular level. *Antioxidants* **9**(8), 1–14. doi:10.3390/antiox9080719

Bisht, B.S., Bankoti, H. & Bharti, T. 2021. A review on therapeutic uses of terpenoids. *J Drug Deliv Ther*. **11**(1), 182–185. doi:10.22270/jddt.v11i1-s.4523

Borah, K.D. & Bhuyan, J. 2017. Magnesium porphyrins with relevance to chlorophylls. *Dalt Trans*. **46**(20), 6497–6509. doi:10.1039/c7dt00823f

Brukhin, V. & Morozova, N. 2011. Plant growth and development - Basic knowledge and current views. *Math Model Nat Phenom*. **6**(2), 1–53. doi:10.1051/mmnp/20116201

Bulawa, B., Sogoni, A., Jimoh, M.O. & Laubscher, C.P. 2022. Potassium Application Enhanced Plant Growth, mineral Composition, Proximate and Phytochemical Content in Trachyandra divaricata Kunth (Sandkool). *Plants*. **11**(22). doi:10.3390/plants11223183

Bustamante, M.Á., Michelozzi, M., Caracciolo, A.B., Grenni, P., Verbokkem, J., Geerdink, P., Safi, C. & Nogues, I. 2020. Effects of soil fertilization on terpenoids and other carbon-based secondary metabolites in Rosmarinus officinalis plants: a comparative study. *Plants* **9**(7), 1–19. doi:10.3390/plants9070830

Fauzan, A., Praseptiangga, D., Hartanto, R. & Pujiasmanto, B. 2018. Characterization of the chemical composition of *Adenostemma lavenia* (L.) Kuntze and *Adenostemma platyphyllum* Cass. *IOP Conf Ser Earth Environ Sci*. **102**(1). doi:10.1088/1755-1315/102/1/012029

Ghatage, S.M., Done, S.R., Akhtar, S., Jadhav, S. & Havaragi, R. 2019. A hydroponic system for indoor plant growth. *Int Res J Eng Technol*. **6**(6), 1279–1286.

Hamamoto, A., Isogai, R., Maeda, M., Hayazaki, M., Horiyama, E., Takashima, S., Koketsu, M. & Takemori, H. 2020. The high content of ent- 11 α -hydroxy-15-oxo-kaur-16-en-19-oic acid in Adenostemma lavenia (L.) O. Kuntze leaf extract: with preliminary in vivo assays. *J. Foods* **9**(73), 1–12. doi:10.3390/foods9010073

Jiaying, M., Tingting, C., Jie, L., Weimeng, F., Baohua, F., Guangyan, L., Hubo, L., Juncai, L., Zhihai, W., Longxing & T. & Guanfu, L. 2022. Functions of Nitrogen, Phosphorus, and Potassium in Energy Status and Their Influences on Rice Growth and Development. *Rice Sci*. **29**(2), 166–178. doi:10.1016/j.rsci.2022.01.005

Lewar, Y. & Hasan, A. 2022. Total leaf area, net assimilation rate, and chlorophyll of red bean leaves of inerie varieties due to application of biological fertilizer (in Indonesian). *Seminar Nasional Politani Kupang Ke-5*, pp. 274–280.

Li, G., Hu, S., Zhao, X., Kumar, S., Li, Y., Yang, J. & Hou, H. 2021. Mechanisms of the Morphological Plasticity Induced by Phytohormones and the Environment in Plants. *International Journal of Molecular Sciences*. https://doi.org/10.3390/ijms22020765

Li, Y., He, N., Hou, J., Xu, L., Liu, C., Zhang, J., Wang, Q., Zhang, X. & Wu, X. 2018. Factors influencing leaf chlorophyll content in natural forests at the biome scale. *Front Ecol Evol*. **6**(64), 1–10. doi:10.3389/fevo.2018.00064

Łukowski, A., Jagiełło, R., Robakowski, P., Adamczyk, D. & Karolewski, P. 2022. Adaptation of a simple method to determine the total terpenoid content in needles of coniferous trees. *Plant Sci*. **314**(2022), 111090. doi:10.1016/j.plantsci.2021.111090

Maeda, M., Suzuki, M., Fuchino, H., Tanaka, N., Kobayashi, T., Isogai, R., Batubara, I., Iswantini, D., Matsuno, M. & Kawahara, N., Koketsu, M., Hamamoto, A. & Takemori, H. 2022. Diversity of Adenostemma lavenia, multi-potential herbs, and its kaurenoic acid composition between Japan and Taiwan. *J Nat Med*. **76**(1), 132–143. doi:10.1007/s11418-021-01565-3

Majid, M, Khan, J.N., Shah, Q.M.A., Masoodi, K.Z., Afroza, B. & Parvaze, S. 2021. Evaluation of hydroponic systems for the cultivation of Lettuce (Lactuca sativa L., var. Longifolia) and comparison with protected soil-based cultivation. *Agric Water Manag*. **245**(2021), 1–13. doi:10.1016/j.agwat.2020.106572

Nurlela, N., Nurfalah, R., Ananda, F., Ridwan, T., Ilmiawati, A., Nurcholis, W., Takemori, H. & Batubara, I. 2022. Variation of morphological characteristics, a total phenolic, and total flavonoid in Adenostemma lavenia, A. madurense, and A. platyphyllum. *Biodiversitas*. **23**(8), 3999–4005. doi:10.13057/biodiv/d230818

Rafi, M., Karomah, A.H., Heryanto, R., Septaningsih, D.A., Kusuma, W.A., Amran, M.B., Rohman, A. & Prajogo, B. 2020. Metabolite profiling of Andrographis paniculata leaves and stem extract using UHPLC-Orbitrap-MS/MS. *Nat Prod Res*. 1–5. doi:10.1080/14786419.2020.1789637

Rajput, A., Rajput, S.S. & Jha, G. 2017. Physiological Parameters Leaf Area Index, Crop Growth Rate, Relative Growth Rate, and Net Assimilation Rate of Different Varieties of Rice Grown Under Different Planting Geometries and Depths in SRI. *Int. J. Pure App. Biosci*. **5**(1), 362-367. doi: 10.18782/2320-7051.2472

Safitri, R., Fuskhah, E. & Karno, K. 2018. Characteristics of photosynthesis and production of soybeans (Glycine max L. Merrill) due to different salinity of watering water (in Indonesian). *J. Agro Complex* **2**(3), 244–247. doi:10.14710/joac.2.3.244-247

Sakuraba, Y. 2022. Molecular basis of nitrogen starvation-induced leaf senescence. *Front Plant Sci*. 13 September:1–15. doi:10.3389/fpls.2022.1013304

Tamsin, A.H.N., Batubara, I., Ridwan, T., Trivadila, Aziz, S.A. 2023. Phenolic and flavonoid production, phytochemical profile, and antioxidant capacity of *Adenostemma platyphyllum* at different concentrations of hydroponic solutions. *Jurnal Tumbuhan Obat Indonesia*. **16**(1), 59-70. doi: 10.31002/jtoi.v16i1.552

Wang, L., Yang, L., Xiong, F., Nie ,X., Li, C., Xiao, Y. & Zhou, G. 2020. Nitrogen fertilizer levels affect the growth and quality parameters of Astragalus mongolica. *Molecules* **25**(2), 1–14. doi:10.3390/molecules25020381

Xu, X., Du, X., Wang, F., Sha, J., Chen, Q., Tian, G., Zhu, Z., Ge, S. & Jiang, Y. 2020. Effects of potassium levels on plant growth, accumulation and distribution of carbon, and nitrate metabolism in apple dwarf rootstock seedlings. *Front Plant Sci*. **11** June:1–13. doi:10.3389/fpls.2020.00904

Agronomy Research **22**(S3), 1531–1542, 2024
https://doi.org/10.15159/AR.24.053

Effect of fermented purple sweet potato flour on physiological conditions and intestinal conditions of broiler chickens

E. Widiastuti, D. Febrianti, H.I. Wahyuni, T. Yudiarti, I. Agusetyaningsih, R. Murwani, T.A. Sartono and S. Sugiharto*

Department of Animal Science, Faculty of Animal and Agricultural Sciences, Universitas Diponegoro, Semarang, 50275 Central Java, Indonesia
*Correspondence: sgh_undip@yahoo.co.id

Received: March 29th, 2024; Accepted: May 22nd, 2024; Published: June 14th, 2024

Abstract. The study investigated the effect of fermented purple sweet potato flour (PSPF) on intestinal and physiological health of broilers. A 189-day-old broiler chicks were divided into T0 (diet based on corn and soybean meal), T1 (diet containing 15% unfermented PSPF), and T2 (diet containing 15% fermented PSPF). Samples collection and measurement were conducted at day 35. The T2 chicks had greater ($p < 0.05$) weight gain than T1, but did not differ from T0. Feed conversion ratio (FCR) was better ($p < 0.05$) in T2 than in T1. The mean corpuscular haemoglobin (MCH) and mean corpuscular haemoglobin concentration (MCHC) were higher ($P < 0.05$) in T2 than in T0 and T1 groups. Haemoglobin tended ($p = 0.08$) to be lower in in T2 than in T0 and T1 groups. Heterophils were higher ($p = 0.05$) in T2 than in T0 and T1 groups. Total cholesterol and high-density lipoprotein (HDL) were higher ($p < 0.05$) in T0 than in T1. Low-density lipoprotein (LDL) tended ($p = 0.06$) to be lower in T1 than that in T0. Total protein and globulin were higher ($p < 0.05$) in T0 than that in T1 and T2. Lactic acid bacteria (LAB) to coliform ratio in the ileum was higher ($p < 0.05$) in T2 than in T0. LAB counts tended ($p = 0.08$) to be greater in T2 than in other chickens. T1 tended ($p = 0.09$) to have a smaller number of lactose negative *Enterobacteriaceae* (LNE) in caecum as compared to that of T0 chicks. T2 tended ($p = 0.09$) to have a lower crypt depth than T0. In conclusion, feeding fermented purple sweet potato flour contributes for the better growth, feed conversion, immune defence, bacterial population and morphology of the small intestine.

Key words: bacteria, broilers, energy source, fermentation, immune response, intestine.

INTRODUCTION

Corn is the main energy source for poultry and contributes more than 70% of the energy needs of poultry (Sultana et al., 2016). The demand for corn increases every year along with the increase in the poultry population. To reduce the use of corn in feed formulations, several attempts have been made by broiler producers, one of which is by using alternative energy source feed ingredients. Despite their widespread availability, using alternative feed ingredients is often challenging due to their low nutritional quality and the presence of anti-nutritional compounds in the ingredients (Helda et al., 2021). Owing to these circumstances, specific processing techniques are required to raise the

nutritional value of these substitute feed ingredients. Fermentation is a commonly employed technique to enhance nutritional value and reduce the amount of anti-nutritional substances present in feed ingredients. Its application is relatively simple and cheap (Sugiharto & Ranjitkar, 2019). Apart from having an impact on improving nutrition, fermentation is also reported to increase the bioactive components in feed ingredients (Sugiharto & Ranjitkar, 2019). Furthermore, according to Sugiharto et al. (2018a), fermentation can raise functional value, which benefits broiler chickens' physiological state and general health.

One alternative feed stuff that can be used as an energy source for broiler chickens and also as a functional feed ingredient is purple sweet potato. Purple sweet potatoes have a relatively high carbohydrate content of 75–90%, which suggests that they could be utilized as an alternative feed ingredient to provide broilers with energy sources (Dapawisi et al., 2022). According to Kusuma et al. (2016), purple sweet potatoes are rich in vitamins, β-carotene and anthocyanins. Indeed, purple sweet potato also shows high antioxidant activity. The antioxidant properties in purple sweet potatoes is beneficial for health because it can ward off free radicals, oxidation in the body and clumping of blood cells. Natural antioxidants in purple sweet potatoes have the advantage of low molecular weight which is effective in suppressing reactive oxygen species (ROS) and preventing oxidative damage to biomolecules. With regard particularly to anthocyanins, because anthocyanins possess antibacterial properties, they can inhibit the growth of harmful bacteria, which in turn encourages the production of mucus by intestinal microbes and improves the digestibility of nutrients (Edi et al., 2018). The high level of carbohydrates in purple sweet potato is inversely proportional to the level of crude protein. Crude protein in purple sweet potatoes is only around 3.2% (Hartadi et al., 2005). Purple sweet potatoes also have anti-nutritional components, one of which is trypsin inhibitor, which can inhibit the work of the trypsin enzyme thereby reducing the level of protein utilization by broiler chickens (Anbuselvi & Muthumani, 2014).

Among the fermentation starters that are often used for the fermentation process is *Saccharomyces cerevisiae* (Nurhayati et al., 2019). *S. cerevisiae* is a yeast that is able to utilize sugar for its growth. *S. cerevisiae* as a fermentation starter is reported to increase protein content and also reduce crude fibre content. In this case, *S. cerevisiae* produces enzymes that can degrade complex carbohydrates into simpler carbohydrates (Kusuma, 2016). Apart from its potential as a fermenter, *Saccharomyces* is utilized extensively as a probiotic, potentially improving the well-being and productivity of chickens (Sugiharto, 2016). Based on the capabilities of this yeast, it was expected that using *S. cerevisiae* as a fermenter for feed ingredients would improve the nutritional quality of the feed ingredients while also serving as a probiotic for poultry. In this study, *S. cerevisiae* was used to ferment purple sweet potato flour. Overall, the demand for corn as the primary energy source in broiler chicken feed continues to rise, and it is frequently unmet because corn production remains unstable throughout the year. Such conditions therefore necessitate efforts to find alternative energy sources other than corn without compromising broiler chicken productivity and health. The scientific purpose of the present study was to look into how fermented purple sweet potato flour affected the intestinal and physiological health of broiler chickens. From the practical broiler production point of view, the present study aimed to find alternative energy source feed ingredients, to reduce the proportion of corn in the feed, for broiler chickens.

MATERIALS AND METHODS

Production of the fermented sweet potatoes

Purple sweet potatoes were purchased from farmers around Semarang, Central Java, Indonesia. Making purple sweet potato flour begun with washing and separating the rotten parts of the sweet potato. Purple sweet potatoes were cut into small pieces, then dried in the sun until dry. The dried purple sweet potato is then ground using a disk mill, then sifted to get purple sweet potato flour. Making fermented purple sweet potato flour begins with sterilizing the purple sweet potato flour using an autoclave at 121 °C for 15 minutes. Next, the sterilized flour was added with yeast containing 6.6×10^8 cfu/g of *S. cerevisiae* (5.5 g of yeast added for every 1 kg of purple sweet potato flour). Then purple sweet potato flour was mixed with water in a ratio of 1:2. In this study, considering that purple sweet potato flour has a high water absorption capacity (ability to absorb and retain water), more water was needed so that the fermentation process could take place optimally through solid state fermentation. Fermentation was carried out in the bucket aerobically for 2 hours at room temperature (~25 °C). Fermentation was halted when alcohol-like smell started to emerge. Fermented purple sweet potato flour was then sun-dried (at the temperature of ~34 °C) until dry (about 2 hours). After drying, a proximate analysis was carried out to determine the nutritional content of the material.

Broiler experiment

The broiler experiment was conducted to met animal welfare principles as approved by Animal Ethics Committee of the Faculty of Animal and Agricultural Sciences, Universitas Diponegoro (No. 59-07d/A-16/KEP-FPP). In total, 189-day-old broiler chicks from the Cobb strain were used in this investigation. Using rice husk as litter, they were raised in an open-sided (naturally ventilated) broiler house for the entire of the rearing process. To manually regulate the temperature and humidity inside the broiler house, plastic curtains, light bulbs, and fans were used. The temperature was kept at 28–30 °C, and the humidity at 80–85%. During the study, the chickens were given light 24 hours a day. The birds, weighing 45.85 ± 3.04 g at arrival, were fed commercial pre-starter feed for seven days. The birds, weighing 142.17 ± 0.34 g, were divided into experimental treatment groups at random starting on day 8. From day 8 to day 21, the birds were fed formulated starter feed (Table 1), and from day 22 to day 35, they were fed finisher feed (Table 2). For the duration of the rearing process, food and water were given freely using round bottom feeder and manual drinker. With three treatment groups and seven replicates (each containing nine chicks), the dietary treatments were set up in a completely randomized manner. From day 8 to 35, the following treatments were given to the chicks: T0 (a diet based on corn and soybean meal), T1 (a diet containing 15% unfermented purple sweet potato flour), and T2 (a diet containing 15% fermented purple sweet potato flour). The chicks were raised in compliance with the Cobb broiler strain rearing guidelines. Using eye drops (day 4) and drinking water (day 18), the chicks received the Newcastle disease vaccination. On day 12, a drinkable vaccine against infectious bursal disease was also administered.

Both the total amount of feed consumed and the body weight were noted. To determine the feed conversion ratio (FCR) value, the ratio of accumulative feed intake (g) to total body weight gain (g)was computed. At the end of experiment, one male chick (in order to prevent gender bias), representing the average body weight of each experimental unit, was chosen to have blood withdrawn from the brachial vein. To produce serum, 3 mL of blood were placed in a non-ethylenediaminetetraacetic acid (EDTA) tube and 1 mL of blood was placed in an EDTA tube for routine blood testing. The same chicks as blood sampled were slaughtered. As soon as the chicken was slaughtered, its intestines were removed. Segments of the duodenum, jejunum, and ileum (about 2 cm) were placed in 10% buffered formalin (Leica Biosystems Richmond, Inc., Richmond, USA) in order to measure the morphology of the small intestine (villus height and crypt depth). After being placed in each sterile sample pot, the ileum and cecum digesta were examined further in the lab to determine the population of particular bacteria present in the intestine.

Table 1. Feed ingredients and nutritional compositions of broilers (day 8–21)

Ingredients (%)	T0	T1	T2
Yellow corn	53.5	36.2	36.4
Palm oil	2.32	2.39	2.55
Soybean meal	40.13	42.36	42.0
DL-methionine	0.19	0.19	0.19
Bentonite	0.75	0.75	0.75
Limestone	1.00	1.00	1.00
Monocalcium phosphate	1.30	1.30	1.30
Premix[1]	0.34	0.34	0.34
Chlorine chloride	0.07	0.07	0.07
Salt	0.40	0.40	0.40
Purple sweet potato flour	-	15.0	-
Fermented purple sweet potato flour	-	-	15.0
Nutritional compositions:			
ME[2] (kcal kg^{-1})	2,900	2,900	2,900
Crude protein	22.0	22.0	22.0
Crude fibre	5.47	4.56	4.75
Ca	1.14	1.09	1.09
P (available)	0.57	0.50	0.50

[1]The following nutrients are provided per kilogram of feed: 1,100 mg Zn, 1,000 mg Mn, 75 mg Cu, 850 mg Fe, 4 mg Se, 19 mg I, 6 mg Co, 1,225 mg K, 1,225 mg Mg, 1,250,000 IU vitamin A, 250,000 IU vitamin D_3, 1,350 g pantothenic acid, 1,875 g vitamin E, 250 g vitamin K_3, 250 g vitamin B_1, 750 g vitamin B_2, 500 g vitamin B_6, 2,500 mg vitamin B_{12}, 5,000 g niacin, 125 g folic acid and 2,500 mg biotin.

[2]ME (metabolizable energy) was calculated according to formula: 40.81 {0.87 (crude protein + 2.25 crude fat + nitrogen-free extract) + 2.5}.

T0: chicks were provided with corn-soybean meal-based diet, T1: chicks were provided with diet containing 15% unfermented purple sweet potato flour, T2: chicks were provided with diet containing 15% fermented purple sweet potato flour.

Laboratory analyses

The routine blood profile tests of the chicks were determined automatically by means of a Hematology Analyzer (Prima Fully-auto Hematology Analyzer, PT. Prima Alkesindo Nusantara, Jakarta, Indonesia) based on the manufacturer's instructions (Sapsuha et al., 2022). Serum lipid profiles (total triglycerides, total cholesterol, low-density lipoprotein [LDL], and high-density lipoprotein [HDL]) and creatinine and uric acid levels were measured using enzyme-based colorimetric techniques. Serum total protein and albumin levels were determined using spectrophotometric and photometric methods. To calculate the globulin concentration, the serum albumin value was

subtracted from the total protein value. All biochemical analyses of serum samples were performed in accordance with the manufacturer's instructions (DiaSys Diagnostic System GmbH, Holzheim, Germany).

Small intestinal segments were histologically examined using 5 µm sections of the ileum, jejunum, or duodenum stained with haematoxylin and eosin. The villous height and crypt depth in each segment were measured with an optical microscope equipped with a digital camera (Leica Microsystems GmbH, Wetzlar, Germany). Five measurements were used to determine the mean values of villous height and crypt depth for each sample. The bacterial population in the ileal and caecal contents was determined according to the total plate count method. After a 24-hour aerobic incubation at 38 °C, coliforms and lactose-negative *Enterobacteriaceae* (LNE) were counted as red and colourless colonies on MacConkey agar (Merck KGaA, Darmstadt, Germany). Lactic acid bacteria (LAB) were counted on de Man, Rogosa, and Sharpe (MRS; Merck KGaA) agar after a 48-hour anaerobic incubation period at 38 °C.

Table 2. Feed ingredients and nutritional compositions of broilers (day 22–35)

Ingredients (%)	T0	T1	T2
Yellow corn	61.74	44.49	44.6
Palm oil	2.41	2.46	2.63
Soybean meal	31.8	34.0	33.72
DL-methionine	0.19	0.19	0.19
Bentonite	0.75	0.75	0.75
Limestone	1.00	1.00	1.00
Monocalcium phosphate	1.30	1.30	1.30
Premix[1]	0.34	0.34	0.34
Chlorine chloride	0.07	0.07	0.07
Salt	0.40	0.40	0.40
Purple sweet potato flour	-	15.0	-
Fermented purple sweet potato flour	-	-	15.0
Nutritional compositions:			
ME[2] (kcal kg^{-1})	3,000	3,000	3,000
Crude protein	19.0	19.0	19.0
Crude fibre	5.57	4.67	4.85
Ca	1.12	1.07	1.07
P (available)	0.59	0.51	0.51

[1]The following nutrients are provided per kilogram of feed: 1,100 mg Zn, 1,000 mg Mn, 75 mg Cu, 850 mg Fe, 4 mg Se, 19 mg I, 6 mg Co, 1,225 mg K, 1,225 mg Mg, 1,250,000 IU vitamin A, 250,000 IU vitamin D_3, 1,350 g pantothenic acid, 1,875 g vitamin E, 250 g vitamin K_3, 250 g vitamin B_1, 750 g vitamin B_2, 500 g vitamin B_6, 2,500 mg vitamin B_{12}, 5,000 g niacin, 125 g folic acid and 2,500 mg biotin.

[2]ME (metabolizable energy) was calculated according to formula: 40.81 {0.87 (crude protein + 2.25 crude fat + nitrogen-free extract) + 2.5}.

T0: chicks were provided with corn-soybean meal-based diet, T1: chicks were provided with diet containing 15% unfermented purple sweet potato flour, T2: chicks were provided with diet containing 15% fermented purple sweet potato flour.

Statistical analyses

To evaluate the data gathered for the study, analysis of variance (ANOVA, SPSS version 16.0) was employed. Duncan'smultiple analysis was conducted when a significant effect ($p < 0.05$) was observed from the treatments. The implementation of tendency occurred when $0.05 \leq p < 0.10$.

RESULTS AND DISCUSSION

Chemical composition and antioxidant activity of non- and fermented purple sweet potato flour are presented in Table 3. The concentrations of crude protein, crude fibre, crude fat and crude ash increased with fermentation using *S. cerevisiae*. There was a

decline in antioxidant activity following fermentation. Typically, fermentation is identical with increasing the nutritional value of feed ingredients (Sugiharto & Ranjitkar, 2019). In line with the latter study, the fermentation carried out increased the crude protein, crude fat and crude ash content in purple sweet potato flour in this study. With protein, crude fat and crude ash content in purple sweet potato flour in this study. With respect to the crude fibre, fermentation using *S. cerevisiae* increased the crude fibre content of the purple sweet potato flour. In contrast, Sugiharto & Ranjitkar (2019) have confirmed that fermentation reduces the amount of crude fibre in feed ingredients. However, our results were consistent with that of Sugiharto et al. (2018a), who found that the fermentation of herbal medicine waste with *Bacillus* bacteria increased its fibre content. They also proposed that the breakdown of complex carbohydrates (polysaccharides) into simpler fibre (oligosaccharides), which led to an increase in crude fibre content and a decrease in carbohydrate content, was the cause of the increased fibre content in the fermented ingredients. In term of antioxidant activity, our finding showed that *S. cerevisiae*-fermentation reduced antioxidant activity of sweet potato flour. In agreement, Sugiharto et al. (2018b) noted the reduced antioxidant activity of the herbal medicine waste with *Bacillus subtilis.* One possible explanation for this situation could be the breakdown of phenolic compounds that occurs during fermentation. In fact, during the fermentation process, phenolics are reactive compounds that can be destroyed by enzymatic and/or non-enzymatic reactions (Sugiharto et al., 2018b).

Table 3. Chemical compositions and antioxidant activity of purple sweet potato flour*

Chemical compositions	Purple sweet potato flour	Fermented purple sweet potato flour
Crude protein (%)	2.55	3.43
Crude fibre (%)	0.60	1.89
Crude fat (%)	1.20	1.39
Crude ash (%)	3.89	4.98
Antioxidant activity (% inhibition)	1.55	0.27

*Analyses were conducted in duplicate, and not statistically analysed.

Fig. 1 shows the weight gain, feed intake and FCR of broilers. It was apparent that T2 chicks had greater ($p < 0.05$) weight gain than the chicks in T1 groups, but did not differ from those in T0 group. FCR was better ($p < 0.05$) in T2 than in T1, but did not vary from that of T0 chicks. There was no substantial effect of dietary treatments on feed intake of broilers. There were no dead or sick chickens found during this present study. The use of purple sweet potato flour, whether fermented or not, was intended to reduce the proportion of corn as an energy source for broiler chickens. In this study, the use of either fermented or non-fermented purple sweet potato flour had no detrimental effects on the broiler chickens' feed intake, weight gain, and FCR during the rearing phase. An interesting finding was seen in this research, in which broiler chickens that were fed fermented purple sweet potato flour had better weight gain and FCR than those that were fed non-fermented purple sweet potato flour. Hence, the benefits of fermentation for maximizing the use of purple sweet potato flour by broiler chickens can be confirmed by these data. As mentioned above, fermentation can improve the nutritional content of purple sweet potato flour. In this respect, improving the nutrient content may increase nutrient availability and chicken growth. Apart from improving nutrition, fermentation of purple sweet potato flour using *S. cerevisiae* could be associated with the use of probiotics in broiler feeds, which has an impact on improving intestinal health and

chicken function. Indeed, *S. cerevisiae* is one of the probiotic microbes that is reported to improve the growth performance of broiler chickens (Sugiharto, 2016). In particular, when it came to feed intake, feeding birds purple sweet potato flour or fermented purple sweet potato flour tended to reduce their feed consumption, even though the difference was not statistically significant. Our results were consistent with those of Maphosa et al. (2003), who observed a drop in broiler feed consumption when fed sweet potato flour because the sweet potato was not well-palatable or well-accepted by the broiler chickens.

The values of MCH and MCHC were higher ($p < 0.05$) in T2 than in T0 and T1 groups, while there was a tendency ($p = 0.08$) that haemoglobin values were lower in in T2 than in T0 and T1 groups. Moreover, there was a strong tendency ($p = 0.05$) that heterophils were higher in T2 than in T0 and T1 groups. The data on complete blood counts are listed in Table 4. Data in the current study showed that the chicks that received fermented purple sweet potato flour had lower MCH and MCHC values than the control group and chicks that received non-fermented purple sweet potato flour. The haemoglobin value was also lower in the fermented purple sweet potato flour group than in the purple sweet potato flour and control groups, which is consistent with these two parameters. According to earlier studies conducted by Pratama et al. (2022), feeding broiler chickens fermented wheat bran reduced the amount of MCH and haemoglobin in the chickens. They suggested that the decline in the risk of infection in chickens fed fermented ingredients was closely related to the decline in haemoglobin and MCH levels.

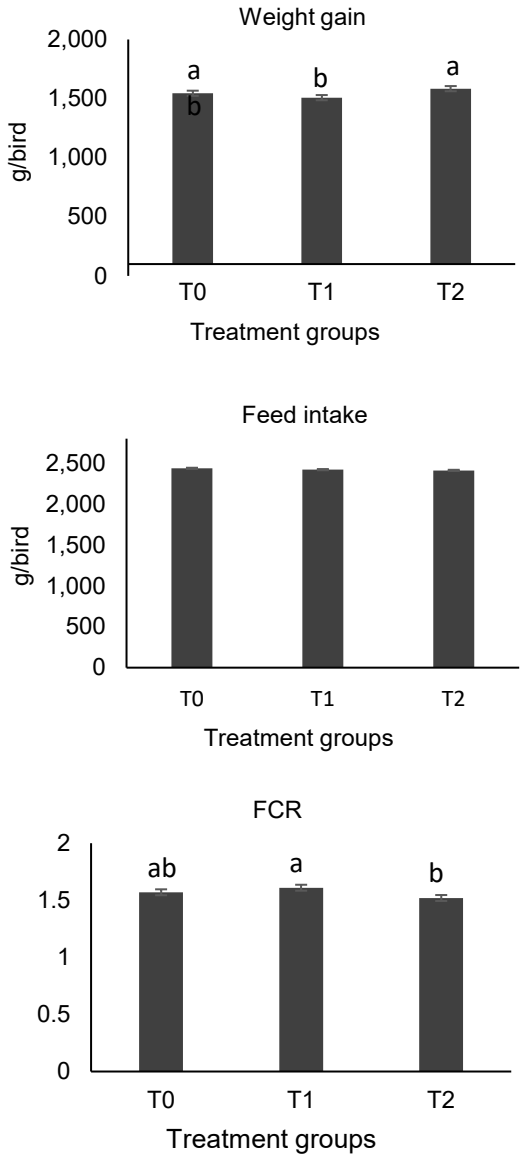

Figure 1. Weight gain, feed intake and FCR of broiler chickens.

[a,b]Means with divergent superscripts among the column differ significantly ($p < 0.05$). T0: chicks were provided with corn-soybean meal-based diet; T1: chicks were provided with diet containing 15% unfermented purple sweet potato flour; T2: chicks were provided with diet containing 15% fermented purple sweet potato flour; FCR: feed conversion ratio.

Haemoglobin typically functions as a transporter of oxygen used for energy metabolism. In many cases, infected chickens require more energy for recovery, so they have higher numbers of haemoglobin and MCH to transport the oxygen supplied to the cells. In regard to the infection, the heterophils value was significantly higher in the fermented purple sweet potato flour group compared to the control group. Hidayah et al. (2021) revealed that the high value of heterophils has an effect on bolstering chicken immunity, reducing the risk of infection in broiler chickens. The mechanism by which fermented feed can improve the immune system in chickens has been discussed in detail by Sugiharto & Ranjitkar (2019). They explained that fermented feed can improve the composition of bacteria in the intestine so that it has a positive impact on the immune response of broiler chickens.

Table 4. Complete blood counts of broiler chickens

Items	T0	T1	T2	SE	*p* value
Erythrocytes (10^{12}/L)	1.66	1.65	1.54	0.04	0.51
Haemoglobin (g dL^{1})	6.63	6.77	5.74	0.20	0.08
Haematocrits (%)	28.4	28.2	26.4	0.80	0.56
MCV (fl)	172	171	172	1.45	0.94
MCH (pg)	39.9[a]	40.8[a]	36.9[b]	0.58	0.01
MCHC (g/dL)	22.7[a]	23.5[a]	21.2[b]	0.34	0.01
RDW-SD (10^{-15} L)	48.9	47.5	34.8	3.22	0.14
RDW-CV (%)	9.81	9.63	13.6	1.75	0.60
Leukocytes (10^{9}/L)	57.9	62.7	63.7	2.02	0.48
Heterophils (10^{9}/L)	1.34	2.11	4.23	0.51	0.05
Lymphocytes (10^{9}/L)	56.6	60.6	59.5	1.73	0.64
Thrombocytes (10^{9}/L)	84.7	87.6	64.4	9.35	0.57

[a,b]Means with divergent superscripts within the similar row differ significantly ($p < 0.05$).
T0: chicks were provided with corn-soybean meal-based diet; T1: chicks were provided with diet containing 15% unfermented purple sweet potato flour; T2: chicks were provided with diet containing 15% fermented purple sweet potato flour; MCV: mean corpuscular volume; MCH: mean corpuscular hemoglobin; MCHC: mean corpuscular hemoglobin concentration; RDW-SD: red cell distribution width standard deviation; RDW-CV: red cell distribution width coefficient variation, SE: standard error of the means.

The data on serum biochemistry of broiler chickens are presented in Table 5.

Table 5. Serum biochemistry of broiler chickens

Items	T0	T1	T2	SE	*p* value
Total cholesterol (mg dL^{-1})	109[a]	78.7[b]	96.1[ab]	5.18	0.04
Total triglyceride (mg dL^{-1})	85.9	80.1	78.2	6.53	0.89
LDL (mg dL^{-1})	17.7	7.20	13.9	1.88	0.06
HDL (mg dL^{-1})	74.6[a]	55.4[b]	66.7[ab]	2.90	0.01
Total protein (g dL^{-1})	2.19[a]	1.10[b]	1.15[b]	0.15	< 0.01
Albumin (g dL^{-1})	0.46	0.49	0.51	0.08	0.96
Globulin (g dL^{-1})	1.74[a]	0.61[b]	0.64[b]	0.18	0.01
Uric acid (mg dL^{-1})	7.92	5.32	6.37	0.52	0.12
Creatinine (mg dL^{-1})	0.33	0.67	0.77	0.21	0.70

[a,b]Means with divergent superscripts within the similar row differ significantly ($p < 0.05$).
T0: chicks were provided with corn-soybean meal-based diet; T1: chicks were provided with diet containing 15% unfermented purple sweet potato flour; T2: chicks were provided with diet containing 15% fermented purple sweet potato flour; LDL: low-density lipoprotein; HDL: high-density lipoprotein, SE: standard error of the means.

The levels of total cholesterol and HDL were higher ($p < 0.05$) in T0 when compared to that in T1, but was not different from T2 chicks. The level of LDL tended ($p = 0.06$) to be lower in T1 than that in T0. Total protein and globulin were higher ($p < 0.05$) in T0 than that in T1 and T2 chicks. In this study, total cholesterol, LDL and HDL values were lower in the group of chickens receiving non-fermented purple sweet potato flour compared to chickens that received control feed. However, significant differences were not found when compared with chickens that received fermented purple sweet potato flour. Various factors influence the cholesterol profile in the serum of broiler chickens, one of which is the antioxidant content in the feed. Shen et al. (2019) confirmed that antioxidant components such as flavonoids and polyphenols can influence metabolism thereby reducing cholesterol content of broiler chickens. Given that purple sweet potato flour has an antioxidant capacity, using it in this study was probably going to enhance that capacity and had an effect on lowering HDL, LDL, and cholesterol in broiler chicken serum. In this study, the chickens fed fermented purple sweet potato flour did not experience significant reductions in cholesterol, LDL, or HDL. As previously mentioned, the antioxidant capacity of purple sweet potato flour is decreased during the fermentation process using *S. cerevisiae*. Because of this, there is little discernible effect of fermented purple sweet potato flour on the cholesterol profile.

The use of purple sweet potato flour or fermented purple sweet potato flour had an impact on reducing total protein and globulin in broiler chicken serum. In this study, serum albumin levels were not affected by the dietary intervention applied during the study. Considering that the globulin value is the difference between total protein and albumin, the decrease in total protein in broiler chicken serum was very likely related to the decrease in globulin in broiler chicken serum. Globulin is a precursor for immunoglobulin which is responsible for the immunity of broiler chickens. As previously mentioned, the low risk of infection in chickens was very likely the reason for the low need for globulin for the production of immunoglobulins. In line with this inference, Wu et al. (2018) reported that the use of oridonin improved *Salmonella*-induced immune responses and reduced immunoglobulin concentrations (IgA and IgG) in the jejunum of broiler chickens.

Table 6. Selected bacteria count in the ileum and caecum of broiler chickens

Items	T0	T1	T2	SE	*p* value
Ileum (log cfu/g)					
LAB	2.38	2.77	4.00	0.31	0.08
Coliform	1.58	1.29	1.53	0.26	0.90
LNE	1.00	1.00	1.32	0.11	0.38
LAB/coliform	1.84[b]	2.25[ab]	3.42[a]	0.27	0.04
Caecum (log cfu/g)					
LAB	8.06	7.91	7.98	0.11	0.87
Coliform	5.11	4.39	4.52	0.14	0.10
LNE	2.80	1.33	2.03	0.28	0.09
LAB/coliform	1.59	1.83	1.82	0.06	0.26

[a,b]Means with divergent superscripts within the similar row differ significantly ($p < 0.05$).
T0: chicks were provided with corn-soybean meal-based diet; T1: chicks were provided with diet containing 15% unfermented purple sweet potato flour; T2: chicks were provided with diet containing 15% fermented purple sweet potato flour; LAB: lactic acid bacteria; LNE: lactose negative *Enterobacteriaceae*; SE: standard error of the means.

The LAB to coliform ratio in the ileum was higher ($p < 0.05$) in T2 than in T0, but did not significantly different from that in T1 chicks (Table 6). The counts of LAB tended ($p = 0.08$) to be greater in T2 than in other treatment groups of chickens. In the

caecum, the T1 chicks tended (p = 0.09) to have a smaller number of LNE as comparedto that of T0 chicks. When compared with the control feed, the use of fermented purple sweet potato flour in the feed significantly increased the population of LAB and the LAB to coliform ratio in the ileum of broiler chickens. These results were as expected, as according to Sugiharto & Ranjitkar (2019), fermented feed with a high organic acid content can support the growth of LAB in the small intestine of broilers. A higher LAB to coliform ratio was observed in the group of chickens fed feed containing fermented purple sweet potato flour due to the high number of LAB in those birds and the comparatively constant number of coliforms in those birds across treatment groups. In this study, it was alsoseen that there was a lower population of LNE in the cecum of broiler chickens that received non-fermented purple sweet potato flour compared to controls. The reason for the lower counts of LNE in the caecum of chickens given purple sweet potato flour remains unclear. However, the content of anthocyanins (possessing antibacterial properties) (Edi et al., 2018) in purple sweet potato flour may inhibit the growth of LNE in the caecum of broiler chickens.

Table 7 shows the morphology of the small intestine of broiler chickens. The group of chicks in T2 tended (p = 0.09) to have a lower crypt depth as compared particularly to the T0 group. The villi height, crypt depth as well as the ratio of villi height to crypt depth did not differ in the duodenum and jejunum of broiler chickens. In this study, it was observed that the use of fermented purple sweet potato flour in feed was associated with the reduced crypt depth, especially in the ileum of broilers. Study shows that crypt depth increases are considered to be a result of damage to epithelial cells lining the villi or increased epithelial cell turnover requiring replacement cells from the crypt to prevent loss of absorptive surface area (Cloft et al., 2023). Based on these conditions, it can be inferred that the use of fermented purple sweet potato flour may result in reduced potential for damage to epithelial cells in the ileum. In this context, the use of fermented purple sweet potato flour could improve the ecological conditions in the intestine, and hence the potential for damage to epithelial cells in the intestine can be minimized (Sugiharto & Ranjitkar, 2019). The latter inference was actually supported by the fact in this study that feeding fermented purple sweet potato flour enhanced the LAB countsand LAB to coliform ratio in the ileum of broilers.

Table 7. Intestinal villous height and crypt depth of broiler chickens

Items	T0	T1	T2	SE	p value
Duodenum					
VH (µm)	1,202	1,304	1,390	61.6	0.48
CD (µm)	221	251	223	8.45	0.28
VH/CD ratio	5.47	5.29	6.39	0.31	0.30
Jejunum					
VH (µm)	1,235	1,307	1,194	80.9	0.85
CD (µm)	255	242	281	11.8	0.40
VH/CD ratio	4.74	5.55	4.25	0.30	0.20
Ileum					
VH (µm)	752	748	676	30.7	0.54
CD (µm)	235	197	178	10.9	0.09
VH/CD ratio	3.31	3.89	3.93	0.19	0.35

T0: chicks were provided with corn-soybean meal-based diet; T1: chicks were provided with diet containing 15% unfermented purple sweet potato flour; T2: chicks were provided with diet containing 15% fermented purple sweet potato flour; VH: villous height; CD: crypt depth; SE: standard error of the means.

Purple sweet potatoes are now becoming increasingly popular as a human food due to their high nutritional value and functional properties (Dereje et al., 2020). This increases the economic value of purple sweet potatoes. Based on these conditions, apart from the positive influence of the fermented purple sweet potato on broiler health and productivity, the use of purple sweet potato or fermented purple sweet potato as an energy source feed ingredient for broiler chickens was considered less efficient, particularly during seasons when corn supplies can meet broiler feed needs. However, the positive values of fermentedpurple sweet potato as a functional feed ingredient may be exploited to improve the physiological and health conditions of broilers, particularly after the ban on the use of antibiotic growth promoters in feed and efforts to reduce chemical-based feed additives for chickens.

CONCLUSIONS

Feeding fermented purple sweet potato flour contributes for the better growth, feed conversion, immune defence, bacterial population and morphology of the small intestine

ACKNOWLEDGEMENTS. The study was supported by the Faculty of Animal and Agricultural Sciences, Universitas Diponegoro through DIPA FPP 2024.

REFERENCES

Anbuselvi, S. & Muthumani, S. 2014. Phytochemical and antinutritional constituents of sweet potato. *J. Chem. Pharm. Res.* **6**(2), 380–383. https://www.jocpr.com/articles/phytochemical-and-antinutritional-constituents-of-sweet-potato.pdf

Cloft, S.E., Miska, K.B., Jenkins, M., Proszkowiec-Weglarz, M., Kahl, S. & Wong, E.A. 2023 Temporal changes of genes associated with intestinal homeostasis in broiler chickens following a single infection with *Eimeria acervulina*. *Poult. Sci.* **102**, 102537. https://doi.org/10.1016/j.psj.2023.102537

Dapawisi, N.E., Mulyantini, N.G.A. & Ballo, V.J. 2022. Combination purple sweet potato flour (*Ipomoea batatas* L.), moringa leaves (*Moringa oleifera*) and coconut oil as a substitute for corn in the quail diet on performance and mortality of quail males. *J. Dryland Livest.* **4**(2), 2181–2184. https://www.doi.org/10.57089/jplk.v4i2.1167

Dereje, B., Girma, A., Mamo, D. & Chalchisa, T. 2020. Functional properties of sweet potato flour and its role in product development: a review. *Int. J. Food Prop.* **23**(1), 1639–1662. https://doi.org/10.1080/10942912.2020.1818776

Edi, D.N., Natsir, M.H. & Djunaidi, I. 2018. The effect of extract tecton leaf (*Tectonagrandis Linn. f*) in diet on performanceof laying hen. *J. Anim. Nutr*. **1**(1), 34–44. https://doi.org/10.21776/ub.jnt.2018.001.01.5

Hartadi, H., Reksohadiprojo, S. & Tilman, A.D. 2005. Feed Composition Table for Indonesia. Gadjah Mada University Press, Yogyakarta. https://www.feedipedia.org/node/22411

Helda, H., Catootjie, L.N. & Jehadu, Y. 2021. Effect of different basal diet and feed additive on the weight, percentage of carcass and component parts of broilers. *J. Trop. Anim. Vet. Sci.* **11**(3), 300–308. https://doi.org/10.46549/jipvet.v11i3.198

Hidayah, N., Yunani, R. & Widhowati, D. 2021. Potency of curcumin derived from ethanol extract of turmeric (*Curcuma longa* l.) as the immunostimulator in broiler. *Adv. Anim. Vet. Sci*. **9**(6), 787–791. http://dx.doi.org/10.17582/journal.aavs/2021/9.6.787.791

Kusuma, A.M., Asarina, Y.I. Rahmawati & Susanti. 2016. Effects of Dayak onion (*Eleutherine palmifolia* L. Merr) and purple yam (*Ipomoea batatas* L) extracts on reducing blood cholesterol and triglyceride levels in male rats. *Indonesian J. Pharm*. **6**(2), 108–116.

Maphosa, T., Gunduza, K.T., Kusina, J. & Mutungamiri, A. 2003. Evaluation of sweet potato tuber (*Ipomea batatas* l.) as a feed ingredient in broiler chicken diets. *Livest. Res. Rural Dev*. **15**(1). http://www.lrrd.org/lrrd15/1/maph151.htm

Nurhayati, N., Berliana, B. & Nelwida, N. 2019. Protein efficiency of broiler chicken fed fermented waste tofu with *Saccharomyces cerevisiae*. *Indonesian J. Anim. Sci*. **22**(2), 95–106. https://doi.org/10.22437/jiiip.v22i2.6725

Pratama, A., Yudiarti, T., Sugiharto, S. & Ayaşan, T. 2022. Blood and intestine profile of broilers fed *Averrhoa bilimbi* fruit, wheat bran, and yeast blends. *Trop. Anim. Sci. J.* **45**(1), 44–55. https://doi.org/10.5398/tasj.2022.45.1.44

Sapsuha, Y., Suprijatna, E., Kismiati, S. & Sugiharto, S. 2022. Possibility of using nutmeg flesh (*Myristica fragrans* Houtt) extract in broiler diet to improve intestinal morphology, bacterial population, blood profile and antioxidant status of broilers under high-density condition. *Agro. Res*. **20**(1), 1134–1150. https://doi.org/10.15159/ar.22.007

Shen, M., Xie, Z., Jia, M., Li, A., Han, H., Wang, T. & Zhang, L. 2019. Effect of bamboo leaf extract on antioxidant status and cholesterol metabolism in broiler chickens. *Animals* **9**(9), 699. https://doi.org/10.3390/ani9090699

Sugiharto, S. 2016 Role of nutraceuticals in gut health and growth performance of poultry. *J. Saudi Soc. Agric. Sci.* **15**, 99–111. https://doi.org/10.1016/j.jssas.2014.06.001

Sugiharto, S. & Ranjitkar, S. 2019. Recent advances in fermented feeds towards improved broiler chicken performance, gastrointestinal tract microecology and immune responses: A review. *Anim. Nutr*. **5**(1), 1–10. https://doi.org/10.1016/j.aninu.2018.11.001

Sugiharto, S., Yudiarti, T., Isroli, I. & Widiastuti, E. 2018a. The potential of tropical agro-industrial by-products as a functional feed for poultry. *Iranian J. Appl. Anim. Sci*. **8**(3), 375–385. https://sanad.iau.ir/journal/ijas/Article/542614?jid=542614

Sugiharto, S., Yudiarti, T., Isroli, I., Widiastuti, E., Wahyuni, H.I. & Suprijatna, E. 2018b. The potential of *Bacillus* strains isolated from the rumen content of dairy cows as natural antibacterial and antioxidant agents for broilers. *J. Indonesian Trop. Anim. Agric*. **43**(2), 115–123. http://ejournal.undip.ac.id/index.php/jitaa

Sultana, F., Khatun, H. & Ali, M.A. 2016. Use of potato as carbohydrate source in poultry ration. *Chem. Biol. Technol. Agric.* **3**(30), 1–7. https://doi.org/10.1186/s40538-016-0081-5

Wu, Q.J., Zheng, X.C., Wang, T. & Zhang, T.Y. 2018. Effect of dietary oridonin supplementation on growth performance, gut health, and immune response of broilers infected with *Salmonella pullorum*. *Irish Vet. J.* **71**(1), 1–6. https://doi.org/10.1186/s13620-018-0128-y

INSTRUCTIONS TO AUTHORS

Papers must be in English (British spelling). Authors are strongly urged to have their manuscripts reviewed linguistically prior to submission. Contributions should be sent electronically. Papers are considered by referees before acceptance. The manuscript should follow the instructions below.

Structure: Title, Authors (initials & surname; an asterisk indicates the corresponding author), Authors' affiliation with postal address (each on a separate line) and e-mail of the corresponding author, Abstract (up to 250 words), Key words (not repeating words in the title), Introduction, Materials and methods, Results and discussion, Conclusions, Acknowledgements (optional), References.

Layout, page size and font

- Use preferably the latest version of **Microsoft Word**, doc., docx. format.
- Set page size to **ISO B5 (17.6×25 cm)**, all **margins at 2 cm**. All text, tables, and figures must fit within the text margins.
- Use single line spacing and **justify the text**. Do not use page numbering. Use **indent 0.8 cm** (do not use tab or spaces instead).
- Use font Times New Roman, point size for the title of article **14 (Bold)**, author's names 12, core text 11; Abstract, Key words, Acknowledgements, References, tables, and figure captions 10.
- Use *italics* for Latin biological names, mathematical variables and statistical terms.
- Use single ('…') instead of double quotation marks ("…").

Tables

- All tables must be referred to in the text (Table 1; Tables 1, 3; Tables 2–3).
- Use font Times New Roman, regular, 10 pt. Insert tables by Word's 'Insert' menu.
- Do not use vertical lines as dividers; only horizontal lines (1/2 pt) are allowed. Primary column and row headings should start with an initial capital.

Figures

- All figures must be referred to in the text (Fig. 1; Fig. 1 A; Figs 1, 3; Figs 1–3). Use only black and white or greyscale for figures. Avoid 3D charts, background shading, gridlines and excessive symbols. Use font **Arial, 10 pt** within the figures. Make sure that thickness of the lines is greater than 0.3 pt.
- Do not put caption in the frame of the figure.
- The preferred graphic format is Excel object; for diagrams and charts EPS; for half-tones please use TIFF. MS Office files are also acceptable. Please include these files in your submission.
- Check and double-check spelling in figures and graphs. Proof-readers may not be able to change mistakes in a different program.

References

- **Within the text**

In case of two authors, use '&', if more than two authors, provide first author 'et al.':

Smith & Jones (2019); (Smith & Jones, 2019);
Brown et al. (2020); (Brown et al., 2020)

When referring to more than one publication, arrange them by following keys: 1. year of publication (ascending), 2. alphabetical order for the same year of publication:

(Smith & Jones, 2019; Brown et al., 2020; Adams, 2021; Smith, 2021)

- **For whole books**

Name(s) and initials of the author(s). Year of publication. *Title of the book* (*in italics*). Publisher, place of publication, number of pages.

Behera, K.B. & Varma, A. 2019. *Bioenergy for Sustainability and Security*. Springer International Publishing, Cham, pp. 1–377.

- **For articles in a journal**

Name(s) and initials of the author(s). Year of publication. Title of the article. *Abbreviated journal title* (*in italic*) volume (in bold), page numbers.
Titles of papers published in languages other than English, should be replaced by an English translation, with an explanatory note at the end, e.g., (in Russian, English abstr.).

Bulgakov, V., Adamchuk, V., Arak, M. & Olt, J. 2018. The theory of cleaning the crowns of standing beet roots with the use of elastic blades. *Agronomy Research* **16**(5), 1931–1949. doi: 10.15159/AR.18.213

Doddapaneni, T.R.K.C., Praveenkumar, R., Tolvanen, H., Rintala, J. & Konttinen, J. 2018. Techno-economic evaluation of integrating torrefaction with anaerobic digestion. *Applied Energy* **213**, 272–284. doi: 10.1016/j.apenergy.2018.01.045

- **For articles in collections:**

Name(s) and initials of the author(s). Year of publication. Title of the article. Name(s) and initials of the editor(s) (preceded by In:) *Title of the collection (in italics)*, publisher, place of publication, page numbers.

Yurtsev, B.A., Tolmachev, A.I. & Rebristaya, O.V. 2019. The floristic delimitation and subdivisions of the Arctic. In: Yurtsev, B.A. (ed.) *The Arctic Floristic Region*. Nauka, Leningrad, pp. 9–104 (in Russian).

- **For conference proceedings:**

Name(s) and initials of the author(s). Year of publication. Name(s) and initials of the editor(s) (preceded by In:) *Proceedings name (in italics)*, publisher, place of publishing, page numbers.

Ritchie, M.E. & Olff, H. 2020. Herbivore diversity and plant dynamics: compensatory and additive effects. In: Olff, H., Brown, V.K. & Drent R.H. (eds) *Herbivores between plants and predators. Proc. Int. Conf. The 38th Symposium of the British Ecological Society*, Blackwell Science, Oxford, UK, pp. 175–204.

Please note

- Use '.' (not ',') for decimal point: 0.6 ± 0.2; Use ',' for thousands – 1,230.4;
- Use '–' (not '-') and without space: pp. 27–36, 1998–2000, 4–6 min, 3–5 kg
- With spaces: 5 h, 5 kg, 5 m, 5 °C, C : D = 0.6 ± 0.2; $p < 0.001$
- Without space: 55°, 5% (not 55 °, 5 %)
- Use 'kg ha^{-1}' (not 'kg/ha');
- Use degree sign ' ° ' : 5 °C (not 5 ^{O}C).